uOttawa

L'Université canadienne
Canada's university

FACULTÉ DES ÉTUDES SUPÉRIEURES ET POSTOCTORALES

uOttawa

L'Université canadienne
Canada's university

FACULTY OF GRADUATE AND POSDOCTORAL STUDIES

Brigitte L. Simons
AUTEUR DE LA THÈSE / AUTHOR OF THESIS

Ph.D. (Chemistry)
GRADE / DEGREE

Department of Chemistry
FACULTÉ, ÉCOLE, DÉPARTEMENT / FACULTY, SCHOOL, DEPARTMENT

In Vacuo Cross-linking of Proteins:
A Novel Approach with Theoretical and Practical Applications to the Study of Proteins

TITRE DE LA THÈSE / TITLE OF THESIS

Harvey Kaplan
DIRECTEUR (DIRECTRICE) DE LA THÈSE / THESIS SUPERVISOR

Mary Alice Hefford
CO-DIRECTEUR (CO-DIRECTRICE) DE LA THÈSE / THESIS CO-SUPERVISOR

EXAMINATEURS (EXAMINATRICES) DE LA THÈSE / THESIS EXAMINERS

Illimar Altosaar

André Beauchemin

Alan Davidson

Ken Storey

Gary W. Slater
LE DOYEN DE LA FACULTÉ DES ÉTUDES SUPÉRIEURES ET POSTDOCTORALES /
DEAN OF THE FACULTY OF GRADUATE AND POSTDOCORAL STUDIES

In Vacuo Cross-linking of Proteins:

A Novel Approach with Theoretical and Practical Applications to the Study of Proteins

Brigitte L. Simons

Thesis submitted to the School of Graduate Studies and Research in partial fulfillment of the degree of Doctor of Philosophy in Chemistry

Ottawa-Carleton Chemistry Institute
Department of Chemistry
University of Ottawa
Ottawa, Ontario
Canada

Candidate

Brigitte L. Simons

Supervisors

Prof. Harvey Kaplan

Prof. Mary Alice Hefford

Your file Votre référence
ISBN: 0-494-11025-2
Our file Notre référence
ISBN: 0-494-11025-2

For my best friend and life partner JJ, who continually inspires me through unconditional love and support, and who has taught me the value of motivation and hard work in order to achieve my personal goals. I am forever true in spirit, life long laughter, and happiness.

ABSTRACT

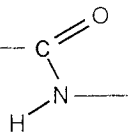

This thesis describes the hypothesis and subsequent demonstration that proteins can be covalently cross-linked without use of chemical reagents by simply incubating the protein or proteins in the lyophilized state under appropriate conditions in a vacuum. This *in vacuo* cross-linking requires the interaction of a protonated positively-charged amino group on one molecule with a deprotonated negatively-charged carboxylate group on a second. A zero-length cross-link is formed by a condensation reaction between the two groups with the release of water. A reaction mechanism is proposed in which amide bond formation occurs by means of a proton transfer from the protonated amino group to an interacting carboxylate group followed by a nucleophilic attack by the deprotonated amino group on the carboxylic acid group (protonated). The reaction is driven by the removal of the released water by the vacuum.

It was observed that proteins appeared to form trace amounts of covalently bonded products, visualized on denaturing and reducing gel electrophoresis and probed with sensitive detection methods, if the protein preparations had been subjected to a vacuum. This observation prompted the hypothesis: can proteins be covalently cross-linked by incubating lyophilized protein under vacuum? This hypothesis was tested using Ribonuclease A (RNase A) as a model protein and the *in vacuo* heating of RNase A demonstrated that covalently cross-linked products arise with dimer being the major product.

Structural characterization of the *in vacuo* RNase A dimer demonstrated that the dimer was composed of a single amide cross-link at positions lysine 66 and glutamic acid 9. This dimeric protein is proposed to adopt a new conformation not previously reported as a

known RNase A X-ray crystallographic structure. The *in vacuo* RNase A dimer also demonstrated a 2-fold increase in enzymatic activity compared to monomeric RNase A towards both double stranded and single stranded RNA, both in the presence and absence of the cytosolic ribonuclease inhibitor.

The *in vacuo* cross-linking of protein was shown to be a general phenomenon as all proteins tested produced covalently cross-linked oligomers. The utility of this cross-linking method was then expanded to the cross-linking of proteins to functionalized solid supports and the covalent cross-linking of enzymes to antibodies to produce highly sensitive immunoconjugates for Western Blot analysis and ELISAs. A discussion of the *in vacuo* cross-linking of a *de novo* designed protein, milk bundle, and its dimeric 4-helix bundle structural characterization is also presented.

ACKNOWLEDGEMENTS

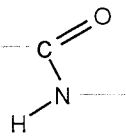

It has been an honour and privilege to have had the guidance, support, encouragement, and wisdom of two outstanding supervisors, Harvey Kaplan (protein chemistry, University of Ottawa) and Mary Alice Hefford (Centre for Biologics Research, Health Canada). I would like to express my sincere gratitude to both of them for allowing me the opportunity to learn and gain valuable research experiences, to achieve academic success, and to reap the benefits of being part of their respective research groups.

I would like to thank my fellow members of these research groups for their technical support, helpful and insightful discussions, and for providing me with daily doses of comic relief: Sophie D'Aoust, Sylvie Fournier, John Mark, Mike Cauchy, Sam Guest, and Russ Taylor at the Centre for Biologics Research and Van Thong Pham, Nicholas Stewart, Mary King, and Erin Ewing at the University of Ottawa. Other people who are deserving of recognition and who endured my continual harassment include: Bozena Jaentschke, Louise Larocque, Diane Bertrand, and Mary Beth Cameron. Many thanks go out to four great scientists at Health Canada, Dr. Terry Cyr, Dr. Bill Casely, and Dr. Sean Li, and Dr. Michel Girard, for their expertise in key components of this research and for their helpful advice. A special thank you goes to Sophie D'Aoust who was an integral to aiding me in completing my thesis through experimental work, technical help, and editing this manuscript.

I would like to acknowledge and express my appreciation for the financial support of NSERC and the University of Ottawa.

TABLE OF CONTENTS

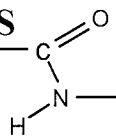

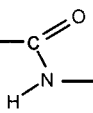

Chapter 1: Main Introduction

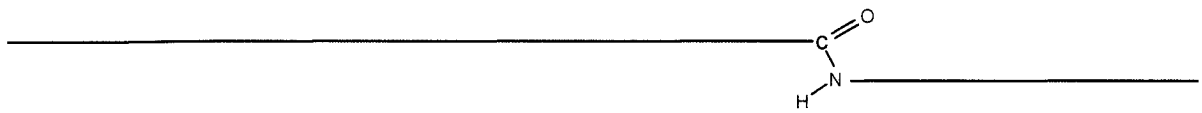

Chapter 2: *In Vacuo* Cross-linking, Mechanism and Methodology

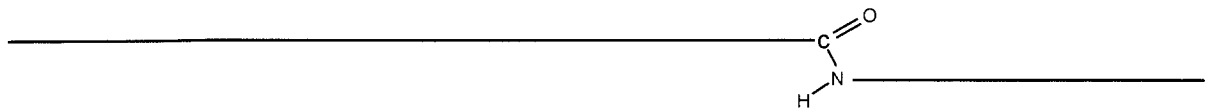

Chapter 3: The *In Vacuo* Cross-linking of RNase A: A Characterization of Structure and Function

Chapter 4: Protein Immobilization onto Soluble and Insoluble Supports

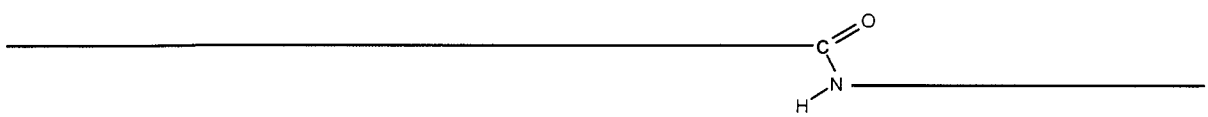

Chapter 5: *In Vacuo* Cross-linking of Antibody-Enzyme Conjugates; Novel Immunoreagents for Western Blot Analysis and ELISA.

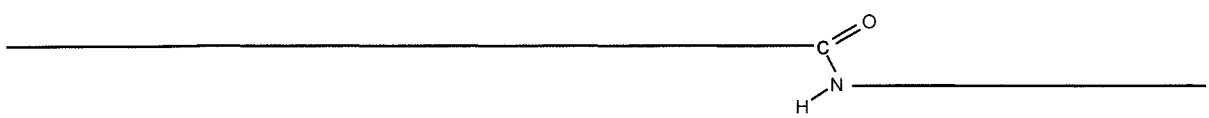

Chapter 6: Dimer Formation from a *De Novo* Designed Protein, Milk Bundle Proteins

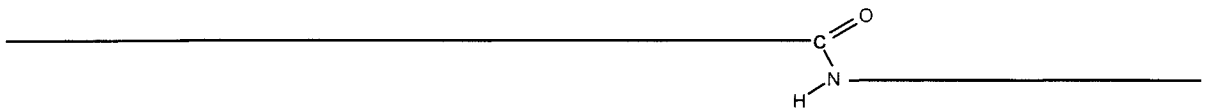

Chapter 7: Conclusions

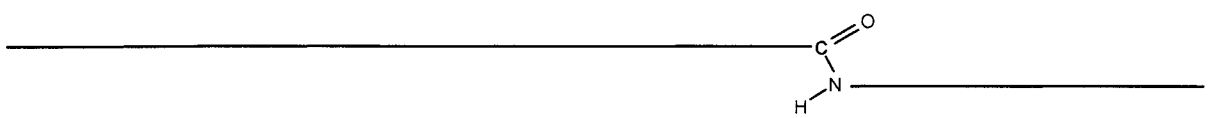

LIST OF FIGURES

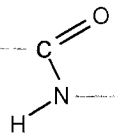

Chapter 1

Chapter 2

Chapter 3

Chapter 4

Chapter 5

Chapter 6

LIST OF TABLES

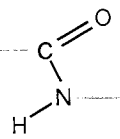

Chapter 1

Chapter 3

Chapter 4

Chapter 5

LIST OF EQUATIONS

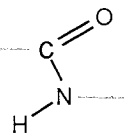

Chapter 3

Chapter 4

Chapter 5

Chapter 6

LIST OF ABBREVIATIONS

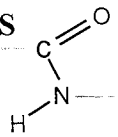

ACN	acetonitrile
APase	alkaline phosphatase
Arg	arginine
Asp	aspartic acid
BCA	bicinchoninic acid
BSA	bovine serum albumin
CD	circular dichroism
CNBr	cyanogen bromide
Cys	cysteine
dH_2O	distilled water
DTT	dithiothreitol
EC_{50}	effective concentration at 50% of measurable effect
EDC	1-ethyl-3-(3-dimethylaminopropyl)carbodiimide
EDTA	ethylenediamine tetraacetic acid
ELISA	enzyme-linked immunoadsorbent assay
ESI-MS	electrospray ionization mass spectrometry
ESI-TOF-MS	electrospray ionization time of flight mass spectrometry
FA	formic acid
FPLC	fast performance liquid chromatography
FTIR	Fourier Transform infrared
Glu	glutamic acid
HPLC	high pressure liquid chromatography
HRP	horseradish peroxidase
His	histidine
IgG	Immunoglobulin G
IPTG	isopropyl-beta-D-thiogalactopyranoside
kDa	*kilo*Daltons
k_{cat}	enzyme turnover number
K_i	enzyme inhibition constant

K_M	Michaelis constant
LC-MS	liquid chromatography followed by mass spectrometry
LpH	lyophilized pH
Lys	lysine
MALDI	matrix assisted laser deadsorption ionization
MB	milk bundle
Met	methionine
M_r	estimated molecular size
MS	mass spectrometry
MeOH	methanol
MW	molecular weight
NMR	nuclear magnetic resonance
ONC	Onconase™
OPD	*ortho* phenyldiamine
PBS	phosphate buffered saline
pK_a	negative logarithm of the ioninzation constant
PMSF	phenylmethyl sulfonyl fluoride
p-NPCF	*para*-nitrophenylchlorformate
poly(glu)	poly-D-glutamic acid
poly(lys)	poly-D-lysine
Poly(A)-Poly(U)	poly adenosine, poly uracil double stranded RNA
RI	ribonuclease inhibitor
RNA	ribonucleic acid
RNase A	ribonuclease A
SDS-PAGE	sodium dodecylsulphate polyacrylamide gel electrophoresis
SEC	size exclusion chromatography
TBS	tris buffered saline
TFA	trifluoroacetic acid
Thr	threonine
Tyr	tyrosine
V_{max}	maximum velocity of enzyme

Chapter 1: Main Introduction

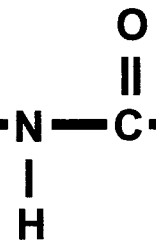

1.1 Thesis Aim and Scope

The research presented in this thesis is based on a discovery that the covalent chemical modification of proteins can be carried out *in vacuo* without the use of chemicals. Throughout the course of experiments, an unexpected reaction was discovered between protein molecules in the dry state and the formation of covalently cross-linked protein complexes was observed. Investigating protein-protein interactions is an underlying theme of much current research dedicated to determining the structure, function, and the physiological importance of proteins in mechanism/regulation in disease. In this thesis, a novel method of investigating protein interactions (by covalently cross-linking through interacting residues in the lyophilized state) is described. Additionally, some approaches are presented describing the construction of protein complexes and the immobilization of proteins to non-protein matrices; these have general applicability in several industrial and therapeutic scenarios. The appeal of this *in vacuo* method is its overall simplicity and the absence of toxic reagents or solvents, which offers the possibility of both reducing manufacturing costs and producing safer products for therapeutics and biomaterials. Through an examination of the cross-linked products generated when this method was applied to selected model proteins, products with potential therapeutic or commercial value were prepared. Their characterization provides insights into the chemistry behind this new *in vacuo* technique and proposes an explanation to this unexpected reaction in the dry state under *in vacuo* conditions.

The starting point of the project was an anomalous result obtained by a colleague studying protein cross-linking using a chemical activating reagent,

p-nitrophenylchloroformate (*p*-NPCF), under *in vacuo* conditions. When the protein cross-linked products of this reaction were examined by denaturing SDS - gel electrophoresis, trace amounts of dimeric protein were observed in the control samples where no reagent had been introduced and, as a result, no dimeric product was expected. The control sample had simply been lyophilized and then incubated under vacuum. The appearance of a small amount of cross-linked material in the control sample of this particular experiment was reminiscent of other unexpected, and unexplained, observations of higher molecular weight species in denaturing gels when samples of lyophilized proteins were examined by sensitive methods like Western Blotting and radiolabeling. These combined observations begged the question: would cross-linking of proteins be observed in lyophilized samples where proteins had been placed under vacuum?

A simple experiment was undertaken to answer this question: A number of proteins (ribonuclease A (RNase A), human growth hormone (hGH), cytochrome c, ubiquitin, and lysozyme) were reconstituted in water from lyophilized preparations purchased from Sigma-Aldrich and subjected to gel electrophoresis without any further treatment. Figure 1.1 shows two SDS-PAGE images where these several different proteins were loaded and subjected to electrophoresis: In the first gel, Figure 1.1A, the proteins are loaded in amounts of 5 µg per lane. The gel is stained with Coomassie Blue. In the second gel, Figure 1.1B, the proteins are loaded in higher amounts, 20 µg of protein per lane, subjected to electrophoresis, then stained, again, with Coomassie Blue. The second gel where the proteins were loaded in high amounts, higher than what is customarily loaded and detected, bands migrating at positions consistent with molecular sizes corresponding to the dimeric products of each protein are visible. The appearance of these apparent dimer bands in all proteins tested suggests that

covalent cross-linking may have occurred when protein samples are subjected to low pressures in the vacuum applied during the lyophilization process that manufacturers commonly use when preparing proteins as powders for distribution. If the bands observed in Figure 1.1 do indeed represent covalently cross-linked dimers formed during lyophilization, the data may also suggest that such a cross-linking reaction could become favourable if a lyophilized sample is heated while under a vacuum. This thesis describes the experimental results obtained from testing this hypothesis, namely, incubating vacuum sealed lyophilized protein samples at elevated temperatures. From the results obtained in a very simple initial experiment, several new avenues of investigation opened up. Firstly, to elucidate the cross-linking reaction that is taking place and secondly to develop methodology for the many practical applications of this discovery. These are described in the following chapters.

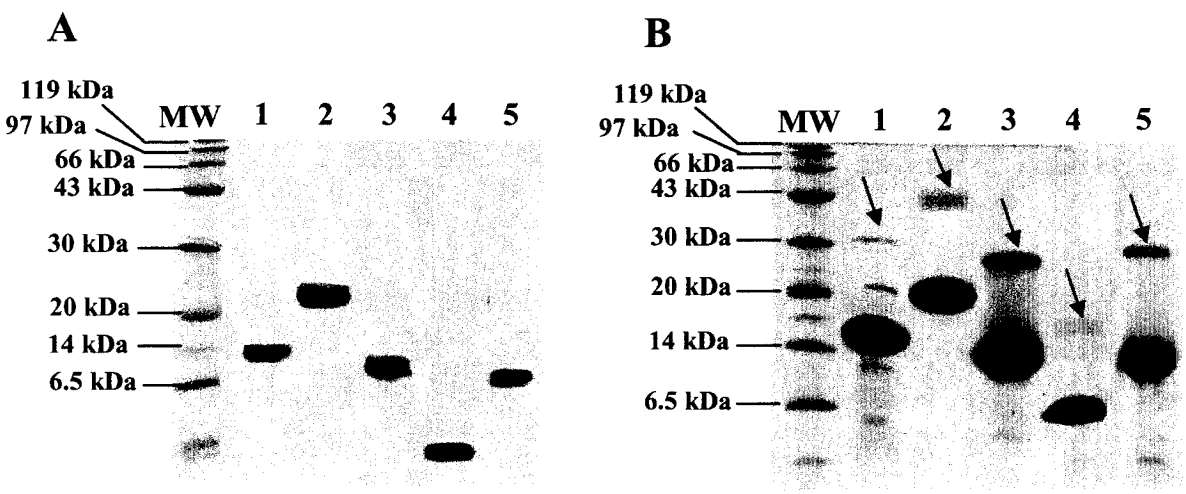

Figure 1.1 SDS gel electrophoresis of 5 µg (A) and 20 µg (B) total protein loadings of various proteins. RNase A (lane 1), hGH (lane 2), cytochrome C (lane 3), ubiquitin (lane 4), and lysozyme (lane 5). Gels stained with Coomassie Blue. Dimeric products are shown by arrows.

1.2 Investigating Protein-Protein Interactions

Many biologically active proteins are members of multi-protein complexes, or interact with other proteins (including themselves or parts of themselves), to modulate or regulate cellular activity. These interactions are often the result of brief, non-covalent forces that bring protein moieties together in close range. These non-covalent forces include hydrogen bonds, ionic bonds, hydrophobic interactions, and Van der Waals (or also called London dispersion) forces. Such molecular interactions bring otherwise distant functional groups together, resulting in the formation of microenvironments and interfaces within the protein structure (Kluger and Alagic, 2004). These microenvironments or interfaces give rise to several structurally important regions such as catalytic sites, binding pockets, allosteric sites, and domain-domain interfaces. Identifying these sites of interaction can provide insights into the biological functions of proteins.

High-resolution methods of protein structural analysis, such as NMR and X-ray crystallography, may help elucidate stable, non-covalent interactions within a protein or protein complex. However, where structural components interact at high motion interfaces under variable circumstances (such as those conditions present in response to inhibitors, effectors, or another protein) these interactions become highly dynamic and thus difficult to resolve by physical methods (Kluger and Alagic, 2004).

One approach to study the complexity and variable nature of protein-protein interactions is to create a permanent record of the sites of interaction, thus facilitating their identification. By analogy, we can presume a fish has approached the end of a fishing line if we find the bait is missing. If the fish becomes permanently attached to the hook, the point of interaction becomes permanently defined. If we "fish" for protein-protein interactions,

one can use chemical "baits" to capture the interaction whereby introducing a chemical cross-link at the site.

1.3 Protein Cross-linking

Protein cross-linking can be used as means of determining protein interactions, by "chemically baiting the hook" to fish for the interaction. In the simplest scenario, a reactive chemical function is attached to an amino acid residue suspected to be at the site of interaction, the strategy being to react it with a residue of another protein molecule that interacts at or near this site. This can be achieved by use of bifunctional reagents flanked by two reactive groups having affinity for specific amino acid residues or types of residues separated by a linker group. Connecting two or more interacting residues into one bifunctional reagent provides a permanent bridge that captures the interaction. Subsequent determination of the sites of cross-linking can reveal where spatially defined interactions occur and one can begin to define the biological significance of that interaction.

There are other reasons to cross-link proteins other than to investigate protein-protein interactions. Structure function relationships can be deduced by modifying the amino acids responsible for biological activity by forming either intermolecular or intramolecular links. Often proteins are cross-linked to chemical labels so they become equipped with a tracking system to determine their binding sites or their cellular location. Cross-linking of proteins may be desired to alter their physical properties, such as to impart structural stability. Lastly, an important use of protein cross-linking is to immobilize proteins to solid supports either to create affinity columns, to easily separate enzymes from reaction mixtures, or so that expensive enzymes can be reused.

1.4 The Chemical Reactivity of Proteins

In order to achieve the desired cross-linking between amino acid residues, one must consider the chemical properties, pK_a and relative reactivity, of amino acid side chains. There are twenty common amino acid side chains of which only nine would normally be considered reactive under conditions where proteins maintain their native structures. These are: (1) thiol groups of cysteine, (2) ε-amino group of lysine, (3) carboxyl groups of aspartic acid and glutamic acid, (4) imidazolyl group of histidine, (5) guanidinyl group of arginine, (6) thioether group of methionine, and (7) phenolic hydroxyl group of tyrosine. In addition to these reactive side chains, the N-terminus amino group and the C-terminus carboxyl group are also reactive. The observed pK_a values of these individual functional groups in aqueous solution are listed in Table 1.1 (Creighton, 1993). The pK_a values of individual functional groups in proteins may well differ from those for the same side chain on an amino acid free in solution (i.e. referring to the pK_a ranges shown in Table 1.1) as both pK_a and reactivity are influenced by the microenviroment of the functional group. Once the primary structure of the protein adopts a 3-dimensional fold or tertiary structure, the side chains of its constituent amino acids are in new microenvironments where they experience non-covalent forces as a result of their proximity to other side chains in the folded structure. These forces, in particular hydrogen and ionic bonding, may create local inductive effects that influence both the pK_a values of the amino acid side chains and their reactivities once the protein is folded (i.e. spatial arrangements of ionizable groups which are placed into close proximity with electron withdrawing groups). The ability of neighboring groups to react is, therefore, highly dependant on pH, steric hinderance, and the ionization states of adjacent functional groups.

Table 1.1 Approximate pK_a values of the amino acid side chains in protein (Modified from Creighton, 1993)		
Amino acid	**Side chain group**	**Observed pK_a**
Aspartic acid	Carboxyl	3.9
Glutamic acid	Carboxyl	4.3 - 4.5
Histidine	Imidazolyl	6.0 - 7.0
Cysteine	Sulfhydryl	9.0 - 9.5
Lysine	Amino	10.4 - 11.1
Tyrosine	Hydroxyl	10.0 - 10.3
Arginine	Guanidinyl	12.0
N-terminus	Amino	6.8 - 8.0
C-terminus	Carboxyl	3.5 - 4.3

1.5 Chemical Cross-linking Reagents

There are several hundreds of chemical reagents designed for cross-linking proteins. The Pierce Chemical Library of Cross-linking Reagents (Pierce Biotechnology, Rockford, Il, USA) is an excellent resource for selecting the appropriate reagent with the proper specificity for the amino acids at the desired site. Glutaraldehyde, a homobifunctional reagent, because of its ease of use and high reactivity, remains the most commonly used reagent to cross-link proteins even though its reaction mechanism is complex. Glutaraldehyde is proposed to react in a two step mechanism as seen in Figure 1.2A. In the first step, the introduction of glutaraldehyde results in rapid reaction of the reagent with

primary amino groups of lysine or the amino terminus to form a Schiff base. Then, a neighboring amino group from lysine residue nucleophilically attacks the carbonyl carbon of the aldehyde of this Schiff base to form a five carbon chain link between two primary amino groups upon subsequent reduction of the Schiff base with $NaBCNH_3$ (Avrameas et al., 1969 a and b; Molin et al., 1978). Glutaraldehyde bifunctional reagents react between the ε-amino groups of neighboring lysine residues close in three dimensional space, however, due to the high reactivity of primary amines towards glutaraldehyde, any one of the lysine side chains on the protein can react and the cross-linking of the protein is often random and incomplete resulting in partially derivitized protein. Another significant drawback to glutaraldehyde cross-linking is the instability of the reagent itself. As shown in Figure 1.2B, glutaraldehyde at pH 9 can polymerize by an aldol condensation type mechanism (Olde Damink et al., 1995). The subsequent reaction with amino functionality on the protein may lead to the formation of large insoluble heterogeneous protein complexes. Glutaraldehyde, when used appropriately, however, can be an efficient reagent to form cross-links between amino groups and is the most commonly used reagent for commercial cross-linking purposes by several manufacturers because of its efficiency and ease of use. None-the-less, glutaraldehyde is toxic at low levels, and is thus not a desirable reagent to be used in the production of biomaterials or therapeutic macromolecules. In addition to glutaraldehyde, there are several other bifunctional reagents used specifically in particular cross-linking applications and their reaction mechanisms and their uses will be discussed in the subsequent relevant chapters of this thesis.

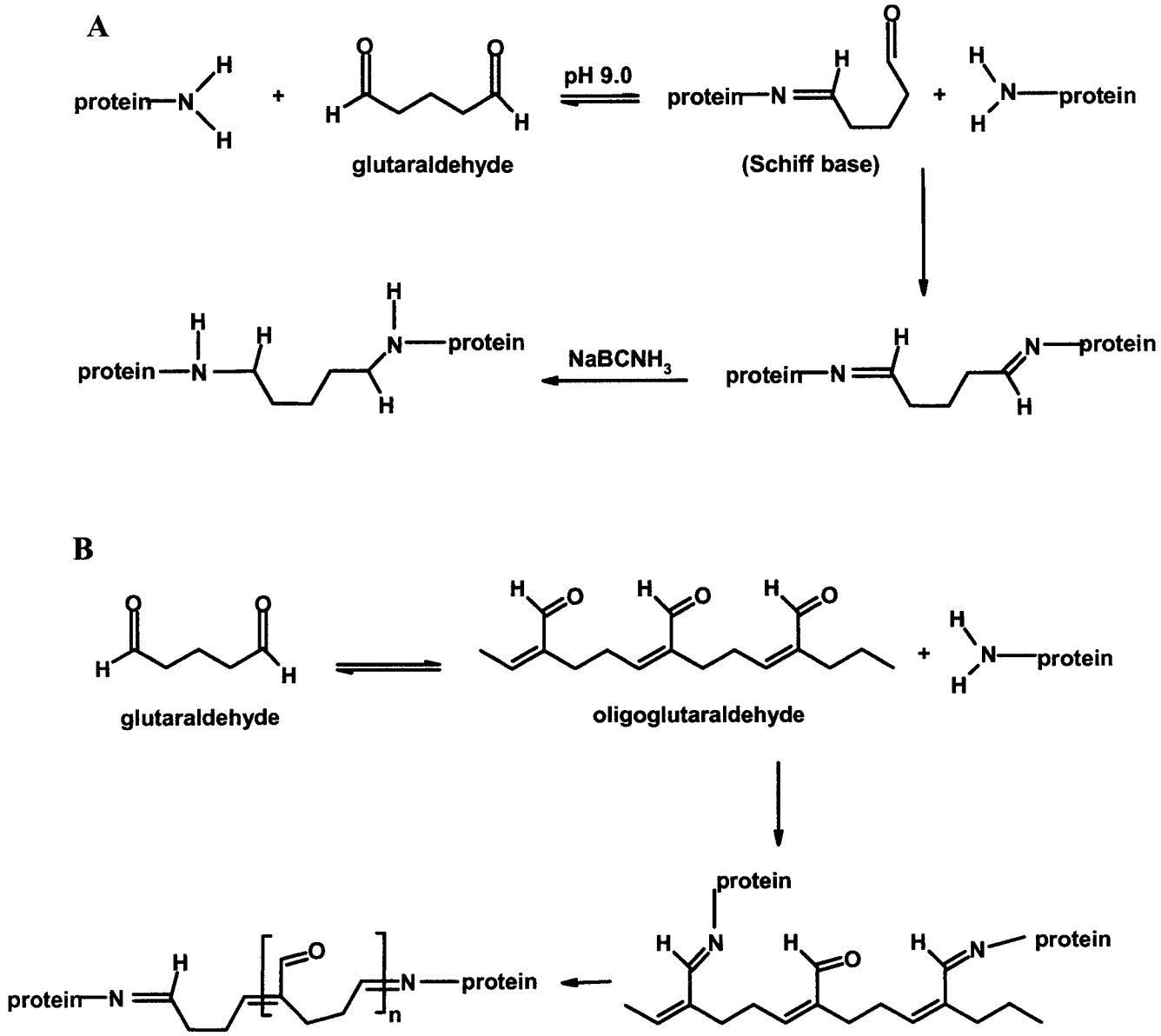

Figure 1.2 The reaction mechanism of glutaraldehyde in the cross-linking between lysine residues in proteins (A). At a reaction pH value of 9, glutaraldehyde can polymerize resulting in large heterogeneous cross-linked protein complexes (B). Modified from Olde Damink et al., 1995.

1.6 *In Vacuo* Protein Modification

Chemical modification of amino acid side chains poses difficulties due to the pH, steric hinderance, and induction effects that take place once a protein folds into its three dimensional structure. Under aqueous reaction conditions, the modification of selected residues often requires strongly activating reagents to overcome the competition from side reactions involving water and oxygen. Proteins, either carrying out reactions or just simply stored in aqueous media, show major chemical and physical instabilities, in particular, oxidation of methionines and histidines, the deamidation of glutamine and asparagine, and disulfide bond scrambling among cysteine residues are quite common. To minimize these destructive chemical reactions, proteins are often lyophilized (or freeze dried) to remove the water in the sample and therefore reduce the possibility of undesirable reactions.

Although protein lyophilization is routinely performed to stabilize protein structure for long-term storage, some proteins experience what is called lyophilization induced denaturation. This denaturation essentially means that upon the addition of water back into the sample, the protein remains aggregated and cannot be returned to its solvated structure (Heller et al., 1999). This inherent physical instability can be controlled by the use of lyoprotectants and cryoprotectants during the freezing and drying stages. These additives are called excipients, and they replace the solvation shell around the protein normally structured by water, and thus prevent hydrophobic collapse and protein self-association. Despite the chance of physical denaturation, lyophilization undoubtedly remains the manufacturing process of choice for preparing protein formulations for therapeutic applications.

Proteins exhibit enhanced thermal stability once freeze dried. Klibanov and Zaks in the 1980's showed that lyophilized protein samples could be heated to temperatures of above

120°C, and upon reconstitution, the proteins retained their full enzymatic activity. They suggested that, once the bulk of the water is removed by lyophilization, tightly bound water or low activity water remains associated with the protein. This minimally solvated structure locks into its lowest energy conformation and all H_2O and O_2 mediated degradation pathways are minimized thus stabilizing the native conformation of proteins even at elevated temperatures. Klibanov then exploited these altered physical properties of lyophilized protein samples to demonstrate the activity of proteins at elevated temperatures in organic solvents (Zaks and Klibanov, 1984; Klibanov, 1983). Further investigations into the behaviour of freeze dried protein samples have developed into significant non-aqueous methodology including chemical modification of proteins in the dried state and the discovery of pH memory effect.

1.6.1 pH memory effect

In solution, the ionizable groups of proteins will be either protonated or deprotonated depending upon the apparent pK_a of the group and the pH of the surrounding medium. During a reaction in solution that exclusively involves one of these moieties, the protonation state of these ionizable groups shifts to the side producing the species that is consumed by the reaction, in accordance with Le Châtelier's Principle (refer to Figure 1.3). This resulting protonation or deprotonation (as the case may be) requires the abstraction or donation of a hydrogen ion and is mediated through water molecules in the solution. Once the protein sample is lyophilized, this protonation/deprotonation to retain equilibrium stops and the ionization state of each individual ionizable functional group on each individual protein molecule is fixed or "frozen-out". This is referred to as "the pH memory effect" because a

protein solution at pH 7, once lyophilized, will retain the relative number of protonated and deprotonated side chains, dictated by their relative pK_a values and the pH of the solution before and during lyophilization (Klibanov, 1983). If a reagent is introduced to the lyophilized sample, in the case of Figure 1.3 the reagent is "E-X", only the deprotonated amine will react allowing for greater control of the reaction.

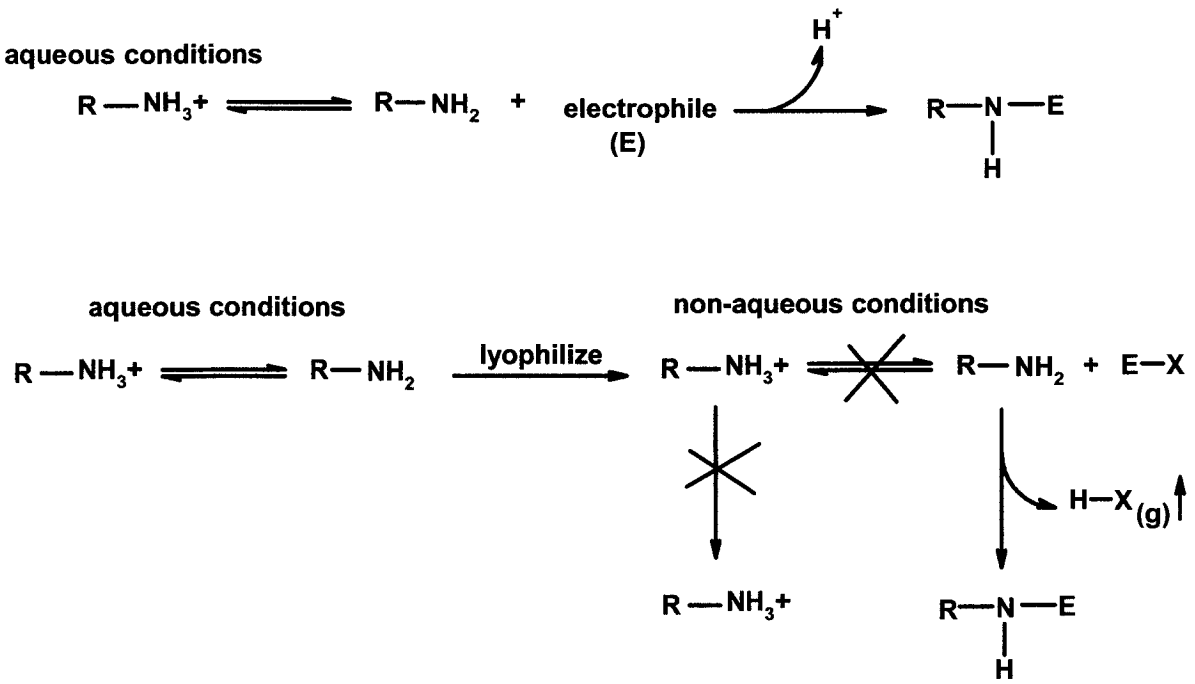

Figure 1.3 The equilibrium between protonated and deprotonated forms of primary amines under aqueous and non-aqueous conditions. The reaction with electrophile (E) will only occur with the deprotonated amino group resulting in a shift in the equilibrium favouring the formation of deprotonated amino groups. If the sample is lyophilized, this equilibrium is frozen-out, and only a fixed amount of deprotonated amino groups are available to react with the electrophilic reagent (E-X).

1.6.2 Chemical reactions *in vacuo*

The early discoveries of Klibanov (1983) and those employing similar methodologies have revealed the practical advantages of modifying proteins in the dry state. Clearly, the major advantage of lyophilizing proteins is to impart chemical and physical stability thus increasing the likelihood of maintaining a native conformation and, consequently, retaining catalytic activity in enzymes and biological activity in therapeutic proteins. A non-aqueous technique was developed by Taralp and Kaplan (1997) to chemically modify lyophilized protein at elevated temperatures under vacuum. An additional benefit of carrying out a protein modification reaction on a dried protein, *in vacuo*, is that any volatile products formed during the reaction are drawn away by the vacuum. This effect of the vacuum thermodynamically drives the reaction by consuming the products and pulling the reaction equilibrium to the products side to compensate for their removal from the equilibrium - Le Châtelier's Principle, in essence. Furthermore, by heating the sample, more favourable reaction conditions can be created and the reaction is further driven to produce products. Incubating *in vacuo* reduces deamidation, degradation, or oxidation which can potentially arise under aqueous conditions, and allows one to carry out chemical modification of proteins using a wide variety of modifying reagents, many of which are too insoluble to be used in aqueous mediums.

1.7 Ribonuclease A - a Model Protein

Bovine pancreatic ribonuclease A (RNase A) is a long-established model for the study of protein structure and function. RNase A was one of the first proteins to have its primary structure (124 amino acid residues) determined (Potts et al., 1962; Smyth et al.,

1963) and one of the first proteins to yield an X-ray crystallographic structure (Kartha et al., 1967). RNase A is a member of an RNase superfamily – a family that shares a 30% sequence homology among all members and is represented in nearly all tissues of mammals and some reptiles (Bientema et al., 1988). Ribonucleases possess a highly specific catalytic activity, namely, the ability to effect the degradation of ribonucleic acid (RNA), through a mechanism involving hydrolysis and transphosphorylation, specifically at cytosine and uracil (pyrimidine) nucleotide residues. This catalytic activity is achieved through highly conserved substrate binding and catalytic sites composed, in bovine pancreatic RNase A, of His-12, Lys-41, Thr-45, and His-119 residues. Despite the high level of conservation of the catalytic site, however, various members of this superfamily catalyze the hydrolysis reaction at very different rates, with k_{cat}/K_M values ranging over six orders of magnitude (Lee and Vallee, 1989).

In 1962, Crestfield et al. reported that RNase A forms dimers and higher oligomers after lyophilization from a solution of 50% acetic acid. These non-covalent RNase A aggregates and other chemically modified RNase A derivatives have since been a major area of study in terms of their characterization (Gotte et al., 1999; Gotte and Libonati, 1998; Liu et al., 1998) their enzymatic activity (Di Donato et al., 1994; Gotte and Libonati, 1998; Park and Raines, 2000; Matousek et al., 2003a and b), their X-ray crystallography (Liu et al., 1998; Fedorov et al., 1996; Liu et al., 2001) and their biological activity (Park and Raines, 2000; Di Donato et al., 1994; Leland et al., 2001; Bretscher et al., 2000). The non-covalent RNase A dimer(s) produced by this method has been shown to display enhanced enzymatic activity toward double and single stranded RNA, as well as an apparent anti-proliferative and cytotoxic activity in specific cancerous tumor cells (Matousek et al., 2003b). Based on this

modulated biological activity, compared to monomeric RNase A, RNase A dimers have been portrayed in the literature as promising pharmaceutical protein candidates in cancer therapy.

1.7.1 Three-dimensional domain swapping

The enhanced biological features of RNase A dimers are thought to arise from its observed structural domain swapping between two monomeric units. In a 3-D domain-swapped dimer (a term coined by Eisenburg (1995)), two identical domains from two molecules exchange and the new domain takes the place of the other in the conformation. Domain swapping, as Eisenberg's work illustrates, occurs, under appropriate conditions, with many proteins other than RNase A and can endow enzyme oligomers with additional properties not present in their monomeric counterparts. Studies involving these unique RNase A domain swapped oligomers may illuminate a further understanding to the structure and biological activities of this enzyme (refer to Introduction, Chapter 3). Indeed, techniques used to elucidate structure(s) and mechanisms of domain swapping in RNase A may prove useful in understanding domain swapped dimers of other proteins.

1.8 Dimer Formation by a *De Novo* Protein Designed to be Monomeric

In 1995, a *de novo* protein enriched in nutritionally important amino acids, was designed to be engineered first into rumen bacteria (Beauregard et al.,1995) and then into cash crops such as wheat and alfalfa. This protein was designed to form a monomeric 4-helix bundle protein, based on considerations of the amino acid requirements and the need to form a stable protein structure that was within the design capabilities of the time. After expression in bacteria, and purification, the *de novo* protein was characterized. Physical

evidence indicated that this protein was dimeric, rather than the originally intended monomeric design (Hefford et al., 1999). Several mutants were designed to modify the original sequence, in hopes of disturbing the dimeric interactions and ensuring a monomeric fold. Despite the attempts to change presumed "problematic" residues responsible for dimer formation, the lack of knowledge of the nature of the dimeric interaction, made it difficult to predict a proper re-design. The design process, coupled with secondary structure predictions, however, suggested that the weakness in the design of a monomeric protein was in the loops between helices of the bundle. Should one or another of these loops fail to form, two molecules of protein rather than one might be needed to bury the hydrophobic residues designed to be in the protein core, forming what, in light of more recent discoveries by others, would now be called a domain swapped dimer.

1.9 Thesis Structure

This thesis is organized into six additional chapters, five describing experimental results and one devoted to concluding remarks. Chapter 2 describes the development of the methodology of *in vacuo* cross-linking; the experimental evidence presented there-in provides proof-of-concept and a proposed reaction mechanism. Chapters 3 and 5 describe the characterization of specific cross-linked products arising from the *in vacuo* cross-linking of RNase A, Onconase™, reporter enzymes (horseradish peroxidase and alkaline phosphatase), and antibodies (immunoglobulins). Chapters 4 and 5 both contain reports of specific applications of the *in vacuo* methodology: protein immobilization, and the labeling of antibodies with enzymes for application in Western Blots and ELISAs. Chapter 6 is the investigation of the dimer formation of milk bundle (MB) proteins, the *de novo* designed 4-

helix bundle protein. In this last chapter, the *in vacuo* method of cross-linking is used as a tool to locate electrostatic interactions within the MB dimer in to elucidate its "mis-designed" structure.

1.10 References

Avrameas, S. Coupling of enzymes to proteins with glutaraldehyde. Use of the conjugates for the detection of antigens and antibodies. *Immunochemistry.* **1969a,** *6* (1), 43-52.

Avrameas, S.; Ternynck, T. The cross-linking of proteins with glutaraldehyde and its use for the preparation of immunoadsorbents. *Immunochemistry.* **1969b,** *6* (1), 53-66.

Beauregard, M.; Dupont, C.; Teather, R. M.; Hefford, M. A. Design, expression, and initial characterization of MB1, a de novo protein enriched in essential amino acids. *Biotechnology (N. Y.)* **1995,** *13* (9), 974-981.

Beintema, J. J.; Schuller, C.; Irie, M.; Carsana, A. Molecular evolution of the ribonuclease superfamily. *Prog. Biophys. Mol. Biol.* **1988,** *51* (3), 165-192.

Bennett, M. J.; Schlunegger, M. P.; Eisenberg, D. 3D domain swapping: a mechanism for oligomer assembly. *Protein Sci.* **1995,** *4* (12), 2455-2468.

Bretscher, L. E.; Abel, R. L.; Raines, R. T. A ribonuclease A variant with low catalytic activity but high cytotoxicity. *J. Biol. Chem.* **2000,** *275* (14), 9893-9896.

Creighton, T.E. Chemical properties of peptides; In *Proteins, Structures and Molecular Properties,* 2nd edition, W.H. Freeman and Company. **1993**. pp. 6-10.

Crestfield, A. M.; Stein, W. H.; Moore, S. On the aggregation of bovine pancreatic ribonuclease. *Arch. Biochem. Biophys.* **1962,** *Suppl 1:217-22.*, 217-222.

Di, Donato. A.; Cafaro, V.; D'Alessio, G. Ribonuclease A can be transformed into a dimeric ribonuclease with antitumor activity. *J. Biol. Chem.* **1994,** *269* (26), 17394-17396.

Fedorov, A. A.; Joseph-McCarthy, D.; Fedorov, E.; Sirakova, D.; Graf, I.; Almo, S. C. Ionic interactions in crystalline bovine pancreatic ribonuclease A. *Biochemistry* **1996,** *35* (50), 15962-15979.

Gotte, G.; Libonati, M. Two different forms of aggregated dimers of ribonuclease A. *Biochim. Biophys. Acta* **1998,** *1386* (1), 106-112.

Gotte, G.; Bertoldi, M.; Libonati, M. Structural versatility of bovine ribonuclease A. Distinct conformers of trimeric and tetrameric aggregates of the enzyme. *Eur. J. Biochem.* **1999,** *265* (2), 680-687.

Hefford, M. A.; Dupont, C.; MacCallum, J.; Parker, M. H.; Beauregard, M. Characterization of MB-1. *Eur. J. Biochem* **1999,** *262* (2), 467-474.

Heller, M. C.; Carpenter, J. F.; Randolph, T. W. Protein formulation and lyophilization cycle design: prevention of damage due to freeze-concentration induced phase separation. *Biotechnol. Bioeng.* **1999,** *63* (2), 166-174.

Kartha, G.; Bello, J.; Harker, D. Tertiary structure of ribonuclease. *Nature.* **1967**, 213: 862-865.

Klibanov, A. M. Stabilization of enzymes against thermal inactivation. *Adv. Appl. Microbiol.* **1983,** *29:1-28.*

Kluger, R.; Alagic, A. Chemical cross-linking and protein-protein interactions - a review with illustrative protocols. *Bioorg. Chem.* **2004,** *32* (6), 451-472.

Lee, F. S.; Vallee, B. L. Binding of placental ribonuclease inhibitor to the active site of angiogenin. *Biochemistry* **1989,** *28* (8), 3556-3561.

Leland, P. A.; Staniszewski, K. E.; Kim, B. M.; Raines, R. T. Endowing human pancreatic ribonuclease with toxicity for cancer cells. *J. Biol. Chem.* **2001,** *276* (46), 43095-43102.

Liu, Y.; Hart, P. J.; Schlunegger, M. P.; Eisenberg, D. The crystal structure of a 3D domain-swapped dimer of RNase A at a 2.1-A resolution. *Proc. Natl. Acad. Sci. U. S. A* **1998,** *95* (7), 3437-3442.

Liu, Y.; Gotte, G.; Libonati, M.; Eisenberg, D. A domain-swapped RNase A dimer with implications for amyloid formation. *Nat. Struct. Biol.* **2001,** *8* (3), 211-214.

Matousek, J.; Soucek, J.; Slavik, T.; Tomanek, M.; Lee, J. E.; Raines, R. T. Comprehensive comparison of the cytotoxic activities of onconase and bovine seminal ribonuclease. *Comp Biochem. Physiol C. Toxicol. Pharmacol.* **2003a,** *136* (4), 343-356.

Matousek, J.; Gotte, G.; Pouckova, P.; Soucek, J.; Slavik, T.; Vottariello, F.; Libonati, M. Antitumor activity and other biological actions of oligomers of ribonuclease A. *J. Biol. Chem.* **2003b,** *278* (26), 23817-23822.

Molin, S. O.; Nygren, H.; Dolonius, L. A new method for the study of glutaraldehyde-induced crosslinking properties in proteins with special reference to the reaction with amino groups. *J. Histochem. Cytochem.* **1978,** *26* (5), 412-414.

Olde Damink, L. H.; Dijkstra, P. J.; Van Luyn, M. J.; Van Wachem, P. B.; Nieuwenhuis, P.; Feijen, J. Influence of ethylene oxide gas treatment on the in vitro degradation behavior of dermal sheep collagen. *J. Biomed. Mater. Res.* **1995,** *29* (2), 149-155.

Park, C.; Raines, R. T. Dimer formation by a "monomeric" protein. *Protein Sci.* **2000,** *9* (10), 2026-2033.

Pierce Chemical Library, Cross-linking reagents, Pierce Biotechnology, **2005**.

Potts, J. T.; Berger, A.; Cooke, J.; and Anfinsen, C. B. The sequencing of bovine pancreatic ribonuclease A. *J. Biol. Chem.* **1962,** *237:1851-1855.*

Smyth, D. G.; Stein, W. H.; Moore, S. The sequence of amino acid residues in bovine pancreatic ribonuclease: revisions and confirmations. *J. Biol. Chem.* **1963,** *238:227-34.*

Sorrentino, S.; Barone, R.; Bucci, E.; Gotte, G.; Russo, N.; Libonati, M.; D'Alessio, G. The two dimeric forms of RNase A. *FEBS Lett.* **2000,** *466* (1), 35-39.

Taralp, A.; Kaplan, H. Chemical modification of lyophilized proteins in nonaqueous environments. *J. Protein Chem.* **1997,** *16* (3), 183-193.

Zaks, A.; Klibanov, A. M. Enzymatic catalysis in organic media at 100 degrees C. *Science* **1984,** *224* (4654), 1249-1251.

Chapter 2: *In Vacuo* Cross-linking, Mechanism and Methodology

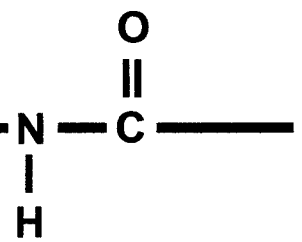

2.1 Introduction

2.1.1 Protein cross-linking

There are many research-based, industrial, and medical incentives to cross-link proteins. Perhaps one of the most common reasons for generating inter or intramolecular cross-links between interacting residues is to investigate protein-protein interactions (Fancy 2001; Phizicky and Fields 1995; Lundblad 1994, pp. 249-257). Many proteins function biologically by interacting with other proteins or as members of multi protein complexes, and the interfaces that are created between interacting proteins can display large ranges of motion and can be stabilized to various degrees by non-covalent forces that can be difficult to identify by physical means. However, cross-linking chemically across these sites of interaction can provide information on: (1) the nature of the interaction (i.e. electrostatic, hydrophobic, and Van der Waals forces); (2) the functionality of the residues involved; and (3) inter-atom distances in 3-dimensional structural arrangements, thus covalently capturing these dynamic interactions for physical examination. Identifying the sites of protein-protein interaction provides a basis for forming an integrated picture of the biological functions of proteins (Woltjer et al., 1992; Onishi and Fujinara, 1989; Carpenter and Harrington, 1972; and comprehensive reviews published by Kluger and Alagic, 2004; and Deisenhofer, 1989).

In 1987, White and Olsen demonstrated the utility of chemical cross-linking by coupling the subunits of hemoglobin, and covalently stabilizing the tetrameric quaternary structure attributed to the protein's enhanced ability for oxygen transport. They also were able to identify key contact sites between the two $\alpha\beta$ subunit interactions and proposed that this particular multimeric arrangement alters the proteins affinity to bind oxygen (White and Olson, 1987). Since then, many research groups have investigated cross-linked hemoglobin

tetramers because of their therapeutic potential as a blood substitute (Manning et. al, 1991, Jones et al, 1996; Chang, 1998; and it has been reviewed by Rudolph, 1994). Despite the success of solving the structural dynamics of hemoglobin in great detail, identifying protein-protein interactions in other protein complexes (such as ligand-receptor binding, assembly of holoenzymes, and proteins involved in catalytic cascades) by chemical cross-linking still remains a challenge with only a few published examples (Woltjer et al., 1992; Uy and Wold, 1977; Cornell, 1989; D'Souza et al., 1988; Rexin et al., 1988).

2.1.2 Cross-linking reagents

The reagent itself is a critical component of the cross-linking reaction and must be selected for its specificity; selection of a non-specific reagent can give rise to a large number of protein oligomerized products resulting in poor yields of the desired complex (Kluger et al., 2004; Uy and Wold, 1977). Glutaraldehyde (as discussed in Chapter 1) still remains the most widely used homobifuctional reagent for a large assortment of applications, ranging from the cross-linking of enzymes and antibodies to the chemical fixation of tissues, and the chemical inactivation of bacterial therapeutic products (Olde Damink et al., 1995). Homobifuctional reagents are used when the same type of functional group is the target on both entities to be cross-linked. Bis(imido) esters, another commonly used homobifunctional reagent, also couples proteins through primary amine groups, as shown below in Figure 2.1.1. Although the reagent is highly reactive and the coupling is efficient and technically undemanding, homobifunctional reagents, like imido esters and glutaraldehyde, tend to produce irregular products and high molecular weight aggregates (Baumert and Fasold,

1989), making them unsuitable for reproducibly preparing homogeneous links between two molecules.

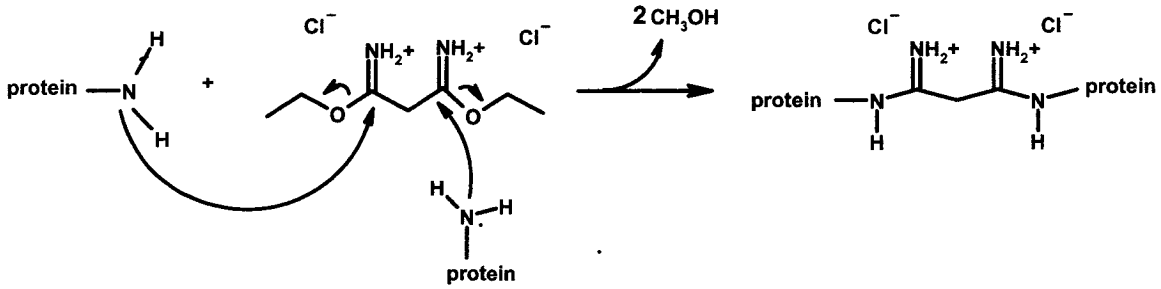

Figure 2.1.1 The reaction of a homobifunctional imidoester with primary amine groups (Lundblad, 1994).

Alternatively, heterobifunctional reagents can be used to identify two sites of different functionality that are either directly involved in or spatially close to the site of interaction between two proteins. While the types of functional groups that can be cross-linked using heterobifunctional reagents is varied, direct cross-linking between an amino group of one protein molecule and a sulfhydryl group on a second molecule is quite common. For instance, succinimidyl *trans*-4-(maleimidylmethyl)cyclohexane-1-carboxylate (SMCC) is a popular reagent for coupling antibodies to other proteins (Yoshitake et al. 1979; Nakagami et al., 1991) because of the chemical stability of the maleimide and its ease of use. In the first step of the reaction (refer to Figure 2.1.2), the protein's free amino groups are reacted with the maleimide to form the activated SMCC protein derivative, a reaction

performed at pH 9. Then, after washing of all unreacted reagent, the antibody, which is rich in sulfhydryl groups, is introduced and reacts to form a stable thioether link at pH ~7.

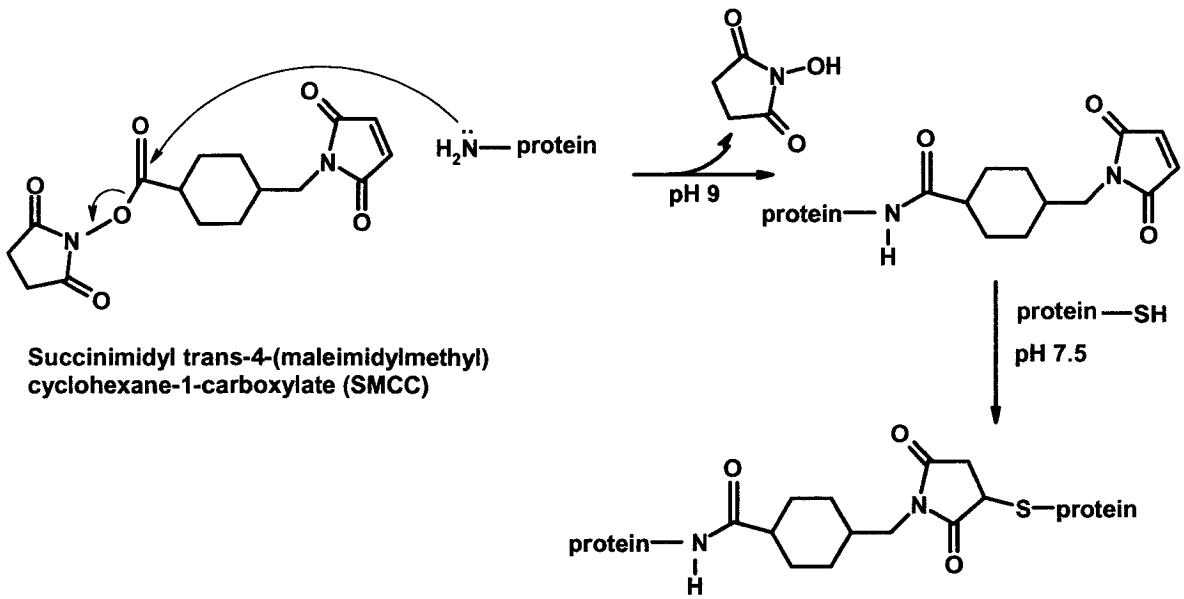

Succinimidyl trans-4-(maleimidylmethyl) cyclohexane-1-carboxylate (SMCC)

Figure 2.1.2 Two step reaction sequence for the cross-linking between amines and thiols using SMCC cross-linking reagent.

Like their homobifunctional counterparts, heterobifunctional reagents can also yield highly aggregated species (Kluger and Alagic, 2004). The extent of conjugation, however, can be more easily controlled by choosing stoichiometric amounts of the cross-linking reagent relative to the first targeted functionality, whereby activating one protein, then washing out excess reagent before introducing the second, with a different targeted functionality, in a stepwise fashion.

In addition to the aforementioned drawbacks of bifunctional mediated cross-linking, it is difficult to control the extent of derivitization of the protein, as it can be expected that several residues can exhibit equal reactivity towards the reagent and multiple residues will be activated for linking. Often large amounts of protein are required to efficiently perform these reactions as partial activation and incomplete reactions at some sites may lead to an alteration in the protein's functionality (Molin et al., 1978). Thus, at the end of the cross-linking process, the reacted protein may be able to function similarly to the native protein – or it may not. Similarly, the reagent itself or the link it introduces may induce electrostatic or hydrophobic interactions, causing sites to react with each other that would normally not associate, perhaps giving false or deceptive results (Kluger and Alagic, 2004). Furthermore, even when a controlled amount of reagent is used, no two sets of proteins will react in the exact same manner, making it difficult to apply a single cross-linking procedure to a variety of different proteins.

2.1.3 Zero-length cross-linking

Zero-length cross-linking, in which peptide chains are covalently linked through existing functional groups without the incorporation of a spacer group, has been extensively used to immobilize proteins on non-protein matrices. This is usually accomplished by activation of carboxyl groups on a protein with a water soluble carbodiimide, typically 1-ethyl-3-(3-dimethylaminopropyl) carbodiimide (EDC), followed by coupling with an amino group on the support to form a stable amide bond (Gratzer and Lee, 2001; Lundblad, 1994). Such cross-links between interacting proteins have been obtained by reaction with carbodiimide among the proteins in the multi-protein electron transport system (Mauk and

Mauk, 1989), but there are very few other reported cases where such zero-length cross-links have been achieved and protein-protein interactions elucidated in multimeric protein complexes. Zero-length cross-linking can therefore provide information about local protein-protein interactions and has the advantage that no foreign linking group is introduced into the protein.

2.1.4 Protein modification *in vacuo*

A novel, non-aqueous, technique of chemically modifying protein has been developed by the Kaplan research group. Functional groups of proteins can be derivitized in the lyophilized state by subjecting the sample to reduced pressures and increased temperatures in the presence of a modifying reagent. The esterification of carboxyl groups of lyophilized proteins in this manner has been shown (Vakos et al., 2001) through the exposure of a lyophilized sample in a sealed tube under vacuum in the presence of gaseous methanol or ethanol and HCl for catalysis. Similarly, modification of amino groups was also achieved by Taralp and Kaplan (1997) who described the increased reactivity of primary amines towards iodomethane *in vacuo* compared to the amino alkylation reaction performed under aqueous conditions (Means and Feeney, 1971). Both the *in vacuo* methylation and reductive methylation reactions are shown in Figure 2.1.3. This work also revealed that the *in vacuo* method of methylation yielded a stable quaternary trimethylated lysine and amino terminus in reactions containing freeze-dried proteins from solutions of high pH. The work was further extended by Stewart et al., (2002) who showed that trimethylated peptides were detected with greater sensitivity than unmodified lysines in MALDI mass spectrometry, most likely as a result of the permanency of the positive charge of the quaternary amine.

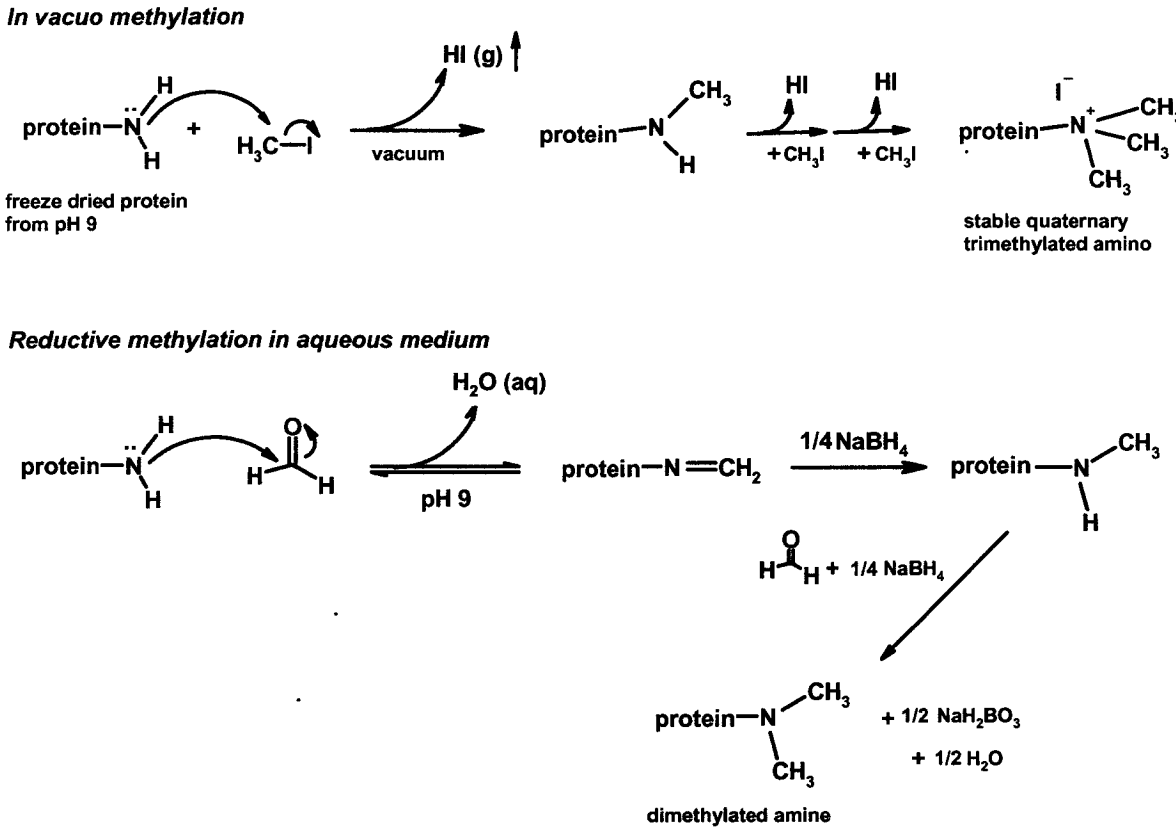

Figure 2.1.3. Methylation of ε-amino groups of lysine residues by *in vacuo* method (Taralp and Kaplan, 1997; Stewart et al., 2002) and reductive methylation (Means and Feeney, 1971 pp. 130-131)

In vacuo modification of protein has several apparent advantages over reaction in aqueous solution: (1) the non-aqueous mediums allow for the use of reagents normally insoluble in water; (2) the procedure can be scaled up or scaled down to any amount; (3) all volatile products are drawn out by the vacuum, shifting the equilibrium and favouring the products over reactants, thus increasing yields; and (4) the method is straightforward and is easily controlled by simply lyophilizing out from a solution of the desired pH.

Previous work by Klibanov (1983) and then further elaborated upon by Wang et al., (2002) and Carpenter et al. (1992) demonstrated that proteins, once freeze-dried, show remarkable stability, both thermal and chemical, presumably because any water-mediated degradation pathways are minimized. This ability of lyophilized protein samples to withstand high temperatures allows sample heating to levels unsuitable for solution protein chemistry, further driving the reaction and increasing product yields. Moreover, for many proteins, native structure is retained in the dried state and upon subsequent reconstitution, and, in the case of enzymes, catalytic activity is retained (Zaks and Klibanov, 1984). This property, coupled with the added stabilization of protein structure conferred by lyophilization, makes the *in vacuo* method less destructive and a more efficient way to chemically modify proteins.

2.1.5 Experimental premise

Observations from previous published work (Vakos et al., 2001; Taralp and Kaplan, 1997; King, Ph.D. thesis, 2004) shows that proteins, lyophilized under certain conditions, have nucleophilic groups that can attack electrophiles *in vacuo*. Such a reaction could be exploited and applied to the cross-linking of proteins. Initially, King and co-workers (Ph.D. thesis, 2003) demonstrated that lyophilized proteins can be covalently cross-linked using an activating reagent, *p*-nitrophenylchloroformate (*p*-NPCF). The particular reactivity of this reagent was initially predicted from its behaviour in solution chemistry, as shown in Figure 2.1.4, where *p*-NPCF reacts with the protein by transforming amino and carboxyl groups into electrophilic sites with good leaving groups. This makes them susceptible to nucleophilic attack from a second molecule bearing a nucleophile, creating a covalent cross-link between two molecules.

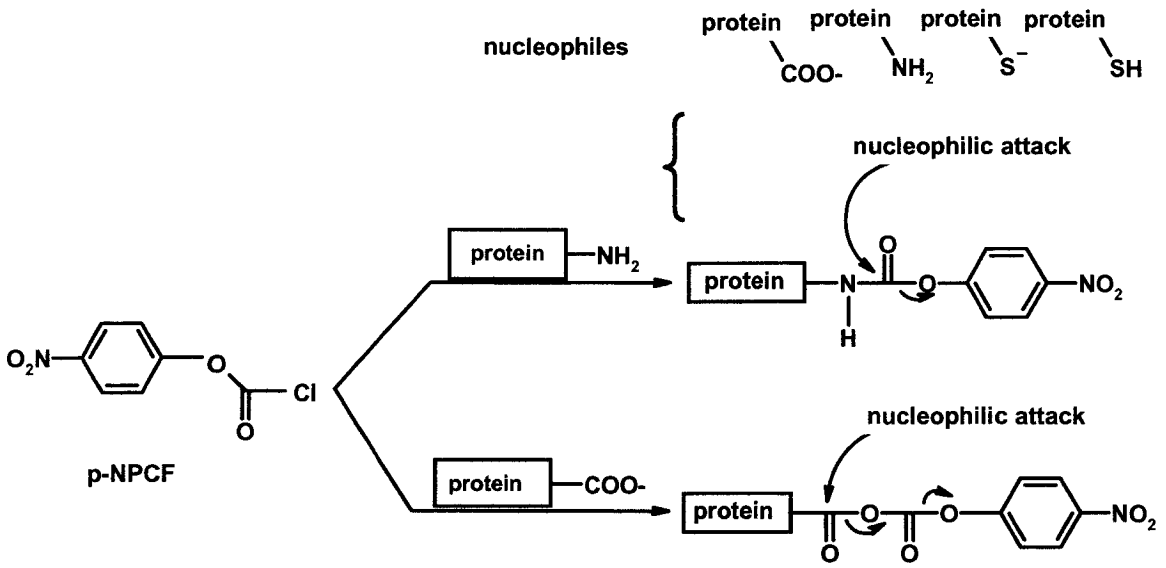

Figure 2.1.4 Reaction to create *p*-NPCF activated species through amino and carboxyl functionalities (King Ph.D. Thesis, 2003).

Using RNase A as a model protein, King and co-workers lyophilized samples from solutions at pH 7 and treated them *in vacuo* with *p*-NPCF. Cross-linked oligomers of RNase A were obtained upon addition of unmodified RNase A in solution. However, it was also observed, that in the control samples (where the protein was simply lyophilized and treated under vacuum without the presence of *p*-NPCF), a small amount of protein consistent with the formation of a covalent dimer was apparent when samples were analyzed by SDS gel electrophoresis. To further investigate this unexpected result, several SDS-PAGE and Western Blot assays of various proteins that had been lyophilized for storage purposes and then reconstituted were reviewed. Particularly of interest is the observation that denaturing

and reducing gels of lyophilized samples of milk bundle protein (MW = 11 kDa) and human growth hormone (MW = 22 kDa) probed using sensitive detection methods often show small amounts of material corresponding to twice the molecular weight of the expected mass of the monomeric protein. (Examples are shown in Figure 2.1.5).

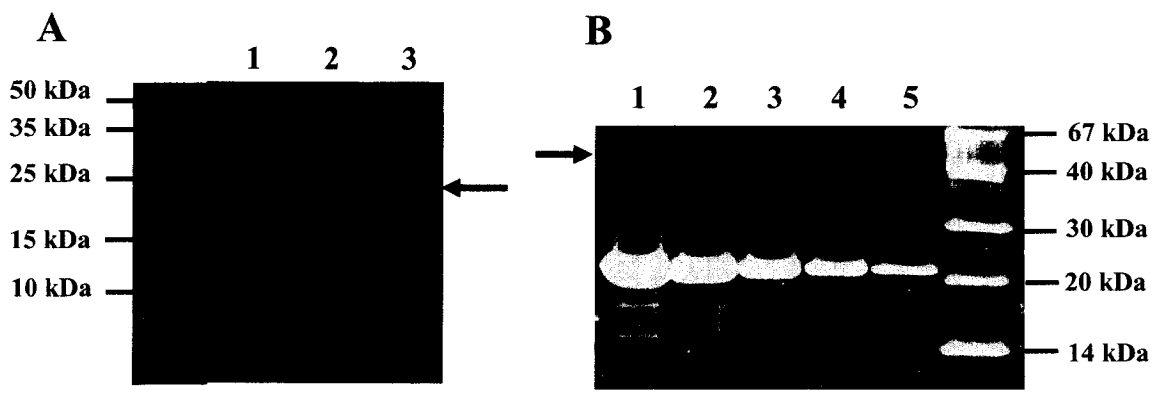

Figure 2.1.5 Western Blot of milk bundle proteins (A) and Sypro® Ruby Red stained 12 % gel of human Growth Hormone (B) to show the appearance of a band at twice the molecular weight of the monomeric band, presumably representing the dimer in each lyophilized sample. (A) Lane 1: 1 µg of MB-1 after lyophilization and reconstitution, lane 2: 5 µg of MB-13/16 after lyophilization and reconstitution, lane 3: 100 ng MB-1, no lyophilization. (B) Lyophilized preparation of human growth hormone loaded onto 12 % gel in amounts of 20 µg (lane 1), 10 µg (lane 2), 5 µg (lane 3), 1 µg (lane 4), and 0.5 µg (lane 5).

These observations raised the possibility that interacting functional groups found on proteins might react *in vacuo* in the absence of activating reagents to form covalently cross-linked protein dimers. Perhaps nucleophilic substitution reactions are possible between nucleophilic groups on one molecule and electrophilic groups on an adjacent molecule reacting in the dried state. It was then hypothesized that the vacuum may be promoting a

condensation reaction between functional groups in the lyophilized protein, by removing water (the product of a condensation reaction). Furthermore, such a reaction should be further promoted by heating. This chapter describes the results obtained in the testing of the hypothesis that proteins, lyophilized under various conditions, can be covalently cross-linked by simply heating lyophilized samples under vacuum.

2.2 Materials and Methods

Bovine pancreatic ribonuclease A (Type I-A), lysozyme, and D(+)-trehalose were purchased from Sigma-Aldrich (Oakville, ON, CAN). All other chemicals, reagents and solvents were high purity preparations obtained from the indicated commercial sources.

2.2.1 In vacuo *cross-linking procedure*

Lyophilized RNase A was obtained from Sigma-Aldrich, reconstituted in dH_2O to a concentration of 10 mg/mL, and the pH of the solution was adjusted to 7.0 with 1 N NaOH. The protein solution was placed in glass tubes and lyophilized. These glass tubes were sealed under a vacuum of approximately 50 mTorr and then placed in an oven at 85°C for 24 hours. The vacuum was released and the protein sample reconstituted with 0.2 M Na_2HPO_4 and 0.15 M NaCl at pH 6.55 to give a final protein concentration of 10 mg/mL.

In some cases, the protein was reconstituted in dH_2O instead of buffer to a concentration of 10 mg/mL, an aliquot was removed, and then the solution was re-lyophilized and heated again under vacuum at 85°C for an additional 24 hours. After four successive cycles of lyophilization, heating, and reconstitution, the final lyophilized protein

sample was reconstituted with 0.2 M Na_2HPO_4 and 0.15 M NaCl at pH 6.55 to give a final protein concentration of 10mg/mL.

2.2.2 The effect of pH, counter ions, or excipients

Protein solutions (10 mg/mL) at pH values varying from 3.0 to 10.0 were prepared by the addition of 1 N NaOH or 1 N HCl with a micro-syringe, as required. The protein solutions were lyophilized and subjected to the *in vacuo* cross-linking procedure.

Protein solutions (10 mg/mL) were also prepared in the presence of different cations by the addition of excess LiCl, NaCl or CsCl followed by dialysis against dH_2O with a 3500 MWCO membrane. Samples were treated as described above except that the pH was adjusted to 7.0 with 1 N LiOH, 1 N NaOH, or 1 N CsOH, as appropriate.

A solution of RNase A (10 mg/mL at pH 7.0) was lyophilized in the presence of D-trehalose at w/w ratios of protein/trehalose of 5:1, 1:1, and 1:5 and then subjected to the *in vacuo* cross-linking procedure. On reconstitution, the excess trehalose was removed by dialysis.

2.2.3 Heterogeneous cross-linking in vacuo

A solution containing RNase A and lysozyme in equal amounts (10 mg/mL) was prepared and the pH was adjusted to 7.0 with 1 N NaOH before lyophilization. The *in vacuo* procedure was carried out on the mixture of these two proteins as previously described.

2.2.4 Detection and quantification of cross-linked protein

Cross-linked products were detected by SDS-PAGE, using the Mini-PROTEAN II electrophoretic cell (BioRad Laboratories, Mississauga, ON, CAN). Protein (5-20 μg) was loaded onto a 16.5% Tricine SDS- PAGE (Schagger and von Jagow, 1987). After electrophoresis at 130 V for 90 min, the gel was stained with Coomassie Brilliant Blue G250. The relative amount of protein present in each band was determined using the pixel counting application in ImageQuaNT 5.1 (Amersham Biosciences (Molecular Dynamics), Baie d'Urfée, PQ, CAN).

Size exclusion chromatography was carried out using two Superdex 75 HR 10/30 columns (Amersham Biosciences) attached, in tandem, to a Pharmacia FPLC system with detection at 210 nm. The mobile phase (0.2 M Na_2HPO_4 and 0.15 M NaCl at pH 6.55 at 4°C) was used at a flow rate of 0.05 mL/min. In general, 0.5 mL fractions were collected. Molecular weight standards (phosphorylase b, 94 kDa; bovine serum albumin, 67 kDa; ovalbumin, 43 kDa; bovine erythrocytes carbonic anhydrase, 29 kDa; trypsin inhibitor, 20.1 kDa; α-lactalbumin, 14.4 kDa) used in column calibration were purchased from Amersham Biosciences. Pooled fractions containing RNase A dimer were concentrated to 0.5 mL using Amicon Ultra® 5 kDa centrifugal filtering devices (Millipore, Nepean, ON, CAN).

2.2.5 RNase A in-gel activity assay

Cross-linked RNase A products were tested for catalytic activity using an RNA agarose gel-based assay (Leland *et al.*, 1998; Gaur *et al.*, 2001). Cross-linked RNase A products (2 ng) were incubated with 5 μg of total rat liver RNA in 100 mM Tris-HCl, pH 7.5, containing 10 mM dithiolthreitol (DTT) in a total reaction volume of 10 μL. The

reaction was allowed to proceed for 10 min at 37°C and was stopped by the addition of 1 µL of diethyl pyrocarbonate and followed by incubation on ice for 2 min. Samples were supplemented with 2 µL of gel loading buffer (10 mM Tris-HCl, pH 7.5, 50 mM EDTA, glycerol (30% v/v), xylene cyanol FF (0.25% w/v), and bromophenol blue (0.25% w/v)) before loading onto 1.5% agarose gel containing 2% formaldehyde and 0.05 M ethidium bromide.

2.2.6 Chemical modification of amino and carboxylic acid groups

Dimethylation of amino groups was carried out on RNase A according to the procedure described by Means and Feeney (1971). In brief, in a 0.2 M sodium borate buffer at pH 9.0, amino groups are reacted with formalydehyde followed by a reduction of the resulting Schiff base with sodium borohydride. Samples of RNase A at a concentration of 15 mg/mL, in a total reaction volume of 5 mL, were placed in an ice bath and 0.3 M $NaBH_4$ was added and stirred. Aliquots of 12.5 µL of formaldehyde (37 wt % solution in water) were added incrementally to the sample over a period of 30 minutes. The samples were then transferred to a 3500 MW cutoff dialysis membrane and excess reagent was removed through 4 changes of 1 L dH_2O over 24 hours.

Amidation of carboxyl groups was carried out in a solution of RNase A (15 mg/mL in a total reaction volume of 2 mL) in 1.33 M glycinamide at pH 4.75 with activation by carbodiimide as describe in Means and Feeney (1971). In brief, samples of RNase A (15 mg/mL) were prepared in 1.33 M glycinamide and pH was adjusted to 4.75 with 2 N NaOH. Aliquots of 0.5 mL of a 0.4 M solution 1-ethyl-3-(3-dimethylaminopropyl)-carbodiimide (EDAC) were added at time 0 minutes and at time 15 minutes, and the reaction was allowed

to proceed for a total of 30 minutes at room temperature. After 30 minutes, the samples were transferred to a 3,500 MW cut-off dialysis membrane and the samples were dialyzed against 1 mM HCl for 4 changes of 1 L dH_2O over 24 hours at 4°C.

2.2.7 Mass Spectrometric Analysis

The nanospray mass spectrum was obtained using a Micromass™ Q-TOF mass spectrometer (Waters, Mississauga, ON, CAN). The RNase A sample was prepared for analysis by standard ZipTip® (Millipore, Nepean, ON, CAN) methodology which includes a 10 µL pipette tip with a micro-volume bed of C_{18} reverse phase chromatography media fixed at its end. Protein is bound to the resin once equilibrated with 0.1 % TFA. Analytes were eluted with 75% methanol/ 25% water/ 0.2% formic acid, the sample was centrifuged (6000 rpm for 2 minutes) and then 2 µL was loaded into a gold coated nanospray PicoTip® (New Objectives, Wobrun, MA, USA). The MS data was deconvoluted using MaxEnt1™ software (MassLynx™, Waters, Mississauga, ON, CAN) to provide the singly charged average masses. The key variable MS voltages include: capillary (+950 V), cone (+47 V), and RF lens 1.05. The source temperature was 80°C, and the data for each scan was collected for 5 seconds over the range of 400 to 2500 Da, using a NaTFA solution for external calibration.

2.3 Results and Discussion

2.3.1 *In vacuo* cross-linking of RNase A and lysozyme

RNase A was chosen as a model protein to investigate the *in vacuo* cross-linking of proteins because of the abundance of literature reporting structure-function relationships and the chemical modification of this protein has been extensively investigated by colleagues in the Kaplan research group. Figure 2.3.1 shows the products found when RNase A, lyophilized at pH 7, is cycled through successive 24 hour heating periods at 85°C under vacuum, re-dissolved, then re-lyophilized after each of a total of four heating periods. A strong band with an apparent molecular mass of ca. 28 kDa, expected for the dimer, becomes evident after only one heating period of 24 hours *in vacuo,* and intensifies somewhat as the heating time increases to 96 hours. Weaker bands corresponding to the expected masses of RNase A trimers (~42 kDa) and tetramers (~56 kDa) are also clearly visible. These results indicate that covalent cross-linking of proteins can be achieved in the absence of chemical reagents merely by heating a lyophilized protein *in vacuo.* It is also apparent that the extent of this cross-linking increases with time, at least initially. Samples that had cycled through re-lyophilization before each heating trial show no increase in dimer formation compared to those kept continuously heating under vacuum for an equal length of time (Lane 7, Figure 2.3.1). Maximum dimer formation was obtained after 96 hours of heating *in vacuo (*data not shown). A band with a slightly higher apparent molecular mass than monomeric RNase A is also evident and is due to the RNase B impurity (glycosylated form of RNase A) present in the preparation (as per product description, Sigma-Aldrich, product number R4875). For the purposes of this study, it was judged unnecessary to further purify RNase A; therefore, the RNase B impurity is apparent in all gels in this thesis.

The cross-linked products of RNase A, detected by gel electrophoresis, must be covalently bonded and not the result of inter-disulfide bond scrambling. All gels were run under the denaturing conditions of SDS (to disrupt any non-covalent interactions between monomers) and reducing conditions of β-mercaptoethanol (to reduce any disulphide bonds between monomeric units). Therefore, the proteins that migrated to the positions consistent with higher oligomers than the expected monomer must be covalently bonded.

Given the efficiency of the *in vacuo* methodology in covalently cross-linking RNase A molecules, the next step was to test the universality of the method. A number of well-characterized proteins with chemical properties different from those of RNaseA were chosen in order to rule out the possibility that it was some unique property of the latter molecule that allowed such ready reaction to form the covalent dimers and higher oligomers observed. Very similar results were obtained with lysozyme (Figure 2.3.2), a protein with no intra-molecular disulfide bonds. Again, the dimer is the major product and a smaller amount of higher oligomer is formed. Lyophilized bovine serum albumin, hemoglobin, human growth hormone, MB-1 protein (Beauregard et al. 1995), and chymotrypsin treated under the same conditions all showed covalent dimer formation to approximately the same extent (data not shown). The *in vacuo* method of cross-linking thus appears to be general in its applicability.

It is interesting to note that even in the untreated, control samples that were not heated under vacuum, some dimeric RNase A and dimeric lysozyme is apparent (Figure 2.3.1, lane 2 and Figure 2.3.2, lane 2). In these experiments, the SDS-PAGE loading was very concentrated, in most cases 20 µg of protein per lane and, while the proteins in these samples had not been lyophilized in the course of this experiment, they were all proteins that had been reconstituted from the manufacturer's lyophilized preparations. While it is unlikely

that the normal preparation of dried protein samples would include the heating to high temperatures used in the *in vacuo* procedure described here, it would very likely involve exposure to similar vacuum conditions during the lyophilization. In fact, these results would predict that most lyophilized protein preparations would contain a small amount of covalent dimer, which could be detected either at high loadings on SDS gels or by the use of highly sensitive detection methods such as Western Blots.

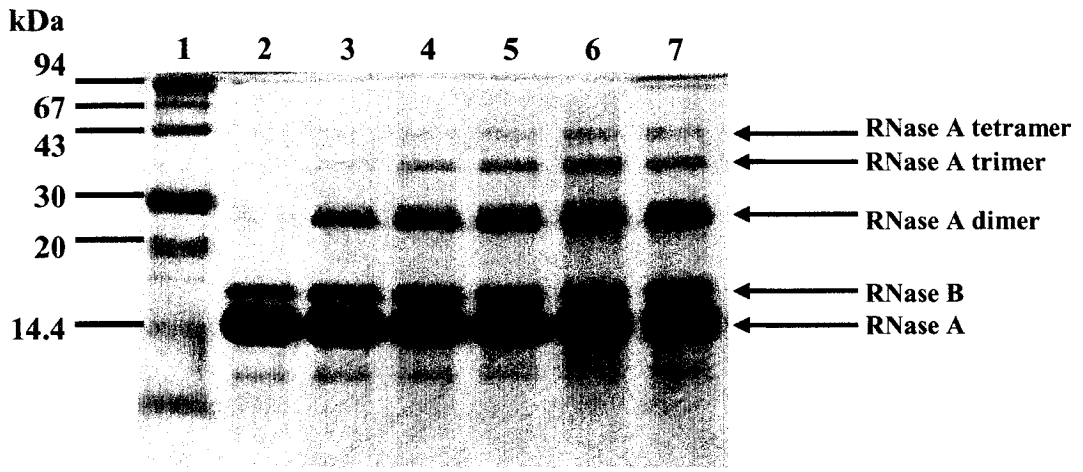

Figure 2.3.1 SDS-PAGE of successive cycles of solubilization of 10 mg of RNase A at pH 7.0, lyophilization, then heating *in vacuo* for 24 hours. Total protein load per lane is 20 μg. Lane 1: low range molecular weight marker; lane 2: lyophilized RNase A, no heating *in vacuo*; lane 3: Cycle 1; lane 4: Cycle 2; lane 5: Cycle 3; lane 6: Cycle 4; lane 7: lyophilized RNase A, heated continuously 96 hours *in vacuo* with only one reconstitution.

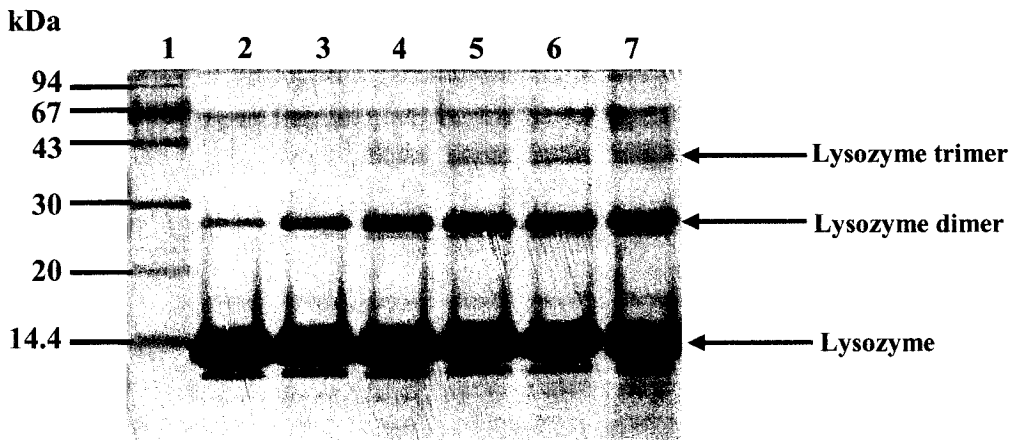

Figure 2.3.2 SDS-PAGE of successive cycles of solubilization of 10 mg of lysozyme at pH 7.0, lyophilization then heating *in vacuo* for 24 hours. Total protein load per lane is 20 μg. Lane 1: low range molecular weight marker; lane 2: lyophilized lysozyme, no heating *in vacuo*; lane 3: Cycle 1; lane 4: Cycle 2; lane 5: Cycle 3; lane 6: Cycle 4; lane 7: lyophilized lysozyme, heated continuously 96 hours *in vacuo* with only one reconstitution.

To quantify the amount of covalent RNase A dimer produced, a photograph of the gel shown in Figure 2.3.1 was imported into the pixel counting application ImageQuaNT™ 5.1 and the amount of dimer was estimated based on pixel density. RNase A dimer yields varied from 20 to 30% of the total treated protein, depending on the length of the heating period. In addition to pixel counting, quantification was also accomplished by separating the reaction products by size exclusion chromatography (Figure 2.3.3) and integrating areas under the resulting peaks. The size exclusion column was calibrated against six protein standards: phosphorylase b, 94 kDa; bovine serum albumin, 67 kDa; ovalbumin, 43 kDa; bovine erythrocytes carbonic anhydrase, 29 kDa; trypsin inhibitor, 20.1 kDa; and α-lactalbumin, 14.4 kDa. The elution profile of the RNase A heated *in vacuo* for 96 hours (Figure 2.3.3B) has peaks consistent with proteins of estimated molecular masses of $M_r \sim 28\,000$, and $M_r \sim 14\,000$, corresponding to the RNase A dimer and monomer, respectively. The dimer represented approximately 30% of the total protein, in agreement with the estimate by pixel counting of the gel photographs.

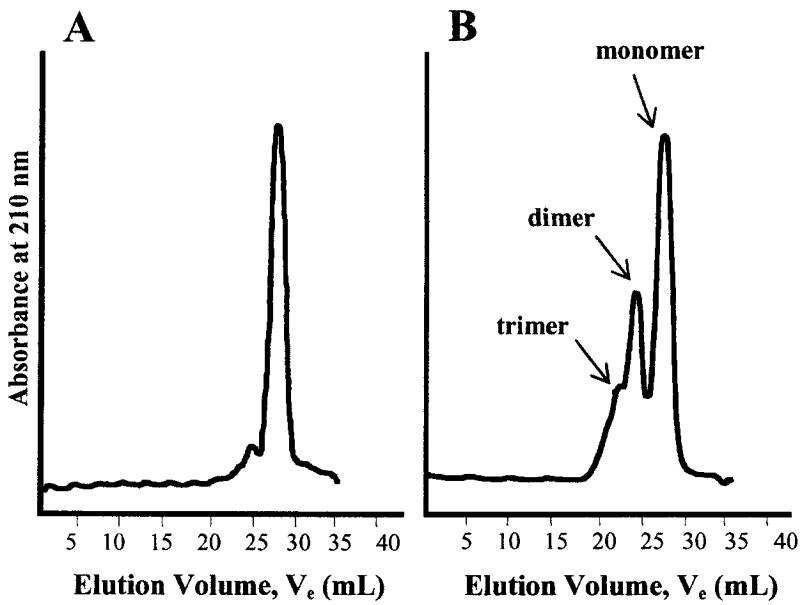

Figure 2.3.3 Size exclusion FPLC of *in vacuo* cross-linked RNase A. Separation of RNase A cross-linked products achieved with two Superdex G75 HR 10/30 G75 columns in tandem using a mobile phase of 0.2 M Na_2HPO_4 and 0.15 M NaCl at pH 6.55 (A) RNase A lyophilized at pH 7.0, no cross-linking; (B) RNase A lyophilized at pH 7.0, then cross-linked *in vacuo*.

The *in vacuo* cross-linking of proteins has shown good efficiency in generating homodimers from homogenous protein samples and was shown to be consistently attainable with many different proteins. The method was then tested for its ability to generate heterodimers. The results obtained when equal amounts (w/w) of RNase A and lysozyme were co-lyophilized, and heated under vacuum, are shown in Figure 2.3.4. Three bands are visible, consistent with the formation of the cross-linked dimeric RNase A, cross-linked dimeric lysozyme and the heterogeneously cross-linked lysozyme/RNase product. A higher extent of cross-linking than that shown could be obtained using longer heating times,

however, the three cross-linked products could not be visualized as distinct bands on SDS-PAGE because of the high intensity of the resulting bands.

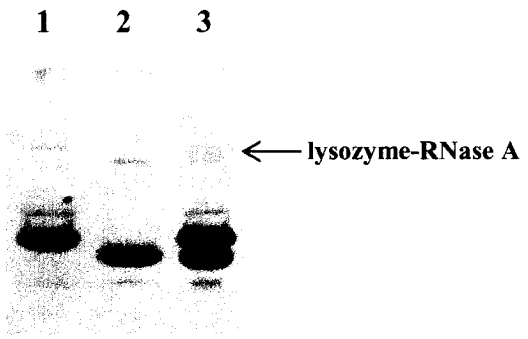

Figure 2.3.4 Heterogeneous cross-linking of RNase A and Lysozyme. RNase A (10 mg) was co-lyophilized with lysozyme (10 mg) at pH 7.0, heated under vacuum for 48 hours, and 15 μg of the treated protein was subjected to SDS-PAGE. Lane 1: RNase A (pH 7.0) alone cross-linked *in vacuo,* 48 hours; lane 2: lysozyme (pH 7.0) alone, cross-linked *in vacuo,* 48 hours; lane 3: RNase A (pH 7.0) and lysozyme (pH 7.0) co-lyophilized and cross-linked *in vacuo,* 48 hours. The lysozyme-RNase A cross-linked product is indicated by the arrow.

2.3.2 The effect of pH on the extent of cross-linking *in vacuo*

The extent of *in vacuo* cross-linking as a function of varying the pH of the lyophilized protein was determined. Due to the pH memory effect (discussed in Chapter 1) (Zaks and Klibanov, 1984), the ionization state of the individual functional groups of the protein in solution essentially gets "frozen-out", and is maintained while the protein is being lyophilized. This experiment was designed to assess the reactivity of possible nucleophilic and electrophilic groups at different pH whereby inducing different protonation states. RNase A solutions were prepared with pH values varying from 3.0 to 10.0. These solutions

were then lyophilized and heated under vacuum. After treatment, the samples were run on SDS-PAGE and stained with Coomassie Blue (Figure 2.3.5). The results show that neutral to slightly alkaline LpH (the pH of the solution before lyophilization) favor formation of dimer. Cross-linking appeared to be less efficient at LpH values below 6.0, with the least amount of dimer being formed at LpH values of 3 and 4. The dependency of efficiency in cross-linking on the pH of the solution before lyophilization implies the involvement of groups with ionizable functionality. Given that the cross-linking reaction appears to be promoted by vacuum, it is reasonable to suspect that it is a condensation reaction in which the loss of one of the reaction products by the vacuum (volatile water vapour) drives the reaction.

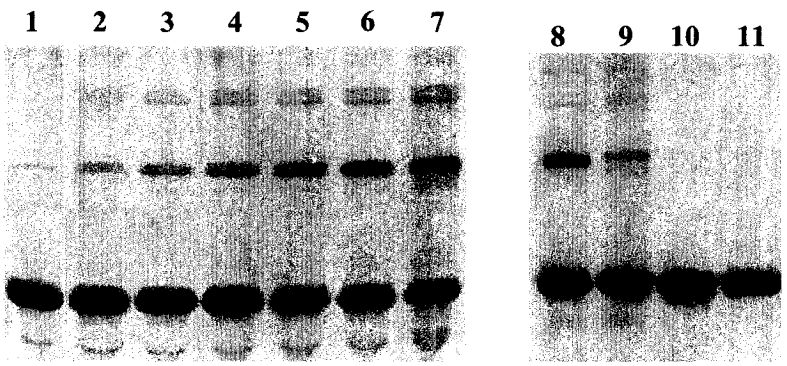

Figure 2.3.5 The effect of pH on the extent of RNase A dimerization. RNase A samples of 10 mg/mL were adjusted to pH values 3.0 to 10.0 with either 1.0 N NaOH or 1.0 N HCl, lyophilized, then cross-linked under vacuum. A 10 µg sample of the treated protein was subjected to SDS-PAGE. Lane 1: RNase A LpH 3; lane 2: RNase A LpH 4; lane 3: RNase A LpH 5; lane 4: RNase A LpH 6; lane 5: RNase A LpH 7; lane 6: RNase A LpH 8; lane 7: RNase A LpH 9; lane 8: RNase A LpH 10; lane 9: RNase A LpH 11; lane 10: RNase A LpH 12; lane 11: RNase A LpH 13. Gel is stained with Coomassie Blue.

2.3.3 Mass Spectrometry analysis of the RNase A *in vacuo* cross-linked dimer

To investigate the possibility of dimer formation through a condensation reaction, the RNase A *in vacuo* cross-linked mixture and the isolated dimer (isolated by size exclusion chromatography) were subjected to electrospray mass spectrometry (Figure 2.3.6 A and B). In the cross-linked mixture, only two major peaks are detected: one of 13682 mass units (m.u.) (which is the expected mass of monomeric RNase A) and the second of 27346 m.u. This latter peak is also the major peak in the spectrum, shown in Figure 2.3.6B, that is obtained when the isolated RNase A dimer was then injected separately. This peak of 27346 m.u. corresponds to twice the mass of the monomer (13682 ± 1 m.u.) minus 18 m.u., i.e. a mass that is expected for a dimer that has been formed through the loss of one water molecule. This evidence shows that a condensation reaction occurs exclusively to form the RNase A dimer and that there are no other modifications to the protein detected.

The RNase A dimer forms from a loss of only one molecule of water, indicating that there is only one link formed, and it is most likely a homogeneous link as more RNase A dimers with masses differing in multiples of 18 would have been detected. It should be also noted that there is a trace amount of a dimer peak at 27327 m.u., as shown in Figure 2.3.6B. This peak may result from the loss of two water molecules and the formation of two cross-links, or it may represent some internal dehydration reaction. Even so, it is detected in a low abundance relative to the singly linked dimer. There is another significant peak at 27361 m.u., and a minor peak at 27377 m.u., 16 and 32 m.u. above the major dimer peak, respectively. The mass spectrum of RNase monomer used to prepare the dimer also shows a component of 16 mass units greater than the monomer and is probably due to the presence of some methionine sulfoxide in the preparation. These two peaks, therefore, are probably due

to dimers formed by condensations of molecules of RNase A containing a residue of methionine sulfoxide.

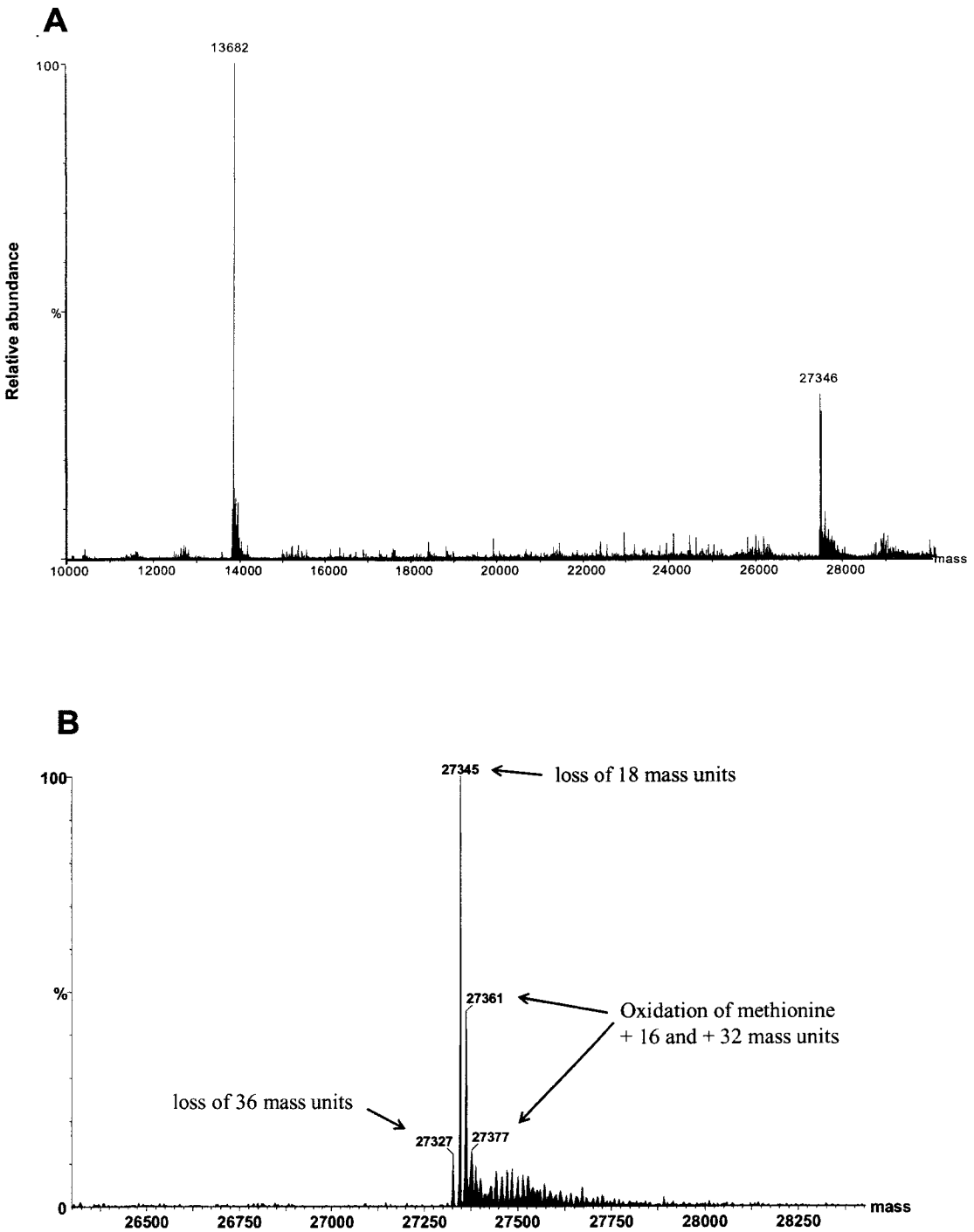

Figure 2.3.6 (A) Deconvoluted ESI-TOF mass spectrum of the RNase A cross-linked mixture containing monomeric RNase A (expected mass 13682 m.u.) and *in vacuo* cross-linked dimeric RNase A (expected mass 27346 m.u.). **(B)** Deconvoluted electrospray TOF mass spectrum of the isolated *in vacuo* cross-linked RNase A dimer.

2.3.4 Chemical modification of lysine and aspartic/glutamic acid residues

The components of the water lost during the condensation reaction are expected to come from the functional groups at the site of cross-linking, either at the N- or C-termini or on side chains of amino acids residues. Carboxylic acid groups, either at the C-terminus or on the side-chains of aspartic and glutamic acid appear likely candidates to participate in the release of a hydroxyl ion to the formation of water. The second hydrogen of the water molecule would be expected to come from the nucleophile. Several amino acids have side chains that are potential nucleophiles: (1) hydroxylate ion from tyrosine; (2) sulfide ion from cysteine; (3) sulfhydyl group for cysteine; (4) imidazole secondary amine of histidine; and (4) ε-amino of lysine. Cysteine residues are not considered to be the nucleophile in this mechanism due to previous results obtained demonstrating the detection of cross-linked products on reducing SDS gels, whereby reducing cysteine to the free thiol. Based on the evidence demonstrating optimal pH values of 7 to10 for the reaction, hydroxylates from tyrosine are expected to be mostly protonated in this pH range (pK_a of hydroxyl ~ 10.5) and not nucleophilic. By elimination, this leaves amino functionality as the most plausible nucleophilic reactant in the cross-linking mechanism, either originating from the N-terminus, the imidazole nitrogen of histidine, or the ε-amino group of lysine.

To verify the involvement of amino and carboxylic acid groups in the condensation reaction, two chemically modified RNase A samples were prepared. In the first the amino groups were dimethylated by reductive methylation; in the second, the carboxyl groups were modified by amidation with carbodiimide and glycinamide. Under conditions used in the reductive methylation, only the primary amine groups at the N-terminus or at the ε-position of the lysine side chain are expected to be modified. The imidazole of the histidine side

chain and the hydroxylate ion of tyrosine are unreactive under these conditions (Means and Feeny, 1971; Creighton, 1993) and RNase A contains no free sulfhydryl. Likewise, the conditions used for the glycinamide reaction result in exclusive modification of the carboxylic acid side chains (Means and Feeny, 1971; Creighton, 1993). Each modified protein was lyophilized individually and heated *in vacuo* under the same conditions as for the unmodified protein. An SDS-PAGE depicting the electrophoretic separation of the products of each of the *in vacuo* cross-linked samples, either chemically modified or un-modified are shown in Figure 2.3.7. When either the amino groups (Figure 2.3.7A, lane 3) or the carboxylic acid groups (Figure 2.3.7B, lane 1) are blocked, *in vacuo* cross-linking does not occur. This result confers the site of cross-linking exclusively to amino and carboxyl functionality.

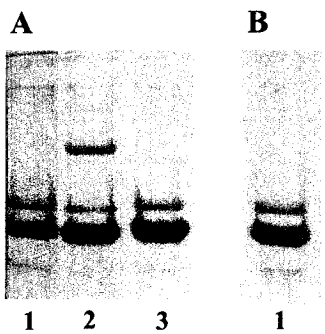

Figure 2.3.7 SDS-PAGE showing the effect of chemical modification of RNase A (15 mg/mL) on *in vacuo* cross-linking. Total protein loaded per lane is 10 μg. (A) Lane 1: RNase A lyophilized at pH 9.0 with no *in vacuo* treatment ; lane 2: RNase A lyophilized at pH 9.0 and heated *in vacuo*, 48 hours; lane 3: reductively methylated RNase A lyophilized at pH 9.0, and heated *in vacuo,* 48 hours. (B) Lane 1: RNase A with amidated carboxyl groups lyophilized at pH 7.0 and heated *in vacuo,* 48 hours.

Based on the chemical evidence indicating that the carboxylic acid group of glutamic or aspartic acid residues is the electrophile in the reaction, there are only three possibilities as to how such cross-linking can occur with the loss of a water molecule: (1) condensation of two protonated carboxylic acid groups to form an anhydride; (2) condensation of a protonated carboxylic with a hydroxyl group of a side chain (tyrosine residue) to form an ester; and (3) condensation of a deprotonated carboxylic acid group with an ammonium group to form an amide. For proteins lyophilized at neutral or slightly alkaline pH values, where optimal *in vacuo* cross-linking occurs (referring to Figure 2.3.5), the carboxylic acid groups are expected to be deprotonated and could not take part in anhydride or ester formation with the loss of a water molecule. Furthermore, covalent dimers formed by anhydrides or esters linkages would not survive the conditions for preparing and running SDS gels, *viz.* high temperatures in the presence of β-mercaptoethanol at an alkaline pH value. Therefore, the result of the mass spectroscopic analysis of the RNase A dimer combined with results obtained from the chemical blocking of amino and carboxylate functional groups provides evidence that the *in vacuo* cross-linking reaction occurs via amide bond formation.

2.3.5 The effect of excipients on *in vacuo* cross-linking efficiency

After it was determined that the *in vacuo* cross-linking reaction is a condensation reaction between amino and carboxyl functionalities, it was necessary to investigate the intermolecular interactions, in particular, salt bridging and hydrogen bonding, that would normally occur between molecules either in solution or in the subsequent lyophilization process. Proteins in aqueous solution are surrounded by water. It is this solvation shell that

separates the protein molecules, prevents them from interacting and thus keeps them soluble. The process of lyophilization removes most of the solvation shell excluding the tightly bound low activity water. As a result, the protein packs against itself and protein-protein interactions may replace those normally contributed by water. Excipients are often added to protein solutions before lyophilization and they can replace the solvent shell, separating molecules, and thereby stabilize the protein. Excipients can also stabilize protein structure by preferentially excluding themselves from the protein, such is the case with trehalose, and consequently increasing the concentration of low activity water bound to the proteins surface (Carpenter et al., 1992; Wang et al, 2002). This physical separation of individual protein molecules by the addition of trehalose in the sample will preclude any intermolecular interactions and may alter the efficiency of cross-linking. RNase A was therefore co-lyophilized with trehalose at different weight ratios, and then heated under vacuum. After treatment, the samples were run on SDS-PAGE and stained with Coomassie Blue (Figure 2.3.8). The results show that as the amount of trehalose present in the lyophilized sample increases, the amount of RNase A dimer produced decreases. At a 1:1 w/w ratio, trehalose appears to prevent any dimer formation, as only a trace of dimer similar to that observed in untreated samples is present. This result indicates that direct interaction of the protein molecules, under lyophilized conditions, is required for the *in vacuo* cross-linking reaction to occur.

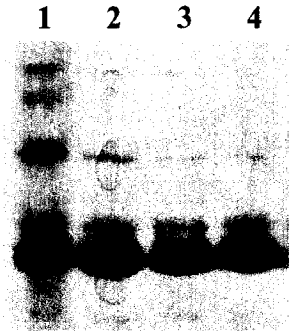

Figure 2.3.8 Cross-linking of RNase A in the presence of trehalose at pH 7.0. RNase A (10 mg) was co-lyophilized with different amounts of trehalose and heated under vacuum for 48 hours. A 20 μg sample of the treated protein was subjected to SDS-PAGE. Lane 1: RNase A alone cross-linked *in vacuo*. Lane 2: RNase A and trehalose in a 5:1 (w/w) ratio, cross-linked *in vacuo*. Lane 3: RNase A and trehalose in a 1:1 (w/w) ratio, cross-linked *in vacuo*. Lane 4: RNase A and trehalose in a 1:5 (w/w) ratio, cross-linked *in vacuo*.

2.3.6 The proposal of a mechanism for *in vacuo* cross-linking

Given the physical and chemical evidence presented thus far, it can be concluded that the *in vacuo* cross-linking is a condensation reaction that occurs between interacting amino and carboxyl functions to yield a zero-length amide bond. The pH dependency of this reaction, limited to a pH range between 7 and 10 for optimal cross-linking, specifies that the carboxyl group must be deprotonated, dictated by its typical pK_a value of 4.5. Also at this pH optimum, one would expect amino groups to be protonated ($pK_a \sim 10$). If this is correct, a positively charged protonated ammonium group reacts via a condensation reaction with a negatively charged, deprotonated carboxylate under vacuum.

The experiments testing the cross-linking method in the presence of excipients indicated that the amino and carboxyl groups must be interacting for the reaction to take place. Positively charged ammonium groups often interact with negatively charged

carboxylates in a salt bridge. Salt bridges play an important role in protein structure and function and are common structural features of enzymes to stabilize domains or motifs. Chymotrypsin, for example, contains a salt bridge between residues Asp_{187} and Lys_{163}, essential for inducing catalytic activity (Ferscht, 1972). Structural salt bridges, such as that observed in chymotrypsin, can be examined by protein X-ray crystallography, whereby the protein molecules are arranged into a highly ordered crystal, and X-ray diffraction information yields three-dimensional atomic arrangements of the amino acids (Anderson et al., 1990). Protein crystallization and protein lyophilization have an apparent similarity; in both cases, salt linkages between interacting molecules can be preserved if the proper pH is applied. The *in vacuo* mechanism of cross-linking presumably requires a strongly interacting ammonium and carboxylate, such as those interacting in a salt bridge, between protein monomers in a lyophilized state in order to initiate a reaction site and the formation of an amide link.

Figure 2.3.9 represents a possible mechanism for the formation of an amide linkage between strongly interacting ammonium and carboxylate groups in the lyophilized state, under vacuum. In the first step of this reaction, it is proposed that a proton transfer occurs from the protonated ammonium to the negative oxygen of the carboxylate. This H^+ transfer is the most critical step of the reaction, and it may be promoted by the strong interaction in the salt bridge, pulling the atoms together in close proximity and thus, facilitating the transfer of the proton. In the second step, the deprotonated amine group can now nucleophilically attack the carbonyl, pushing out the water as a leaving group. Despite the difficulty of the initial H^+ transfer and the fact that water is a poor leaving group, the water vapour produced, is drawn-out of the reaction by the vacuum. Le Châtelier's Principle states

"if a system in chemical equilibrium is altered in any way, the system will shift so as to minimize the effect of the change" (Masterston and Slowinski, 1969). In this particular reaction, the effect of the vacuum removing a volatile product, i.e. water, induces a shift in the equilibrium to the products side, favouring the condensation reaction, and the result is the formation of an amide bond.

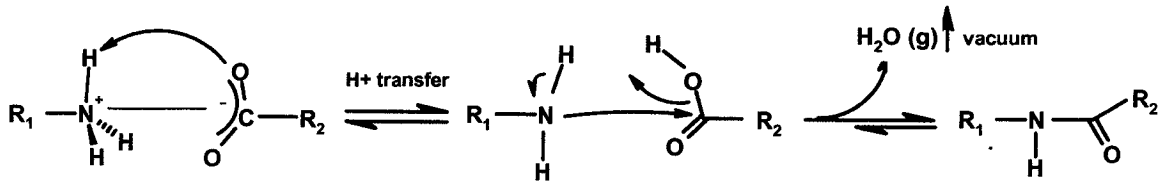

Figure 2.3.9 Proposed mechanism of amide bond formation by *in vacuo* cross-linking.

This mechanism for *in vacuo* cross-linking is supported by the mechanism for the decomposition of ammonium bicarbonate under vacuum (Figure 2.3.10). Most quaternary ammonium salts, such as ammonium bicarbonate, decompose via sublimation into volatile gases (Masterston and Slowinski, 1969). Ammonium bicarbonate, in solid form, will therefore, naturally decompose into ammonia, water, and carbon dioxide gases. If placed under vacuum, this reaction is further encouraged due to the evacuation of the gaseous products by the vacuum. Like the mechanism proposed for *in vacuo* cross-linking, this mechanism is also proposed to proceed via a proton transfer from the ammonium to the bicarbonate hydroxyl. Once the resulting carbonic acid is formed, H_2CO_3 breaks down into CO_2 and H_2O gas by either forming a 4 or 6 membered transition state complex with water

(as shown in Figure 2.3.10) (Loerting et al., 2000). Although the proposed mechanism of *in vacuo* cross-linking does not involve a decomposition, the evidence of ammonia, water, and carbon dioxide gas formed by the decomposition of ammonium bicarbonate is indicative of a proton transfer in the dry state, therefore, such a similar proton transfer mechanism is plausible for the reaction of *in vacuo* cross-linking.

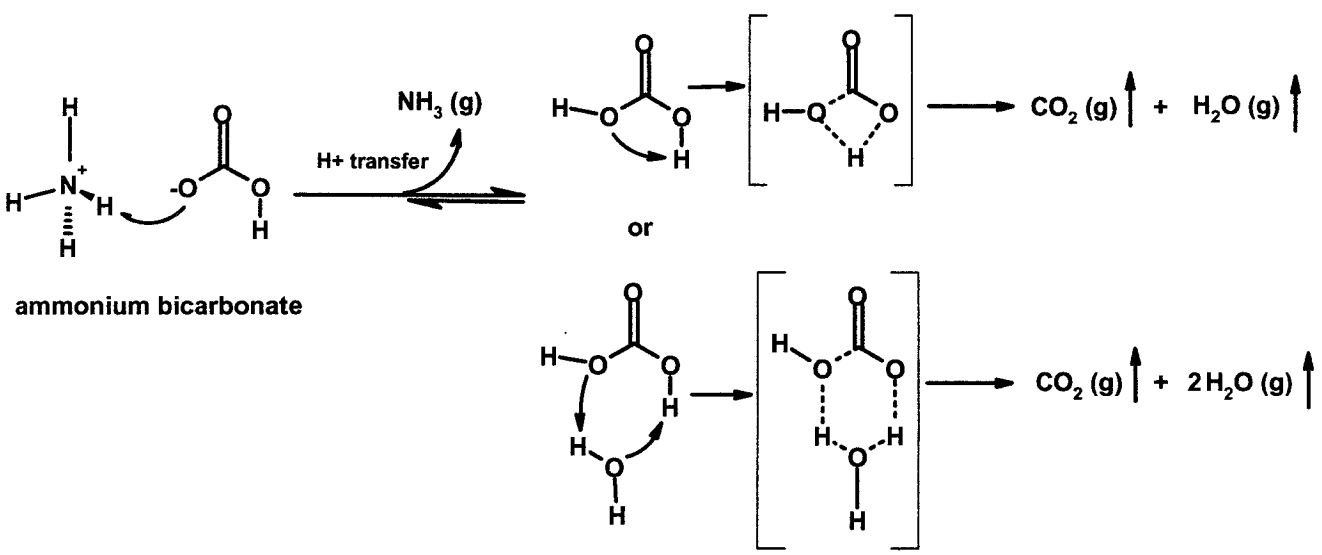

Figure 2.3.10 Proposed mechanism of the decomposition of ammonium bicarbonate *in vacuo* (Modified from Loerting et al., 2000).

2.3.7 The effect of counter-ions on the extent of *in vacuo* cross-linking

The yield of dimer obtained with RNase A was approximately 30%. A possible explanation for this apparent limit is the presence of counter-ions, especially Na^+, in association with carboxyl groups. This association could obstruct the salt bridge interaction between protein molecules and reduce the cross-linking efficiency. Therefore, the effect of

small and large cations present as counter-ions on the extent of cross-linking *in vacuo* was determined by addition of excess LiCl or CsCl followed by dialysis. The pH of the samples prior to lyophilization was adjusted with LiOH or CsOH. It was found that these counter-ions had no affect whatsoever on the extent of dimerization (data not shown). The reason why the yield in cross-linked dimer was limited to 30 % remains obscure, however, the presence and size of the counter-ions does not appear to be a factor.

2.3.8 Activity of cross-linked RNase A

In vacuo cross-linked proteins would be expected to retain their biological activity when returned to an aqueous environment, as this is the case for most lyophilized proteins (Carpenter, 1992). The RNase A dimer was tested for its enzymatic activity by an RNase in-gel assay as previously described by Leland et al. (1998) as a "quick and easy test of ribonuclease activity". Basically, samples of RNase A monomer and dimer are incubated with total rat RNA, then, the resulting solutions are loaded onto an agarose gel and subjected to electrophoretic analysis followed by staining with ethidium bromide (data not shown). The *in vacuo* cross-linked dimer was shown to be active, as equally observed by monomeric RNase A treated in the exact same manner (results not shown, as it is a blank gel, corresponding to the complete degradation of RNA and no bands are detected on the gel). The structural and activity characterization of RNase A dimer formed by *in vacuo* cross-linking will be shown in great detail in Chapter 3.

2.4 Conclusions

The objective of this study was to determine if cross-linking of protein could take place between two molecules, lyophilized, and heated under vacuum. Originating from such a simple concept, heating lyophilized protein samples in vacuum sealed tubes, the *in vacuo* method of cross-linking has demonstrated the ability to efficiently link protein molecules without the use of chemical activating reagents. The chemical and physical evidence reported clearly indicates the formation of amide bonds between strongly interacting ammonium and carboxylates, creating zero-length cross-links. At its optimum reaction pH between 7.0 and 10.0, this reaction is thermodynamically unfavourable in solution, as one would expect that protonated amino groups are not nucleophilic, as also carboxylic acid groups are not electrophilic once deprotonated and thus, no condensation reaction would occur. However, if a protonated amino group is strongly interacting with a deprotonated carboxylic acid group in a salt bridge, this condensation reaction can be made favourable by heating the lyophilized protein under vacuum and driving the condensation reaction towards the formation of the volatile product, water. This novel *in vacuo* chemistry redefines the classical nucleophilic substitution mechanisms ordinarily deemed impossible for solution chemistry.

The cross-linked proteins generated by this *in vacuo* mechanism have a significant advantage over products produced by means of chemical activation. It is predicted that in most proteins, *in vacuo* cross-linking will generate very few and selective cross-links whereby preventing the formation of highly polymerized and insoluble aggregated products. The mass spectrum results obtained with RNase A show that the covalent dimer is formed by only one dominant amide cross-link. Through this very selective linking reaction, number

and location of zero-length cross-links observed in RNase A and their effects on its activity should provide novel information on protein-protein interactions and structure-function relationships (results of such a study are described in Chapter 3). Studies evolving from the *in vacuo* cross-linking of RNase A may potentially evolve a general method for investigating protein-protein interactions in a wide variety of proteins complexes.

The apparent novelty of this cross-linking method is summarized as follows: (1) no activating reagents are used in this procedure, thereby reducing the likelihood of denaturing or aggregating the protein; (2) the cross-links formed are few in number and highly selective to sites containing strongly interacting salt bridges; (3) proteins can be lyophilized out from any pH, perhaps at biologically relevant pH's, to ensure optimal activity of the protein and/or proper formation of salt bridges; (4) the extent of cross-linking can be controlled by altering the ratios of the proteins, prior to lyophilization, or by co-lyophilizing with excipients; (5) any uncross-linked material can be re-covered and re-used, and (6) this method is general and can be applied to any sets of interacting proteins, as all protein tested resulted in the production of cross-linked dimers.

2.5 References

Anderson, D. E.; Becktel, W. J.; Dahlquist, F. W. pH-induced denaturation of proteins: a single salt bridge contributes 3-5 kcal/mol to the free energy of folding of T4 lysozyme. *Biochemistry* **1990,** *29* (9), 2403-2408.

Baumert, H. G.; Fasold, H. Cross-linking techniques. *Methods Enzymol.* **1989,** *172:584-609.*, 584-609.

Beauregard, M.; Dupont, C.; Teather, R. M.; Hefford, M. A. Design, expression, and initial characterization of MB1, a de novo protein enriched in essential amino acids. *Biotechnology (N. Y.)* **1995,** *13* (9), 974-981.

Carpenter, F. H. Interactions of stabilizing additives with proteins during freeze-thawing and freeze-drying. *Dev Biol Stand.* **1992,** 74:225-38; discussion 238-9.

Carpenter, F. H.; Harrington, K. T. Intermolecular cross-linking of monomeric proteins and cross-linking of oligomeric proteins as a probe of quaternary structure. Application to leucine aminopeptidase (bovine lens). *J. Biol. Chem.* **1972,** *247* (17), 5580-5586.

Chang, T. M. Modified hemoglobin blood substitutes: present status and future perspectives. *Biotechnol. Annu. Rev.* **1998,** *4:75-112.*, 75-112.

Cornell, R. Chemical cross-linking reveals a dimeric structure for CTP:phosphocholine cytidylyltransferase. *J. Biol. Chem.* **1989,** *264* (15), 9077-9082.

Creighton, T.E. Chemical properties of peptides; In *Proteins, Structures and Molecular Properties,* 2nd edition, W.H. Freeman and Company. **1993**. pp. 6-10.

D'Souza, S. E.; Ginsberg, M. H.; Burke, T. A.; Lam, S. C.; Plow, E. F. Localization of an Arg-Gly-Asp recognition site within an integrin adhesion receptor. *Science* **1988,** *242* (4875), 91-93.

Deisenhofer, J.; Michel, H. The photosynthetic reaction centre from the purple bacterium *Rhodopseudomonas viridis*. *Biosci. Rep.* **1989,** *9* (4), 383-419.

Fancy, D.A. Elucidation of protein-protein interactions using chemical cross-linking or label transfer techniques. *Curr. Opin. Chem. Biol.* ***2001***, **4**: 28-33.

Fersht, A. R. Conformational equilibria in -and -chymotrypsin. The energetics and importance of the salt bridge. *J. Mol. Biol.* **1972,** *64* (2), 497-509.

Fersht, A. R. Conformational equilibria and the salt bridge in chymotrypsin. *Cold Spring Harb. Symp. Quant. Biol.* **1972,** *36:71-3.*, 71-73.

Gaur, D.; Swaminathan, S.; Batra, J. K. Interaction of human pancreatic ribonuclease with human ribonuclease inhibitor. Generation of inhibitor-resistant cytotoxic variants. *J. Biol. Chem.* **2001,** *276* (27), 24978-24984.

Gratzer, P. F.; Lee, J. M. Control of pH alters the type of cross-linking produced by 1-ethyl-3-(3-dimethylaminopropyl)-carbodiimide (EDC) treatment of acellular matrix vascular grafts. *J. Biomed. Mater. Res.* **2001,** *58* (2), 172-179.

Hefford, M. A.; Dupont, C.; MacCallum, J.; Parker, M. H.; Beauregard, M. Characterization of MB-1. A dimeric helical protein with a compact core. *Eur. J. Biochem.* **1999,** *262* (2), 467-474.

Jones, R. T.; Shih, D. T.; Fujita, T. S.; Song, Y.; Xiao, H.; Head, C.; Kluger, R. A doubly cross-linked human hemoglobin. Effects of cross-links between different subunits. *J. Biol. Chem.* **1996,** *271* (2), 675-680.

King, M.C. Ph. D. Thesis, **2003.** Novel Conjugation Strategies for Hybrid Biomacromolecules. University of Ottawa.

Klibanov, A. M. Stabilization of enzymes against thermal inactivation. *Adv. Appl. Microbiol.* **1983,** *29:1-28.*, 1-28.

Kluger, R.; Alagic, A. Chemical cross-linking and protein-protein interactions-a review with illustrative protocols. *Bioorg. Chem.* **2004,** *32* (6), 451-472.

Leland, P. A.; Schultz, L. W.; Kim, B. M.; Raines, R. T. Ribonuclease A variants with potent cytotoxic activity. *Proc. Natl. Acad. Sci. U. S. A* **1998,** *95* (18), 10407-10412.

Loerting, T.; Tautermann, C; Kroemer, R. T.; Kohl I., Hallbrucker, A.; Mayer, E., Liedl, K.R. On the Surprising Kinetic Stability of Carbonic Acid, H_2CO_3. *Angew Chem Int Ed Engl.* **2000**, 39(5): 891-894.

Lundblad, R. *Techniques in Protein Modification.* CRC Press. **1994**. pp. 249-252. Boca Raton, FL.

Manning, L. R.; Morgan, S.; Beavis, R. C.; Chait, B. T.; Manning, J. M.; Hess, J. R.; Cross, M.; Currell, D. L.; Marini, M. A.; Winslow, R. M. Preparation, properties, and plasma retention of human hemoglobin derivatives: comparison of uncrosslinked carboxymethylated hemoglobin with crosslinked tetrameric hemoglobin. *Proc. Natl. Acad. Sci. U. S. A* **1991,** *88* (8), 3329-3333.

Masterston, W.L., and Slowinski, E. J. Equilibria in chemical systems: In *Chemical Principles.* 2nd Edition, W.B. Saunders Company. **1969.** pp.315-320. Philidelphia, USA.

Mauk, M.R., Mauk, A.G. Crosslinking of cytochrome c and cytochrome b5 with a water-soluble carbodiimide. Reaction conditions, product analysis and critique of the technique. *Eur. J. Biochem.* **1989**, 186: 473-486.

Means, G.E., Feeney, R.E. *Chemical modification of proteins.* Holden-Day press. **1971**. pp. 130-132, 144-148, 216-217, 222-223. San Francisco, CA.

Molin, S. O.; Nygren, H.; Dolonius, LA new method for the study of glutaraldehyde-induced cross-linking properties in proteins with special reference to reaction with amino acids. *J. Histochem Cytochem.* **1978,** *26* (5), 412-414.

Nakagami, S.; Matsunaga, H.; Oka, N.; Yamane, A. Preparation of enzyme-conjugated DNA probe and application to the universal probe system. *Anal. Biochem.* **1991,** *198* (1), 75-79.

Olde Damink, L. H.; Dijkstra, P. J.; Van Luyn, M. J.; Van Wachem, P. B.; Nieuwenhuis, P.; Feijen, J. Influence of ethylene oxide gas treatment on the in vitro degradation behavior of dermal sheep collagen. *J. Biomed. Mater. Res.* **1995,** *29* (2), 149-155.

Onishi, H.; Maita, T.; Matsuda, G.; Fujiwara, K. Carbodiimide-catalyzed cross-linking sites in the heads of gizzard heavy meromyosin attached to F-actin. *Biochemistry* **1989,** *28* (4), 1905-1912.

Onishi, H.; Fujiwara, K. The rigor configuration of smooth muscle heavy meromyosin trapped by a zero-length cross-linker. *Biochemistry* **1990,** *29* (12), 3013-3023.

Park, C.F. and Raines, R.T. Dimer formation by a "monomeric" protein. *Protein Sci.* ***2000.*** 9, 2026 – 2033.

Phizicky, E.M., Fields, S. Protein-protein interactions: methods for detection and analysis. *Microbiol. Rev.* **1995,** 59: 94-123.

Rexin, M.; Busch, W.; Gehring, U. Chemical cross-linking of heteromeric glucocorticoid receptors. *Biochemistry* **1988,** *27* (15), 5593-5601.

Rudolph, A. S. Biomaterial biotechnology using self-assembled lipid microstructures. *J. Cell Biochem.* **1994,** *56* (2), 183-187.

Schagger, H.; von Jagow, G. Tricine-sodium dodecyl sulfate-polyacrylamide gel electrophoresis for the separation of proteins in the range from 1 to 100 kDa. *Anal. Biochem.* **1987,** *166* (2), 368-379.

Stewart, N. A.; Pham, V. T.; Choma, C. T.; Kaplan, H. Improved peptide detection with matrix-assisted laser desorption/ionization mass spectrometry by trimethylation of amino groups. *Rapid Commun. Mass Spectrom.* **2002,** *16* (15), 1448-1453.

Taralp, A.; and Kaplan, H. Chemical modification of lyophilized proteins in nonaqueous environments. *J. Protein Chem.* **1997,** *16* (3), 183-193.

Uy, R and Wold, F. Protein cross-linking, Plenum, New York, **1997.** pp. 56-89.

Wang, X.; Minasov, G.; Shoichet, B. K. Noncovalent interaction energies in covalent complexes: TEM-1 beta-lactamase and beta-lactams. *Proteins* **2002,** *47* (1), 86-96.

Vakos, H.T., Black, B., Dawson, B., Hefford, M.A. and Kaplan, H. *In vacuo* esterification of caroboxyl groups in lyophilized proteins. *J. Protein Chem.* **2001,** 26(1), 215-222.

White, F.L., Olsen, K.W.. Effects of crosslinking on the thermal stability of hemoglobin. I. The use of bis(3,5-dibromosalicyl) fumarate. *Arch. Biochem. Biophys.* **1987,** 258: 51-57.

Woltjer, R. L.; Weclas-Henderson, L.; Papayannopoulos, I. A.; Staros, J. V. High-yield covalent attachment of epidermal growth factor to its receptor by kinetically controlled, stepwise affinity cross-linking. *Biochemistry* **1992,** *31* (32), 7341-7346.

Yoshitake, S.; Hamaguchi, Y.; Ishikawa, E. Efficient conjugation of rabbit Fab' with beta-D-galactosidase from Escherichia coli. *Scand. J. Immunol.* **1979,** *10* (1), 81-86.

Zaks, A. "Protein-water interactions: Role in protein structure and stability" in *The stability of proteins*. T. J. Ahern, M. C. Manning ed. Plenum Press. **1992** pp.249-274. New York.

Zaks, A.; Klibanov, A. M. Enzymatic catalysis in organic media at 100 degrees C. *Science* **1984,** *224* (4654), 1249-1251.

Zale, S. E.; Klibanov, A. M. Mechanisms of irreversible thermoinactivation of enzymes. *Ann. N. Y. Acad. Sci.* **1984,** *434:20-6.*, 20-26.

Chapter 3: The *In Vacuo* Cross-linking of RNase A: A Characterization of Structure and Function

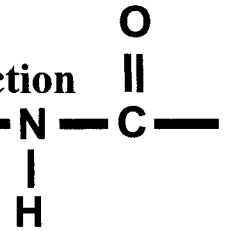

3.1 Introduction

3.1.1 RNase A dimers formed by *in vacuo* cross-linking

Bovine pancreatic ribonuclease A (RNase A), one of the most extensively studied and characterized proteins of the last three decades, was used as our model protein to develop the *in vacuo* method of cross-linking proteins described in Chapter 1. Like most other members of the RNase superfamily, it is a monomeric protein, however, it shares a 80% sequence homology with bovine seminal ribonuclease (BS-RNase) - a uniquely homodimeric ribonuclease that has demonstrated both highly effective anti-tumor activity and cytotoxicity (D'Alessio et al., 1991; D'Alessio, 1999; Di Donato et al., 1994, Kim et al., 1995; and reviewed by Matousek, 2001). In solution, BS-RNase forms an equal mixture of two distinct conformers (Piccoli et al., 1992), both of which are composed of two identical monomers linked by two disulfide bonds. In one of the two dimeric conformers, the two monomeric subunits appear to fold independently of one another. The other dimeric conformer, however, is assembled by the exchange of the N-terminal α-helix between subunits – a process that is commonly termed 3D domain swapping; in essence, the two subunits exchange identical domains (Mazzeralla et al., 1993; Bennett et al., 1995). It is this latter conformer that is shown to be cytotoxic towards cancer cells (Piccoli et al., 1992).

BS-RNase is the only ribonuclease known to form highly stabilized domain swapped dimers under physiological conditions. Given the structural similarities between BS-RNase and RNase A, engineering RNase A to form dimers has been extensively investigated with the hope of endowing RNase A with new biological functions. In 1962, Crestfield observed that stable, dimeric RNase A aggregates could be formed by lyophilization from a concentrated solution of 50 % acetic acid. Crestfield and colleagues, in 1967, further

proposed and then demonstrated that these non-covalent RNase A dimers were two monomeric units that had exchanged their N-terminal segments, thus forming a domain swapped conformation (as shown in Figure 3.1.1), very similar to that observed in BS-RNase, many years later. More recently, numerous groups have begun to characterize the non-covalent RNase A dimers generated by Crestfield's method of lyophilization from acidic media (Gotte et Libonati, 1998; Di Donato et al, 1994; Sorrentino et al, 2000; Park and Raines, 2000). Rather than a single dimeric RNase A species, recent work had shown that, after lyophilization out of dilute acid solutions, RNase A dimers can exist in two distinctly different conformers: the N-terminal α-helix swapped dimer (Liu et al, 1998) and the C-terminal β-strand swapped dimer (Park and Raines, 2000; Liu et al, 2001). The latter is shown in Figure 3.1.2. The N-terminal α-helix (residues 1-15) swapped conformer can be separated from the more dominant C-terminal β-strand (residues 116-124) swapped conformer by cation exchange chromatography and an equilibrium mixture (in a ratio of 1:4, N- to C-terminal domain swapped dimer) was observed (Gotte et al., 1999; Nenci et al., 2001; Liu et al., 2001).

Figure 3.1.1 Crystal structure of 3D domain-swapped bovine pancreatic RNase A, N-terminal α-helix exchange. Protein Data bank entry 1A2W. Monomer 1 is in pink and monomer 2 is in blue (Lui et al., 1998).

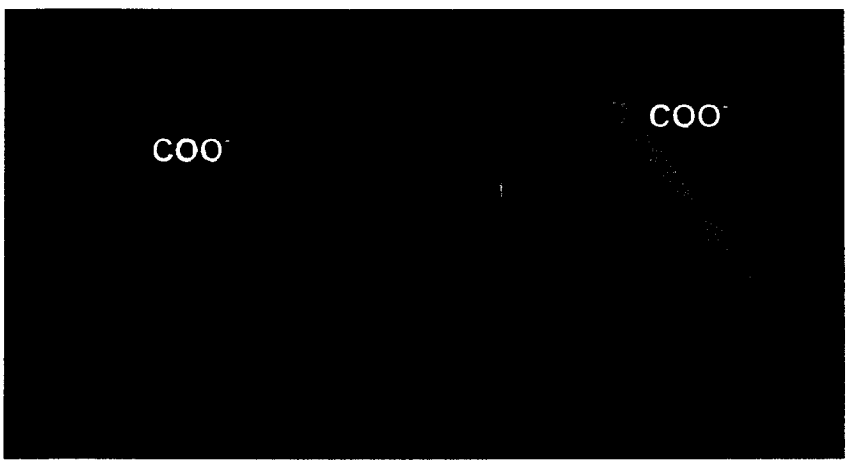

Figure 3.1.2 Crystal structure of 3D domain-swapped bovine pancreatic RNase A, C-terminal β-strand exchange. Protein Data bank entry 1F0V. Monomer 1 is in pink and monomer 2 is in blue (Lui et al., 2001).

In addition to the structural characterization of these non-covalent RNase A dimers, recent work has demonstrated the apparent increase in catalytic activity of dimeric RNase A towards dsRNA substrates (Gotte and Libonati, 1998; Gotte et al., 1999; Park and Raines, 2000). This increase in activity has been explained by the coordinative destabilizing effect of the dimeric moiety on the nucleic acid secondary structure: the increased number of positive charges in the composite active site of the dimer tends to dissociate the double stranded polyribonucleotide structure thus, facilitating enzymatic attack.

Enzymatic studies of the non-covalent RNase A dimers have also been pursued in the presence of the known cellular inhibitor, cytosolic ribonuclease inhibitor (RI) (Kim et al., 1995; Matousek, et al., 2001; Dickson et al., 2003; and reviewed by Haigis et al., 2003). BS-RNase has the ability to resist inhibition by RI – a property believed to make an important contribution to its cytotoxicity (Matousek, et al., 2001). Conversely, RNase A forms a tight 1:1 complex with RI ($K_d = 4 \times 10^{-14}$ M) and is completely encapsulated by the large horse-shoe-like structure of RI which prevents it from interacting with and cleaving RNA. Like BS-RNase, the non-covalent RNase A dimers produced by Crestfield's lyophilization procedure have been shown to remain completely active in the presence of RI (Gotte and Libonati, 1998).

The literature to date therefore indicates that: (1) RNase A, like BS-RNase (a cytotoxic ribonuclease), can, under certain conditions, have dimeric quaternary structure; (2) N-terminal and C-terminal domain-swapped non-covalent RNase A dimers are stable enough to be formed by lyophilization from acetic acid; (3) RNase A non-covalent dimers are more enzymatically active than monomeric RNase A; and (4) RNase dimers resist inhibition by RI. Based on this innate potential to be transformed into a cytotoxic ribonuclease, RNase A

dimers are highly sought after and several strategies for producing such dimers have been reported in the literature, such as protein modeling from BS-RNase sequences (Di Donato et al., 1994), covalent dimerization (Bartholeyns and Baudhuin, 1976; Tarnowski et al., 1976; and Gotte et al., 1997), and numerous variants produced by site directed mutations of monomeric RNase A (Piccolli et al., 1992; Park and Raines, 2000; and Leland et al., 1998).

Given the therapeutic potential of dimeric RNase species, we sought to characterize the covalently cross-linked RNase A dimer produced by the *in vacuo* method to ascertain if it has the stability, enzymatic activity, and resistance to inhibition by RI that other RNase dimers exhibit. While chemical cross-linking of RNase A is still thought to be a fast and easy method of producing RNase A covalent dimers, methods used to produce dimeric RNases to date have met with only limited success. Bartholeyns and Moore, in 1974, prepared a synthetic RNase A dimer by cross-linking with the bifunctional reagent dimethyl submerimidate – a method that was further exploited by Gotte and Libonati, (1998) and Wang and co-workers (Wang et al., 1998). Although it is reported that the resulting cross-linked dimers demonstrated an increase in activity towards double stranded RNA substrates compared to monomeric RNase A, Gotte and Libonati reported yields of only 3 to 5 % of the cross-linked dimer. They attributed these poor yields to inefficiency in the cross-linking procedure. Wang and colleagues reported higher yields of 16 % dimeric RNase A, but they also obtained a large percentage of higher oligomers in addition to the dimer that were unresolved by gel filtration chromatography. The fact that there are no current publications describing a method and a reagent to cross-link RNase A with good yields while retaining catalytic activity and the fact that the *in vacuo* cross-linking methodology is a rapid and

facile way to produce dimeric proteins with relatively high yields added further impetus to characterize the covalent RNase A dimer produced by this method.

The first part of this chapter describes the characterization of the *in vacuo* cross-linked RNase A dimer for its stability, catalytic activity, structural properties, and efficiency of the *in vacuo* cross-linking process.

3.1.2 Novel cytotoxic RNase A derivatives as cancer therapeutics

The molecular basis for cell susceptibility to ribonuclease cytotoxicity is poorly understood. The proposed mechanism of ribonuclease-mediated cytotoxicity involves cell surface binding and internalization, translocation to the cytosol, evasion of the cytosolic ribonuclease inhibitor protein, and degradation of cellular RNA (Haigis et al., 2003). The efficiency at which the ribonuclease accomplishes any of these steps relates directly to cell toxicity and, hence, to its utility as a new protein therapeutic.

Recent advances in the development of ribonucleases as cancer therapeutics have lead to the discovery of Onconase™ (Alfacell, Bloomfield, NJ, USA), a homologue of RNase A from the Northern Leopard frog (*Rana pipiens*). Onconase™ is now in Phase III clinical trials as an anti-tumor drug (Klink and Raines, 2000). A comparison between Onconase™ and RNase A in terms of activity, stability, and structural similarities is essential to understanding the mechanisms of ribonuclease cytotoxicity and the further development of novel human RNase A cytotoxic derivatives. Onconase™ and RNase A are both monomeric proteins but have a low degree of sequence homology (30 %). Despite the low percentage homology, Onconase™ shows a similar topology to that of RNase as well as sequence conservation of the active site residues (Wu et al., 1993). Due to the structural

similarities of the active site, both RNase A and Onconase™ cleave RNA by similar mechanisms, however, RNase A is more active than Onconase™ in ribonuclease assays using double stranded RNA (dsRNA) and single stranded RNA (ssRNA) substrates (Boix et al., 1996). Onconase™, however, is not inhibited by the cytosolic ribonuclease inhibitor, a property unique to Onconase™ among monomeric ribonucleases. Also, Onconase™ was shown to interact with a cell surface receptor on tumor cells whereas RNase A showed no such affinity (Wu et al., 1993). The inherent abilitiy of Onconase™ to interact with a cellular receptor (thereby facilitating its entry into cells) and to evade inhibition from RI compensates for its poor catalytic activity and gives it a cytotoxic property.

Early clinical trial data indicated that treatment with Onconase™ resulted in a significant reduction in tumor growth for various carcinomas. However, in the late stages of phase III clinical trials, undesirable side effects such as high renal toxicity were observed which detract from its appeal as a long term therapeutic. An Onconase™-RNase A heterodimer, on the other hand, provides an opportunity to decrease the therapeutic dosage and the potential risk of adverse side effects by combining a high efficiency in RNA degradation (a property from RNase A) with a mode of cellular entry (a property of Onconase™). The *in vacuo* method of cross-linking can be used to covalently attach Onconase™ to RNase A generating a new dimeric ribonuclease with modulated biological activity. This can be accomplished without the use of chemicals and, unlike methods that rely on the creation of fusion proteins by recombinant technology, can be either scaled up or down easily.

The second part of this chapter describes the design of preliminary experiments in the development of this newly proposed heterodimeric ribonuclease, including the expression

and purification of an in-house version of Onconase™ , called ONC, (required both as a control and a precursor of the proposed dimer) and the characterization of RNase A and ONC monomers in terms of their cytotoxicity towards a cancer cell line. The experiments form the basis for future comparisons of cytotoxic properties of RNase A homodimers and RNase A - ONC heterodimers.

3.2 Materials and Methods

3.2.1 In vacuo *cross-linking of ribonuclease A*

Bovine pancreatic ribonuclease A (Type I-A) was obtained from Sigma-Aldrich (Oakville, ON, CAN) (R4875), reconstituted in distilled water to a concentration of 5 mg/mL, and the pH of the solution was adjusted to 7.0 with 1 N NaOH. The protein solution was placed in glass tubes and lyophilized. These glass tubes were sealed under a vacuum of approximately 50 mtorr and then incubated at 85°C for 96 hours. The vacuum was released and the protein sample reconstituted with 40 mM NaH_2PO_4 at pH 6.67 to give a final protein concentration of 5 mg/mL.

3.2.2 Purification of RNase A dimers

RNase A dimers were purified by two chromatography steps. The first step was size-exclusion chromatography which was carried out using two Superdex 75 HR 10/30 columns (Amersham Biosciences, Baie, d'Urfée, PQ, CAN) attached, in tandem, to an FPLC system (Amersham Biosciences) with detection at 210 nm. Mobile phase (0.2 M Na_2HPO_4 and 0.15 M NaCl at pH 6.55 at 4°C) was used at a flow rate of 0.05 mL/min. In general, 0.5 mL fractions were collected. Molecular weight standards (phosphorylase b, 94 kDa; bovine serum albumin, 67 kDa; ovalbumin, 43 kDa; bovine erythrocytes carbonic anhydrase, 29

kDa; trypsin inhibitor, 20.1 kDa; α-lactalbumin, 14.4 kDa) used in column calibration were purchased from Sigma-Aldrich. Pooled fractions containing RNase A dimer were concentrated to 0.5 mL and the buffer was exchanged to 40 mM NaH_2PO_4 at pH 6.67 using Amicon® Ultra 5 kDa MWCO centrifugal filtering devices (Millipore, Nepean, ON, CAN) and several washing cycles.

The second chromatography step was necessary to ensure no non-covalent dimer was eluting with and contaminating the covalent dimer sample and this was performed using a strong cation exchange Source 15S resin (Amersham Biosciences) and a 8 mL column (Bio-Rad Laboratories, Mississauga, ON, CAN) attached to an FPLC system (Amersham Biosciences) at room temperature. The running buffer used was 40 mM NaH_2PO_4 at pH 6.67 at a flow rate of 1mL/min. Approximately 3mg of the protein collected from the size exclusion column was loaded onto the column at 1 mL/min and monomer, dimer, and trimer were eluted and collected in this respective order by a step wise sodium phosphate linear gradient: 40 mM to 200 mM NaH_2PO_4 at pH 6.7 over 1 hour as indicated in Figure 3.3.1. Dimeric RNase A was collected then concentrated by Amicon® Ultra 5 kDa MWCO centrifugal filtering devices to a volume of approximately 1mL. Samples were kept in 40 mM NaH_2PO_4 at pH 6.67 at 4°C until needed.

The concentration of the *in vacuo* cross-linked RNase A dimer present in each sample was estimated spectrophotometrically by the BCA protein quantification method. Briefly, solutions of unknown protein concentration and 6 standard protein solutions of bovine serum albumin (BSA) of concentrations ranging between 0 and 5 mg/mL were reacted with bicinchoninic acid and copper sulfate (50:1 v/v ratio) for 30 minutes at 37°C. The solutions were transferred into 2 mL disposible cuvettes and their absorbance at 562 nm

was measured using a Beckman DC530 spectrophotometer (Beckman Coulter, Mississauga, ON, CAN). Protein concentrations in the samples were estimated from interpolation of the standard curve obtained for the BSA solutions.

3.2.3 Acid hydrolysis of RNase A dimers

The mixture of cross-linked RNase A dimer and monomer present after lyophilization and incubation (1 mg samples) was reconstituted to 200 µL in one of the following acid solutions: 0.1% (v/v) trifluoroacetic acid (TFA), 1% (v/v) TFA, 0.2% (v/v) formic acid, 2% (v/v) formic acid, 5% (v/v) formic acid, and 10% (v/v) formic acid. Samples were incubated at 50°C for 3 hours then neutralized with 1.0 N NaOH. A 5 µl aliquot (5µg total protein) was taken from each sample, added to 10 µL of SDS loading buffer, then run on a 16.5% Tricine SDS-PAGE at 130 volts for 80 min, and stained with Coomassie Blue for visualization.

3.2.4 Thermal denaturation of RNase A monomer and dimer

A Jasco® 810 circular dichroism (CD) spectrometer (Jasco Inc., Easton, MD, USA) was used to monitor the far-UV region (180 nm to 260 nm) to assess the secondary structures and thermal stability of the RNase A monomer and dimer. Samples contained 0.5mg/mL of protein in 25mM sodium phosphate buffer, pH 7.2 and were placed in a cell of 0.2 cm optical path. In the thermal denaturation experiments, spectra were recorded at 5°C increments as the sample was heated from 25 to 95°C and each spectrum represents the average of 5 accumulations. The molar ellipticities at 222 nm and 208 nm were monitored at each temperature. The fraction of unfolded RNase A molecules was calculated by Equation

3.1 (Navon et al., 2001), where y_{folded} is the molar ellipticity at 222 nm at 25°C (where the protein is expected to be fully folded), y_{temp} is the molar ellipticity at 222 nm at each temperature increment, and $y_{unfolded}$ is the molar ellipticity at 222 nm at 95°C (where the protein is expected to be fully unfolded). The y_{temp} , y_{folded} , and $y_{unfolded}$ were also retrieved from the molar ellipticity data collected at 208 nm. An average of these quotients, as shown in Equation 3.1, gives an estimate of the fraction of folded molecules for RNase A. The % unfolded was plotted against temperature to estimate the melting temperature (T_M) of the protein.

$$\%\ unfolded = \frac{\left(y_{folded} - y_{temp}\right)_{222nm}}{\left(y_{folded} - y_{unfolded}\right)_{222nm}} + \frac{\left(y_{folded} - y_{temp}\right)_{208nm}}{\left(y_{folded} - y_{unfolded}\right)_{208nm}} / 2$$

Equation 3.1 Percent unfolded calculation from molar ellipticity values taken at 222 nm and 208 nm at each 5°C incremental increase (Navon et al., 2001).

3.2.5 Kunitz Ribonuclease Activity Assay

Ribonuclease activity was measured by monitoring the hyperchromaticity induced by cleavage of poly(A)·poly(U) double stranded RNA (Kunitz, 1946). One Kunitz unit of activity corresponds to the initial change in absorbance at 260 nm under first order kinetics (i.e. linear portion of the A_{260} against time curve) divided by the total measurable increase at 260 nm measured after completion of the reaction (refer to Equation 3.2). The substrate used was double stranded RNA, poly(A)·poly(U). Enzyme solutions at a concentration of 50

µg/mL were prepared in Kunitz buffer (0.15 M NaCl, 0.015 M citrate, pH 7.5). After the poly(A)·poly(U) substrate solutions (at concentrations varying from 4 to 80 µg/mL, in 0.15 mL of Kunitz buffer) were equilibrated at 25°C for 30 min, an aliquot of enzyme solution (0.05 mL) was added to each giving a final reaction volume of 0.2 mL. The same reaction, with buffer rather than enzyme addition, was used as a blank for correction at each substrate concentration. The absorbance at A_{260} was monitored over 3 hours on a Tecan® SPECTRAFluorPlus multifunction microplate reader (Tecan US, Durham, NY, USA). After subtraction of the appropriate blanks, the kinetic analysis of each reaction was determined by non-linear regressional analysis of the data using SigmaPlot® (Systat Software Inc., Point Richmond, CA, USA). The resulting hyperbolic curves were plotted in Microsoft Excel® (Microsoft Canada, Mississauga, ON, CAN). The number of "Kunitz units" per mg of enzyme used is equivalent to the k_{cat}/K_M and determines the specific activity of the enzyme, as shown in Equation 3.3.

$$Kunitz\ unit = \frac{dA/dt}{\Delta A}$$

Equation 3.2 Kunitz unit of ribonuclease activity where dA/dt is the slope of the linear part of the curve and ΔA is the maximum absorbance obtainable (i.e. the plateau of the A_{260} versus time curve).

$$k_{cat} / K_M = \left(\frac{dA/dt}{\Delta A} \right) \frac{1}{[E]}$$

Equation 3.3 The activity is measured under first order conditions, k_{cat}/K_M calculation, where the number of "Kunitz units", divided by the amount of enzyme in milligrams will equal the k_{cat}/K_M.

RNase A activity was determined in the presence or absence of cellular ribonuclease inhibitor (RI), (Ambion Technologies, Austin, TX, USA). The Kunitz assay was performed as described above, except 2000 units of RI (from a stock solution of 40 U/µL, provided by the supplier) or an equivalent volume of buffer was added to the samples as indicated.

3.2.6 Enzymatic digestion of RNase A dimer

Disulphide bonds in RNase A dimer and monomer were reduced and alkylated as described by McWherter et al, 1984. Samples (~ 2mg/mL) were denatured in 0.5 M Tris-HCl, 2.5 mM EDTA, and 6 M guanidinium-HCl, pH 8.5 at 37°C for 1 hour. 2.5 mM DTT was added and N_2 was bubbled through the sample for 5 min followed by a further incubation at 37°C for 1 hour. 0.3 M iodoacetamide was added and allowed to react, in the dark at 37°C, with the protein for 30 min. The alkylation reaction was stopped by the addition of 100 µL (1.42×10^{-3} mol) of β-mercaptoethanol and samples were dialyzed extensively against 50 mM ammonium bicarbonate (pH 8.0) to remove all excess reagents.

Trypsin (Promega, Madison, WI, USA) was added to each RNase sample at an enzyme to substrate ratio of 1:25 and the protein samples were allowed to digest overnight at 37°C. The next day, the samples were heated to 100 °C for 3 min, and then evaporated down to 10 µL using a Vacfuge™ speed rotorvac (Ependorff North America, Westbury, NY, USA).

Reverse phase HPLC was used to separate the tryptic RNase A peptides of both monomeric and dimeric samples. Trypsin digested samples were reconstituted in the mobile phase solvent A (5% ACN, 0.1 % TFA) then injected by Waters 770E autosampler into Waters 600E HPLC system (Waters Limited, Mississauga, ON, CAN) interfaced by

millennium HPLC software into a 0.46 x 30 cm C_{18} column provided by Vydac (Grace Vydac, Hesperia, CA, USA). A linear gradient changing from 100% mobile phase solvent A to 35% mobile phase solvent B (95% ACN, 0.1% TFA over 60 min) at a flow rate of 1 mL/min was used to elute the peptides. Peptides were collected individually and the volume of each fraction reduced to approximately 10 µL by evaporation.

3.2.7 Peptide mapping by LC-Mass spectrometry

In preparation for mass spectrometry (MS), 0.2 % formic acid (v/v) was added to each of the evaporated samples containing eluted fragments to give an estimated final concentration of 50 pmol/µL per sample. Samples were analyzed by LC-ESI-MS with use of a Waters Q-TOF Ultima Global (Waters Inc., (Micromass™), Mississauga, ON, CAN) mass spectrometer coupled to a Waters CapLC XE system. Tryptic peptides were loaded (1.0 µL) and desalted, at a flow rate of 20 µL/min, on a C_{18} Pepmap trapping column (300 µm id x5mm) (LC Packings Dionex, Sunnyvale, CA, USA). The peptide mixture was eluted using an acetonitrile solvent gradient from 0 to 40% B running over 60 min followed by a second gradient from 40 to 95% B achieved in 60 to 70 min (solvent A: 98% dH_2O, 0.2% formic acid, 2% ACN; solvent B: 90% ACN, 0.2% formic acid). The solvent stream, flowing at a rate of 10 µL/min, was split prior to the analytical column to achieve a flow rate of 200 nL/min on the analytical column - an Atlantis™ Waters C_{18} 75 µm x 150 mm NanoEase™ column (Waters Inc.). Mass spectral data acquisitions were piloted by MassLynx™ software using automated switching between MS and MS/MS modes. The survey scan (1s) was obtained over the mass range m/z 300-1200 in the positive ion mode with a cone voltage of 40 V. When the signal reached a user-defined threshold (10 counts/sec), and the isotope

pattern demonstrated that the ion was multiply charged, then peptide precursor ions were selected for MS/MS scan (2 s) over the mass range m/z 50-2000. Fragmentation was performed using argon as the collision gas and with a collision energy profile (20-40 eV) that is depended on the state and the mass of the precursor ion. External calibration was achieved using a multipoint calibration from the MS/MS of doubly charged glu-fibrinopeptide B (Sigma-Aldrich) at various concentrations in 0.2% formic acid.

3.2.8 Expression and purification of Onconase™

An in-house version of Onconase™ (ONC) was expressed and produced as a His-tagged protein in *E. coli* using pONC, a PET-22b(+) (Bio S & T Inc., Montreal, PQ, CAN) vector encoding 6 histidines before an N-terminal methionine residue to allow cleavage (to produce the encoded recombinant protein sequence without the His-tag) upon treatment with cyanogen bromide. Bacterial growth and induction of the gene encoding ONC followed standard procedures. Several hours (2 to 4) after induction, the cells were harvested by spinning at 56 000 rpm for 30 min at 4°C. The cell pellet was resuspended in 10 mL of lysis buffer (50mM Tris-HCl, 100 mM NaCl at pH 7.0) to which 0.5 mM PMSF (phenylmethyl sulfonyl fluoride) and 0.3 mg/mL lysozyme had been added and then incubated 30 min on ice. After incubation, 1.3 mg/mL of sodium deoxycholate was added and the cell pellets were incubated a further 30 min at 30°C. 6.7 µg/mL of DNase was added, and then the suspension was sonicated according to standard procedures to release cellular contents.

After sonication, the cell lysates were centrifuged at 20 000 x g for 30 min at 4°C. The insoluble fraction (ONC is produced as an inclusion body) was resuspended in 10 mL of lysis buffer and 0.5% Triton X-100 and then incubated for 10 min at room temperature. The

lysate was centrifuged for a second time at 20 000 x g for 30 min at 4°C. The insoluble pellets were re-washed with distilled water and re-centrifuged as described above. This re-washed, insoluble pellet was then re-suspended in 10 mL of denaturing buffer (6 M guanidinum hydrochloride, 50 mM Tris-HCl, 300 mM NaCl at pH 7.0). Reduced glutathione was added to the now solubilized pellet at a final concentration of 100 mM and the sample was incubated under nitrogen for 2 hours at room temperature. After the reduction reaction was complete, the pH of the sample was re-adjusted to pH 7.0.

The reduced and solubilized pellet was loaded onto a pre-equilibrated 5 mL Talon® metal affinity (BD Biosciences, Mississauga, ON, CAN) column at a rate of 1 mL/min and the eluant monitored by a 280 nm UV detector. The His-tagged ONC was retained on the column until eluted with 50 mM imidazole in denaturing buffer at pH 7.0. His–ONC was collected and concentrated by Amicon®Ultra 5 kDa centrifugal filtering device to a final volume of 2 mL.

The His-ONC sample was dialyzed against 20 mM Tris-acetate with 0.5 M arginine at pH 6.0 for 3 changes of 1 L over 3 hours. To cleave the His tag from native ONC, CNBr in formic acid was added at a final concentration of 1 mg/mL and the sample was incubated in the dark for 24 hours. After the CNBr reaction, the sample was again dialyzed against denaturing buffer for 2 changes of 500 mL over 2 hours, to rid the sample of His-tag.

To insure the purification of the His-cleaved native ONC from any uncleaved His-ONC a second affinity chromatography step was used, employing a 5 mL Talon® metal affinity resin column (BD Biosciences) in a 6 M guanidinium hydrochloride, 20 mM Tris-HCl, 300 mM NaCl, at pH 7.0 running buffer. The protein mixture was loaded onto the column (at a flow rate of 1 mL/min) and native ONC, completely unretained, was eluted

from the column and collected while the His - labeled protein remained bound to the column. The sample was then concentrated using Amicon Ultra® MWCO 5 kDa centrifugal filtering device to a final volume of approximately 2 mL.

The refolding of ONC out from the 6 M guanidinium hydrochloride denaturing buffer conditions was performed by oxidative refolding in a Tris-arginine buffer. The sample was dialyzed against 20 mM Tris-HCl, 0.5 M arginine at pH 7.8 for 3 changes of 1 L over 3 hours to effectively exchange the buffer. It was transferred to a 15 mL tube, and 8 mM oxidized glutathione added before incubation overnight at 4°C. After oxidation, the sample was transferred into a 3500 MWCO dialysis membrane (Spectrum Laboratories Inc., Rancho Dominguez, CA, USA) and the refolding of ONC was performed by a slow, stepwise gradient from 100% 20 mM Tris-HCl, 0.5 M arginine at pH 7.8 to 100% phosphate buffered saline (4.3 mM Na_2HPO_4, 137 mM NaCl, 2.7 mM KCl, and 1.4 mM KH_2PO_4 at pH 7.4) in a total volume of 1L over 8 hours.

Following the refolding, the ONC protein sample was concentrated to a volume of less than 1 mL using Amicon Ultra® MWCO 5 kDa centrifugal filtering devices. A 10 µL aliquot was taken for protein quantification by the bicinchioninic acid assay, to determine the final concentration.

3.2.9 Fluorescence ribonuclease assay

ONC thus produced was tested for its ribonuclease activity using the RNaseAlert™ (Ambion, Austin, TX, USA) ribonuclease activity assay kit. This assay is composed of a single stranded RNA substrate with a fluorescent tag that fluoresces once the RNA substrate has been cleaved by the enzyme. Each reaction was conducted in a 96 well fluorescent microtitre plate (Corning, NY, USA) containing 50 pmol of substrate and 200-300 pg of

enzyme in TBS (20 mM Tris-HCl, 137 mM NaCl, at pH 7.2) in a total reaction volume of 50 µL. In selected reactions, 40 units of ribonuclease inhibitor (Ambion) was added from a stock solution at a concentration of 40 units/µL. The catalytic activity of the enzyme was monitored by TECAN® GENious fluorimeter (excitation filter: 485 nm; emission filter: 535 nm) (San Jose, CA, USA) and relative fluorescent units (RFU) were measured over 90 min.

Plots of RFU as a function of time generated hyperbolic curves in which the linear portion of the curve gives the initial velocity of the enzyme, according to a first order steady state kinetics model. The specific activity of the enzyme can be calculated by using Equation 3.4. The term dRFU/dt represents the slope of the linear portion of the RFU over time curve and $RFU_{max} - RFU_o$ is the difference in fluorescence intensity of the maximum (once the reaction is brought to completion) minus the initial measurement. This defines an activity unit according to this assay (all values are corrected for the dRFU/dt of blank reaction, in the absence of enzyme). The specific activity, therefore, is estimated by the activity units divided by the total amount of enzyme given in pg.

$$activty\ \ unit = \frac{\frac{dRFU}{dt}}{RFU_{max} - RFU_o}$$

$$specific\ \ activity = \frac{activity\ \ unit}{[E]}$$

Equation 3.4 An activity unit in the ribonuclease fluorescence assay is calculated by the slope of the linear portion of the RFU over time curve divided by the difference in total fluorescent units obtainable after the reaction is brought to completion. The specific activity is, therefore, defined as the activity units divided by the amount of enzyme in pg.

3.2.10 Cell proliferation assay

ONC and RNase A were tested for their cytotoxic effects on a HL-60 lymphocytic leukemia cell line (American Type Culture Collection, Manassas, VA, USA) by performing a cell proliferation assay which measures the incorporation of methyl[^{3}H]thymidine into DNA by ^{3}H scintillation counts. HL-60 cells are plated at 1 x 10^7 cells per 5 mL well in 500 µL of media (Dulbecco's medium supplemented with 10% fetal calf serum) (Invitrogen Canada Inc., Burlington, ON, CAN) and 50 units/mL penicillin and 50 µg/mL streptomycin (Sigma-Aldrich) was added. From a sample of ONC or RNase A (~2 mg/mL in PBS, pH 7.2), 50 µL of the enzyme was added to the plated cells and the plate was incubated at 37°C with 5% CO_2 for 72 hours. Cyclohexamide (CHX) (0.3 µg/µL in PBS) was added to selected wells as positive control (stops protein synthesis, *viz.* cell death).

After this 72 hours incubation period, 0.5 µCi of methyl[^{3}H]thymidine was added and the plate was further incubated for an additional 4 hours. The cells were then centrifuged at 1600 rpm for 5 min and washed with cold PBS to remove excess methyl[^{3}H]thymidine. Precipitation of nucleic acid material was achieved by adding 0.5 mL of ice cold trichloroacetic acid (TCA) to each well and incubating at 4°C for 30 minutes. The unreacted TCA was removed by centrifugation at 1600 rpm for 5 min, washed with PBS and repeated. At room temperature, 0.5 mL of 0.5 N NaOH and 0.5 % SDS was added to permeate and loosen the cell membrane to allow for the precipitation of DNA by NaOH. Linearized DNA was removed and transferred to scintillation vials, containing 4.5 mL scintillation fluid, and the ^{3}H counts were read on a Beckman scintillation counter (Beckman Coulter, Mississauga, ON, CAN) in triplicate.

3.3 Results and Discussion

3.3.1 Purification of the *in vacuo* cross-linked RNase A dimer

From the cross-linked mixture obtained after the *in vacuo* treatment of RNase A, the dimer was separated from the free (uncross-linked) monomer by a series of liquid chromatography steps. Size exclusion chromatography using a Superdex G75 HR 10/30 column, an FPLC system, and a high salt buffer was determined to be the best method of separating the bulk of the dimer (this separation is shown in Figure 2.3.3 of Chapter 2). Because trace amounts of non-covalent dimer also eluted at the same position as the covalent dimer, a second FPLC step was necessary to assure homogeneity of the dimer. Using a strong cation exchange column, the monomer and dimer were separated by their differences in positive charges (Gotte and Libonati, 1998) and eluted according to the profile shown in Figure 3.3.1. A gel depicting the separated products is shown in Figure 3.3.2 below.

The second purification step, the strong cation exchange chromatography of RNase A cross-linked mixture shown in Figure 3.3.1, revealed two separated peaks eluting in the fraction that, on subsequent examination by SDS-PAGE, appears to contain predominantly covalently cross-linked dimer. Based on the earlier findings of Gotte and Libonati (1998), who characterized two different forms of the aggregated non-covalent RNase A dimer, these are postulated to be two domain swapped dimeric species differing in the portion of the monomers that are swapped. To date, there is no evidence that the two domain swapped dimers separated by Gotte and Libonati (1998) are formed when RNase A is lyophilized from anything but dilute acetic acid solutions. Park and Raines (2000) did note the transient formation of an unstable dimer of inactive but complementary RNase A mutants at neutral pH. This latter dimer was not characterized for its behaviour on cation exchange resins. The

presence of the dimer peak doublet, however, need not indicate a non-covalent dimer formation as it may also be explained by the covalent dimerization of RNase B (the glycated form of RNase A) that is present as a contaminant in the commercial preparation or the production of an RNase A-RNase B heterodimer. The RNase A covalent trimer elutes last.

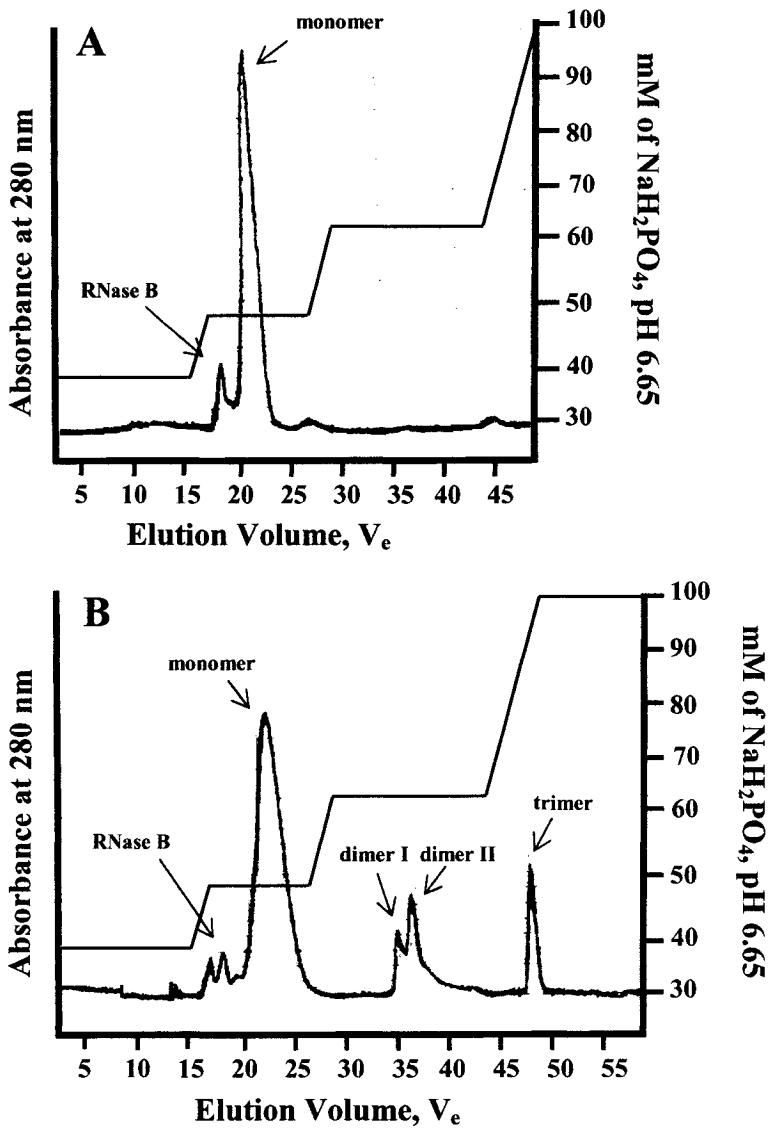

Figure 3.3.1 Strong cationic exchange chromatography of RNase A uncross-linked (A) and *in vacuo* cross-linked mixture (B). Elution of monomer, dimer and trimer by a step-wise gradient of NaH_2PO_4 between 40 and 100 mM (red line) and eluted products are as indicated.

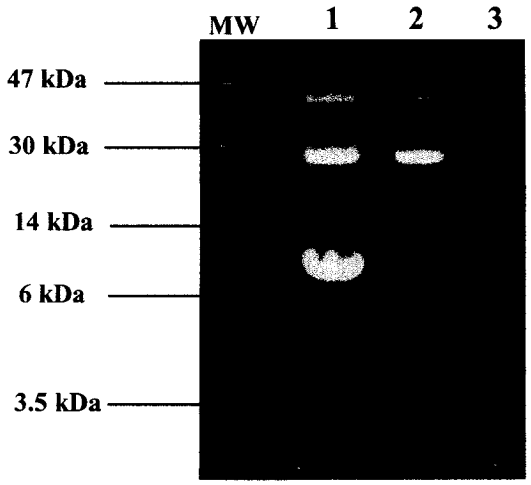

Figure 3.3.2 16.5% SDS Tricine gel electrophoresis, stained with Sypro® Ruby Red stain of RNase A monomer and *in vacuo* cross-linked RNase A dimer. 10 µg of RNase A cross-linked mixture (lane 1), and ~ 5ug RNase A dimer isolated by size exclusion FLPC (lane 2). Further separation of non-covalent dimer from covalent dimer by ionic exchange FLPC, and eluted dimer product seen in lane 3.

3.3.2 Acid hydrolysis of the amide link in the RNase A dimer

Having obtained a high-purity preparation of the covalently cross-linked dimer, it was now possible to attempt identification of the sites of cross-linking. This was envisioned to be a rather simple process: merely to produce and compare peptide maps from purified preparations of both monomer and covalent dimer and then analyze the ensuing peptides by mass spectrometry (MS) to identify those involved in cross-linking to produce the dimer. Efforts to locate the amide linkage in the RNase A dimer, however, were complicated by the observation that the amide link might be acid labile and certain techniques, such as attempts at peptide mapping using cyanogen bromide in formic acid or analysis by electrospray mass spectroscopy (with its concomitant dissolution of isolated peptides in acid for injection into the spectrometer), would return a monomeric profile, presumably because the amide link

holding the dimer together was breaking. Experiments to test the acid lability of the *in vacuo* cross-linked dimer were then performed using different concentrations of trifluoroacetic acid (TFA) and formic acid (FA). Figure 3.3.3 is a set of two gels depicting the RNase A cross-linked mixture after incubation in acid at different concentrations at 50°C for 3 hours. Incubation in 0.1 % TFA does not cause dissociation of the dimer, however, a 1.0 % TFA solution was sufficient to break down the dimer and produce monomer (as shown in Figure 3.3.3 Gel A). A higher concentration of FA also caused dissociation of the dimer: incubation in concentrations above 5 % FA resulted in a loss of the dimer band on the gel and an intensified monomeric band. It should be noted that the acid treatment at 50°C does not appear to break peptide bonds in the backbone chain of the monomer as no breakdown products are visible on the gel. Figure 3.3.3 Gel B shows a similar experiment using a sample of purified covalent dimer and trace amounts of higher oligomer and treating it in 1 % TFA at 50°C for 3 hours. After treatment in acid, all cross-linked products seemed to disappear (only a faint band was seen at the dimer position) resulting in one major band at the monomeric position. These results indicate that amide linkages holding the dimer together and those found in larger oligomers as a result of the cross-linking method appear to be unstable and easily hydrolyzed in mild acid. This may be because of the strain on these bonds and because they are presumably exposed and do not experience steric hindrance contributions from neighboring side groups (as do the peptide bonds in the backbone chain), and thus are easily accessible to water. While most amide linkages in proteins and peptides are stable in these relatively mild acid conditions, some peptide bonds, because of exposure and straining are quite labile. It is well known that amide linkages between aspartic acid (Asp) and proline (Pro) residues, for example, are extremely sensitive to acid and such Asp-

Pro amide bonds in most proteins hydrolyze readily when incubated, without heating, at pH 2 (Creighton, 1993). As well, Asp-Pro bonds and Gln-Pro bonds have been shown to have chemical instabilities under gas phase acidic vaporization induced by mass spectrometric methods (Yu et al., 1993; Skribanek et al., 2002).

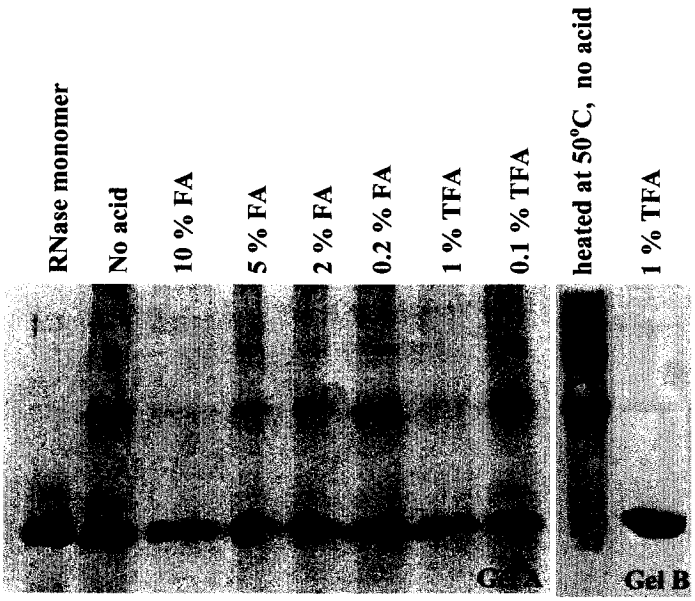

Figure 3.3.3 16.5% Tricine SDS-PAGE of cross-linked mixture of RNase A monomer and dimer (~5 µg total load) after hydrolysis with the acid indicated at 50°C for 3 hours (Gel A). Gel B shows the purified *in vacuo* cross-linked RNase A dimer (with traces of trimer and tetramer) heated at 50°C for 3 hours in the presence and absence of 1 % TFA.

3.3.3 Thermal denaturation of RNase A dimer

Because of the observed chemical instability of the RNase A dimer towards acid hydrolysis, a comparison of the thermal stability of both the dimer and monomer was pursued next. Neither the covalently cross-linked dimer nor the monomer undergo any covalent bond breaking, even when heated to 100°C under atmospheric pressure. The dimer

remains dimeric and does not revert to monomer as it does when exposed to acid. For example, the sample preparation for the SDS-PAGE analysis that initially revealed the presence of dimer in lyophilized protein samples involve a step of boiling the protein in denaturant for several minutes before loading on the gel. Therefore, the effect of heating the dimer in solution at elevated temperatures is not likely to be the source of amide bond breakage, but rather the effect of the acid.

While exposure to high temperature does not result in amide bond breakage (a type of chemical degradation of proteins) in either the monomer or the covalent dimer of RNase A, it is expected to break the non-covalent linkages that hold the primary structure specified by the amide linkages between amino acid residues in a specific tertiary structure or conformation. Thermal denaturation (conformational denaturation), monitored by far-UV circular dichroism (CD), evaluates the retention in secondary structure as a protein is heated from 25 – 95°C. Most proteins, however, unfold in a co-operative manner and lose secondary structure and tertiary structure simultaneously (Johnson, 1999; Greenfield, 1996; Creighton, 1993, pp. 287-301). Thermal denaturation provides information about the protein's unfolding mechanisms as well as its thermal stability. Comparison of the denaturation profile of monomeric and dimeric RNase A, therefore, had the potential to reveal some differences in the tertiary structure, the overall fold of the two molecules, and yield some clues as to the suspected strain on the linkage between monomeric units in the dimer.

According to the X-ray crystallographic structure in the protein database (PDB id = 1RCN; Fontacillia-Camps, 1994) RNase A is an α/β-structured protein, containing three α-helices and seven β-strands. The CD spectrum of RNase A at room temperature shows a

typical trough at 205 to 230 nm which shifts to a minimum at 200 nm as the protein denatures and becomes a random coil type structure (Stelea et al., 2001). RNase A monomer and dimer were analyzed by CD, scanning at 5°C temperature increments, and their spectra are shown in Figure 3.3.4. The monomer (Figure 3.3.4A) shows a confirmed two state unfolding mechanism, indicated by the sharp transition in the spectra from 55 to 70°C and the isobestic point at about 208 nm (Stelea et al., 2001). The dimer also shows a two-state transition, though scans from 55 to 70°C indicate a slightly less abrupt transition from folded to unfolded (Figure 3.3.4B). In general, the thermal denaturation profiles of the RNase A monomer and covalently cross-linked dimer as judged by the composite spectra below appear very similar, both in general shape and in the temperature at which the transition in spectral shape occurs, indicating that the *in vacuo* cross-linking has not significantly altered the structure of RNase A or its folding and unfolding mechanisms.

This observation of similar conformational denaturation is typically assessed more precisely by monitoring the shift in the spectral minima from 222 nm and 208 nm to 200 nm (Greenfield, 1996). This shift in the maxima of mean residue ellipticity is indicative of the unfolding of the α-helices (responsible in part for the negative ellipticity at 222 nm) and the β-sheet structure (responsible in part for the negative ellipticity at 208 nm) into random coil (resulting in the ellipticity minimum at about 200 nm typical for coil). By monitoring the degree of negative ellipitiy at 222 nm and 208 nm, the fraction of folded molecules and unfolded molecules can be calculated using the Equation 3.1 as described in Materials and Methods section 3.2 above and plotted as a function of temperature, as shown in Figure 3.3.5. From this plot, the melting temperature or T_M is determined by the inflection of the sigmoid curve at the temperature at which 50 % of the protein is unfolded.

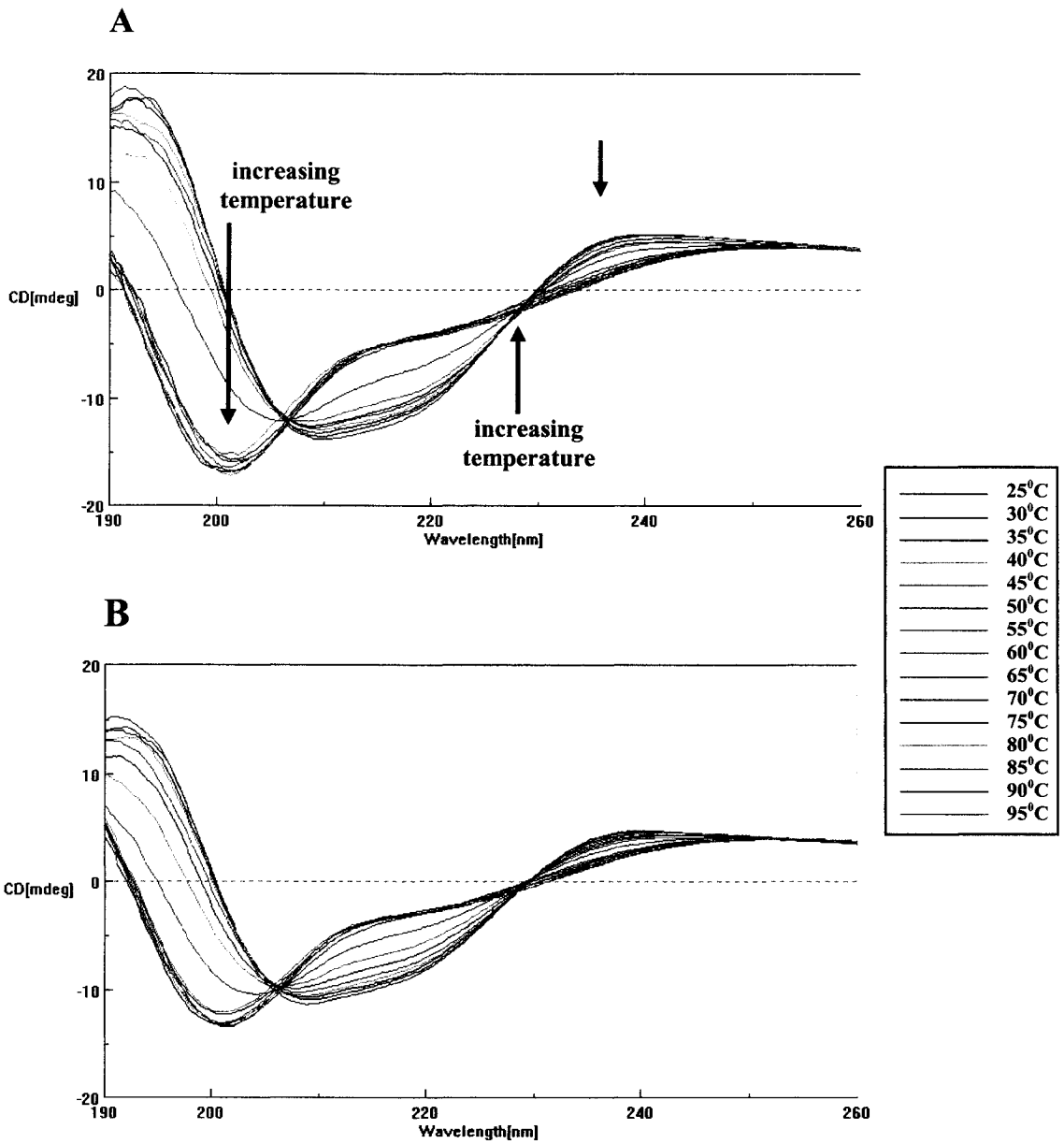

Figure 3.3.4 Circular dichroism spectra of RNase A monomer (A) and *in vacuo* cross-linked dimer (B) measured at different temperature increments. Thermal denaturation of proteins at 0.5 mg/mL in 10 mM phosphate, pH 7.4, measured by Jasco 810 CD and spectrums calculated from an average of 5 scans per increment in temperature.

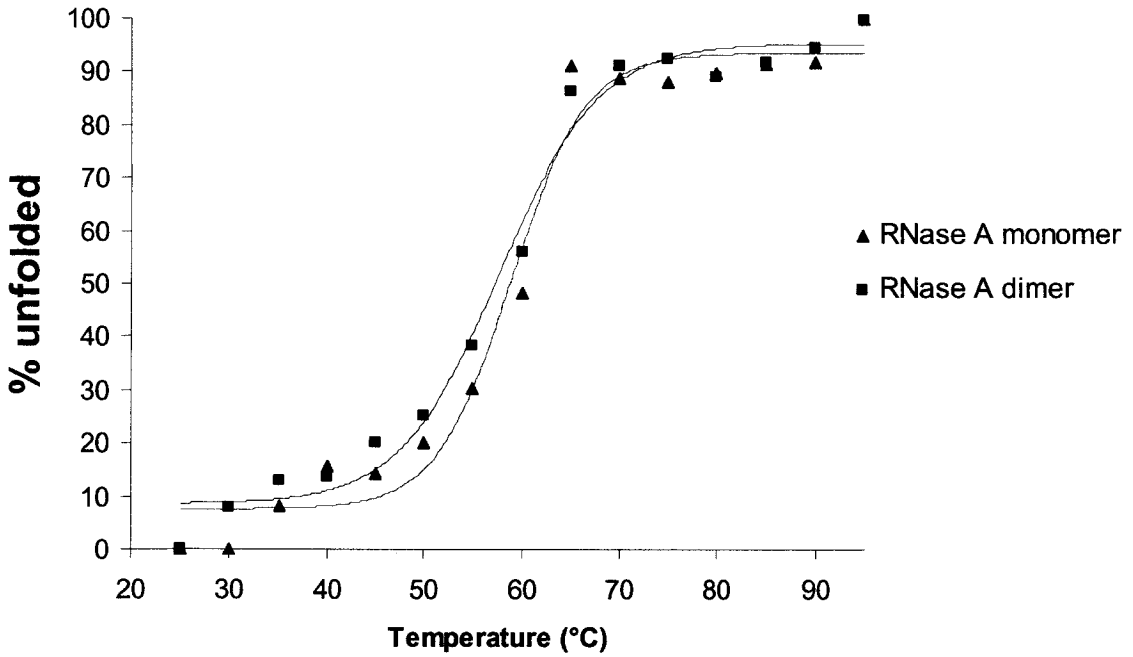

Figure 3.3.5 Percentage of unfolded RNase A protein molecules as a function of temperature; thermal denaturation curves of RNase A monomer (blue line) and *in vacuo* cross-linked dimer (red line) to determine melting temperature (T_M).

Table 3.3.1 lists the results of the melting temperatures obtained from the CD thermal denaturation analysis of the monomer and dimer respectively. As is evident from the similarity in T_M values for the isolated monomer and dimer formed by the *in vacuo* cross-linking procedure, there is no gross conformation difference between the two molecules. Unfolding of the dimer, however, does appear to be slightly less co-operative, as indicated by the fact that the denaturation curve in Figure 3.3.5 is less steep through the transition. This observation and the slight decrease in T_M value for the dimer compared to the monomer can be taken as indicating that the dimer is slightly less well packed (less tightly folded) than the monomer – an interpretation that is at least consistent with the postulation of a monomer-monomer amide linkage in the dimer which is slightly strained.

Table 3.3.1 Melting temperatures of RNase A monomer and dimer	
Ribonuclease Species	**Melting Temperature, T_M (°C)**
RNase A (Stelea et al., 2001)	63.2
RNase A monomer	59.8
In vacuo RNase A dimer	57.6

Table 3.3.1 also lists the T_M value of RNase A as determined by (Stelea et al., 2001; and also confirmed by Klink and Raines (2000)) using differential scanning calorimetry at concentrations of 1 mg/mL in phosphate buffered saline at pH 6.8. This value is slightly higher than that observed for either the isolated monomer or the isolated dimer but is in the general range of the results obtained. Differences in the experimental results compared to the literature value may be due to the experimental differences between T_M determination via differential scanning colorimetry versus that by circular dichroism and in sample treatment prior to analysis, in particular sample buffers of different pH and ionic strength. None-the-less, the *in vacuo* treated RNase A dimer does not show any large structural deviations from native RNase A as a result of cross-linking.

3.3.4 Peptide mapping of the *in vacuo* cross-linked dimer to identify the amide linkage

While the results of the thermal denaturation and enzymatic activity (below) indicate that there is no reason to suppose that the overall conformation of individual monomers in the dimer are grossly dissimilar to that of the RNase A monomer, both the relative position of the monomeric units in dimer and the actual amino acid residues involved in the cross-link required further investigation. The RNase A *in vacuo* cross-linked dimer is formed by a

condensation reaction between interacting ammonium and carboxylate groups from a lysine residue and an acid residue (either aspartic acid or glutamic acid) as previously described in Chapter 2. To locate this amide linkage within the primary structure of the RNase A dimer, a peptide mapping strategy was employed. This strategy involved the enzymatic digestion of the RNase A dimer, the separation of the peptides by reverse phase HPLC (RP-HPLC) followed by peptide identification by electrospray mass spectrometry of both native RNase A and the *in vacuo* cross-linked dimer. Care was taken in the choice of enzymes for digestion to avoid digestion conditions that would expose the dimer to acid conditions determined above to result in cleavage of the linkage between monomeric units. In addition, the results of all these experiments were interpreted in light of the possibility that the linkage between these monomeric units is strained and relatively exposed and hence may be overly susceptible to cleavage during the additional derivation processes preceding enzymatic digestion or in the sample handling in the mass spectrometric analysis.

To prepare the protein samples for peptide mapping, both the native RNase A and the *in vacuo* cross-linked dimer were separately reduced with dithiothreitol (DTT) and then cysteine residues were S-carbaminomethylated using iodoacetamide to effectively break then cap the sulfhydryl groups and thus preventing them from re-oxidizing and reforming disulphide bonds. After the reducing and capping, both RNase A monomer and dimer samples were enzymatically digested with trypsin to achieve selective cleavages after lysine and arginine residues and to generate a tryptic digestion profile in which the tryptic peptides are separated by RP-HPLC.

The RP-HPLC chromatograms depicting the digestion profiles of the RNase A monomer and dimer are shown in Figures 3.3.6 A and B. Based on the primary structure of

native RNase A, which indicates thirteen tryptic cleavage sites, fourteen tryptic peptides are expected to elute. However, only 13 peaks (see explanations below) are observed and these have been labeled with the letters A through N, as shown in Figure 3.3.9 A - a representative digestion of native RNase A. This digestion profile is consistent with that obtained in peptide mapping studies by McWherter et al., 1984, and Hirs et al., 1956 and accounts for the relative resistance to trypsin cleavage at $Lys_1 - Glu_2$ and $Lys_{41} - Pro_{42}$ (attributed to steric hindrance resulting from the 'bulky' side chains of residues following the lysine at the recognition site). In addition to resistant tryptic sites, the partial cyclization of the N-terminal glutamine forms a pyroglutamate, from cleavage of the $Lys_{10} - Gln_{11}$ bond, resulting in a difference in mobility through the HPLC column (peaks J and K) (in Figure 3.3.6) which represent the same peptide with and without the pyroglutamate. The digestion profile is also consistent with previously reported results pertaining to peak H (residues 92-98) and peak I (residues 86-98) which arise due to an occasionally missed tryptic cleavage site at Arg_{91} that is routinely observed due to the steric hinderance that surrounds this arginine residue (McWherter et al., 1984). Therefore, 13 lysine and arginine tryptic cleavage sites contained within the native RNase A sequence only generates 13 eluted peaks (not 14), A – N, as shown in Figure 3.3.6. The identity of each of the labeled peaks was eventually confirmed using mass spectroscopy (data not shown - but explanation is shown below) and is consistent with that which would be predicted by comparing the elution profile to that of the previously cited peptide maps in the literature.

Mass spectrometric and chemical evidence presented in Chapter 2 indicated that the product of *in vacuo* cross-linking is mainly a dimer composed of a single amide link formed between two RNase A monomers and further that this link is formed between amino acid

side chains at a lysine and an aspartic or glutamic acid residues. Because an ε-amino group of a lysine is involved in the amide link, this lysine residue will no longer be cleaved by trypsin and the abundance of peptide fragments on the C- and N-terminal sites of this lysine residue will be reduced by half since they will only arise from the identical cleavage site on the opposite chain. Using the same reasoning, the peak representing the tryptic peptide containing the acid functionality of the amide link will also decrease by half as this peptide from one of the monomeric units is now covalently attached in the formation of a new cross-linked peptide, but the noncross-linked acid residue is also present on the opposite monomeric chain. However, the cross-link is expected to produce a new peak which should appear as a new peak in the elution profile, comprised of the uncleaved lysine fragment and the covalently linked fragment containing the acid residue.

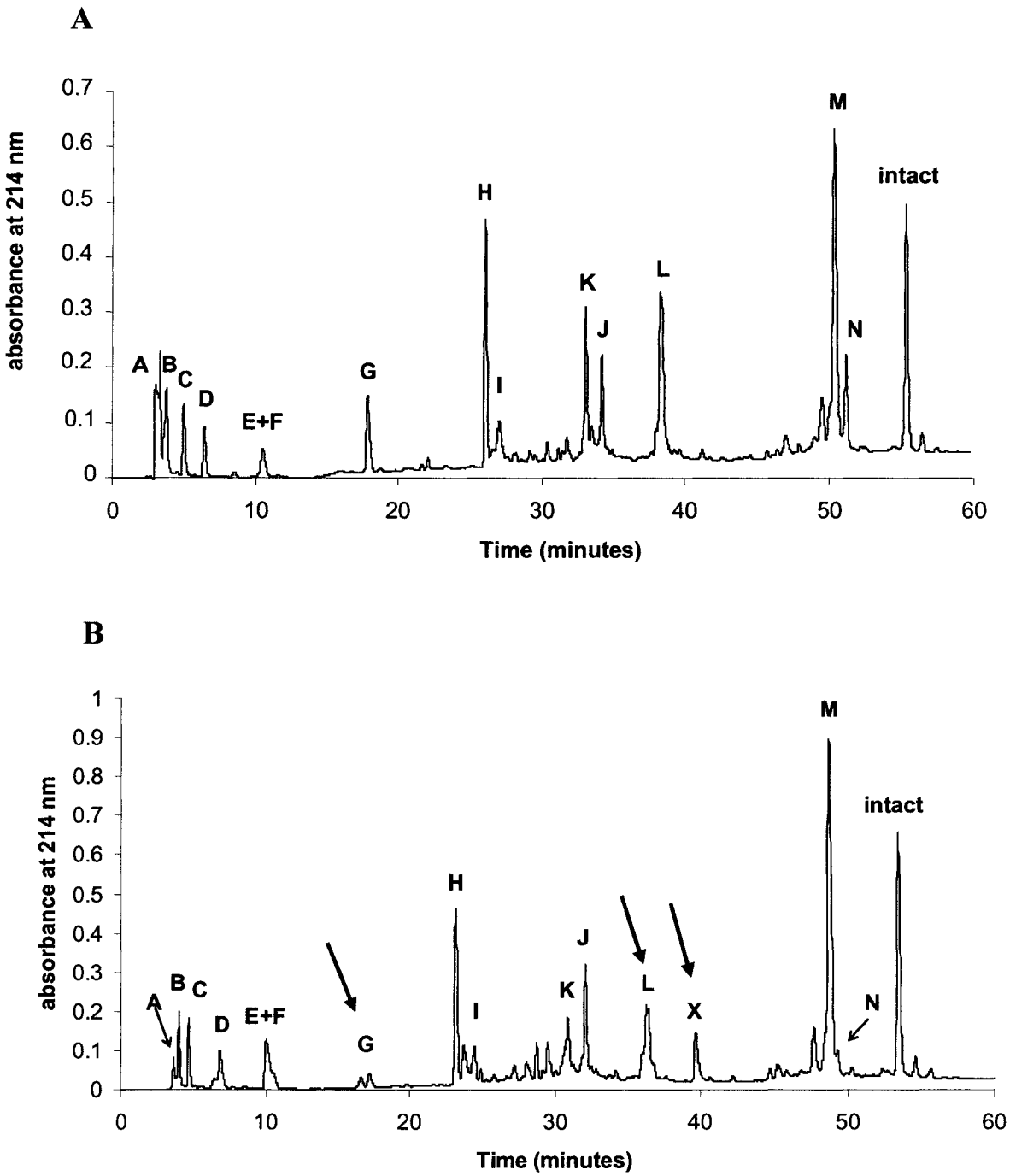

Figure 3.3.6 Tryptic peptide map of S-carbaminomethylated native monomeric RNase A **(A)** and S-carbaminomethylated *in vacuo* cross-linked RNase A dimer **(B)**. Peptides from the tryptic digest were separated on a 0.46 x 30 cm C_{18} reverse phase column using solvent systems A (5 % ACN, 0.1% TFA) and B (95% ACN, 0.1% TFA). A linear gradient of 0 to 35% B from 5 to 65 mins was employed. The flow rate was 1 mL/min and the column effluent was monitored at 214 nm. The red arrows indicate the reduction in height of peak G and L, as well as, the appearance of peak X in the dimer tryptic digest.

The differences in the monomeric and dimer tryptic digest RP-HPLC chromatograms are shown by the red arrows in Figure 3.3.6B. The height of the tryptic peak labeled "G" in the dimer digestion profile appears to have decreased compared to its relative height in the monomer digest. Also, peak "L" also appears to have decreased in height relative to the corresponding peak on the monomeric profile. A new peak was observed in the dimer digestion chromatogram, labeled peak "X", which eluted at 40 minutes. At this elution time, there is no corresponding peak observed in the monomeric digest; therefore, it was presumed that this peak represents the elution of the cross-linked peptide. Referring to the amino acid sequences of peak G and L, it was learned that peptide G must contain the carboxylic acid component (G is only a tripetide: Phe-Glu-Arg) and the peptide preceding L in the sequence, peptide F should contain the missed tryptic lysine site, the lysine presumed to be contained in the link. Peptide F would therefore be also expected to be reduced in abundance on the RP-HPLC chromatogram, however, its co-elution time with peptide E made this loss difficult to observe.

3.3.5 Mass spectrometric analysis of the *in vacuo* cross-linked peptide

The decrease in abundance of peaks G, and L and the appearance of a new peak, labeled peak X, in the tryptic peptide map of the covalent dimer leads to the speculation that the cross-linking of peptide G to peptide F-L has generated a new peptide, which elutes as peak X. The eluted G and L peaks from the RNase A monomer digest and the eluted peak X from the dimer digest were individually collected and samples were prepared for electrospray ionization time of flight mass spectrometry (ESI-TOF-MS) to allow some preliminary identification of the peptide fragments present in each peak. ESI-TOF-MS of

peak G from the monomeric RNase A sample generated a peak at 452 m.u. which corresponds to a tripeptide, residues 8-10, of the RNase A amino acid sequence (data not shown). This peptide contains only three amino acids, $Phe_8 - Glu_9 - Arg_{10}$, therefore, if it is involved in the amide link in the RNase A dimer, the only possible link site is the carboxylic acid functionality of the glutamic acid residue. Peak L from the monomeric RNase A sample was also analyzed by ESI-TOF-MS and its resulting spectrum depicted a peak of mass 2364 m.u., representing the peptide containing residues 67-85 (data not shown). This fragment results from the expected trypsin cleavage sites at Lys_{66} and Arg_{85}. Given that this peptide is reduced in the dimer digestion profile, it can be presumed that the peptide preceding peptide L, the peptide containing Lys_{66} (peptide F) bears the lysine involved in the amide link.

The newly observed peak X eluted from the dimer digest HPLC separation was subjected to analysis by ESI-TOF-MS and its mass spectrum is shown in Figure 3.3.7. The spectrum shows three dominant peaks: a singly charged ion of mass 453.3, a triply charged ion of mass 953.6 and a doubly charged ion of mass 1430.5. The peak at mass 453.3 ± 1 m.u. represents the mass of the tripeptide observed from the mass spectrometric analysis of peak G, corresponding to residues 8-10 of the native RNase A sequence and is singly charged as expected. The triply charged ion at 953.6 and doubly charged at 1430.5 both deconvolute to an identical peptide of an average mass equal to 2858.8 ±1 m.u. which corresponds to a peptide containing residues 62-85 of the native RNase A sequence. This fragment contains Lys_{66}, which would normally be a tryptic cleavage site, but is appearing as a resistant tryptic site, presumably because it is involved in the amide link, and confirms the presence of the peptide F-L. Peak X is argued to represent the cross-linked peptide comprised of the peptide from residues 62-85 attached to residues 8-10 through an amide

bond formed from the ε-amino group of Lys_{66} and the carboxyl group of Glu_9. The appearance of peak G in this mass spectrometric analysis of peak X (where peak G is not expected to co-elute, as seen by the monomer digest) and the previous demonstration that the acidic conditions (required to ensure the peptides adopt a positive charge and become ionized) and high voltages (required for the subsequent vapourization in the vacuum chamber of the mass spectrometer) lends credence to this argument by suggesting that the cross-linked peptide contained in peak X is breaking down to generate peak G, the tripeptide containing Glu_9 and peptide F-L, the peptide containing the lysine partner of the cross-link. These data therefore strongly suggest that the amide cross-link in the *in vacuo* cross-linked dimer is formed between Lys_{66} and Glu_9.

This conclusion is further strengthened by close examination of the deconvolution of the ESI-TOF-MS spectrum of peak X eluted from the *in vacuo* cross-linked dimer RP-HPLC separation shown in Figure 3.3.8. The deconvoluted spectrum shows the appearance of a peak of 2858 ± 1 m.u., which corresponds to the Lys_{66} – containing "F-L" peptide fragment. In addition, a smaller peak is detected at 3292 ± 1 m.u. The observed mass of this latter peak is equal to the mass of this "F-L" peptide containing Lys_{66} (2858 m.u.) plus the mass of the Glu_9-containing tripeptide (452 m.u.) minus 18 m.u. (loss of one water molecule). This mass of this peak, therefore, corresponds exactly to that expected for the intact cross-linked peptide and indicates that a small amount of residual cross-linked peak X remains even after the acid treatment and vaporization required for mass spectrometric analysis. Figure 3.3.8 shows a schematic of the cross-linked peptide demonstrating the location of the amide cross-link.

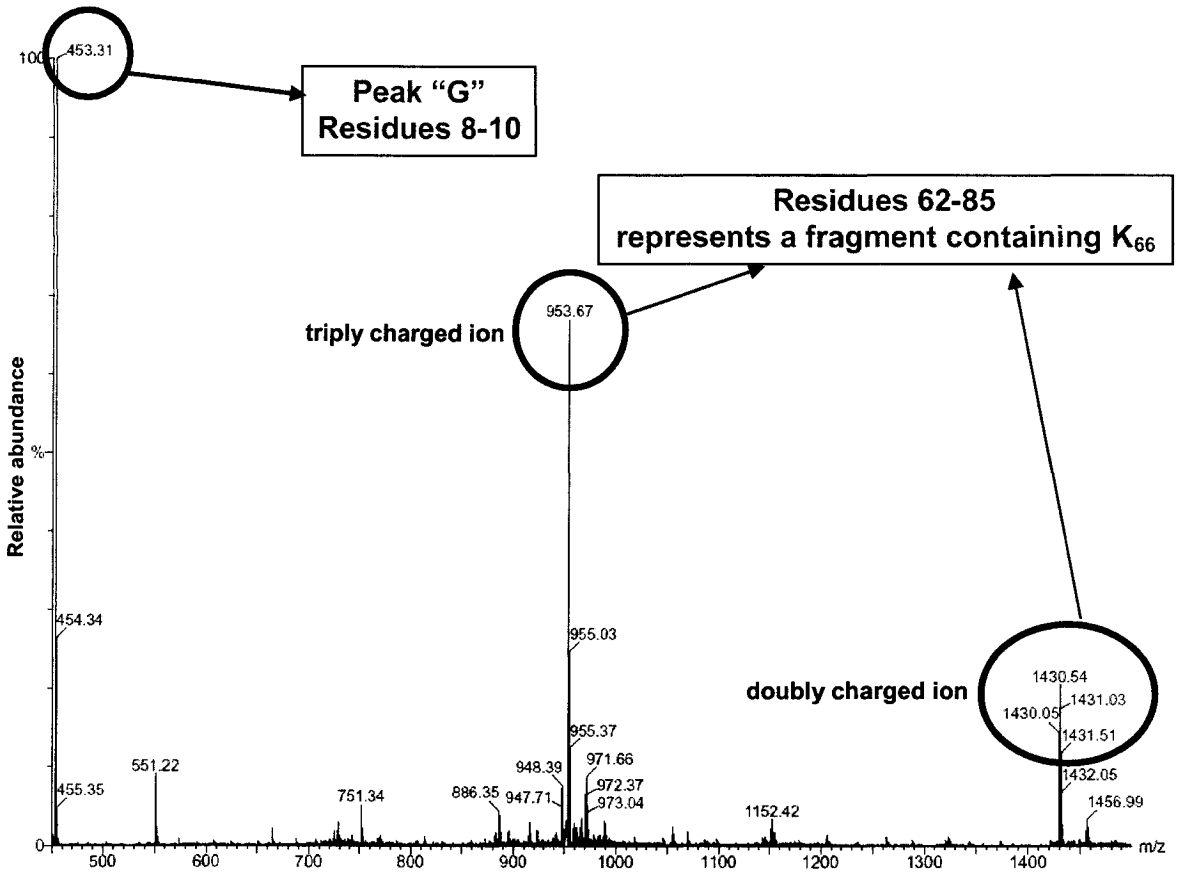

Figure 3.3.7 Electrospray ionization TOF mass spectrum of the eluted peak "X" from the tryptic digestion profile of the *in vacuo* cross-linked RNase A dimer collected from RP-HPLC. The mass peak of $453.3^{+} \pm 1$ m.u. corresponds to residues 8 -10 of the native RNase A sequence and mass peaks at 953.6^{+++} and 1430.5^{++} both deconvolute to the same peptide containing residues 62-85 of the native RNase A sequence.

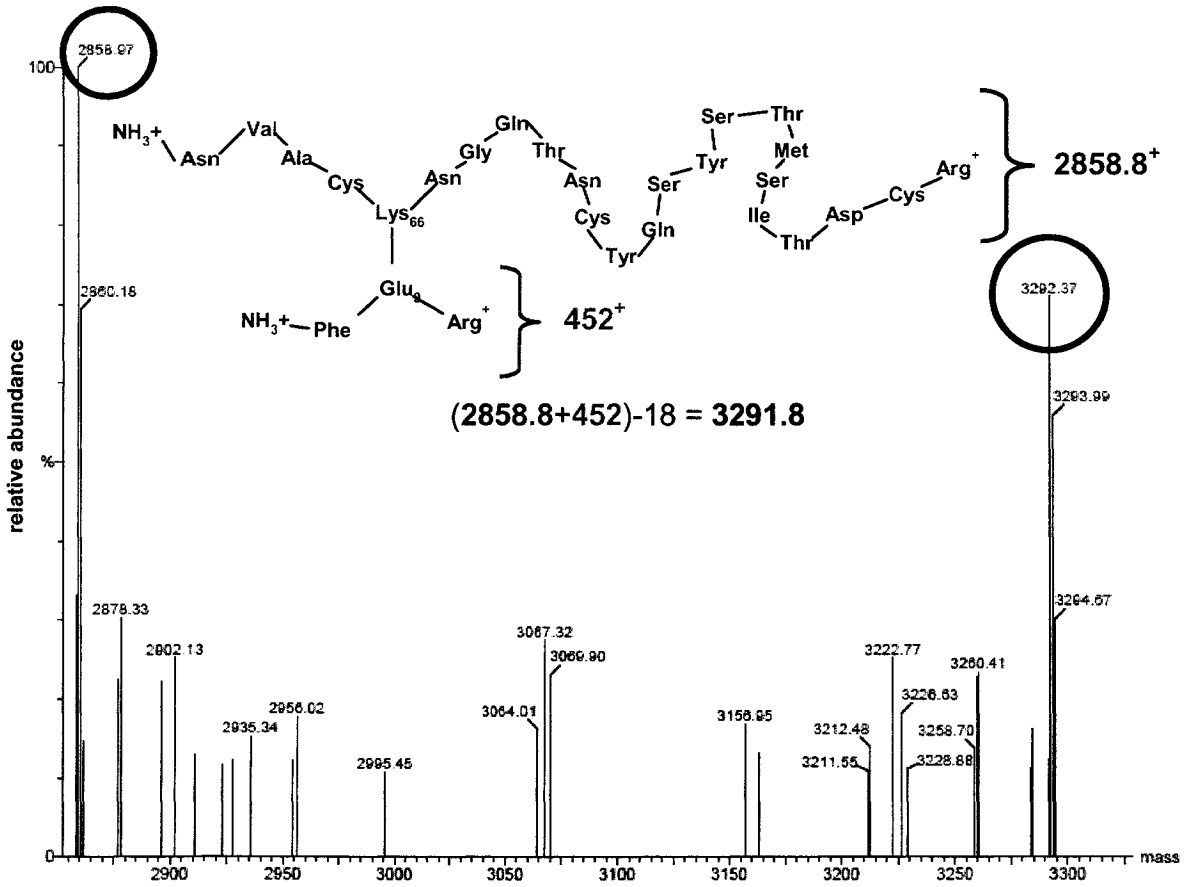

Figure 3.3.8 Deconvoluted Electrospray ionization TOF mass spectrum of the eluted peak "X" from the tryptic digestion profile of the *in vacuo* cross-linked RNase A dimer collected from RP-HPLC. The mass at 2858 ± 1 m.u. corresponds to the Lys_{66} containing fragment (sequence in blue). The intact cross-linked peptide (schematic shown) equals 3292.3 ± 1 m.u.

3.3.6 Analysis of X-ray crystallographic structures of RNase A

Having identified the point of cross-linking in the RNase A dimer formed by the *in vacuo* procedure, one naturally wonders whether the dimer thus formed is a covalent capture of one of the known conformers of non-covalent RNase A dimers or is, in fact a novel dimeric structure. The structures of the two non-covalent domain swapped dimers (formed when RNase A is lyophilized acetic acid) have been solved (Liu et al, 1998, PBD id =

1A2W; Liu et al., 2001, PBD id = 1F0V). The first non-covalent dimer, the "N-dimer", is the result of the N-terminal α-helix (residues 1-15) swapping with a second molecule. The second dimer, the "C-dimer", is formed by the swapping of the C-terminal β-strand (residues 116-124) of each monomer. These dimers were viewed using two different molecular modeling programs, Modeller (version 6.2, Accelerys, BC, CAN) and SETOR, a visualization program developed by Dr. Stephen Evans (Evans et al., 1993). Once the structures of the known domain-swapped dimers were imported into the modeling program, the side chain of the lysine residue corresponding to Lys_{66} was highlighted on one of the monomeric units. The side chain of the Glu_9 residue on the other monomeric unit was then highlighted in a second colour and the distance between the two measured. Figure 3.3.9A shows the X-ray crystallographic structure of the N-dimer with Lys_{66} from one monomer and Glu_9 from the second monomer highlighted and the corresponding distance measured. In this particular N-dimer swapped conformer, the distance between Lys_{66} and Glu_9 is 20.09 Å. The C-dimer structure is shown in Figure 3.3.9B, and the same measurement between Lys_{66} and Glu_9 resulted in a distance of > 30Å. In order for the Lys and the Glu residues to participate in a salt-bridge, the distance between the ε-N of the lysine side chain and the γ-O or β-O (these are electronically equivalent in resonance structure of the deprotonated form of the acid) of the glutamic acid side chain must be between 3 and 5 Å. Given the large distances measured between Lys_{66} and Glu_9 in both domain swapped conformers, it is highly unlikely that the *in vacuo* cross-linked dimer represents either of these structures.

Because the distances between these residues in both domain swapped dimers are much too great to allow for the formation of the salt bridge which we have demonstrated to be a necessary prerequisite for *in vacuo* cross-linking to occur (see results and discussion

below), the side chains of all acidic residues on the second monomeric unit in each dimer were then highlighted and compared to the location of Lys_{66} on the first monomeric unit. The distance from each γ-O or β-O from a glutamic or aspartic acid in this second monomer to the ε-N of the Lys_{66} of the first monomeric unit was then measured. Alternately, the side chain of Glu_9 was highlighted on the first molecule and the distances between its terminal oxygen atoms and the ε-amino nitrogens of all other lysine residues in the second monomeric unit were measured. These subsequent measurements were made to ascertain whether, if one of these dimers were indeed formed during the *in vacuo* procedure, a different cross-link would be expected to ensue. As shown in Figure 3.3.10A, Lys_{66} (coloured in green) is not close to any acidic residue (coloured in blue) from the domain swapped partner in the N-dimer. A similar conclusion is drawn if the same examination is made using Glu_9 of the first monomer to any Lys residue in the other monomer in the N-dimer (data not shown).

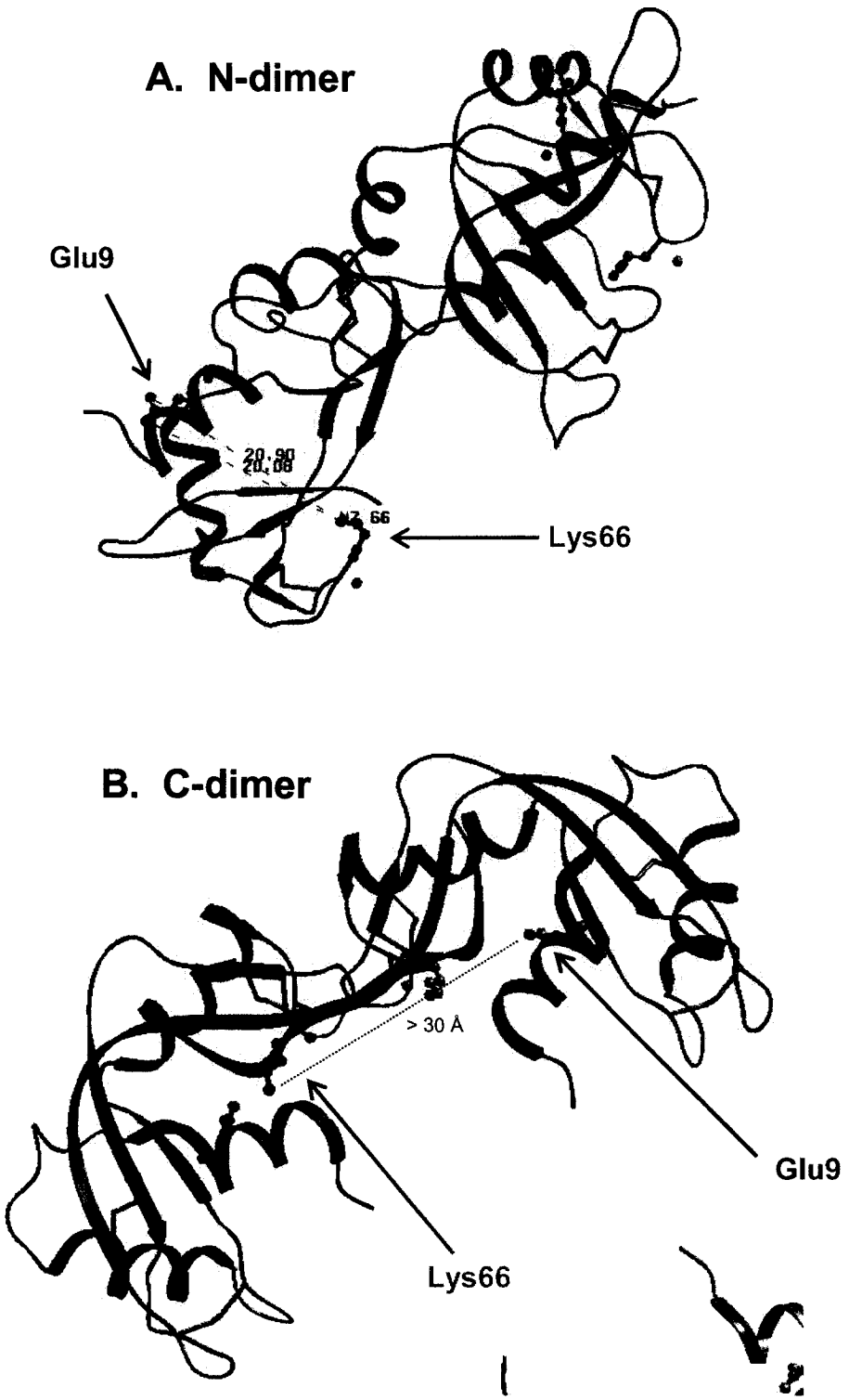

Figure 3.3.9 X-ray crystallographic structures of the N-terminal domain swapped dimer (A) and the C-terminal domain swapped dimer (B) displaying the position and distances between Lys_{66} and Glu_9. Structures (N-dimer PBD id = 1A2W and C-dimer PBD id = 1F0V) are viewed by SETOR (Evans, 1993).

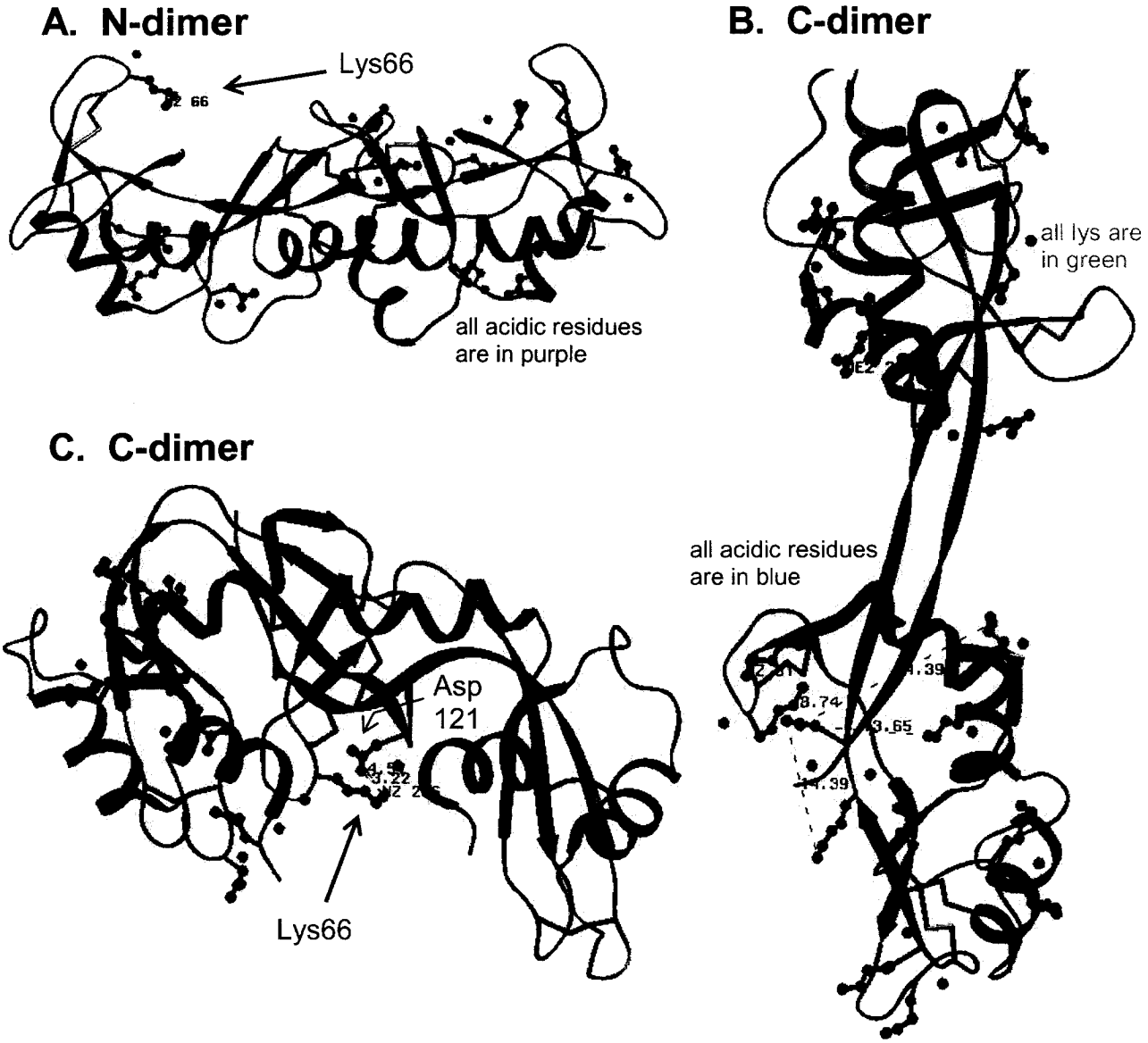

Figure 3.3.10 X-ray crystallographic structures of the N-terminal domain swapped dimer displaying the relative distances between Lys_{66} of one monomer to all the acidic residues on a second monomer **(A).** In the crystallographic structure of the C-dimer **(B),** all Lys residues are highlighted in green on one monomer and all the acidic residues are highlighted on a second monomer and some salt-bridging distances are shown. The salt-bridge between Lys_{66} and Asp_{121} in the C-dimer is shown in **(C).** Structures (N-dimer PBD id = 1A2W and C-dimer PBD id = 1F0V) are viewed by SETOR (Evans, 1993).

To determine if any salt-bridges of the required 3 to 5 Å interatomic distance exist in the C-dimer as formed in the crystal structure, all Lys residues from one C-dimer monomeric unit were examined for their location relative to all the acidic residues on the opposite interacting molecule. In Figure 3.3.10B, all the lysine residues are coloured in green and all acidic residues from a second monomer are coloured in blue. Measurements of distances between the ε-amino groups of lysine and the carboxyl groups from aspartic or glutamic acid residues reveal the possibility of salt-bridge interaction, between Lys_{66} and Asp_{121}. (The requisite groups are at an interatomic distance of 3.22 Å in this particular C-dimer conformer, as shown in Figure 3.3.10C). If indeed the RNase A dimer produced by the *in vacuo* procedure yielded a C-terminal domain swapped conformation, this salt-bridge, between Lys_{66} and Asp_{121}, would be expected to be the site of cross-linking and the linkage that we observed would not be expected to be formed. These data indicate, therefore, that neither the N-terminal domain swapped dimer nor the C-terminal domain swapped dimer are likely to represent the dimeric structure formed by the *in vacuo* cross-linking of RNase A.

Given the results of the inspection of the N-dimer and the C-dimers and the findings that Lys_{66} and Glu_9, in both of these dimeric conformations are located on opposite sides of the molecule, it was then necessary to determine whether these two residues are close in proximity, close enough to presume a salt-bridge interaction, in the crystallographic packing of the RNase A monomer unit cell. As the protein crystallizes out of solution, protein molecules can also associate by packing one distinct and separate monomeric unit against another to form the unit cell. It is difficult to predict *a priori,* however, if the driving force for packing of one surface against another would simulate the conditions of lyophilization, where all but the most essential water molecules are likely to be progressively removed as

the freeze-drying progresses. Proteins also undergo an exclusion of water at their surfaces during the process of crystallization, albeit through a different mechanism and often in the presence of salts, detergents, heavy metals, and in aqueous solutions. None-the-less, the unit cells of X-ray crystal structures do show monomeric units packed against each other in relatively dehydrated conditions that might approximate those of the lyophilization process used to generate the *in vacuo* cross-linked covalent dimer. The monomer-monomer interfaces in the unit cells of monomeric RNase A (PDB id 1RTB), the N-dimer (PDB id 1A2W), and the C-dimer (PDB id 1F0V) were all examined as described above using SETOR both to pack individual molecules in the unit cell and to visualize the positions of the pertinent functional groups. Six RNase A monomeric units, all coloured differently, are shown in Figure 3.3.11 packed into one unit cell. The Lys_{66} and Glu_9 side chains (labeled NZ 66 and OE1 9) on each monomeric unit are shown and the Lys_{66} and Glu_9 acid residues easily visible on two appropriately positioned monomeric units are highlighted. The distance between this lysine residue and the glutamic acid between monomeric units is 22.1 Å, a distance too great to presume a salt-bridge interaction between these two residues. The packing of monomeric RNase A in the unit cell in its crystalline form, therefore, does not explain of the linkage observed in the *in vacuo* covalently cross-linked dimer.

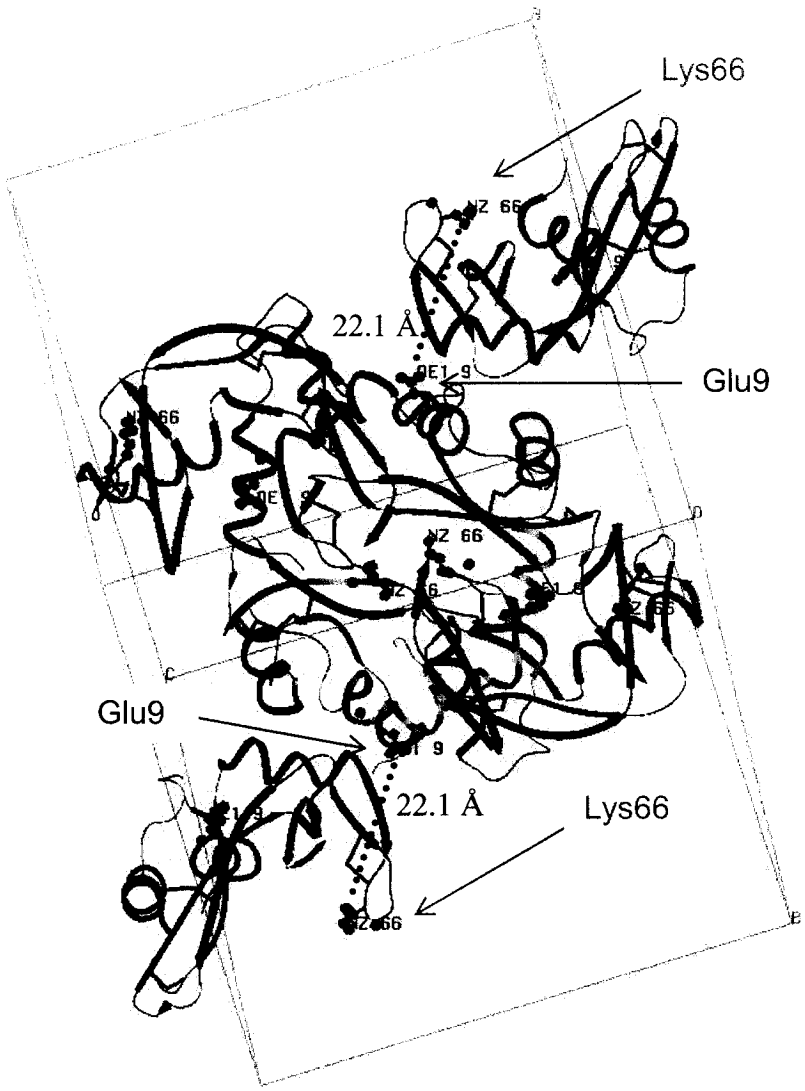

Figure 3.3.11 Six RNase A monomeric units (all coloured differently) packed into a unit cell. The distance between Lys_{66} and Glu_9 is shown by the dashed red line. Molecule viewing and unit cell packing optimization using PDB file id 1RTB and the figure was done by SETOR (Evans, 1993).

The question was then asked "if the lyophilization process had produced a packing similar to that observed in the unit cell of crystalline RNase A, would the *in vacuo* method have been able to capture that dimer?" To answer this question all lysine residues and all glutamic acid residues in the unit cell were highlighted and their relative distances examined

to determine if any inter-monomeric salt-bridging are present that would be covalently captured by the cross-linking procedure (model not shown). Indeed, an interatomic distance of 3.96 Å was measured between the requisite groups on Lys_{61} and Glu_9 between monomeric units - a short distance well within the range of an expected salt-bridge interaction. This salt-link, between Lys_{61} and Glu_9, was also observed by Fedorov et al., (1996). The results obtained by peptide mapping and mass spectrometry, however, do not indicate the involvement of Lys_{61} in the amide cross-link produced by the *in vacuo* procedure. These data also support the conclusion that this particular packing of RNase A into its unit cell is not representative of the packing of monomeric units in the lyophilized state.

Fedorov et al (1996), however, claim that different crystallization reagents and procedures may influence the positioning of the ε-amino group of Lys_{61} and perturb the salt-bridge interaction. The majority of the RNase A crystallographic structures reported in the literature, including that of Fedorov and co-workers (1996) as well as those of others (Dong and Bell, 1997; Campbell and Petsko, 1987) were generated from crystals grown from 30% ammonium sulfate, 3.0 M CsCl, and 0.1 M sodium acetate at pH 5. At this pH, the carboxyl groups from aspartic and glutamic acid residues are predicted to be only partially deprotonated (expected pK_a is ~ 4.5), and therefore, these particular crystallographic structures may not accurately represent the inter-monomeric salt bridge interactions that exist between monomeric units in lyophilization samples from solutions of neutral to slightly alkaline pH. In addition to the ionic and acidic conditions used in crystallography of RNase A, solvent molecules are shown to be an integral part of the crystal, where as many as 188 molecules of water are associated in the active site, binding site and N-terminal helix of RNase A (Fedorov et al., 1996). The extent of hydration of the RNase molecule in the

crystal may certainly differ from the low activity water that remains strongly bound to the protein after lyophilization. Upon lyophilization, the secondary structure content of RNase A demonstrates a slight decrease in helical content and an apparent increase in β-sheet (Griebenow and Klibanov, 1995; Bell, 1999). This slight conformational change in secondary structure would vary with different orientations of adjacent molecules, leading to perhaps a heterogeneous mix of ionic interactions in lyophilized preparations. It would be therefore reasonable to presume that RNase A molecules may adopt a different conformation in the lyophilized state.

The known crystallographic unit cell packing arrangements of all the structures of RNase A, the N-dimer and the C-dimer were also examined to ascertain the relative locations of Lys_{66} and Glu_9 in the dimers packed in the unit cell. The modeling of the unit cell of the C-dimer conformer indicates an interatomic distance of > 30 Å between Lys_{66} and Glu_9 in adjacent C-dimer molecules and therefore these residues are presumed as non-interacting (model not shown). A similar examination of the N-dimer crystal packing of the unit cell showed an interatomic measurement of 8.10 Å between Lys_{66} and Glu_9 in adjacent dimeric units (Figure 3.3.12 A and B). In Figure 3.3.12A, one N-dimeric molecule (in green) is interacting with a second dimer (silver) and Lys_{66} and Glu_9 are labeled in green and blue respectively at a distance of 8.10 Å. A clearer view is depicted in Figure 3.3.12B, where the same two molecules are displayed, however in this depiction, the non-covalent monomeric partners of each N-dimer are removed, showing only the conformation of one partner of the dimer. The crystallographic packing of the N-dimer unit cell results in a structure where the pertinent lysine and glutamine residues are in close proximity and close to the range that is expected for a salt-bridge interaction. While the two pertinent residues are close enough to

imagine that, with some adjustment, they may indeed form a salt bridge, the remaining parts of the monomeric units are not properly configured to give an active molecule without either major refolding or the participation of the non-covalent partner. There is no evidence for the presence of such non-covalent or covalent partners in the active covalent dimer formed by the *in vacuo* method. Likewise, to postulate the formation of the N-dimer, condensation to a crystal-like unit cell, covalent cross linking and then major refolding on dehydration, while possible, seems an unduly complex explanation for the formation of the covalent dimer. This examination of the known monomeric and dimeric X-ray crystal structures of RNase A therefore strongly suggests that the *in vacuo* RNase A dimer (with an amide linkage at Lys_{66} and Glu_9) does not result from a condensation reaction between interacting residues in a structure that is represented by one of these X-ray structures and is indeed a new dimeric structure not previously observed.

The examination of the known crystal structures also suggests that if, for example, the C –dimer was indeed pre-formed, it should be possible, under appropriate conditions, to "capture" this dimer covalently using the *in vacuo* procedure. Thus performing the *in vacuo* procedure on RNase A samples, lyophilized from 50% acetic acid solutions may yield an amide bond between Lys_{66} and Asp_{121}, if a salt linkage is present under these conditions. In addition to covalently capturing the major (and more active) conformer of non-covalent dimers, successful completion of this experiment would provide further evidence for the mechanism proposed for the *in vacuo* method, namely the condensation reaction of a pre-existing salt bridge.

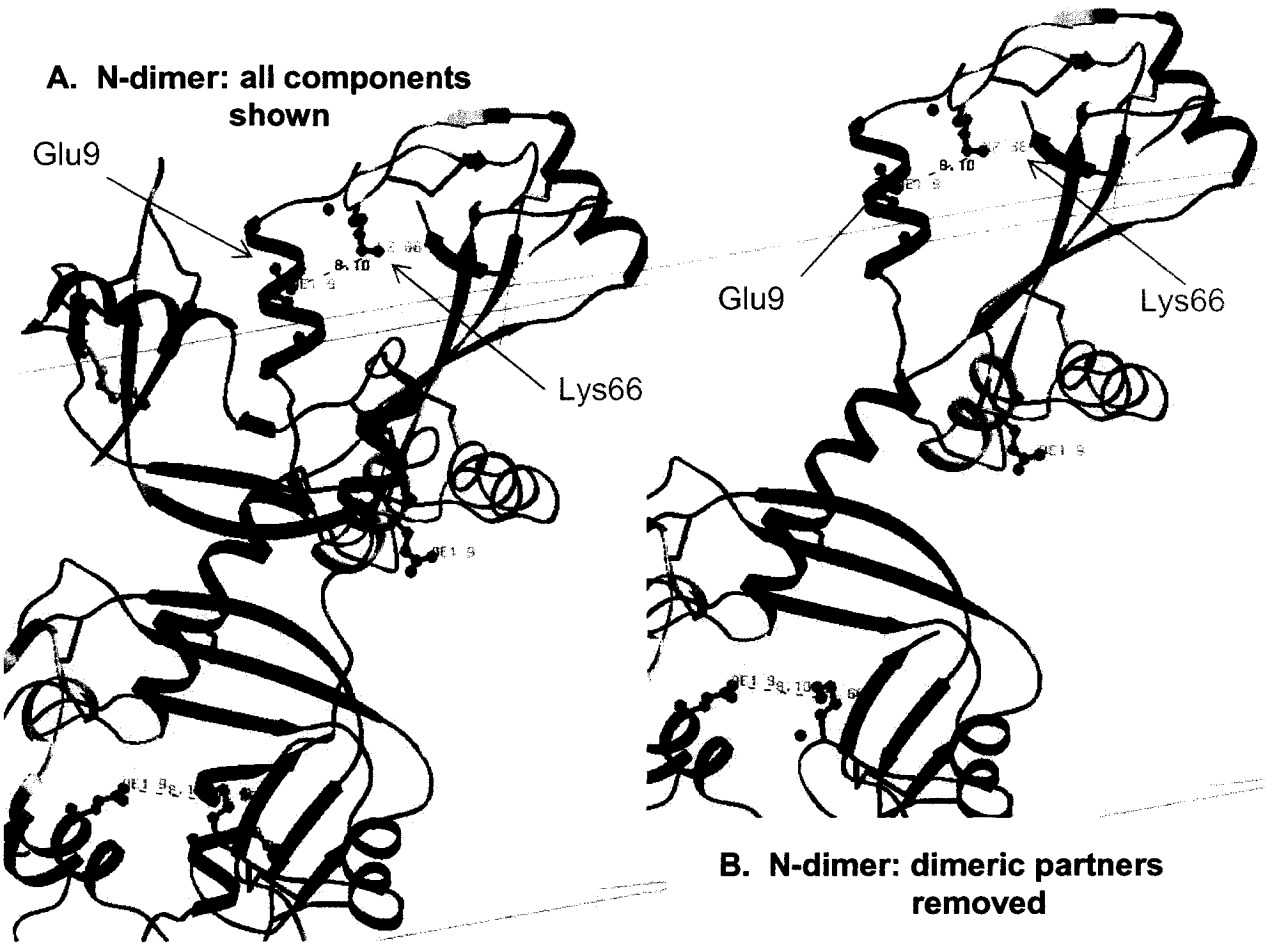

Figure 3.3.12 The crystallographic packing of the N-terminal domain swapped RNase A dimer into its unit cell. **(A)** shows a N-dimer molecule in green interacting with another N-dimer molecule coloured silver. Lysine 66 and glutamic acid 9 are labeled in green and blue respectively. **(B)** shows the same two N-dimer molecule as in A, with the non-covalent dimeric counterparts removed. N-dimer originates from the PDB file 1AW2 and the figure is generated from the modeling software SETOR (Evans, 1993).

3.3.7 Activity of the RNase A dimer

Earlier studies with non-covalent dimers of RNase A (Gotte and Libonati, 1998; Gotte et al., 1999; Park and Raines, 2000) and covalent dimers produced by traditional chemical cross-linking reactions (Gotte et al., 1997) indicate that the dimerization of RNase A can result in changes to the enzymatic behavior of the protein, changes that make dimeric RNases potential therapeutic agents. It was, therefore, of interest to determine the enzymatic properties of the RNase A dimer produced by the *in vacuo* cross-linking procedure. The ability of the dimer to cleave RNA substrates was compared to that of the RNase monomer using a well-known assay developed by Kunitz (1946). This method is based upon a hypsochromic shift in the absorption maximum of the UV of the polynucleotide substrate, in this case, Poly(A)·Poly(U) dsRNA upon digestion to smaller fragments. The activity is determined by measuring the difference in absorbance at 260 nm as a function of time; the initial velocity is determined by the following equation:

$$V_o = \frac{dA / dt}{\Delta A}$$

The dA/dt term represents the slope of the linear part of the curve and ΔA is the maximum absorbance obtainable (i.e. the plateau of the absorbance versus time curve). The slope divided by ΔA represents the initial velocity (V_o) is also referred to as a "Kunitz Unit". Figure 3.3.13 shows the effect of different substrate concentrations on the rate of change of absorbance as a function of RNase digestion time on both the dimer and monomer. The activity is measured in the linear part of the curve taken between 11-27 minutes, where the reaction is first order in substrate concentration.

The k_{cat}/K_M is therefore defined as:

$$k_{cat} / K_M = \frac{V_o}{[E]}$$

The initial velocity, divided by the amount of enzyme in milligrams, therefore equals k_{cat}/K_M. Michaelis-Menton analysis of this kinetic assay is calculated and initial velocity is plotted against substrate concentration, as shown in Figure 3.3.14. From this plot, it is apparent that the slope of the dimer curve (red) is twice that of the monomer curve (blue). Because of the limitations of this assay, such as the parallel absorbance of the substrate and the enzyme in exactly the same UV region as the product absorbance measurement at 260 nm, it is impossible to measure V_{max} or K_M independently in this assay. Therefore, k_{cat}/K_M, which also equals $V_o/[E]$ and gives a measure of the catalytic efficiency of the enzyme was used as a standard of comparison. In order to compare the catalytic efficiency of single monomeric units in the dimer with single molecules of monomeric RNase A, the k_{cat}/K_M values are expressed per mg of protein present in the assay and, thus expressed, give a measure of the specific activity of monomeric units in the dimer and monomer. These values are shown in Table 3.3.2. The k_{cat}/K_M of the dimer is twice that of the monomer (per mg of protein), 0.34 ±0.0007 and 0.17± 0.0007 $\mu g/mL \cdot min^{-1} \cdot mg^{-1}$ respectively.

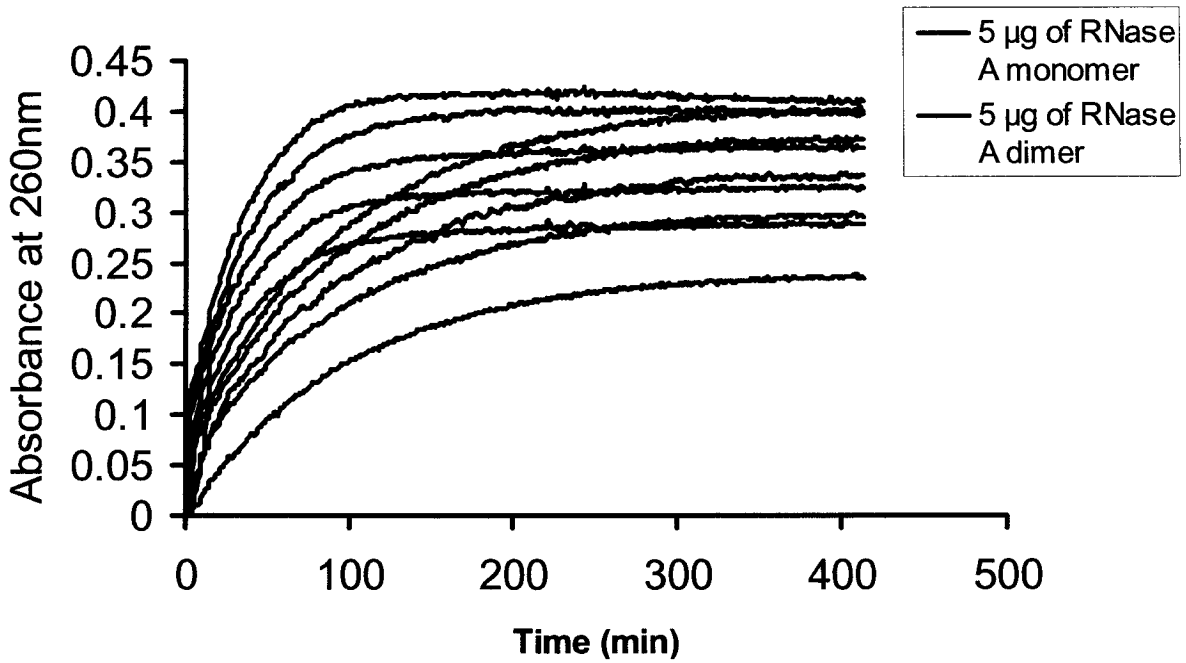

Figure 3.3.13 Kunitz ribonuclease activity assay. The difference in absorbance at 260 nm measured over time monitors the catalytic activity of 5 µg of RNase A monomer and 5 µg of the *in vacuo* cross-linked dimer towards dsRNA substrate Poly(A)·Poly(U) in amounts of 12, 14, 16, 18, and 20 µg..

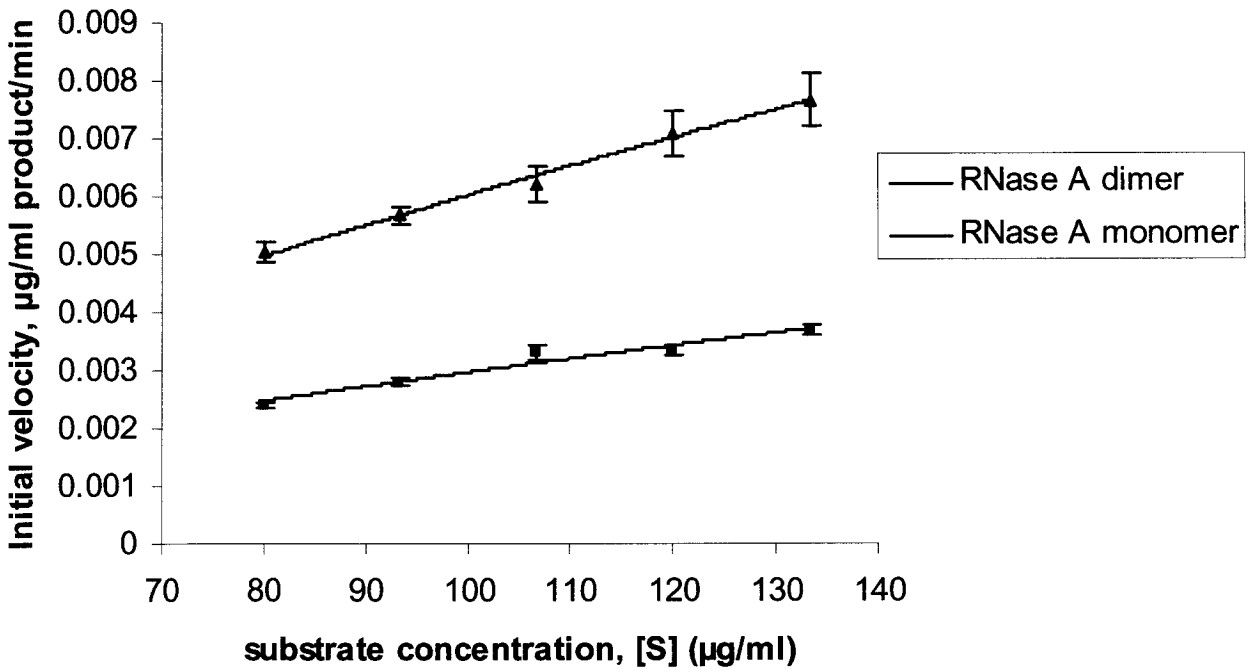

Figure 3.3.14 Michaelis-Menton analysis of RNase A monomer and the *in vacuo* cross-linked dimer. Initial velocity (V_o), calculated from the linear region of the absorbance over time curve shown in Figure 3.3.13, is plotted against substrate concentration.

Table 3.3.2 A comparison between the specific activities of RNase A monomer and the *in vacuo* cross-linked dimer.		
Ribonuclease A species	***Kunitz units ($\mu g/mL \cdot min^{-1}$)**	****k_{cat}/K_M Kunitz unit/mg protein**
monomer	0.008 ± 0.0009	0.17 ± 0.0007
***in vacuo* cross-linked dimer**	0.018 ± 0.0004	0.35 ± 0.000696

* Kunitz unit is calculated as an increase in absorbance per min/total measurable increase for [Poly(A)·Poly(U)] = 20 µg
**Specific activity can be estimated by the Kunitz units/mg protein or k_{cat}/K_M

The doubling of enzymatic activity per mg of enzyme displayed by the RNase A dimer and the fact that the dimeric ribonuclease molecule now has two active sites may be coincidental. However, this heightened activity of RNase A dimers against dsRNA was also observed by Gotte and Libonati, 1998; Gotte et al., 1999; Lui et al., 1998; and Park and Raines, 2000. These groups reported a doubling of the dimeric activity, even in different ribonuclease activity assays using different types of dsRNA substrates. This doubling in activity is explained by a presumed destabilization effect on polynucleotide substrates from an increase in surface positive charge density on the dimer molecule acting upon the negatively charged backbone of RNA (Matousek et al., 2003). The transient single stranded stretches of RNA that are exposed are now susceptible to attack from two composite active sites (one from each monomeric unit) and it is this effect that is thought to account for a coincidental increase in catalytic efficiency attributed to a dimeric structure. The *in vacuo* cross-linked RNase A dimer also demonstrates this doubling of enzymatic activity, per mg of total enzyme, which suggests that the *in vacuo* cross-linked dimeric RNase A possess similar catalytic properties to the naturally occurring and acetic acid lyophilized non-covalent

dimeric aggregates reported in the literature (Gotte et al., 1999). The retention of at least full catalytic activity of the dimer reinforces the conclusion (from Chapter 2) that the *in vacuo* method of cross-linking does not destroy the structure or function of the proteins being treated.

The activity of the dimer and monomer were also evaluated in the presence of the known cytosolic Ribonuclease Inhibitor (RI). Figure 3.3.15 represents the Kunitz assay with and without 2000 units of RI added to the enzyme assay. According to first order kinetics, the initial velocity of the enzyme is evaluated by the slope of the linear portion of the curve. The *in vacuo* cross-linked dimer with (orange line) and without 2000 units of RI (red curve) shows identical slopes in the region between 0 to 80 minutes and the curves almost completely superimpose. The reaction plateau of these curves, however, does not reach identical points. This observation, however, is not unexpected: the addition of 2000 units of RI into the reaction increases the total amount of protein in the mixture and protein molecules contribute to the overall absorbance at this wavelength, which consequently also increases the total obtainable absorbance at 260 nm. The RNase A monomer activity (blue line) without RI, again, shows an initial velocity which is half that of the dimer reaction. However, the addition of 2000 units of RI into the monomer activity reaction completely destroys the activity of the monomer and there is no measured increase in absorbance at 260 nm. Once again, this effect of RI on RNase A is and reflects its well known inhibition constant (K_i) equal to 6.9 nM (Haigis et al., 2003).

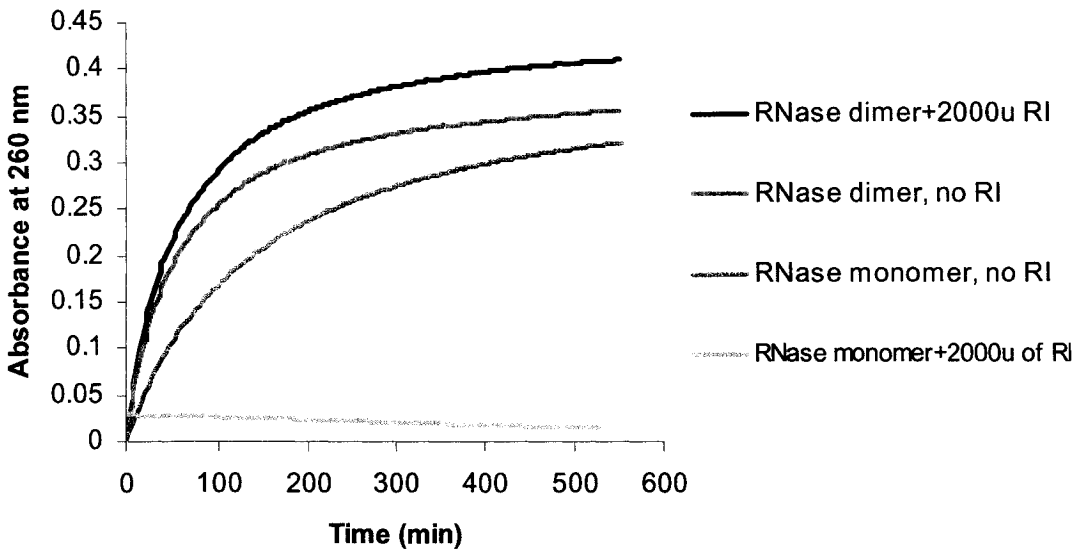

Figure 3.3.15 Kunitz ribonuclease activity assay in the presence of cytosolic Ribonuclease Inhibitor (RI). The difference in absorbance at 260 nm measured over time monitors the catalytic activity of 5 µg of RNase A monomer and RNase A dimer was added to 20 µg of Poly(A)·Poly(U) substrate with 0 units or 2000 units of RI.

These results demonstrate that the *in vacuo* cross-linked RNase A dimer is resistant to inhibition by RI. This escape from inhibition by RI was also observed by RNase A dimeric derivatives prepared by the chemical cross-linking of RNase A using the bifunctional reagent dimethyl suberimidate (Gotte and Libonati, 1998; and Gotte et al., 1999). It is proposed that, once inside the cell, RI binds with monomeric RNase A and this interaction prevents the catalytically degradation of RNA (Haigis et al., 2003). This regulatory mechanism can also be defeated if RNase A forms a natural non-covalent dimer, through 3D domain swapping (Monti and D'Alessio, 2004). These authors propose that it is the sheer size of the dimeric forms of RNase that prevents it from binding and interacting with the large horse-shoe-like structure of RI. As a result of their increased catalytic activity

towards dsRNA and their ability to evade inhibition by the naturally-occurring cellular inhibitor RI, RNase A dimers appear to remain completely operable at all times and thus have a greater cellular toxicity (by degrading RNA and stopping protein synthesis). Stable, chemically cross-linked, RNase A dimers are viewed as promising cancer therapeutics (Kim et al., 1995; Cafaro et al., 1998; Leland et al., 1998 and reviewed by Youle et al., 1993) since they are presumed to mimic and enhance the modulated cellular activity of the natural non-covalent RNase A dimer inside the cell. The *in vacuo* cross-linked dimer may be an even more suitable candidate for cancer therapeutics than the aggregated, non-covalent forms of RNase A dimers or the dimeric forms produced by conventional methods of chemical cross-linking, because the *in vacuo* product would have a higher conformational stability than the former moieties (by virtue of the covalent nature of the linkage between monomeric units) and, unlike the latter, was not produced using activating reagents or other chemicals, (traces of which may be present in other purified preparations of those RNase dimers, compromising their potential for safe therapeutic use).

3.3.8 A comparison of enzymatic activity between RNase A and ONC

Onconase™ (a registered trade mark of Alfacell Inc.) and RNase A share a 30% sequence homology and have similar tertiary structure, yet have been reported to differ in catalytic activity and affinity for the cytosolic ribonuclease inhibitor (Haigis et al., 2003). Since Onconase™ has shown to display both antitumor and antiviral activity, and is now in Phase III clinical trials for the treatment of malignant mesothelioma (Wu et al., 1995), a comparison of ribonuclease activity the *in vacuo* cross-linked RNase A to that of Onconase™ seemed appropriate. This initial kinetic analysis was undertaken with a view to

compare ribonuclease activities of *in vacuo* cross-linked RNase A dimers, ONC, our in-house version of Onconase™, and an *in vacuo* cross-linked RNase A-ONC heterodimer which would be created in the hope of combining the positive attributes of both enzymes, thus generating an improved therapeutic ribonuclease.

The activities of *in vacuo* cross-linked RNase A dimer, ONC, and monomeric RNase A were measured by monitoring the fluorescence generated when a fluorescently labeled ssRNA substrate is cleaved upon digestion by a ribonuclease enzyme. The relative fluorescence units (RFU) were measured over time with a fluorimeter equipped with an excitation/emission filter set at 485/535 nm. Enzyme velocity curves were generated, as shown in Figure 3.3.16. A unit of activity by this fluorometric assay is defined by the rate of relative fluorescence detection over time divided by the total fluorescent counts obtainable per reaction (Equation 3.4, Materials and Methods section 3.2). The activity units, divided by the total amount of enzyme (in pg) gives an estimate of the specific activity of the enzyme. These values are listed in Table 3.4. As demonstrated by the slope of the linear portion of the RFU against time curves, the *in vacuo* RNase A dimer shows an increase in activity compared to the activity of monomeric RNase A, as previously shown in the Kunitz assay using dsRNA substrates. The activity of the ONC sample, with approximately the same total amount of protein, generates a lower activity that those seen with RNase A monomer and dimer, almost a 3-fold decrease in activity compared to monomeric RNase A.

Interesting to note is the apparent ability of the *in vacuo* cross-linked dimer to catalyze the degradation of a ssRNA substrate, a property that the non-covalent, acetic acid lyophilized dimers demonstrate with a significantly reduced specific activity compared to native RNase A. Park and Raines (2000) report that the acid lyophilized non-covalent dimer

displayed a 4-fold decrease in specific activity towards poly(cytidylic acid), a single stranded polyribonucleic acid polymer. The enhanced ribonuclease activity of the *in vacuo* cross-linked dimer compared to monomeric RNase A towards the fluoro-ssRNA substrate used in this assay further establishes reason to suspect that the *in vacuo* dimer may display a novel dimeric conformation.

In the presence of the cytosolic ribonuclease inhibitor, monomeric RNase A is completely inactive as shown by the flat line in Figure 3.3.16. Both ONC and the *in vacuo* cross-linked RNase A dimer do, however, remain completely active in the presence of 40 units of RI and do not show any decrease in catalytic efficiency compared to the enzyme assayed alone. The ability of ONC to remain active in the presence of RI is thought to endow it with unique biological activity important to its cytotoxicity (Haigis et al., 2003). The ability of the RNase A dimer to do the same may be likewise important.

It should be noted that ONC preferentially cleaves the phosphodiester bond between uridine and guanosine residues, a different site than RNase A's specificity for uridine and cytosine nucleotides (Lee and Raines, 2003). The fluoro-RNA substrate used in this assay (a kit purchased commercially) may not contain an equal amount of both ONC and RNase cleavage sites resulting, perhaps, in a misrepresentation of the exact catalytic efficiencies of the two enzymes. However, the objectives of this experiment were to determine whether RNase A is indeed a more catalytically active enzyme than ONC and to determine the effect of RI on the enzymatic efficiency of both ribonucleases. The differences in catalysis between the ONC and both the RNase A monomer and RNase A dimer in the absence of inhibitor are striking and any minor errors resulting from an unequal number of preferred cleavage sites in the substrate are unlikely to change the interpretation of the result.

Likewise, the retention of ONC activity in the presence of RI is what is expected from the literature (Haigis et al., 2002 and Boix et al., 1996) and indicates that the in-house version of ONC behaves very much like the Onconase™ and can be used as a positive control in cytotoxicity assays. In addition, the confirmation of the ability of the *in vacuo* cross-linked dimer to evade inhibition warrants it further testing for cytotoxicity.

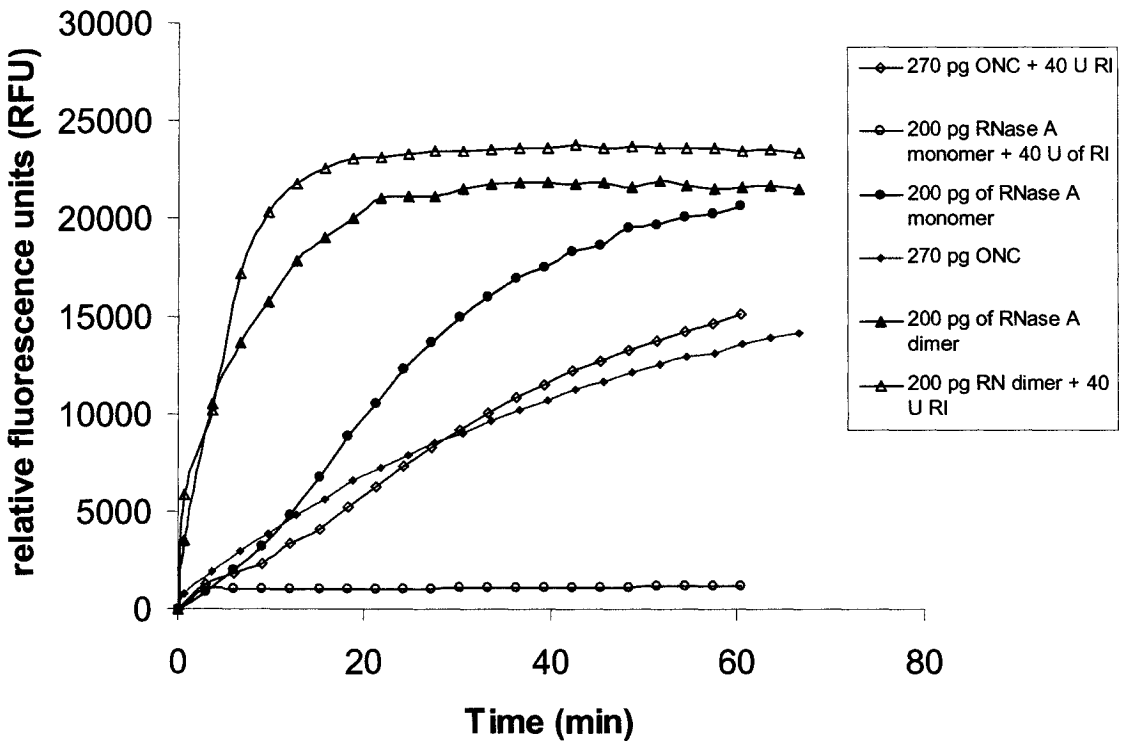

Figure 3.3.16 Fluorometric ribonuclease assay of ONC (green line), RNase A monomer (blue line), and *in vacuo* cross-linked RNase A dimer (red line) in the presence of cytosolic Ribonuclease Inhibitor (RI) (open symbols) and absence (closed symbols). Assay performed with 50 pmol of fluoro-ssRNA substrate per reaction and 40 units of RI, where indicated. Total enzyme per reaction is 200 pg or 270 pg in the case of ONC. Reaction was monitored using a fluorometer at excitation/emission = 485/535 nm, readings were taken every 3 minutes over 1 hour.

Table 3.3.3 Fluoro-activity units over total amount of enzyme in *pico*grams to determine enzyme efficiency	
Ribonuclease species	**Units/pg enzyme (units/pg)**
RNase A monomer	1.7×10^{-4}
RNase A in the presence of RI	0
In vacuo cross-linked dimer	4.2×10^{-4}
In vacuo cross-linked dimer in the presence of RI	4.6×10^{-4}
ONC	1.0×10^{-4}
ONC in the presence of RI	9.5×10^{-5}

In addition, because both ONC and the dimeric RNase A produced here can evade inhibition by RI, one would predict that a ribonuclease heterodimer composed of an *in vacuo* cross-link between RNase A and ONC would also be active in the presence of RI. Such a dimer, with one monomer (RNase A) showing enhance activity against the desired substrate and the other monomer (ONC) able to effectively gain entrance into target cells, may well be a more effective cytotoxic agent than Onconase™ itself. The *in vacuo* cross-linking of RNase A (14 kDa) and ONC (12 kDa) yielded a combination of what appeared to be (based on the estimation of molecular size on SDS-PAGE) the following cross-linked products: RNase A homodimer, ONC homodimer, and ONC-RNase A heterodimer. These products were not easily resolved by gel electrophoresis (data not shown), even with varying degrees of polymerized gel matrices. By reducing the length of time incubating under vacuum, the amount of each dimeric species generated was reduced, improving resolution on gel electrophoresis. However, reduced yield of each dimeric species make it difficult to subject the cross-linked mixture to chromatographic methods and effectively isolate and purify the RNase A – ONC dimer. Some scale-up of the methodology is therefore required. Such a

project, though of both theoretical and practical interest, is beyond the scope of this thesis work. This opportunity to further develop a method for the production and purification of the RNase A-ONC heterodimer was, therefore, left for others to pursue.

3.3.9 Cytotoxicity testing of ONC and RNase A derivatives

Given the enzymatic activity and inhibition results of the *in vitro* ribonuclease assay, and the observation that ONC is less active towards RNA substrates than either the RNase A monomer or dimer, the next step was to assess the cytotoxicity of the ribonucleases in an HL-60 lymphocytic leukemia cell line. Cytotoxicity was assessed by examining the extent of cell proliferation in the presence of the ribonuclease. A cell viability assay was performed by quantifying the incorporation of [methyl-^{3}H]thymidine into replicating DNA; the total ^{3}H content of the cells was measured with liquid scintillation counting. The ^{3}H counts per minute (CPM) in each experimental sample was compared to the media control, a sham assay that did not contain any exogenous ribonuclease, and gives an assessment of the cytotoxicity (*viz* non-proliferating cells) at each concentration of each ribonuclease tested.

Figure 3.3.18 shows the total ^{3}H counts in each HL-60 cell cultured sample after the indicated dosages of ONC or cyclohexamide (CHX). (Cyclohexamide is an agent which blocks protein synthesis and the cells stop proliferating; this sample culture is used as a positive control to ensure that the assay is functioning properly.) Upon increasing the concentration of ONC from 0.42 μM to 13.5 μM, the CPM measured droped dramatically indicating that at a concentration at 13.5 μM, the cells were no longer replicating. This result that ONC induces a cytotoxic effect on this particular cell line at a μM dosing range is

consistent with results reported in the literature (Wu et al., 1995; Klink and Raines, 2000; and Haigis et al., 2001).

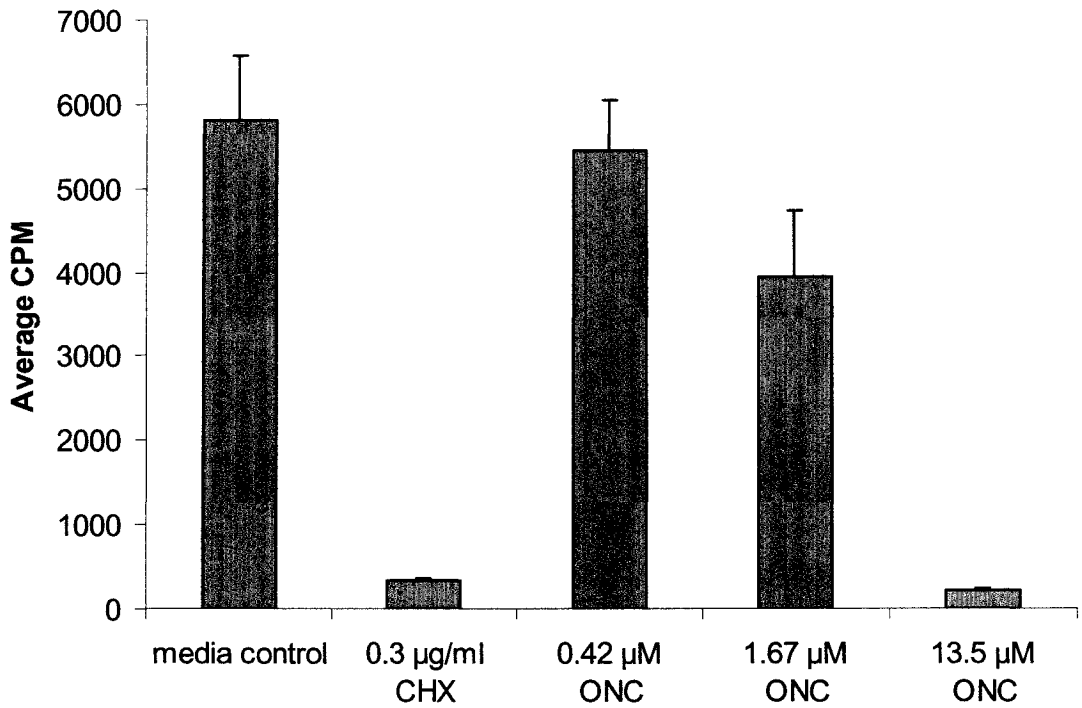

Figure 3.3.17 Effect of concentration of ONC on the cell proliferation of HL-60 cells. Proliferation was measured by the incorporation of [methyl-^{3}H]thymidine into replicating DNA after a 4 hour incubation with ONC. Values reported are the average from three cultures.

RNase A monomer and the *in vacuo* cross-linked RNase A dimer were then assayed for cytotoxicity against the same HL-60 cell line at increasing concentrations of ribonuclease in µg/mL (Figure 3.3.18). At a concentration range of 10 – 50 µg/µL (or 1 – 2 µM), monomeric RNase A showed only a very slight and inconsistent decrease in CPM compared to the media control, however, this small difference may not be significant as shown by the

error bars representing the standard deviation of triplicate trials. RNase A is not expected to disrupt cell proliferation and is not known to be cytotoxic, even at M concentrations (Di Donato et al., 1994). In this preliminary experiment dimeric RNase A showed a similar slight decrease in CPM as the concentration increased from 10 µg/mL to 50 µg/mL. While cell viability did tend to decrease consistently with increasing concentrations of the *in vacuo* cross-linked dimer, there is a relatively large standard deviation resulting from triplicate trials. The concentration effect suggested by these data, therefore, is not significant enough to conclude that RNase A dimer is indeed displaying cytotoxic capabilities. Careful reading of the literature in light of these results (Lee and Raines, 2003; Leland et al., 1998; Klink and Raines, 2002; Wu et al., 1995) indicates that, in addition to increased concentrations of dimeric RNase species, several other precautions should be taken in preparation of the samples. One research group cautions that samples be tested for cytotoxicity only when "freshly prepared" (Lee and Raines, 2003). (In the present, preliminary work, ONC samples were tested immediately after preparation but RNase A monomers and dimers were stored for significant lengths of time before use in cytotoxicity assays). Several parameters, including methods and the timing of sample concentration and length of storage of each preparation before cytotoxicity testing remain to be tested. In addition, this preliminary cytotoxicity experiment requires further testing of both monomeric and dimeric RNases at higher concentrations, such as those in the 10-50 µM ranges, to confidently report the presence or absence of a cytotoxic effect on this cancer cell line.

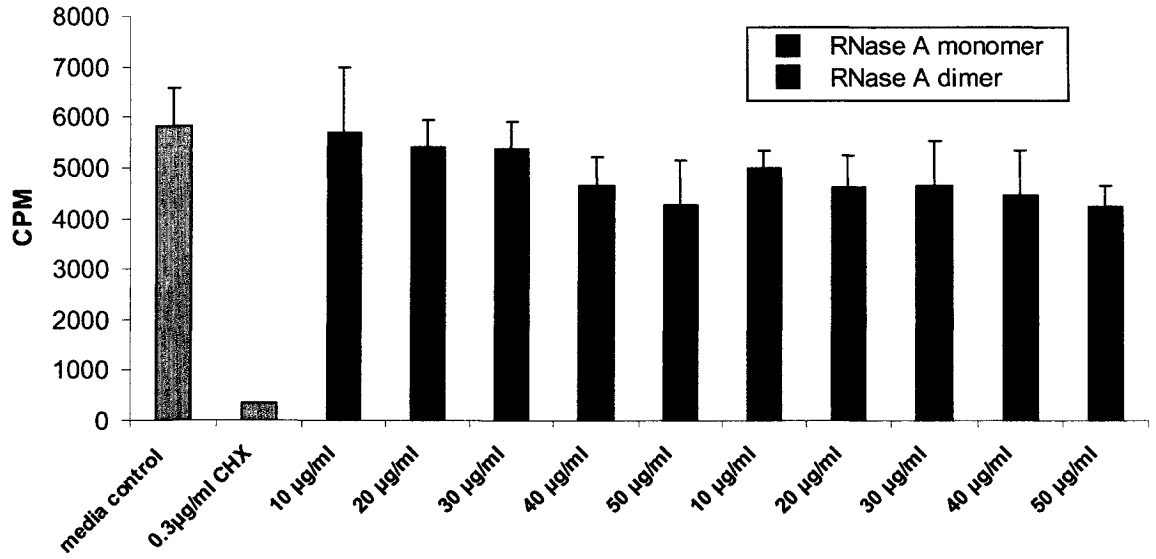

Figure 3.3.18 Cell proliferation assay of HL-60 cells treated with 10 µg/mL to 50 µg/mL of RNase A monomer (dark blue bars) and dimer (red bars). Proliferation was measured by the incorporation of [methyl-^{3}H]thymidine into replicating DNA after a 4 hour incubation with ONC. Values reported are the average from three cultures.

The objectives in this initial work were to simply establish a method and control samples for testing the cytotoxicity of these ribonucleases. The cytotoxicity assessment of the *in vacuo* cross-linked RNase A homodimer and the ONC-RNase A heterodimer in terms of EC_{50} values (effective concentration to kill 50% of the cells) has lead to work beyond the scope of this thesis and was left for others to investigate further.

3.4 Conclusion

Studies of RNase A have made great contributions to our understanding of protein structure and function in the past and, more recently, to the understanding of the formation of non-covalent oligomers by 3D-domain swapping. RNase A can form two different domain

swapped conformers, an N-terminal α-helix swap and a C-terminal β-strand swap, by an artificial procedure – lyophilization from a concentrated solution in 50% acetic acid (Crestfield et al., 1962). The X-ray crystallographic structures of these domain swapped dimers have been solved (Liu et al., 1998, and Liu et al., 2001). In addition to the structural and theoretical interest in the oligomerization of this enzyme, RNase A natural dimers exhibit an enhanced catalytic activity towards dsRNA substrates and a modulated biological activity *in vivo*. A strong correlation has been made between the biological activities of dimeric RNase A and the natural dimeric BS-RNase and the monomeric Onconase™ ribonucleases each of which demonstrate cytotoxicity effects on selected cancer cell lines (Leland et al., 1998; Matousek et al., 2003). This high catalytic efficiency of RNase A dimers in the degradation of several different types of RNA and their ability to resist inhibition by the cytosolic ribonuclease inhibitor has resulted in great interest in the development of RNase A dimeric variants in cancer therapy. Moreover, endowing mammalian ribonucleases with cytotoxicity could yield cancer chemotherapeutics that lack the undesirable side effects seen with foreign proteins.

The *in vacuo* cross-linking of RNase A and the structural and enzymatic characterization of the covalent dimer has lead to the discovery of a novel dimeric ribonuclease a unique structure, distinctly different from the non-covalent dimers produced by Crestfield's lyophilization procedure. As previously determined from the chemical and mass spectrometric results presented in Chapter 2, the *in vacuo* RNase A dimer is composed of two monomeric units attached by a single amide cross-link between a lysine residue and an acidic residue. Through further experimentation to investigate the location of the amide cross-link, it was determined that the bond introduced by the *in vacuo* procedure does not

induce any gross conformational changes to the overall structure of RNase A, yet is quite acid labile and, therefore, presumably exposed and conformationally strained. Careful examination of peptide mapping followed by mass spectrometric analysis revealed that the amide cross-link occurs at positions Lys_{66} and Glu_9 between interacting monomeric units.

Evidence is presented, through the review of the known crystal structures for the non-covalent domain swapped dimers by modeling that none of these known structures can easily account for the cross-link observed. In both the N-dimer and C-dimer molecular models, Lys_{66} and Glu_9 were not close enough to envision the *in vacuo* dimer adopting such conformations. As well, Lys_{66} and Glu_9 are not in close proximity in the crystallographic structure of RNase A monomeric packing arrangements in the unit cell. The crystallographic packing of the N-dimer into its unit cell, however, does show Lys_{66} and Glu_9 within a distance of 8 Å but considerable refolding of the monomeric units subsequent to amide bond cross-linking would be necessary to achieve the active covalent conformer observed. It is reasonable to presume that these X-ray crystallographic structures do not represent the true electrostatic interactions between molecules of the RNase A in the lyophilized state. Further experiments to systematically investigate the effect of lyophilization from acetic acid and the characterization of the resulting *in vacuo* cross-linked product may provide further proof to the unique conformation of the *in vacuo* covalent RNase A dimer produced by this method. Indeed sufficient evidence as to the novelty of the dimer produced by the *in vacuo* method has been obtained to justify an attempt to crystallize this dimer and determine its structure.

Given the unique structural properties of the *in vacuo* RNase A dimer, an assessment of the enzyme's catalytic properties and biological activities was pursued. The *in vacuo* RNase A dimer exhibits a 2-fold increase in activity over monomeric RNase A on a per

weight basis. This doubling of enzymatic activity was shown using two different types of RNA substrates, one a dsRNA and the other a ssRNA. Although some reports indicate that the non-covalent C-dimer can show catalytic activity values 20 times above that expected for monomeric RNase A in assays using dsRNA substrates (Gotte and Libonati, 1998; Gotte et al., 1999), unlike this covalent dimer, the non-covalent dimers consistently show a reduced catalytic activity towards ssRNA substrates (Park and Raines, 2000; Leland et al., 2001). In addition to this enhanced ability to degrade RNA, inhibition studies involving ribonuclease inhibitor protein (RI) in the ribonuclease activity assays determined that the *in vacuo* dimer is resistant to inhibition by RI – ascribing this dimer with a property linked to *in vivo* cytotoxicity.

Preliminary experiments were initiated to compare the enzymatic activity and the cytotoxicity of RNase A monomer and covalent dimer relative to ONC. The expression and purification of our in-house version of Onconase™ (ONC) yielded a cytotoxic ribonuclease that established a cell viability positive control sample to which to compare monomeric RNase A and *in vacuo* dimeric RNase A in cell proliferation assays. Despite the lack of conclusive data in the preliminary trials in testing the cytotoxicity of the *in vacuo* RNase A dimer, the experimental controls and the assay set-up is now established to systematically assay the ribonuclease derivatives, including a proposed RNase A – ONC heterodimer, in the appropriate dosing ranges.

The *in vacuo* cross-linked RNase A dimer appears to possess key features that are encouraging for its development as a novel protein therapeutic: (1) the *in vacuo* cross-linking procedure is a facile and cost-effective method of forming RNase A dimers and the process can be scaled-up for producing larger quantities; (2) *in vacuo* RNase A dimer displays

enhanced enzymatic activity and is not inactivated by the cytosolic inhibitor; (3) the *in vacuo* procedure can be applied easily to the formation of a human pancreatic RNase A dimer which is thought to reduce the immunogenic side reactions that are incurred by the foreign ribonucleases such as bovine seminal RNase and Onconase™ (Indeed a heterodimer consisting of a monomeric unit of RNase A and a monomeric unit of ONC produced by the *in vacuo* method may possess the enhanced catalytic efficiency with a stronger cytotoxicity); and (4) no chemical reagents are used in the cross-linking method thereby creating safer protein conjugates for human pharmaceutical use.

3.5 Acknowledgements

Due to the interdisciplinary nature of the work surrounding the characterization of the *in vacuo* RNase A dimer, several people contributed both in technical assistance and in intellectual output to portions of the research presented in this chapter. I would like to acknowledge Sylvie Fournier in aiding in the Kunitz enzymatic studies along with Corinne Hoesli, who established the initial set-up and experimental conditions. Also, Sam Guest for helping me with some circular dichroism experiments and Sophie D'Aoust for electrophoresis and MALDI-MS analysis. My sincere gratitude extends to Dr. Michel Girard for the use of his HLPC, in which I did all of my chromatography using this instrument and its many components over the time course of my graduate work. Dr. Martin Kalmakof kindly donated his FLPC and several moments of his time to helping me establish chromatographic methods in which to do endless amounts of protein separations. Our in-house version of Onconase™ was cloned and sequenced originally by Dr Sean Li with the help of Louise Larocque, Ding Ding Huang, and Bozena Jaentchnske. I would like to individually thank Bozena for the several times she expressed ONC and prepared the bacterial cultures and Louise, who performed all tissue culture and cell proliferation assays. Mass spectrometric analysis and instrumentation was done with help from Dr. Terry Cyr's lab: Mary-Beth Cameron and Diane Bertrand and former lab mate, Jean-Claude Ethier. These people were pivotal in many analytical experiments.

Outside of Centre for Biologics Research, Health Canada – I would like to thank Dr. Carole Huber (University of Ottawa) for the intellectual input into the molecular modeling programs and X-ray crystallography. Equally, I would like to thank Dr. Steve Evans (University of Victoria) for the software SETOR. Mary King (Ph.D., University of Ottawa) also paralleled this work in similar experiments – in which she provided endless inspiration for the work.

3.6 References

Bartholeyns, J.; Moore, S.; Stein, W. H. Ribonuclease activity in the pancreas. *Arch. Int. Physiol Biochim.* **1974,** *82* (5), 966-967.

Bartholeyns, J.; Baudhuin, P. Inhibition of tumor cell proliferation by dimerized ribonuclease. *Proc. Natl. Acad. Sci. U. S. A* **1976,** *73* (2), 573-576.

Beintema, J. J.; Schuller, C.; Irie, M.; Carsana, A. Molecular evolution of the ribonuclease superfamily. *Prog. Biophys. Mol. Biol.* **1988,** *51* (3), 165-192.

Bell, J. A. X-ray crystal structures of a severely desiccated protein. *Protein Sci.* **1999,** *8* (10), 2033-2040.

Bennett, M. J.; Schlunegger, M. P.; Eisenberg, D. 3D domain swapping: a mechanism for oligomer assembly. *Protein Sci.* **1995,** *4* (12), 2455-2468.

Boix, E.; Wu, Y.; Vasandani, V. M.; Saxena, S. K.; Ardelt, W.; Ladner, J.; Youle, R. J. Role of the N terminus in RNase A homologues: differences in catalytic activity, ribonuclease inhibitor interaction and cytotoxicity. *J. Mol. Biol.* **1996,** *%19;257* (5), 992-1007.

Bretscher, L. E.; Abel, R. L.; Raines, R. T. A ribonuclease A variant with low catalytic activity but high cytotoxicity. *J. Biol. Chem.* **2000,** *275* (14), 9893-9896.

Cafaro, V.; Bracale, A.; Formiggini, F.; Notomista, E.; D'Alessio, G.; Di, D. A. Protein engineering of ribonucleases. *Biochimie* **1998,** *80* (11), 905-909.

Campbell, R. L.; Petsko, G. A. Ribonuclease structure and catalysis: crystal structure of sulfate-free native ribonuclease A at 1.5-A resolution. *Biochemistry* **1987,** *26* (26), 8579-8584.

Carpenter, F. H.; Harrington, K. T. Intermolecular cross-linking of monomeric proteins and cross-linking of oligomeric proteins as a probe of quaternary structure. Application to leucine aminopeptidase (bovine lens). *J. Biol. Chem.* **1972,** *247* (17), 5580-5586.

Creighton, T.E. Chemical properties of peptides; In *Proteins, Structures and Molecular Properties,* 2nd edition, W.H. Freeman and Company. **1993**. pp. 6-10.

Crestfield, A. M.; Stein, W. H.; Moore, S. On the aggregation of bovine pancreatic ribonuclease. *Arch. Biochem. Biophys.* **1962,** *Suppl 1:217-22.*, 217-222.

D'Alessio, G.; Di, D. A.; Parente, A.; Piccoli, R. Seminal RNase: a unique member of the ribonuclease superfamily. *Trends Biochem. Sci.* **1991,** *16* (3), 104-106.

D'Alessio, G. The evolutionary transition from monomeric to oligomeric proteins: tools, the environment, hypotheses. *Prog. Biophys. Mol. Biol.* **1999,** *72* (3), 271-298.

Dickson, K. A.; Dahlberg, C. L.; Raines, R. T. Compensating effects on the cytotoxicity of ribonuclease A variants. *Arch. Biochem. Biophys.* **2003,** *415* (2), 172-177.

Di, Donato. A.; Cafaro, V.; D'Alessio, G. Ribonuclease A can be transformed into a dimeric ribonuclease with antitumor activity. *J. Biol. Chem.* **1994,** *269* (26), 17394-17396.

Evans, S. V. SETOR: hardware-lighted three-dimensional solid model representations of macromolecules. *J. Mol. Graph.* **1993,** *11* (2), 134-138.

Fedorov, A. A.; Joseph-McCarthy, D.; Fedorov, E.; Sirakova, D.; Graf, I.; Almo, S. C. Ionic interactions in crystalline bovine pancreatic ribonuclease A. *Biochemistry* **1996,** *35* (50), 15962-15979.

Fontecilla-Camps, J. C.; de, L. R.; le Du, M. H.; Cuchillo, C. M. Crystal structure of ribonuclease A.d(ApTpApApG) complex. Direct evidence for extended substrate recognition. *J. Biol. Chem.* **1994,** *269* (34), 21526-21531.

Gaur, D.; Swaminathan, S.; Batra, J. K. Interaction of human pancreatic ribonuclease with human ribonuclease inhibitor. Generation of inhibitor-resistant cytotoxic variants. *J. Biol. Chem.* **2001,** *276* (27), 24978-24984.

Gotte, G.; Libonati, M. Two different forms of aggregated dimers of ribonuclease A. *Biochim. Biophys. Acta* **1998,** *1386* (1), 106-112.

Gotte, G.; Bertoldi, M.; Libonati, M. Structural versatility of bovine ribonuclease A. Distinct conformers of trimeric and tetrameric aggregates of the enzyme. *Eur. J. Biochem.* **1999,** *265* (2), 680-687.

Gotte, G.; Testolin, L.; Costanzo, C.; Sorrentino, S.; Armato, U.; Libonati, M. Cross-linked trimers of bovine ribonuclease A: activity on double-stranded RNA and antitumor action. *FEBS Lett.* **1997,** *415* (3), 308-312.

Greenfield, N. J. Methods to estimate the conformation of proteins and polypeptides from circular dichroism data. *Anal. Biochem.* **1996,** *235* (1), 1-10.

Griebenow, K.; Klibanov, A. M. Lyophilization-induced reversible changes in the secondary structure of proteins. *Proc. Natl. Acad. Sci. U. S. A* **1995,** *92* (24), 10969-10976.

Haigis, M. C.; Kurten, E. L.; Raines, R. T. Ribonuclease inhibitor as an intracellular sentry. *Nucleic Acids Res.* **2003,** *31* (3), 1024-1032.

Haigis, M. C.; Kurten, E. L.; Abel, R. L.; Raines, R. T. KFERQ sequence in ribonuclease A-mediated cytotoxicity. *J. Biol. Chem.* **2002,** *277* (13), 11576-11581.

Heller, M. C.; Carpenter, J. F.; Randolph, T. W. Protein formulation and lyophilization cycle design: prevention of damage due to freeze-concentration induced phase separation. *Biotechnol. Bioeng.* **1999,** *%20;63* (2), 166-174.

Hirs, C. H.; Moore, S.; Stein, W. H. Peptides obtained by tryptic hydrolysis of performic acid-oxidized ribonuclease. *J. Biol. Chem.* **1956,** *219* (2), 623-642.

Johnson, W. C. Analyzing protein circular dichroism spectra for accurate secondary structures. *Proteins* **1999,** *35* (3), 307-312.

Kim, J. S.; Soucek, J.; Matousek, J.; Raines, R. T. Mechanism of ribonuclease cytotoxicity. *J. Biol. Chem.* **1995,** *270* (52), 31097-31102.

Klink, T. A.; Raines, R. T. Conformational stability is a determinant of ribonuclease A cytotoxicity. *J. Biol. Chem.* **2000,** *275* (23), 17463-17467.

Klibanov, A. M. Stabilization of enzymes against thermal inactivation. *Adv. Appl. Microbiol.* **1983,** *29:1-28.*, 1-28.

Lee, J. E.; Raines, R. T. Contribution of active-site residues to the function of onconase, a ribonuclease with antitumoral activity. *Biochemistry* **2003,** *42* (39), 11443-11450.

Leland, P. A.; Schultz, L. W.; Kim, B. M.; Raines, R. T. Ribonuclease A variants with potent cytotoxic activity. *Proc. Natl. Acad. Sci. U. S. A* **1998,** *95* (18), 10407-10412.

Leland, P. A.; Staniszewski, K. E.; Kim, B. M.; Raines, R. T. Endowing human pancreatic ribonuclease with toxicity for cancer cells. *J. Biol. Chem.* **2001,** *276* (46), 43095-43102.

Liu, Y.; Hart, P. J.; Schlunegger, M. P.; Eisenberg, D. The crystal structure of a 3D domain-swapped dimer of RNase A at a 2.1-A resolution. *Proc. Natl. Acad. Sci. U. S. A* **1998,** *95* (7), 3437-3442.

Liu, Y.; Gotte, G.; Libonati, M.; Eisenberg, D. A domain-swapped RNase A dimer with implications for amyloid formation. *Nat. Struct. Biol.* **2001,** *8* (3), 211-214.

Matousek, J. Ribonucleases and their antitumor activity. *Comp Biochem. Physiol C. Toxicol. Pharmacol.* **2001,** *129* (3), 175-191.

Matousek, J.; Soucek, J.; Slavik, T.; Tomanek, M.; Lee, J. E.; Raines, R. T. Comprehensive comparison of the cytotoxic activities of onconase and bovine seminal ribonuclease. *Comp Biochem. Physiol C. Toxicol. Pharmacol.* **2003,** *136* (4), 343-356.

Matousek, J.; Gotte, G.; Pouckova, P.; Soucek, J.; Slavik, T.; Vottariello, F.; Libonati, M. Antitumor activity and other biological actions of oligomers of ribonuclease A. *J. Biol. Chem.* **2003,** *278* (26), 23817-23822.

Mazzarella, L.; Capasso, S.; Demasi, D.; Di, L. G.; Mattia, C. A.; Zagari, A. Bovine seminal ribonuclease: structure at 1.9 A resolution. *Acta Crystallogr. D. Biol. Crystallogr.* **1993,** *49* (Pt 4), 389-402.

McWherter, C. A.; Thanhauser, T. W.; Fredrickson, R. A.; Zagotta, M. T.; Scheraga, H. A. Peptide mapping of bovine pancreatic ribonuclease A by reverse-phase high-performance liquid chromatography. I. Application to the reduced and S-carboxymethylated protein. *Anal. Biochem.* **1984,** *141* (2), 523-537.

Monti, D. M.; D'Alessio, G. Cytosolic RNase inhibitor only affects RNases with intrinsic cytotoxicity. *J. Biol. Chem.* **2004,** *279* (38), 39195-39198.

Navon, A.; Ittah, V.; Laity, J. H.; Scheraga, H. A.; Haas, E.; Gussakovsky, E. E. Local and long-range interactions in the thermal unfolding transition of bovine pancreatic ribonuclease A. *Biochemistry* **2001,** *40* (1), 93-104.

Nenci, A.; Gotte, G.; Bertoldi, M.; Libonati, M. Structural properties of trimers and tetramers of ribonuclease A. *Protein Sci.* **2001,** *10* (10), 2017-2027.

Nenci, A.; Gotte, G.; Maras, B.; Libonati, M. Different susceptibility of the two dimers of ribonuclease A to subtilisin. Implications for their structure. *Biochim. Biophys. Acta* **2001,** *1545* (1-2), 255-262.

Park, C.; Raines, R. T. Dimer formation by a "monomeric" protein. *Protein Sci.* **2000,** *9* (10), 2026-2033.

Piccoli, R.; Tamburrini, M.; Piccialli, G.; Di, D. A.; Parente, A.; D'Alessio, G. The dual-mode quaternary structure of seminal RNase. *Proc. Natl. Acad. Sci. U. S. A* **1992,** *89* (5), 1870-1874.

Schagger, H.; von, Jagow. G. Tricine-sodium dodecyl sulfate-polyacrylamide gel electrophoresis for the separation of proteins in the range from 1 to 100 kDa. *Anal. Biochem.* **1987,** *166* (2), 368-379.

Schlunegger, M. P.; Bennett, M. J.; Eisenberg, D. Oligomer formation by 3D domain swapping: a model for protein assembly and misassembly. *Adv. Protein Chem.* **1997,** *50:61-122.*, 61-122.

Simons, B. L.; King, M. C.; Cyr, T.; Hefford, M. A.; Kaplan, H. Covalent cross-linking of proteins without chemical reagents. *Protein Sci.* **2002,** *11* (6), 1558-1564.

Smyth, D. G.; Stein, W. H.; Moore, S. The sequence of amino acid residues in bovine pancreatic ribonuclease: revisions and confirmations. *J. Biol. Chem.* **1963,** *238:227-34.*, 227-234.

Skribanek, Z.; Mezo, G.; Mak, M.; Hudecz, F. Mass spectrometric and chemical stability of the Asp-Pro bond in herpes simplex virus epitope peptides compared with X-Pro bonds of related sequences. *J. Pept. Sci.* **2002,** *8* (8), 398-406.

Sorrentino, S.; Barone, R.; Bucci, E.; Gotte, G.; Russo, N.; Libonati, M.; D'Alessio, G. The two dimeric forms of RNase A. *FEBS Lett.* **2000,** *466* (1), 35-39.

Stelea, S. D.; Pancoska, P.; Benight, A. S.; Keiderling, T. A. Thermal unfolding of ribonuclease A in phosphate at neutral pH: deviations from the two-state model. *Protein Sci.* **2001,** *10* (5), 970-978.

Tarnowski, G. S.; Kassel, R. L.; Mountain, I. M.; Blackburn, P.; Wilson, G.; Wang, D. Comparison of antitumor activities of pancreatic ribonuclease and its cross-linked dimer. *Cancer Res.* **1976,** *36* (11 Pt 1), 4074-4078.

Wang, D.; Wilson, G.; Moore, S. Preparation of cross-linked dimers of pancreatic ribonuclease. *Biochemistry* **1998,** *15* (3), 660-665.

Wu, Y.; Mikulski, S. M.; Ardelt, W.; Rybak, S. M.; Youle, R. J. A cytotoxic ribonuclease. Study of the mechanism of onconase cytotoxicity. *J. Biol. Chem.* **1993,** *268* (14), 10686-10693.

Wu, Y.; Saxena, S. K.; Ardelt, W.; Gadina, M.; Mikulski, S. M.; De, L. C.; D'Alessio, G.; Youle, R. J. A study of the intracellular routing of cytotoxic ribonucleases. *J. Biol. Chem.* **1995,** *270* (29), 17476-17481.

Yu, W.; Vath, J. E.; Huberty, M. C.; Martin, S. A. Identification of the facile gas-phase cleavage of the Asp-Pro and Asp-Xxx peptide bonds in matrix-assisted laser desorption time-of-flight mass spectrometry. *Anal. Chem.* **1993,** *65* (21), 3015-3023.

Chapter 4: Protein Immobilization on Soluble and Insoluble Supports

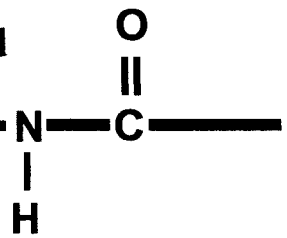

4.1 Introduction

4.1.1 Protein immobilization

A challenging goal in biotechnology, biosensory, and process chemistry is the immobilization of proteins onto solid surfaces with the retention of activity and stabilization against physical and chemical degradation. Recent advances in proteomic technology and the introduction of protein microarrays (which are prepared by immobilizing thousands of different proteins onto separate surfaces and thus allow several parallel experiments using very small amounts of protein and reagents) have resulted in renewed interest in developing efficient and effective methods for protein immobilization. Macbeath and Schreiber (2000), for example, immobilized a series of proteins on aldehyde-terminated glass slides and showed dynamic interactions between theses proteins and their substrates in solution. Recently, Wang et al. (2002) reported designing a surface-modifying procedure for attaching peptides to polyurethane matrices for use in cardiovascular implantation. These and other examples (Weetall, 1969; Shenoy et al., 1992; and Yeo et al., 2001) speak to the importance of efficient methods for immobilizing proteins for medical, diagnostic, and industrial applications.

4.1.2 Protein immobilization onto solid supports

Traditionally, the most common methods of protein immobilization to solid surfaces have been (and remain) non-specific adsorption, physical entrapment in gel matrices, non-covalent ligand-protein association, and covalent cross-linking using chemical reagents. Adsorption of a protein to surfaces is the most widely used method - used in many applications, such as the coating of antibodies on immunoassay plates in Enzyme-Linked

Absorption Immunoassays (ELISAs). (ELISAs are discussed in Chapter 5 of this thesis). During adsorption, protein molecules are immobilized passively through hydrophobic or ionic interactions with the surface, usually without any selectivity. This generates heterogeneous surfaces with protein bound in random orientations. The technique is difficult to control and often fails, particularly if the protein binds too weakly or the attachment sterically hinders protein action (Jeanson et al., 1988; Barnes et al., 1993). In such cases, covalent immobilization may result in better activity of the biomolecule, and may reduce non-specific adsorption, and increase stability of the protein.

The first step in covalent immobilization to solid supports usually involves the chemical modification of the support to render it reactive towards the protein. While this modification can be accomplished in a number of ways, consideration must be given to the types of covalent bonding between the surface and protein in order to obtain a link of desired length, flexibility, and reactivity. Cross-linking through amino groups is a commonly used approach, as proteins tend to have a comparatively large number of surface lysine residues and many solid supports are available (Kluger and Alagic, 2004). For example, the immobilization of a luteinizing hormone receptor onto polystyrene beads functionalized with amino groups was successfully achieved using homobifunctional N-hydroxysuccinimide ester cross-linkers (Moenner et al, 1986). The cross-linking reagent (shown below in Figure 4.1.1) induces a nucleophilic substitution reaction exclusively with available amine groups, forming a stable amide bond and inserting a 12 carbon hydrophilic arm between the surface and the protein. It was demonstrated that the use of this particular reagent and the resulting link it introduced between the protein and polystyrene bead was successful for "hooking-in" peptide-receptor interactions in an affinity chromatography system.

Ethylene glycol disuccinate di(N-succinimidyl) ester (EGS)

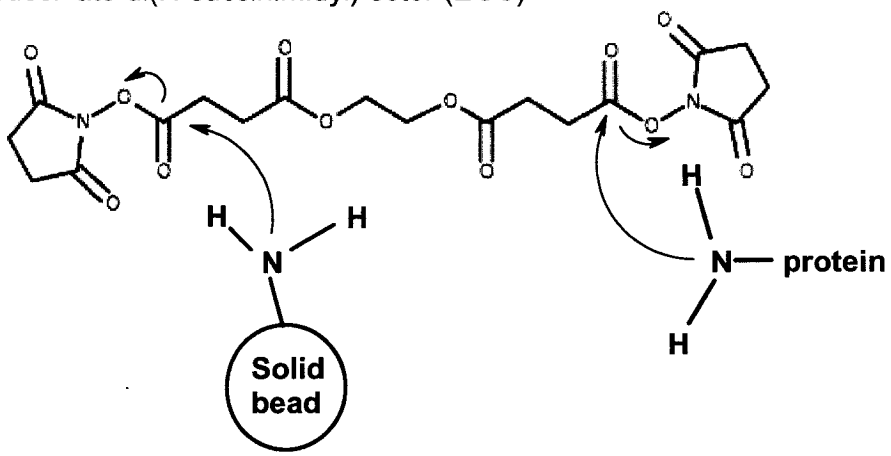

Figure 4.1.1 The coupling of protein to amino derivatized beads by ethylene glycol disuccinate di(N-succinimidyl) ester, a homobifunctional reagent. Sigma-Aldrich cross-linker, product no. 73912.

One of the most commonly used method for immobilizing enzymes on a research-based scale requirement (i.e. less than a gram of enzyme) involves sepharose resin activated by cyanogen bromide. Sepharose is a readily available beaded polymer which is highly hydrophilic and composed of the polysaccharide, poly-(β-1,3-D-galactose-α-1,4-(3,6-anhydro)-L-galactose, generating a surface plentiful of hydroxyl groups (Wilchek and Miron, 1974). The hydroxyl groups react with cyanogen bromide to produce a reactive cyclic imido-carbamate which can then react with primary amino groups of the enzyme under mildly basic conditions (as shown in Figure 4.1.2) (Woodward, 1985). Pre-cyanogen bromide activated sepharose beads are now commercially available and sold as immobilization kits for laboratory research (Sigma-Aldrich, Oakville, ON, CAN). Consequently, the high toxicity of cyanogen bromide has lead to the development of more expensive, less toxic methods of activating sepharose surfaces for the immobilization of enzymes using reagents such as chlorofomate, which react with sepharose in a similar

manner as CNBr. As shown by these examples which are exploited for commercial purposes, there exists a need for improved methods that efficiently immobilize proteins to solid surfaces.

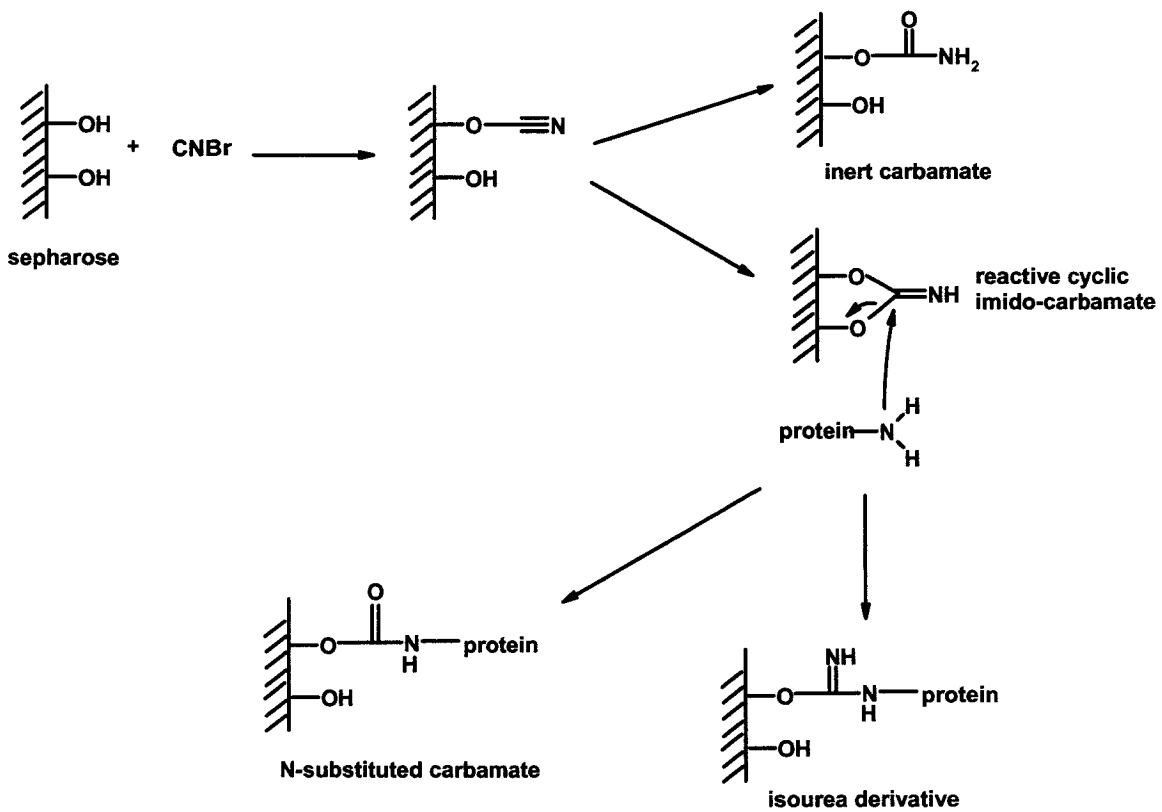

Figure 4.1.2 The cyanogen bromide activation of sepharose beads for the immobilization of protein (Woodward, 1985).

Solid support phases come in a variety of forms: membrane filters, beads, glass slides, silicon wafers, and polystyrene products such as multiple well plates. Each has a unique surface characteristic that may affect its use in various assays and applications. The derivatization of inorganic silica or glass surfaces is thought to produce an ideal support

matrix because of silica's inert nature and resistance to chemical and enzymatic degradation (Weetall, 1969; Stark and Holmberg, 1989; Taylor et al., 2005). Weetall and Hersh, (1969) devised a method to chemically modify the silica hydroxyl functionality of glass with 3-aminopropyltrimethoxysilane to result in an aminoalkylsilane-glass derivative, as shown in Figure 4.1.3.

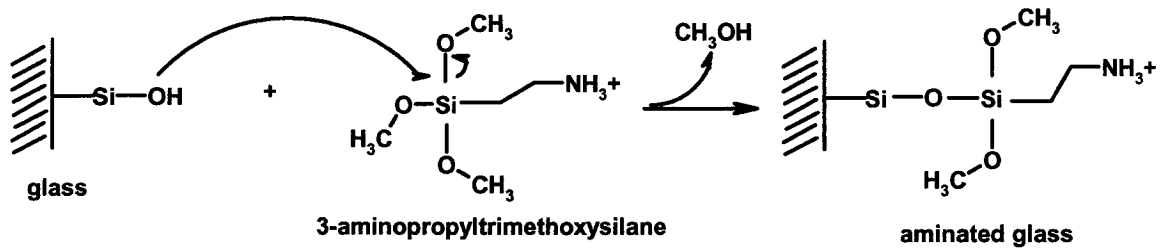

Figure 4.1.3 Preparation of trisylated-silica (modified from Stark et al, 1989).

Introduction of amino groups onto the glass surface allows amino-activated reagents to couple proteins to the surface via primary amino groups on the protein surface. A wide variety of cross-linking strategies can now be employed, including *in vacuo* cross-linking, the method developed in and described by Chapter 2 of this thesis. Because no chemical activating reagents are used in the *in vacuo* cross-linking method, the likelihood of irreversible chemical denaturation of the protein during attachment to the surface is reduced. Thus, the *in vacuo* cross-linking methodology is expected to afford a significant advantage in many applications over current methods used to immobilize proteins to glass surfaces and other supports.

This chapter describes the *in vacuo* cross-linking of enzymes to aminated glass supports. At pH 7, the aminated glass will be coated with protonated amino groups, and, if protein is lyophilized against the surface of the glass, salt bridge interactions will form between deprotonated carboxylate ions on the protein surface. Under vacuum and high temperatures, amide bonds are expected to be formed between the aspartic and glutamic resides of the protein and the amino groups of the glass, covalently attaching the protein. This facile method of covalent cross-linking can be easily tested for its efficiency as an immobilizing procedure, as the protein can be lyophilized directly on the surface of the glass, in the absence of reagent, and all uncross-linked protein can be simply washed away.

One key goal in developing any procedure for immobilizing a protein to a surface is to maximize the consistency and performance of the immobilized protein system in terms of stability, biological activity of the protein, and reproducibility of the experimental procedure. The *in vacuo* method of cross-linking of protein has already demonstrated the ability to effectively cross-link proteins while maintaining their activity. The applicability of this process to solid supports may well prove to be extremely practical, with a considerable savings in enzyme, labour and overhead costs for scaled-up industrial processes.

4.1.3 Protein immobilization to soluble polypeptide supports

While protein immobilization to glass supports is applicable in several scenarios, there are many situations where attachment of proteins to soluble supports would be more preferable. Polypeptide polymers are one type of these soluble supports and have been used in several biological applications. In particular, poly-D-lysine is used as an adhesive for attaching tissue specimens to glass slides for immunohistochemical examination (Mazia et

al., 1975 and Huang et al., 1983). The polycationic nature of this molecule encourages strong interactions between the anionic sites of tissue sections and the thiol functionality of the glass slide. The reported application of poly-lysine in the immobilization of tissues and proteins to surfaces, raises the possibility that proteins can be oligomerized by cross-linking them to chains of poly-lysine. In addition to the potential utility of the products, success in creating such protein "oligomers" by *in vacuo* cross-linking would provide further evidence for the proposed dehydration mechanism: As discussed in Chapter 2, *in vacuo* cross-linking is proposed to involve the amide bond formation between interacting ammonium and carboxylate functional groups in the lyophilized state. If the mechanism is as general as proposed, this cross-linking should be applicable to polypeptide chains with ammonium or carboxylate groups, such as poly(glu)tamic acid and poly-lysine. Enzymes cross-linked to these polypeptides should also yield soluble and active products. This chapter will describe the cross-linking of proteins to polypeptide supports, with the objective of clearly showing the generality of the proposed *in vacuo* method of cross-linking proteins.

4.2 Materials and Methods

4.2.1 In vacuo *cross-linking of RNase A to poly-glutamic acid and poly-lysine*

Bovine pancreatic RNase A (Type I-A) (Sigma-Aldrich, R4875, Oakville, ON, CAN), and poly-D-glutamic acid (poly(glu)) (Sigma-Aldrich P4033), and poly-D-lysine (poly(lys)) (Sigma-Aldrich P7886) were subjected to the *in vacuo* cross-linking procedure as previously described in Chapter 2, section 2.2.2. Briefly, poly-D-lysine (M_r ~ 340 000) or poly-D-glutamic acid (M_r ~ 38 000) was mixed with RNase A in an unbuffered aqueous

solution in a 5:1 w/w (protein/polymer) ratio. After adjusting the pH to 7.0, the mixture was lyophilized and incubated *in vacuo* for 96 hours at 85°C.

After incubation the lyophilized mixture was reconstituted into 0.1 M Tris-HCl, 0.15 M NaCl at pH 7.5, in preparation for size exclusion chromatography. The separation of the RNase A-poly(lys) or RNase A-poly(glu) complexes was achieved by TSK G3000SWxl and a G4000SWxl size exclusion column (TOHAAS, Supelco, PA, USA) and a Waters 600E HPLC system (Waters, Mississauga, CAN) using 0.1 M Na_2HPO_4, 0.15 M NaCl pH 7.5 as the mobile phase. The cross-linked proteins were separated by an isocratic method (single mobile phase) at a flow rate at 0.5 mL/min. The high molecular weight fractions were collected and concentrated using Amicon® Ultra 10 kDa MWCO centrifugal filtering devices (Millipore, Nepean, ON, CAN) to approximately a final volume of 1 mL.

4.2.2 RNase A in-gel activity assay

Cross-linked polypeptide - RNase A products were tested for catalytic activity using an RNA agarose gel-based assay (Leland *et al.*, 1998; Gaur *et al.*, 2001). Cross-linked RNase A products were quantified by the bicinchocinic acid (Sigma -Aldrich B9643) protein assay before activity determination experiments (developed by Smith et al., 1985 and Wiechelman et al., 1988). Briefly, sulfhydryl and amino groups on proteins reduce alkaline Cu(II) to Cu(I) in a concentration dependant manner. Bovine serum albumin was used to generate a standard curve. A total protein amount of 2 ng was incubated with 5 µg of total rat liver RNA in 100 mM Tris-HCl, pH 7.5, containing 10 mM DTT in a total reaction volume of 10 µL. Reaction was allowed to proceed for 10 min at 37°C and was stopped by

the addition of 1 µL of diethyl pyrocarbonate and followed by incubation on ice for 2 min. Samples were supplemented with 2 µl of RNA gel loading buffer (10 mM Tris-HCl, pH 7.5, 50 mM EDTA, glycerol (30% v/v), xylene cyanol FF (0.25% w/v), and bromophenol blue (0.25% w/v)) before loading onto a 1.5% agarose gel containing 2% formaldehyde and 0.05 M ethidium bromide. RNase activity is assessed qualitatively by the disappearance of the distinctive 18S and 28S rRNA band set (visualized by UV at 312 nm) that are present if the RNA remains intact in the absence of ribonuclease activity.

4.2.3 Kunitz ribonuclease activity assay

This ribonuclease assay uses the hyperchromaticity shift in UV absorbance induced by cleavage of RNA chains as an indication of ribonucleolytic activity (Kunitz, 1946). One Kunitz Unit of activity corresponds to the initial change in absorbance at 260 nm under first order kinetics (i.e. linear portion of the A_{260} over time curve) divided by the total measurable increase of absorbance at 260 nm measured after completion of the reaction (refer to Equation 4.1). The substrate used was double stranded RNA, poly(A)·poly(U). Enzyme solutions at 50µg/mL were prepared in Kunitz buffer (0.15M NaCl, 0.015M citrate, pH 7.5). After the poly(A)·poly(U) substrate solutions (4 – 80 µg/mL substrate diluted in Kunitz buffer) were placed in individual wells of a microtiter plate and equilibrated at 25°C for 30 min, the enzyme solution (0.05 mL) was added to each reaction to give a final reaction volume of 0.2 mL. The increase in absorbance (A_{260}) was monitored over 3 hours on a Tecan® SPECTRAFluorPlus multifunction microplate reader (Tecan, US Inc., Durham, NC, USA). The kinetic parameters were determined by non-linear regression analysis of kinetic

data using SigmaPlot® (Systat Software Inc., Point Richmond, CA, USA) and the hyperbolic curves were plotted in Microsoft Excel (Microsoft, Mississauga, ON, CAN).

$$Kunitz\ unit = \frac{dA/dt}{\Delta A}$$

Equation 4.1 Kunitz unit of ribonuclease activity where dA/dt is the slope of the linear part of the curve and ΔA is the maximum absorbance obtainable (i.e. the plateau of the A_{260} versus time curve).

$$k_{cat} / K_M = \frac{Kunitz\ unit}{mg\ enzyme}$$

Equation 4.2 The activity is measured under first order conditions, k_{cat}/K_M calculation, where the *Kunitz unit*, divided by the amount of enzyme in milligrams will equal the k_{cat}/K_M.

4.2.4 Activation of silica filter disks

Glass fiber filter disks (2.4 cm in diameter) were purchased from Millipore (Nepean, ON, CAN) (APFC02500) and refluxed with 12 N HCl for 2 hours. Disks were then washed with excess dH_20 using a Buchner funnel and oven dried at 80°C for 30 minutes. A 10% (v/v) solution of 3-aminopropyltrimethoxysilane (Sigma-Aldrich 28,177-8) in toluene was used to aminate the glass surface, as described by Stark et al., 1989. The filter disks were added to this solution and refluxed for 18 hours. Finally, after refluxing, the disks were rinsed three times each first with toluene, acetone, and then dH_20.

4.2.5 Immobilization of alkaline phosphatase (APase)

A 10mg/mL aqueous stock of bovine intestinal mucosa alkaline phosphatase (Sigma-Aldrich P7640 Lot. 121K7078) was prepared and adjusted to pH 7.0 with 1 N NaOH. Activated glass filter disks were soaked in 200 µl of the stock solution until saturated (approximately 10 seconds). These moist filter disks were flash frozen with liquid nitrogen and lyophilized. Next, these dried APase-disks were sealed under vacuum (~50mTorr) and incubated at 80°C for 96 hours as described by the *in vacuo* cross-linking procedure reported in Chapter 2. Disks with APase immobilized by cross-linking were rinsed in a Buchner funnel with excess 0.1 M NaCl then dH_20, lyophilized, and stored at 4°C.

4.2.6 Immobilized alkaline phosphatase activity assay

The APase activity was determined using standard methods involving the dephosphorylation of *p*-nitrophenylphosphate (*p*-NPP) to *p*-nitrophenol whereby the latter can be measured by absorbance at 405 nm (Walter and Schiit, 1974). Briefly, a stock solution of 350µM *p*-NPP (Sigma-Aldrich N6260, Lot 091K5315) in 25 mM glycine was prepared and adjusted to pH 9.6 with 1.0 N NaOH. The glass fiber filter disk containing the immobilized APase was tethered, using 2 mm plastic tubing, below the midline of a 25 mm x 150 mm culture tube. At time 0 minutes, 20.0 mL of *p*-NPP solution was added to the culture tube with constant stirring. Every minute thereafter, a 90 µL aliquot was removed from the mix and placed in a well of a microtiter plate containing 10 µL of a stop solution composed of 0.1 M NaOH and 0.1 M EDTA. The absorbance at 405 nm of the ensuing solution in each well was measured using a Tecan® GENios spectrophotometer (Tecan®

Systems Inc, San Jose, CA). The activity, in Units/mL, of immobilized APase was calculated using the formula shown in Equation 4.3, where ΔA_{405}/min is the slope of the linear region of the A_{405} against time plot, $V_{aliquot}$ is the volume of the aliquot read (0.1 mL), $V_{reaction}$ is the volume of the reaction (20 mL) and ε is the extinction coefficient for *p*-nitrophenol, which is 18.5 mM·cm^{-1}.

$$volume\ acitvity\ \ (U/mL) = \frac{(\Delta A_{405\,nm}/\min)\dfrac{(V_{reaction})}{(V_{aliquot})}}{\varepsilon}$$

Equation 4.3 Volume activity, units/mL, of immobilized alkaline phosphatase taken in aliquots of 90 µL from a total reaction volume of 20 mL.

4.2.7 Quantification of immobilized enzyme

A standard activity curve was generated using 20 mL of the 350 µM *p*NPP substrate and free, soluble APase. At time 0 min, the substrate was stirred vigorously and 0.5, 1, 5, 20, 100 or 400 µg of soluble APase were added. Aliquots were taken as described in Section *4.2.6* and the change in absorbance at 405 nm was calculated. Five different concentrations of soluble APase were assayed, each in duplicate, and the mean values plotted on a standard curve. This standard curve was used to estimate the amount of immobilized APase per soluble equivalent.

The amount of protein immobilized on each filter disk was also quantified by reaction with dansyl chloride, measurement of the total fluorescence of the sample (after acid

hydrolysis and reconstitution) and interpolation using a standard curve. The standard fluorescence curve was made by weighing 5.00 mg APase, dissolving it in a solution of 6 M urea and 0.1 M sodium bicarbonate pH 8.3 and reacting it with dansyl chloride. A 10% molar excess of dansyl chloride (Sigma-Aldrich D2625 Lot 11K2620) in dimethylformamide (DMF) was added per mole of lysine residue in APase. The reaction was allowed to proceed, with agitation, at room temperature for 30 min before termination by the addition of 100 mg of glycine. The sample was then transferred to 12-14000 MW cut-off dialysis tubing and thoroughly dialyzed against water. The dansylated - APase was acid hydrolyzed in 6 N HCl in an evacuated, sealed tube (vacuum at 75 mtorr) by heating to 110°C for 28 hours. After hydrolysis, HCl was removed by lyophilization and the dried sample was reconstituted to a concentration of 5.00 mg/mL hydrolysate in 0.05 N NaOH. This hydrolysate was used to create a dilution series. Each diluted sample was excited at 340 nm and the fluorescence emission at 465 nm was measured.

APase immobilized on filter disks was dansylated in a solution of 6 M urea and 0.1 M sodium bicarbonate at pH 8.3. An excess (~100 fold) of dansyl chloride in DMF was added drop-wise and reacted for 30 minutes as described above. Each filter disk was rinsed with methanol and then dH_20 to remove unreacted reagent and dansyl sulphonic acid. Acid hydrolysis of dansylated, immobilized APase was carried out as described above. After reconstitution, total fluorescence was measured and the amount of protein determined from the standard curve. An activated disk without immobilized protein was also used as a control.

4.2.8 Washing and reuse of filter disks

Between each trial the filter disk containing the immobilized APase was rinsed three times with excess (approximately 3 x 10mL) 1 M NaCl then dH_20 by placing the disk in a Buchner funnel attached to a water aspirator.

4.3 Results and Discussion

4.3.1 *In vacuo* cross-linking of RNase A to polypeptide polymers

The *in vacuo* cross-linking of RNase A to itself has shown to produce a covalent dimer with a zero-length amide link and has demonstrated enhanced activity, as shown in Chapter 3. To further test the generality of this cross-linking methodology, the idea that RNase A could be attached to any molecule bearing the proper functionality, i.e. either carboxylic acids or amino groups, was tested. Polypeptide polymers such as poly-lysine (poly(lys)) or poly-glutamic acid (poly(glu)) acid were obvious choices for polymeric supports due to their abundant potential cross-linking sites present as long as care was taken to ensure the co-lyophilized mixture retained the proper pH (pH 7-10) to ensure salt bridge formation between RNase A and the polymer.

In initial experiments, RNase A was *in vacuo* cross-linked to a 69 000 Da polymer of poly(lys) in a (w/w) ratio of 5:1 respectively, and, after the reaction, the cross-linked mixture was injected (in a relatively hypertonic (0.2 M of NaCl) mobile phase) onto a TSK G4000SWxl size exclusion column attached to an HPLC system to assess the extent of polymerization (as shown in Figure 4.3.1A). The early eluting peaks containing the large molecular weight cross-linked products, and expected (based on the demonstrated elution position of the monomeric enzyme) to be free of any unbound RNase A were collected and

assayed for ribonuclease activity. These fractions demonstrated high activity towards a total rat RNA substrate in an in-gel RNase assay (results not shown).

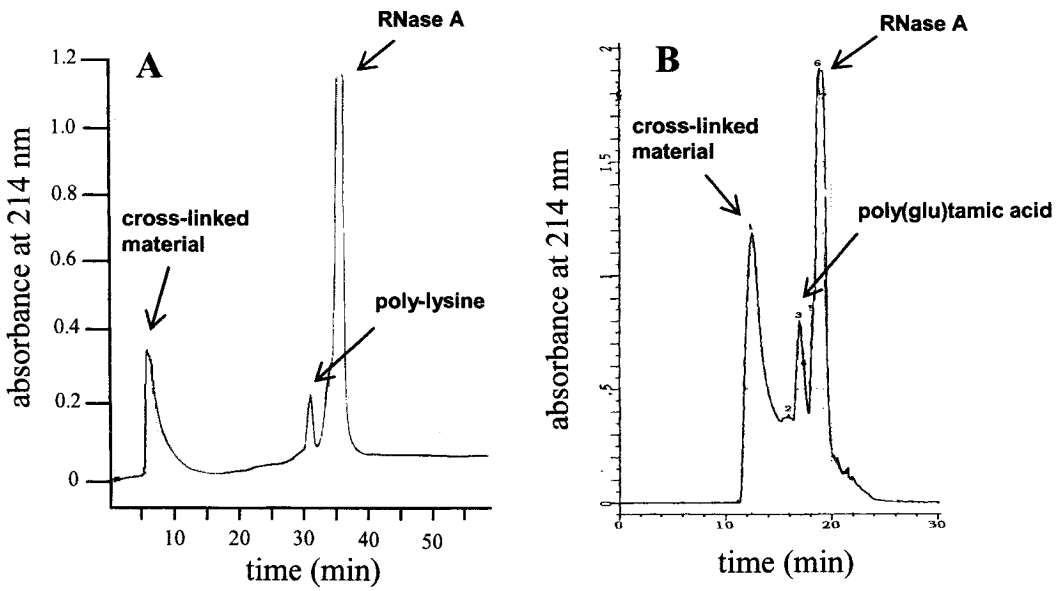

Figure 4.3.1 Size exclusion chromatography of *in vacuo* cross-linked mixtures of RNase A to poly-lysine **(A)** and RNase A to poly-glutamic acid **(B)** in a 5:1 (w/w) protein/polymer ratio. Cross-linked mixture (~0.25 – 0.5 mg) was injected into a TSK G3000SWxl or G4000SWxl (poly-lysine cross-linked mixture) column and the components were separated by HPLC in a 0.1 M NaH_2PO_4, 0.2 M NaCl, pH 7.5 running buffer over the indicated time.

Given this retention of ribonuclease activity demonstrated by the poly(lys) - RNase A conjugate, a similar cross-linking experiment was carried out using poly(glu) (thereby further validating the applicability of the cross-linking methodology to carboxylic acid polymers). In this case, RNase A was *in vacuo* cross-linked to a 38 000 Da polymer of poly(glu) in a 5:1

w/w (protein/polymer) ratio. Once the cross-linked mixture was reconstituted, size exclusion chromatography (Figure 4.3.1B) separated the free RNase A from that attached to the polymer. The early eluting peak containing the RNase – poly(glu) conjugates were collected and assayed for ribonuclease activity. This time, a more quantitative assay (the Kunitz assay (Kunitz et al., 1946)) was used to measure and compare ribonuclease activity of monomeric RNase A and the poly(glu) - RNase conjugate. In the Kunitz assay, the difference in absorbance at 260 nm is monitored as an assessment of the degradation of poly(A)·poly(U) RNA substrate over time. Figure 4.3.2 shows the plot of A_{260} of an assay mixture containing 5 µg of monomeric RNase A, 5 µg of the RNase-poly(glu) conjugate and 5 µg of a control sample (5 µg of RNase A mixed with 5 µg of poly(glu) (uncross-linked)) over time. Table 4.1 lists the k_{cat}/K_M values of each ribonuclease sample tested; these were calculated using Equations 4.1 and 4.2, as previously described in Materials and Methods, section 4.2 and also in Chapter 3. As demonstrated by the steepness in the hyperbolic curve representing the initial velocity of the enzyme, the poly(glu) - RNase A conjugate shows substantially increased activity towards the substrate (0.59 $mM \cdot min^{-1} \cdot mg^{-1}$) when compared to the monomeric RNase A sample in the presence and absence of free poly(glu). The specific activity of this latter sample is, 0.16 $mM \cdot min^{-1} \cdot mg^{-1}$ and identical to that of the monomeric RNase A which indicates that the presence of poly(glu) in the assay mixture does not interfere with the activity of RNase A towards degrading dsRNA. Indeed, if RNase A is covalently attached to poly(glu), and 5 µg of the total RNase A bound is assayed for activity, the oligomerized RNase A shows increased activity, almost 4-fold more, per equal weight of enzyme assayed. Even though equal amounts of total protein (5 µg) and substrate (20 µg) were assayed by this method, the plateaus of the activity curve do not match-up due to the

lack of equivalency in the absorbance of enzyme and poly(glu) at 260 nm and the variable make-up of each sample tested.

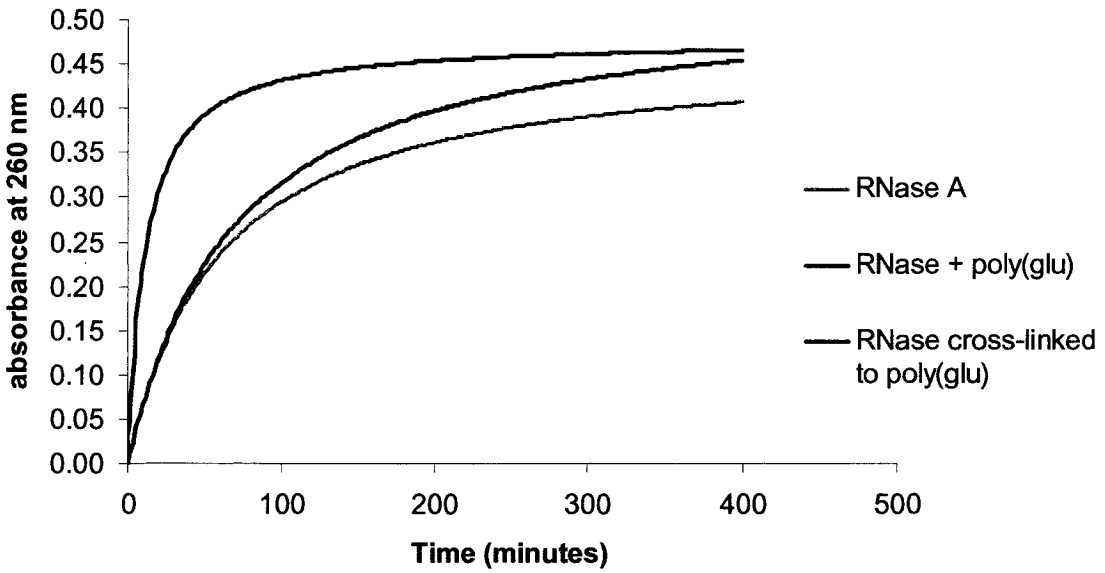

Figure 4.3.2 Kunitz ribonuclease activity assay of poly(glu)-RNase A conjugates. Difference in absorbance at 260 nm measured over time to monitor the catalytic activity of 5 µg of monomeric RNase A (light blue line), 5 µg of RNase A + 5 µg of poly(glu) uncross-linked (dark blue line), and 5 µg of cross-linked poly(glu)-RNase (red line) towards 20 µg of Poly(A)-Poly(U). Enzyme kinetic data was fitted to a hyperbolic function by SigmaPlot.

Table 4.3.1 A comparison between the specific activities of monomeric RNase A, RNase A in the presence of 5 µg of poly(glu) and RNase-poly(glu) conjugate

RNase A species	**k_{cat}/K_M $mM \cdot min^{-1} \cdot mg^{-1}$**
RNase A monomeric wild type	0.16 ± 0.0007
Rnase A with 5 µg of poly(glu), uncross-linked	0.16 ± 0.0007
RNase A cross-linked to poly(glu)	0.59 ± 0.0009

4.3.2 Alkaline phosphatase immobilized onto amino functionalized glass

In light of the effective attachment of RNase A to amino and carboxylic acid functionalized polymers, the *in vacuo* cross-linking of enzymes onto solid, non-protein supports, which had been derivatized with either amino or carboxylic acid functionality, was performed in an effort to further investigate the generality of this methodology and to test another practical application of the procedure. Silica and glass surfaces can be aminated according to a procedure described by Stark and Holmberg, 1989 generating a solid support coated in amino groups. Using the *in vacuo* method, it should be possible to covalently attach alkaline phosphatase (APase) to such a surface by lyophilizing a solution of alkaline phosphatase at pH 7.0 in the presence of the prepared, reactive surface. Amide bond formation is expected as a result of interactions between carboxylates of APase and the ammonium groups on the silica present at the time of co-lyophilization. The results shown in Figure 4.3.3 demonstrate that this is indeed the case for glass fiber filter disks derivatized with amino groups, and then subsequently, APase is attached using the *in vacuo* cross-linking procedure. After the reaction, excess APase was vigorously washed off under high ionic conditions, and the remaining bound APase was assayed using the standard colorimetric detection of the dephosphorylation of *p*-nitrophenolphosphate (*p*-NPP) to *p*-nitrophenol (*p*-NP) monitored by an increase in absorbance at 405 nm.

Figure 4.3.3 shows the rate of *p*-NPP dephosphorylation by APase immobilized on a typical glass fiber filter disk. The enzymatic activity of the immobilized enzyme immediately after preparation and initial washing is depicted as "Trial 1". Trials 2, 3, and 4 represent subsequent washing, rinsing and reusing of the same filter disk in repeated assays.

The process was repeated with APase immobilized on four separate glass filter disks to determine an average enzymatic activity per gram of silica fiber.

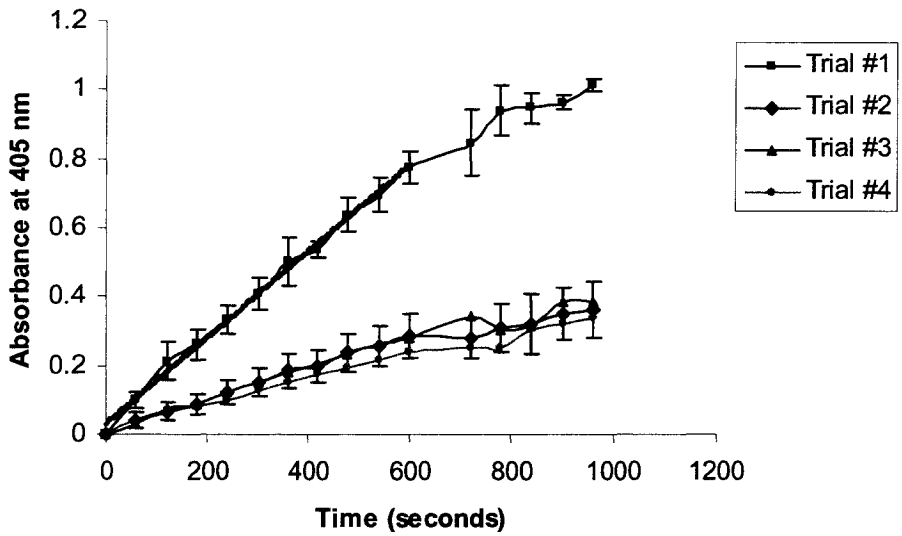

Figure 4.3.3 Activity of APase immobilized onto glass filter disks by *in vacuo* cross-linking after subsequent washing and reuse of the glass disk for 4 repeated trials. For each trial, 20 mL of 350 µM *p*-NPP was used and a 90 µL aliquot was taken every 60 seconds, for 25 minutes and placed in 10 µL of stopping solution. A_{405} monitors the dephosphorylation of *p*-NPP to *p*-NP over time in seconds.

Activity of alkaline phosphatase, in terms of "activity units per mL", is calculated by the Equation 4.3, where ΔA/min is the slope of the A_{405} over time plot taken from the linear portion of the curve, $V_{aliquot}$ is the volume of the aliquot read (0.1 mL), $V_{reaction}$ is the volume of the total reaction (20 mL) and ε is the extinction coefficient for *p*-nitrophenol, which is 18.5 mM cm^{-1}. Table 4.2 lists the immobilized APase volume activity calculated for each trial. In the first trial, 0.0141 ± 0.0005 units/mL of activity was detected. After the glass filter disk was washed and the APase assay was repeated, a loss of activity was detected, 0.0063 ± 0.0003 units/mL. The assay repeated for a third and fourth trial, detected a volume

activity of 0.0058 ± 0.0003 units/mL, with no further loss in APase activity. Therefore, after the first trial, the disk lost approximately 60% of its activity. In subsequent washing cycles, however, the losses were minimal and over 90% of the activity present after the first trial remained after additional washings.

$$volume\ acitvity\ \ (U/mL) = \frac{(\Delta A_{405}/\min)\dfrac{(V_{reaction})}{(V_{aliquot})}}{\varepsilon}$$

Equation 4.3 Volume activity, units/mL, of immobilized alkaline phosphatase taken in aliquots of 100 µL from a total reaction volume of 20 mL.

Table 4.3.2 Volume activity of APase immobilized onto glass filter disks after 4 repeated trials.

	Volume activity* (Units/mL)
Trial 1	0.0141 ± 0.0005
Trial 2	0.0063 ± 0.0003
Trial 3	0.0058 ± 0.0003
Trial 4	0.0058 ± 0.0002

*Standard deviation is calculated from the activity results obtained from 4 separate APase - filter disks, each assayed and reused 4 times.

These results also indicate that filter disks containing immobilized enzymes have the potential for repeated use without significant loss of activity. It was expected that the washing steps in the procedure before trial 1 would remove any non-covalently associated

protein. Nevertheless, a large decrease in activity between trial 1 and trial 2 is consistently observed. This decrease in activity after the first assay was also observed in activity assays evaluating the efficiency of immobilization of trypsin to glass beads, *in vacuo* cross-linked in the same manner (Kaplan unpublished results, 2005). Kaplan and co-workers demonstrated a loss in 50% of tryptic activity in a second trial, after completing one full cycle of assay, wash and reuse of the same glass beads, however, no subsequent loss was observed there after and the amount of bound trypsin seemed to remain constant as well. While the source of this loss of activity is not clear, it may be that, despite the attempts to remove any non-covalently bound enzyme using 0.1 M NaCl, some still remains associated with the glass matrix during the first trial. Indeed, if the non-covalent association of enzyme with the glass were not ionic in nature, the high concentration NaCl washes used would not disrupt it. Alternately, the loss of activity after the first trial may be associated with properties of the particular enzyme chosen in this experiment. Although monomeric APase is catalytically active, APase exists primarily as a dimer and undergoes a conformational change (Chappelet-Tordo et al., 1974) as it dephosphorylates *p*-NPP. This intramolecular contortion may be sufficient to disrupt the residual non-covalent interactions in the dimer and liberate any of the non-covalently-associated enzyme from the silica. The similar loss of activity observed by Kaplan and co-workers with covalent attachment of trypsin to glass, however, is not explained by this mechanistic argument: trypsin exists (and acts) in solution primarily in its monomeric form. However, perhaps an intramolecular contortion occurs as the enzyme interacts with its substrate in the first trial, and any weakly bound material becomes liberated from the surface. Regardless of the mechanism, the covalently immobilized enzyme remaining after the first

trial and washing was stable; the losses of activity with five subsequent washes of the disk were minimal.

4.3.3 Quantification of immobilized APase

The amount of APase remaining on the disk, after the first trial, was estimated as the soluble equivalent, i.e. the amount of soluble enzyme that would give the same activity as the immobilized enzyme in Figure 4.3.3. On average (n=4), it was found that 185 ± 30 µg of protein was present during the first trial and 35 ± 15µg for the second trial. After the fourth trial, the total amount of protein remaining on the disk was quantified by comparing its fluorescence (see Methods section *4.2.7*) to that of a similarly treated sample of soluble enzyme used to make the standard curve (data not shown). The result indicates that 52.7 µg of protein can be bound to a 24 mg filter disk with a diameter of 2.4 cm. This represents 2.16 mg of total protein remaining immobilized per gram of silica fiber and approximately 67% of the apparent specific activity of the soluble enzyme can be retained after immobilization and several reuses.

In 1969, Weetall reported that 0.74 mg of APase per gram of glass could be immobilized by adding the enzyme to glass beads chemically activated with diazo groups. The results presented in this chapter show a larger amount of active immobilized enzyme (2.16 mg per gram of silica fiber) and a 67% retention in specific activity after several trials. This value compares favourably with examples of APase immobilized on other surfaces (1% of specific activity retained on an ethylene-maleic anhydride co-polymer (Zingaro and Uziel, 1970) and 56 to 72% on various vanacryls (Brown and Joyeau, 1974) as well as to values obtained for acid phosphatases immobilized on plain and glycerol coated glass (4 and 14%,

respectively (Van Hekken et al., 1990)). These data suggest that the *in vacuo* immobilization process is at least as effective as more traditional chemical methods of immobilization in preserving the activity of the enzyme molecules immobilized on the glass.

4.4 Conclusion

Enzymes have been immobilized on a variety of surfaces (Surinenaite, et al., 1996; Wiley et al., 2001; Filmon et al, 2002) but, to our knowledge, there are very few reports describing the immobilization of enzymes onto glass supports (Weetall, 1969; Macbeath and Schreiber, 2000; Van Hekken et al., 1990). The successful covalent immobilization of alkaline phosphatase without the use of activating chemicals demonstrates that the *in vacuo* method is a practical and efficient process for immobilizing proteins, especially small amounts of valuable proteins. As well, any uncross-linked material remains completely unmodified and therefore can be recovered and reused – an added benefit for use with especially expensive proteins. This work has initiated several projects including the immobilization of commercially valuable proteins, such as trypsin and chymotrypsin, onto functionalized glass beads. Current and on going work in the Kaplan research group has demonstrated the enhanced thermal stability of glycated forms of trypsin, immobilized onto finely ground glass beads via *in vacuo* cross-linking. This covalent cross-linking methodology would allow for scaled-up production of large quantities of immobilized enzymes for industrial processing at low costs and with high potential for enzyme reuse. Also, this procedure can be scaled-down, for custom immobilization of enzymes, ligands, or antibodies onto chromatographic resins for bench-top research purposes. In re-iteration, the *in vacuo* method of immobilizing protein is an efficient method of attaching protein to either

solid or soluble surfaces without the use of chemical activating agents to produce safer and more biologically active molecules.

4.5 Acknowledgements

The immobilization of proteins to derivatized glass and polymer surfaces was a project with numerous contributors other than myself, namely Russell Taylor and Sylvie Fournier (Centre for Biologics Research, Health Canada), and Van Thong Pham (University of Ottawa). I would like to thank everyone for their technical and intellectual assistance.

4.6 References

Barnes, C. S.; Upadrashta, B.; Pacheco, F.; Portnoy, J. Enhanced sensitivity of immunoblotting with peroxidase-conjugated antibodies using an adsorbed substrate method. *J. Chromatogr.* **1993,** *613* (2), 281-288.

Brown, E. and Joyeau, R. Immobilized enzymes: Use of vanacryls in preparation of immobilized arginase and alkaline phosphatase. *Polymer* **1974,** 15, 546-552.

Chappelet-Tordo, D.; Fosset, M.; Iwatsubo, M.; Gache, C.; Lazdunski, M. Intestinal alkaline phosphatase. Catalytic properties and half of the sites reactivity. *Biochemistry* **1974,** *13* (9), 1788-1795.

Filmon, R.; Grizon, F.; Basle, M. F.; Chappaard, D. Effects of negatively charged groups (carboxymethyl) on the calcification of poly(2-hydroxyethyl methacrylate). *Biomaterials* **2002,** *23* (14), 3053-3059.

Fosset, M.; Chappelet-Tordo, D.; Lazdunski, M. Intestinal alkaline phosphatase. Physical properties and quaternary structure. *Biochemistry* **1974,** *13* (9), 1783-1788.

Gaur, D.; Swaminathan, S.; Batra, J. K. Interaction of human pancreatic ribonuclease with human ribonuclease inhibitor. Generation of inhibitor-resistant cytotoxic variants. *J. Biol. Chem.* **2001,** *276* (27), 24978-24984.

Huang, W. M.; Gibson, S. J.; Facer, P.; Gu, J.; Polak, J. M. Improved section adhesion for immunocytochemistry using high molecular weight polymers of L-lysine as a slide coating. *Histochemistry* **1983,** *77* (2), 275-279.

Immoto, T, and Yamada, H.(1989) Chapter 10, In Protein Function, A Practical Approach. T. E. Creighton, (Ed.) Oxford University Press. pp. 247-277.

Jeanson, A.; Cloes, J. M.; Bouchet, M.; Rentier, B. Preparation of reproducible alkaline phosphatase-antibody conjugates for enzyme immunoassay using a heterobifunctional linking agent. *Anal. Biochem.* **1988,** *172* (2), 392-396.

Kluger, R. and Alagic, A. Chemical cross-linking and protein-protein interactions - a review with illustrative protocols. *Bioorg. Chem.* **2004,** *32* (6), 451-472.

Kunitz, M. A spectrophotometric method for measurement of ribonuclease activity. *J. Biol. Chem.* **1946,** *164*: 563-568.

Leland, P. A.; Schultz, L. W.; Kim, B. M.; Raines, R. T. Ribonuclease A variants with potent cytotoxic activity. *Proc. Natl. Acad. Sci. U. S. A* **1998,** *95* (18), 10407-10412.

Lundblad, R.L. Chapter 15, in Techniques in Protein Modification, CRC Press Inc., **1995** Boca Raton, Florida, pp. 249-262.

MacBeath, G.; Schreiber, S. L. Printing proteins as microarrays for high-throughput function determination. *Science* **2000,** *289* (5485), 1760-1763.

Mazia, D.; Schatten, G.; Sale, W. Adhesion of cells to surfaces coated with polylysine. Applications to electron microscopy. *J. Cell Biol.* **1975,** *66* (1), 198-200.

Moenner, M.; Chevallier, B.; Badet, J.; Barritault, D. Evidence and characterization of the receptor to eye-derived growth factor I, the retinal form of basic fibroblast growth factor, on bovine epithelial lens cells. *Proc. Natl. Acad. Sci. U. S. A.* **1986,** *83* (14), 5024-5028.

Shenoy, N. R.; Bailey, J. M.; Shively, J. E. Carboxylic acid-modified polyethylene: a novel support for the covalent immobilization of polypeptides for C-terminal sequencing. *Protein Sci.* **1992,** *1* (1), 58-67.

Simons, B. L.; King, M. C.; Cyr, T.; Hefford, M. A.; Kaplan, H. Zero-length cross-linking of lyophilized proteins. *Protein Sci.* **2002**, 11(1), 1558-1564.

Smith, P.K.; Krohn, R.I.; Hermanson. G.T.; Mallia, A.K.; Gartner, F.H.; Provenzano, M. D.; Fujimoto, E.K.; Goeke, N.M.; Klenk, D.C. Measurement of protein using bicinchoninic acid. *Anal. Biochem.* **1985,** *150* (1), 76-85.

Stark, M. B., and Holmberg, K. Covalent Immobilization of Lipase in Organic Solvents. *Biotechnology and Bioengineering* **1989**, 34: 942-950.

Surinenaite, B.R.; Bendikene, V.G. and Iuodka, B.A. (1996). Immobilization of enzymes on carriers with magnetic properties: the search for optimum conditions for immobilization of alkaline phosphatase from the chicken graft. Prikl. Biokhim. Mikrobiol. 32:609-614.

Taylor, R., Fournier, S. M., Simons, B. L., Kaplan, H., Hefford, M. A. Covalent immobilization of alkaline phosphatase. *J. Biotech.* accepted, **2005**.

Walter, K. and Schütt, C. in *Methods of Enzymatic Analysis* Bergmeyer, H.U. (Ed.) 2nd edition,Volume II, Academic Press, Inc., NY **1974**, pp 860-864.

Wang, C. H.; Chen, S. M.; Wang, C. M. Co-immobilization of polymeric luminol, iron(II) tris(5-aminophenanthroline) and glucose oxidase at an electrode surface, and its application as a glucose optrode. *Analyst* **2002,** *127* (11), 1507-1511.

Wang, D. A.; Ji, J.; Sun, Y. H.; Shen, J. C.; Feng, L. X.; Elisseeff, J. H. In situ immobilization of proteins and RGD peptide on polyurethane surfaces via poly(ethylene oxide) coupling polymers for human endothelial cell growth. *Biomacromolecules.* **2002,** *3* (6), 1286-1295.

Weetall, H. H. Trypsin and papain covalently coupled to porous glass: preparation and characterization. *Science* **1969,** *166* (905), 615-617.

Weetall, H. H. Alkaline phosphatase insolubilized by covalent linkage to porous glass. *Nature* **1969,** *223* (209), 959-960.

Weetall, H. H.; Hersh, L. S. Urease covalently coupled to porous glass. *Biochim. Biophys. Acta* **1969,** *185* (2), 464-465.

Wiechelman, K. J.; Braun, R. D.; Fitzpatrick, J. D. Investigation of the bicinchoninic acid protein assay: identification of the groups responsible for color formation. *Anal. Biochem.* **1988,** *175* (1), 231-237.

Wilchek, M.; Miron, T. Stable, high capacity and non charged agarose derivatives for immobilization of biologically active compounds and for affinity chromatography. *Mol. Cell Biochem.* **1974,** *4* (3), 181-187.

Wiley, J. P.; Hughes, K. A.; Kaiser, R. J.; Kesicki, E. A.; Lund, K. P.; Stolowitz, M. L. Phenylboronic acid-salicylhydroxamic acid bioconjugates. 2. Polyvalent immobilization of protein ligands for affinity chromatography. *Bioconjug. Chem.* **2001,** *12* (2), 240-250.

Woodward, J. Immobilised enzymes: Adsorption and covalent coupling. In *Immobilised cells and enzymes, A practical approach*, ed. J. Woodward, **1985** pp 3-17. Oxford: IRL Press Ltd.

Van Hekken, D. L., Thompson, M. P. And Strange, E. D. Immobilization of potatoe acid phosphatase on succinamidopropyl glass beads for the dephosporylation of bovine whole casein. *J. Dairy Sci.* **1990**, 73, 2720-2730.

Yeo, W. S.; Hodneland, C. D.; Mrksich, M. Electroactive monolayer substrates that selectively release adherent cells. *Chem biochem.* **2001,** *2* (7-8), 590-593.

Zingaro, R. A. and Uziel, M. Preparation and properties of active, insoluble alkaline phosphatase *Biochim. Biophys. Acta* **1970**, 213, 371-379.

Chapter 5: *In Vacuo* Cross-linking of Antibody-Enzyme Conjugates; Novel Immunoreagents for Western Blots and ELISAs.

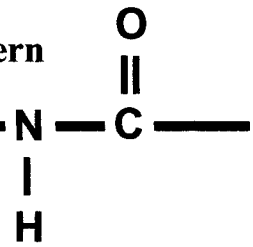

5.1 Introduction

Enzyme-Linked Immunosorbent Assay (ELISA) and Western Blot assays are well established and widely used methods of choice for screening and quantifying antigens and antibodies. Indeed a variety of enzyme-linked antibodies from various suppliers are now commercially available. Different enzymes, different cross-linking procedures, and inconsistencies in efficiency reporting, however, have made standardization of the protocols using these enzyme-antibody complexes difficult (O'Sullivan and Marks, 1981).

Enzyme-antibody conjugates are most commonly prepared by cross-linking the enzyme to the antibody through functional groups on proteins such as primary amines, sulfhydryls, or sugar moieties. One fairly common way of cross-linking the reporting enzyme, horseradish peroxidase (HRP) to immunoglobulins (i.e. IgG) uses homobifunctional reagents such as glutaraldehyde in a two step synthesis, as demonstrated in work published by Avrameas and Ternynck in 1969 (Figure 5.1.1). Glutaraldehyde reacts with the amino groups in HRP, through the formation of a Schiff base; then all free glutaradyhyde is removed. The activated enzyme is now allowed to react with the antibody, forming a five carbon link between molecules. Coupling via glutaraldehyde often occurs in very low yields, and the antibody-enzyme complexes generated by this method can be heterogeneous and highly polymerized (Avrameas, 1968; Kluger and Alagic, 2004). Larger and irregular antibody-enzyme complexes may lead to steric hinderance effects on the IgG molecule, which may affect antigen binding ability and compromise the sensitivity of the subsequent immunological assay in which the complex is used.

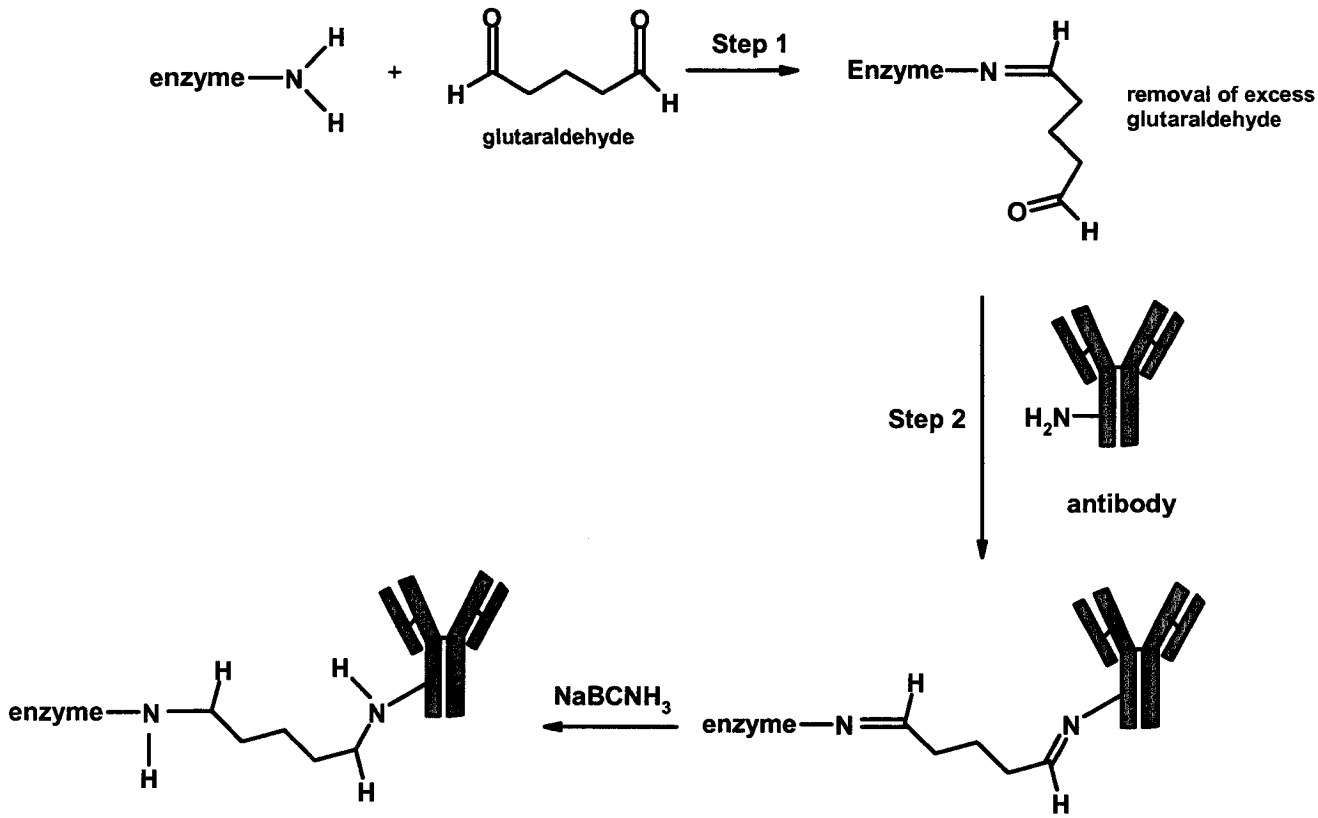

Figure 5.1.1 Enzyme-antibody coupling by the two-step glutaraldehyde procedure (Avrameas and Ternynck, 1969).

To alleviate the potential of destroying the catalytic activity of the signaling enzyme, some companies that manufacture and market IgG labeled with HRP, have adopted a "glutaraldehyde-like" cross-linking strategy taking advantage of the sugar moieties (not part of the active site of the enzyme) present on HRP. Sigma-Aldrich, the company whose enzyme-linked IgG products were purchased and used as a comparison in this study, use a periodate oxidation method developed by Wilson and Nakane (1978) that takes advantage of the constituent carbohydrate in HRP to form a bifunctional reagent and cross-links IgG, to

the antibody, thereby creating a flexible link and a product with good solubility. In the first step of this cross-linking reaction (Figure 5.1.2), vicinal hydroxyl groups of the sugar on HRP are oxidized by periodate to aldehyde groups. After excess oxidizing agent is removed, the antibody is added and the primary amino groups of the antibody cross-link through the aldehyde groups of HRP and are stabilized by reductive amination with $NaCNBH_3$.

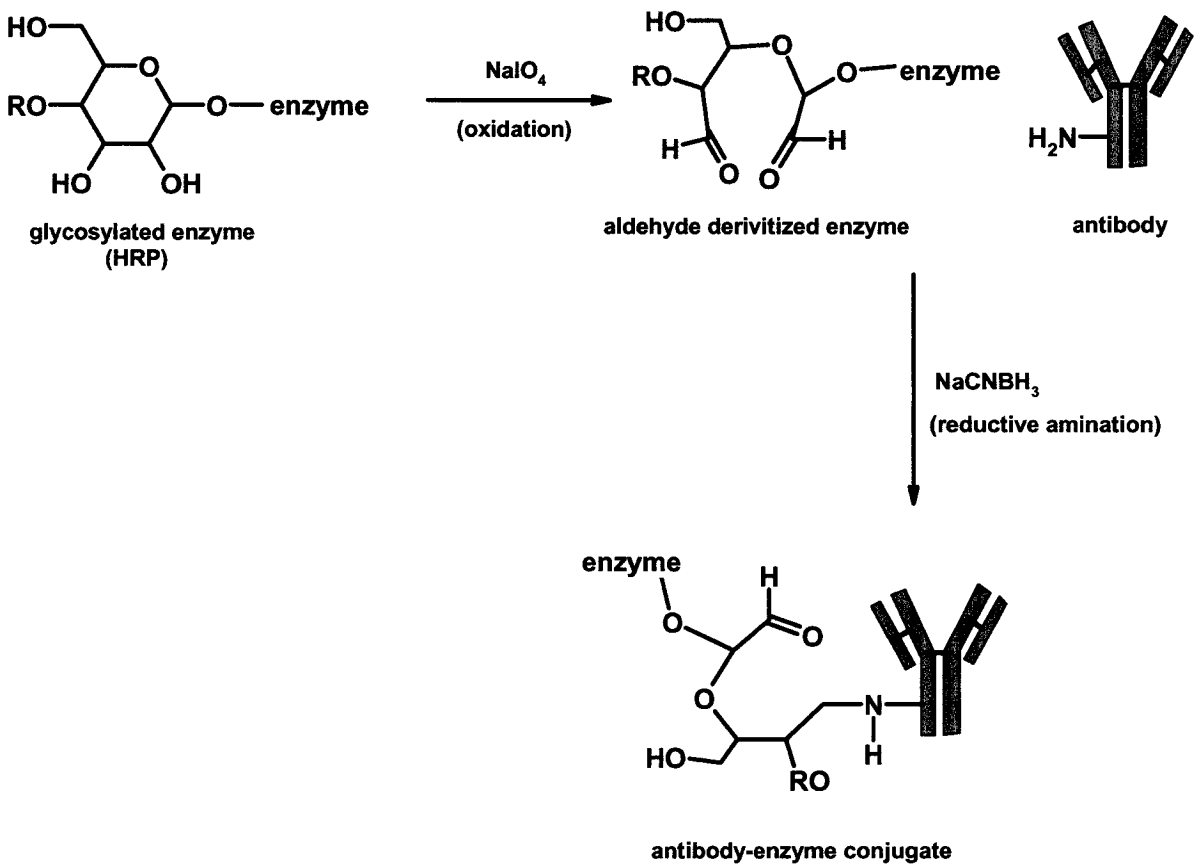

Figure 5.1.2 Coupling of HRP to IgG using the periodate oxidation method developed by Wilson and Nakane, 1978.

In general, bifunctional cross-linking reagents have several drawbacks when applied to antibody-enzyme coupling. Firstly, the chemical activation of the target residues on either the enzyme or antibody tends to be random and thus, competing side reactions are difficult to control. These side reactions generate enzyme-enzyme and antibody-antibody complexes which contaminate the antibody-enzyme conjugate of interest. Secondly, any method of chemical derivitization using activating reagents has the potential to destroy the activity of the enzyme and/or antibody by modifying the residues responsible for biological function or by altering the native structure of the protein, which may weaken antigen-antibody interactions or damage the signaling ability of the reporter enzyme. Lastly, large molecular weight oligomers formed by uncontrolled cross-linking may produce insoluble aggregates that are impossible to manipulate in immunoassays. It is evident that the quality of the antibody-enzyme conjugate and the efficiency of the conjugation procedure are key to designing an immunoassay antibody reagent of optimal performance.

The *in vacuo* method of cross-linking proteins offers an alternative methodology for designing novel antibody-enzyme conjugates which eliminates many of the drawbacks of the conventional protein cross-linking procedures. Using this technique, a zero-length amide bond is formed as a result of ionic interactions of ammonium and carboxylate groups between molecules in the lyophilized state, without the use of chemical modifying reagents (as described in Chapter 2). Any strong salt bridge interactions existing between an antibody molecule and an enzyme molecule in solution, which are present after lyophilization, will be few in number and likely homogeneous in nature. This in fact may result in the formation of covalent cross-links between the antibody and enzyme that are highly selective and thereby reduce the likelihood of large heterogeneous complexes being formed.

Immunoglobulins may show instabilities under prolonged aqueous conditions, especially in solutions of low-pH, due to multiple domains that are associating through disulfide bridges and non-covalent forces (Vermeer and Norde, 2000). Co-lyophilizing enzymes with IgGs followed by incubating the lyophilized mixture under vacuum is less likely to disrupt protein structure, as proteins do show greatly enhanced stability in the lyophilized state. The *in vacuo* method, therefore, has an apparent advantage over chemical derivitization by aqueous chemistry in the protection of the biological function of IgGs. Based on the results obtained in the initial experiments on the in *vacuo* cross-linking of proteins (Chapter 3), it is expected that enzymes such as alkaline phosphatase and HRP can be cross-linked to IgG *in vacuo* to form soluble antibody-enzyme conjugates that retain their full biological activity. A feature that is potentially extremely advantageous, especially with valuable proteins samples, is that noncross-linked protein remains in its native unmodified state and can be recovered and reused.

Despite the wide use and considerable success of enzyme conjugated antibodies and secondary antibodies in antigen detection, the sensitivity or detection afforded is not adequate for all applications. In particular, diagnostic immunoassays of biological fluids containing very low levels of antigen or experiments where the antigen is partially obstructed by gel matrices (in-gel assays) are in need of more sensitive detection methods. Efforts to improve sensitivity of these reagents have led to the design of multi-enzyme based conjugates (Dhawan, 2002). This approach is based on the strategy that if one IgG can carry multiple units of enzyme the detection signal will be amplified many fold beyond that achieved with the conventional 1:1 ratio of one enzyme per antibody. Some investigators have designed conjugates using amino-derived polystyrene microparticles to chemically

attach thousands of HRP molecules through activated amino sites and then attach one antibody molecule, through a specific thiol coupling reaction, to each particle (Dhawan, 2002; and Kala et al, 1997). Although bulky and insoluble, these polystyrene microparticles do show a significant increase in signal in immunoassays for detection of very low levels of antigen, however, the precise amount detected is not clearly reported. Aside from the bulk and insolubility of these conjugates, they do not appear to be ideal in several other ways. In order to achieve signal enhancement of 5-8 fold, much higher concentrations of their immuno-particles were required than would be conventionally used in an assay using a direct IgG-HRP conjugate, creating limitations of this procedure in terms of cost and long-term usage. Furthermore, these immuno-particles have not been shown to be applicable to Western Blot analyses.

To the best of our knowledge, there are no multi-enzyme based immunoconjugates that have versatility and practicality in ELISAs and Western Blot analyses and that have shown an increase in the sensitivity of signal detection. This shortcoming in the current technology provided the incentive for designing multi-enzyme antibody conjugates using the *in vacuo* method to cross-link enzymes and antibodies to soluble polypeptide chains (as described in Chapter 4). Poly-glutamic acid (poly(glu)) or poly-lysine (poly(lys)) can be used as soluble supports to attach several HRP molecules to one IgG in a two step *in vacuo* cross-linking procedure, as shown in Figure 5.1.3. Basically, in the proposed method, several molecules of HRP would be covalently cross-linked to poly(glu) in step 1 and large molecular weight species are separated from the low molecular weight material that did not cross-link. The IgG would then be introduced in a limiting ratio, and attached to the HRP-poly(glu) complex in step 2. The IgG-poly(glu)-$(HRP)_n$ conjugates that would be formed by

in vacuo cross-linking are expected to be soluble, their size could be controlled based on the ratios of the starting materials, and their coupling does not require any chemical activation steps. One would therefore anticipate that such a strategy would result in soluble IgG-poly(glu)-$(HRP)_n$, where $n > 1$, demonstrating significantly enhanced detection signals in ELISA and Western Blot assays.

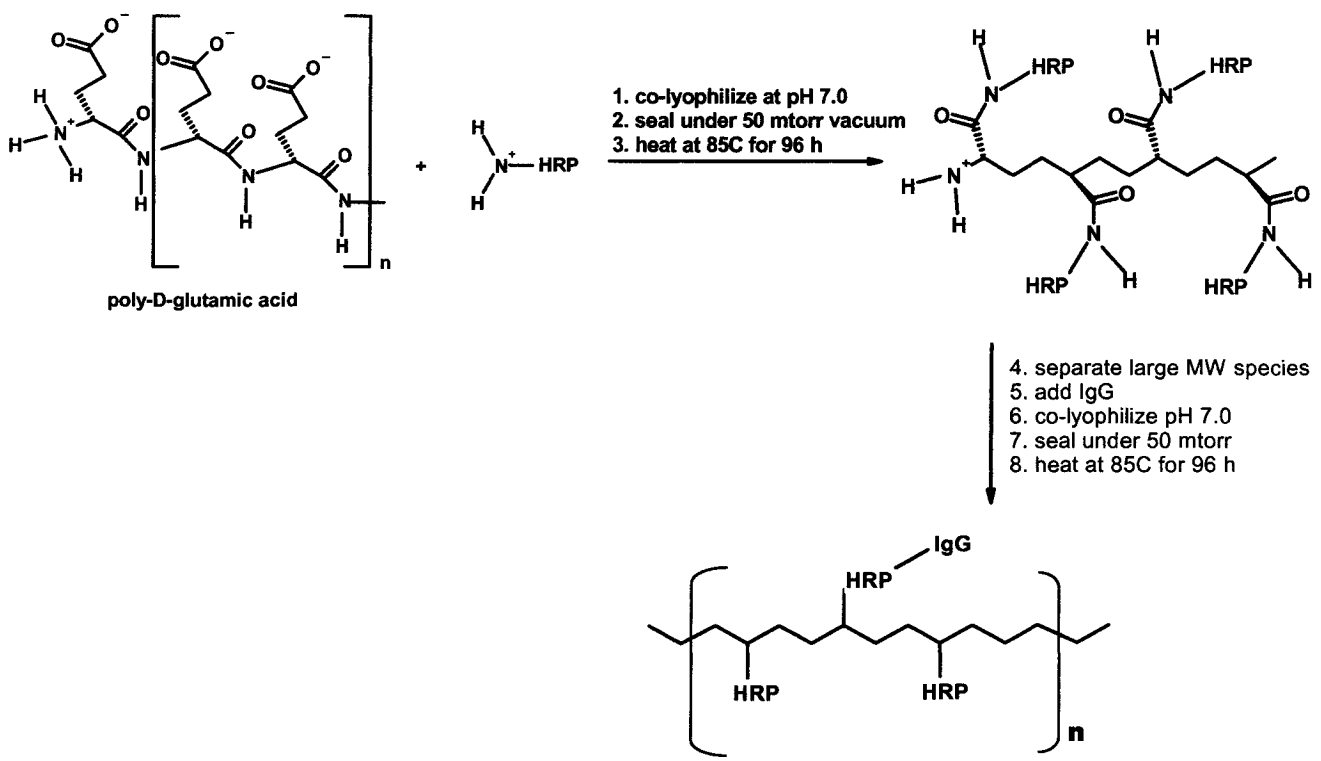

Figure 5.1.3 General procedure for the formation of IgG-poly(glu)-$(HRP)_n$ conjugates via *in vacuo* cross-linking.

This chapter describes the results obtained from the cross-linking of antibodies to reporter enzymes and their evaluation in terms of biological activity towards binding antigens or other antibodies in Western Blot assays and ELISAs.

5.2 Materials and Methods

5.2.1 Materials

Affinity purified goat anti-rabbit IgG whole molecule (R2004), horseradish peroxidase (P6782), alkaline phosphatase (P7640), anti-chick egg ovalbumin (C6534), goat anti-rabbit IgG peroxidase conjugate (A6154), and goat anti-rabbit IgG alkaline phosphatase conjugate (A3687) were purchased from Sigma-Aldrich, Oakville, ON, CAN. Superdex G-200 gel filtration chromatography column, and ECL™ Western Blot detection system kit was purchased from Amersham Biosciences (Baie d'Urfée, PQ, CAN). All other reagents were purchased from Sigma-Aldrich, unless otherwise indicated.

5.2.2 Conjugation of alkaline phosphatase to rabbit anti-ovalbumin and anti-rabbit IgG

Goat anti-rabbit IgG (Sigma-Aldrich R2004) and rabbit anti-chick egg ovalbumin anti-serum (Sigma-Aldrich C6534) were both covalently attached to alkaline phosphatase (APase) (Sigma-Aldrich P7640) independently by *in vacuo* cross-linking. Briefly, 2 mg of APase and 2 mg IgG or 2 mL of anti-ovalbumin anti-serum were mixed in an unbuffered solution to a total volume of 2 mL. The solution was dialyzed in a 50 kDa MWCO dialysis bag against dH_2O (4 changes of 1 L over 5 hours) to remove glycerol, sodium azide, and storage buffers present in commercial antibody preparations. The APase and IgG mixture was then placed in a long glass tube, pH was re-adjusted to 7.5 with 1 N NaOH, and the

sample was lyophilized. Once the protein was dried, the glass sample tube was narrowed, placed under vacuum (< 50 mtorr), then sealed and placed in an oven at 85°C for 96 hours. Following the reaction, the tube was cracked and the dried sample was reconstituted in 1 mL of 0.1 M Tris-HCl, 0.15 M NaCl at pH 7.5.

5.2.3 Conjugation of HRP to IgG

Goat anti-rabbit IgG (Sigma R2004) was covalently attached to HRP (Sigma P6782) by *in vacuo* cross-linking using the same protocol that was described in Section 5.2.2 with the following exceptions; (a) 5 mg of HRP and 2 mg IgG were used, mixed in an unbuffered solution of total volume equaling 2 mL; and (b) dialysis was performed in a 10 kDa MWCO dialysis membrane against dH_2O for 4 changes of 1 L each over 5 hours.

5.2.4 Purification of antibody-enzyme conjugates

The separation of uncross-linked material and antibody-enzyme conjugates was achieved by gel filtration chromatography using a Superdex 200 10/300 GL purchased from Amersham Biosciences. The column was equilibrated in running buffer (0.1 M Tris-HCl, 0.15 M NaCl at pH 7.5, TBS) pumped through by a P-500 FPLC system (Amersham Biosciences), connected to a UV detector (Bio-Rad Laboratories, Mississauga, ON, CAN) reading at 280 nm, and then calibrated using the following protein standards: dextran blue ($M_r \sim 2\ 000\ 000$), thrombin ($M_r \sim 669\ 000$), anti-rabbit IgG ($M_r \sim 160\ 000$), and HRP ($M_r \sim 42\ 000$). The reconstituted cross-linked mixture was applied and eluted at a flow rate of 0.5 mL/min and large molecular weight fractions, (those species eluting before IgG

(M_r ~ 160 000) is expected to elute), were collected and concentrated with Amicon® Ultra 50 kDa MWCO centrifugation filtering device (Millipore Corp., Nepean, ON, CAN) to a volume of approximately 1 mL. This sample is presumed to contain the antibody-enzyme conjugates as they are expected to be approximately 200 000 Da in size and they are expected to have elution times before free IgG (M_r ~ 160 000) and after thrombin (M_r ~ 669 000).

5.2.5 Conjugation of HRP to Poly-D-glutamic acid

HRP was covalently attached to poly-D-glutamic acid (average MW 38,000; Sigma-Aldrich P1370) in a similar manner to the procedure described in section 5.2.2. Poly(glu) and HRP were mixed together in a 1:100 (w/w) ratio, pH was adjusted to 7.5, and the mixture was lyophilized. The sample was then sealed under vacuum and heated at 85°C for 96 hours. After heating, the sample was reconstituted to 1 mL in TBS (0.1 M Tris-HCl, 0.15 M NaCl at pH 7.5), in preparation for separation of conjugates by size exclusion chromatography.

Separation of uncross-linked poly(glu) and HRP was performed by SEC-HPLC on a TSK-Gel® G3000SW_{XL} 7.8 mm x 30 cm column (Sigma-Aldrich) with a TBS running buffer as described above in section 5.2.3. The early eluted peaks containing the higher cross-linked poly(glu)-HRP conjugates were collected and concentrated by Amicon® Ultra 50 kDa MWCO centrifugation concentrators (Millipore, Mississauga, ON, CAN) to a volume of approximately 2 mL. Goat anti-rabbit IgG was then added in a weighted ratio of 1:10 with the poly(glu)-HRP conjugate, dialyzed against dH_2O for 4 changes of 1 L each. The pH of the resulting solution was adjusted to 7.5, then the sample was subjected to the

cross-linking procedure as described in section 5.2.2. After *in vacuo* cross-linking procedure was complete, the IgG-poly(glu)-HRP was separated from the unlabeled antibody by gel filtration chromatography as described in section 5.2.3. Large oligomers eluting in the void volume were collected and concentrated using Amicon® Ultra 100 kDa MWCO centrifugation concentrators to a volume of approximately 1 mL.

5.2.6 Quantification of antibody-enzyme conjugates

The APase and the HRP labeled antibodies were quantified using the bicinchoninic acid protein assay (Sigma-Aldrich B9643) developed by Smith et al., 1985 and Wiechelman et al., 1988. Briefly, sulfhydryl and amino groups (and tryptophan or tyrosine to a small extent) on proteins reduce alkaline Cu(II) to Cu(I) in a concentration dependant manner. Bicinchoninic acid is a highly specific chromogenic reagent of Cu(I), forming a purple complex with an absorbance maximum at 562 nm. Therefore protein concentration can be estimated in direct proportion to the absorbance at 562 nm. Three standard curves with corresponding line equations were developed using HRP, bovine serum albumin (used as a standard protein provided in the assay kit), and IgG at increasing concentrations to assess the reactivity of all three proteins in the bicinchoninic assay (Figure 5.2.1). These standard curves allow for the estimation of protein concentration of samples by interpolation into the appropriate line equation depending on the components of the sample. Because of the differences in reactivity between IgG, HRP, and BSA, a choice between each of the three line equations was made to reflect the major component of the antibody-enzyme conjugate. For example, for the quantification of IgG-HRP conjugate, the standard curve of IgG ($y = 0.0104x + 0.0509$) was used to estimate the concentration of the sample, since IgG is a major

component with high reactivity towards this assay. All antibody-enzyme conjugates, including those purchased from commercial suppliers, were quantified using the correct standard curve and then standardized to 0.7 mg/mL through dilution in TBS.

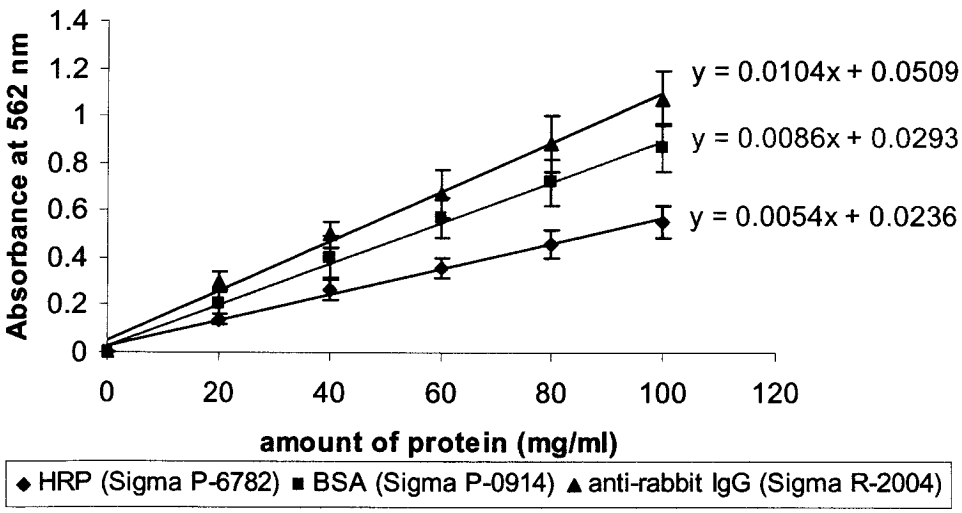

Figure 5.2.1 Bicinchoninic acid protein assay standard curves using HRP, BSA, and IgG in increasing amounts. Error bars represent the standard deviation of the results from three trials.

5.2.7 Detection of antibody-enzyme complexes on Western Blots

Western Blotting involves the transfer of protein, previously separated by size, from a polyacrylamide gel to a membrane to which the protein is adsorbed and immobilized. The membrane is then probed with a primary antibody with specificity for its antigen, next probed with a secondary antibody which has specificity for the primary antibody. The secondary antibody, in most cases, is labeled with a reporter enzyme whose catalytic activity

can be monitored, upon the introduction of a substrate, and a measurable property, i.e. flurorescence, chemiluminescence, or colourimetric, detects the antigen on the blot.

Ovalbumin was loaded in decreasing amounts (5 µg to 1 pg) and electrophoresed on a 12.5 % SDS-PAGE at 200 volts for 55 minutes. A typical gel of ovalbumin was fixed with 7 % acetic acid and 10% methanol for 30 minutes, and then stained with SYPRO® Ruby Red stain (Molecular Probes, Woodburn, CA, USA) for 3 hours to visualize bands. Unstained gels were electrophoretically transferred to PDVF membranes (Millipore Immobilon-P Corp., Nepean, ON, CAN) overnight at 30V using standard protocols, blocked with 1% casein blocking solution (Amersham Biosciences), washed with three changes of TBS-Tween (20 mM Tris-HCl at pH 7.6, 100 mM NaCl, and 1% Tween-20), and incubated for 1 hour at room temperature with a solution of rabbit anti-chick egg ovalbumin (3.9 mg/mL), which had been diluted 1:300 in TBS. If the antibody conjugate tested involved a primary antibody, such as that described in the cross-linking of alkaline phosphatase to anti-ovalbumin, this latter step was omitted and the primary antibody conjugate was applied directly to the blot and detected as described above.

5.2.7.1 The detection of alkaline phosphatase labeled antibodies on Western Blots

A blot of ovalbumin, identical to that described in section 5.2.7, was prepared for the testing of APase labeled IgG conjugates. After incubation of primary antibody and subsequent washing steps, IgG-APase secondary antibody (0.7 mg/mL) was applied to the blot in a dilution of 1:20 000 and incubated for 1 hour at room temperature. Ovalbumin was detected indirectly using the enzymatic activity of APase measured by the formation of a purple precipitate using nitro-blue tetrazolium chloride (NBT) (0.5 mg/mL) and 5-bromo-4-

chloro-3-indolylphosphate toluidine (BCIP) (0.5 mg/mL) reagent solution prepared as follows; 0.1 M Tris, 0.1 M NaCl, 0.005 M $MgCl_2$, 0.5 % (v/v) BCIP, and 0.5 % (v/v) NBT at pH 9.6. Detection times varied between 30 sec and 1 min. The reaction was stopped by the addition of 20 mM EDTA and phosphate buffered saline (PBS)(0.1 M Na_2HPO_4, 0.1 M KH_2PO_4, 0.15 M NaCl, 0.05 M KCl, at pH 7.2).

5.2.7.2 The detection of HRP labeled antibodies on Western Blots

After incubation with primary antibody and subsequent washing steps with TBS-Tween, anti-rabbit IgG-HRP and IgG-poly(glu)-HRP antibody conjugates were incubated for 2 hours at room temperature with the blotted membrane at various concentrations, however, a typical 1:20 000 dilution of a stock concentration of 0.7 mg/mL was used on most blots. Detection of HRP labeled antibodies was performed with ECL™ Western Blotting detection system (a chemiluminescent detection reaction), as described by Amersham Biosciences. The blot was exposed to an X-ray film for 15 seconds, and developed by a Kodak2000 X-OMAT system (Kodak Canada, Toronto, ON, CAN).

5.2.8 Detection of HRP conjugates by direct ELISA

The solution of primary polyclonal antibody (anti-chick egg ovalbumin) was prepared by dilution to 5 µg/mL in 0.5 M carbonate-bicarbonate buffer at pH 9.6. This solution (200 µL) was used to coat a 96 well EIA microtiter plate (Corning Inc, NY, USA) through exposure for 24 hours at 4°C. The coated plate was washed with three changes of PBS-Tween (PBS containing 0.5% Tween-20 (v/v)). A blocking step was performed by the addition of 0.5% casein blocking solution (200 µL) (Amersham Biosciences) diluted in PBS

into each coated well followed by an incubation of the plate for 1 hour at room temperature. After washing with PBS-Tween to remove excess blocking solution, the plate was incubated for 2 hours at room temperature with either IgG-HRP or IgG-poly(glu)-HRP antibody conjugates, diluted appropriately with a final volume of 200 µL. After this incubation, the plate was washed with three changes in PBS-Tween. The 0.4 M *o*-phenylenediamine (OPD) substrate solution used for the colourimetric detection of HRP was prepared by dissolving one SigmaFast® OPD tablet into 20 mL dH_2O as described by Sigma's product description P9187. Substrate was added to each well to give total volumes of 200 µL, and the plate was incubated for 30 minutes in the dark at room temperature. The reaction was stopped by the addition of 50 µL of 3 M HCl and the plate was read at 492 nm by a Tecan GENios spectrophotometer (Tecan Systems Inc, San Jose, CA) microtitre plate reader.

5.2.9 Competitive binding of unlabeled IgG

To evaluate the binding affinity of the antibody conjugates produced by *in vacuo* cross-linking and to quantify the amount of antibody in the sample, competitive ELISA experiments were designed. In these experiments, HRP-labeled antibodies were displaced by the addition of known amounts of IgG (Sigma R2004) and the remaining HRP labeled antibody was measured after the detection of HRP by the addition of its substrate. These data were used to generate competition curves from which the amount of unlabeled antibody required to displace 50% of the signal (EC_{50}) could be determined simply by interpolation. Briefly, all wells of an EIA polystyrene microtitre plate were coated with 200 µL of 5 µg/mL solution of anti-chick egg ovalbumin through incubation for 24 hours at 4°C. After successive washings and blocking steps, as described in section 5.2.8, 0.7 mg/mL of each

conjugate, diluted with PBS to yield a 1:20 000 proportion in a final volume of 200 µL, was mixed with samples of unlabeled IgG (0.35 ng/µL, 0.7 ng/µL, 1.4 ng/µL, 2.1 ng/µL, 2.8 ng/µL, and 3.5 ng/µL) and pipetted into successive wells on the plate. The plate was then incubated for 2 hours at room temperature. After washing with PBS-Tween, OPD substrate was then added in the manner described above, and after a 30 minute incubation in the dark at room temperature, the reaction was stopped with 50 µL of 3 M HCl. Absorbance readings were taken at 492 nm for each sample.

5.2.10 Generation of antibody binding curves

The A_{492} data accumulated from the direct ELISA experiments was compiled and processed using Microsoft Excel® (Microsoft, Mississauga, ON, CAN) and SigmaPlot® V.8.02 (Systat Software Inc., Point Richmond, CA, USA). The A_{492} against ln (antibody dilution) for each antibody conjugate (Figure 5.3.5) were mathematically fitted to create a sigmoidal calibration curve according to the following equation.

$$y = \frac{a}{1 + e^{-\left(\frac{x - x_o}{b}\right)}}$$

Equation 5.1 Sigmoidal curve-five parameters, where *a, b,* and x_o are coefficients determined by the regression analysis.

The mean and standard deviation was derived from triplicate readings of each microtitre plate and from triplicate assays performed with different antibody preparations to ensure

reproducibility of the data. The results of the non-linear regression analysis used in curve fitting were exported into Microsoft Excel® and plots/error bars were generated.

The A_{492} data from the competitive ELISA was similarly analyzed using SigmaPlot®. The plot of A_{492} against concentration of unlabeled IgG (Figure 5.3.6) fits a hyberbolic decay curve with the equation shown in Equation 5.2. The mean and standard deviation of the competitive binding ELISA data were also determined using data from triplicate readings of three independent assays.

$$y = \frac{ab}{b + x}$$

Equation 5.2 Hyberbolic decay - two parameters, where *a* and *b* are coefficients determined by the regression analysis.

In the analysis of the data from the competitive binding ELISA experiment, the A_{492} reading of each IgG conjugate in the absence of unlabeled IgG, or zero dose value is symbolized as B_o. B_o represents the total bound signal resulting from binding of the HRP-labeled antibody in the absence of competition from unlabeled antibody. The signal detected in the presence of any concentration of unlabeled IgG is symbolized as B. The ratio B/B_o was plotted against increasing concentration to unlabeled IgG (Figure 5.3.8) and hyberbolic decay curves were constructed and fitted to Equation 5.2 in the exact same manner as previously described. Interpolation into the hyberbolic curve when y = 0.5, when 50% of the signal is displaced by unlabeled IgG, yields an effective concentration of unlabeled IgG

(EC_{50}) which can be used to compare the quantity and quality of the antibody in the immunoconjugates.

5.3 Results and Discussion

5.3.1 *In vacuo* cross-linking of antibodies to enzymes

The *in vacuo* method of cross-linking proteins has demonstrated efficient and effective coupling of enzymes to form homodimers (as described in Chapter 3) and attachment of enzymes to solid supports (as described in Chapter 4) with retention of full biological activity. This method was extended to an application for the conjugation of enzymes to antibodies to generate improved conjugates for immunoassays. The cross-linking experiments described in this chapter were designed with a view to test the efficacy of the *in vacuo* procedure in cross-linking reporter enzymes, alkaline phosphatase (APase) and horseradish peroxidase (HRP), to either primary or secondary antibodies directly or indirectly using poly-glutamic acid as a support. In these proof-of concept experiments, ovalbumin was chosen as the antigen. Ovalbumin is readily available (and relatively inexpensive) as are anti-ovalbumin primary antibodies. Rabbit anti-ovalbumin antiserum was chosen as a primary antibody and anti-rabbit IgG was chosen as the secondary antibody to be conjugated by this process. These pre-labeled enzyme-linked antibodies are also readily available commercially and thus allowed for the comparison between antibody conjugates made by the *in vacuo* method and those made by chemical cross-linking methods. In each case, the *in vacuo* cross-linking yielded high molecular weight products which could be separated by size exclusion chromatography (data not shown). Their performance in both Western Blots analysis and ELISA were evaluated.

5.3.2 *In vacuo* cross-linking of antibodies to alkaline phosphatase

Initial experiments involved alkaline phosphatase (APase), cross-linked to either a primary antibody (rabbit anti-ovalbumin) or a secondary antibody (anti-rabbit IgG). APase activity can be detected in a colorimetric assay that uses BCIP/NBT in the detection system. Figure 5.3.1 shows a series of Western Blots of gels on which ovalbumin was loaded in decreasing amounts and APase labeled antibodies are used as probes. These preliminary results showed that when APase is cross-linked to rabbit anti-ovalbumin antiserum by the *in vacuo* cross-linking method, amounts as low as 1 µg of ovalbumin can be detected as demonstrated by the appearance of a weak band at an apparent molecular mass of 43 kDa (Figure 5.3.1B, lane 2).

Comparison of panels A (Sypro® Ruby Red staining) and B of Figure 5.3.1 indicates that detection of ovalbumin using an enzyme-linked primary antibody created by the *in vacuo* cross-linking procedure is actually less sensitive than staining, albeit with a staining reagent known to have extremely high detection capabilities. The relatively poor sensitivity of the primary antibody was not surprising and many of the underlying reasons for it relate to the antigen-primary antibody system itself and have little to do with the method used to link the enzyme to the antibody. Anti-ovalbumin, as available commercially, is a polyclonal antibody and this antiserum contains multiple proteins most of which are blood proteins and have no immunological properties. Thus, the cross-linking of APase by any method to this unseparated mixture will most likely yield a variety of heterogeneous complexes. Because the separation of APase cross-linked mixture was accomplished by size exclusion chromatography and the large molecular weight products collected were used directly on the blotted membranes, this complexity results in a *de facto* dilution of reactive moieties

available at a given total protein concentration. Given that this particular APase labeled antibody demonstrated a poor detection of antigen (ovalbumin), the further cross-linking of primary antibodies to enzymes was judged inefficient and required a separation method to purify the primary antibody prior or post conjugation to the enzyme reporter protein. Therefore, monoclonal anti-rabbit IgG secondary antibodies are used for the remainder of this chapter to evaluate the efficiency of cross-linking enzymes to antibodies.

Using the *in vacuo* method of cross-linking, a monoclonal secondary antibody, anti-rabbit IgG, was cross-linked to APase and this antibody-enzyme conjugate produced was compared with a commercially available APase-linked secondary antibody (also anti-rabbit IgG but produced by chemical cross-linking) with respect to its immunological properties on blotted amounts of ovalbumin, pre-incubated with its appropriate primary antibody, rabbit anti-ovalbumin. The IgG-APase conjugate was detected with the standard BCIP/NBT reagents, to yield a purple precipitate, and the results of this comparison are shown in the blots of Figure 5.3.1 C and D.

These results show that, in this initial screen, IgG-APase generated by *in vacuo* cross-linking is comparable to the commercially available product if equal amounts of antibody conjugate are used under the same conditions.

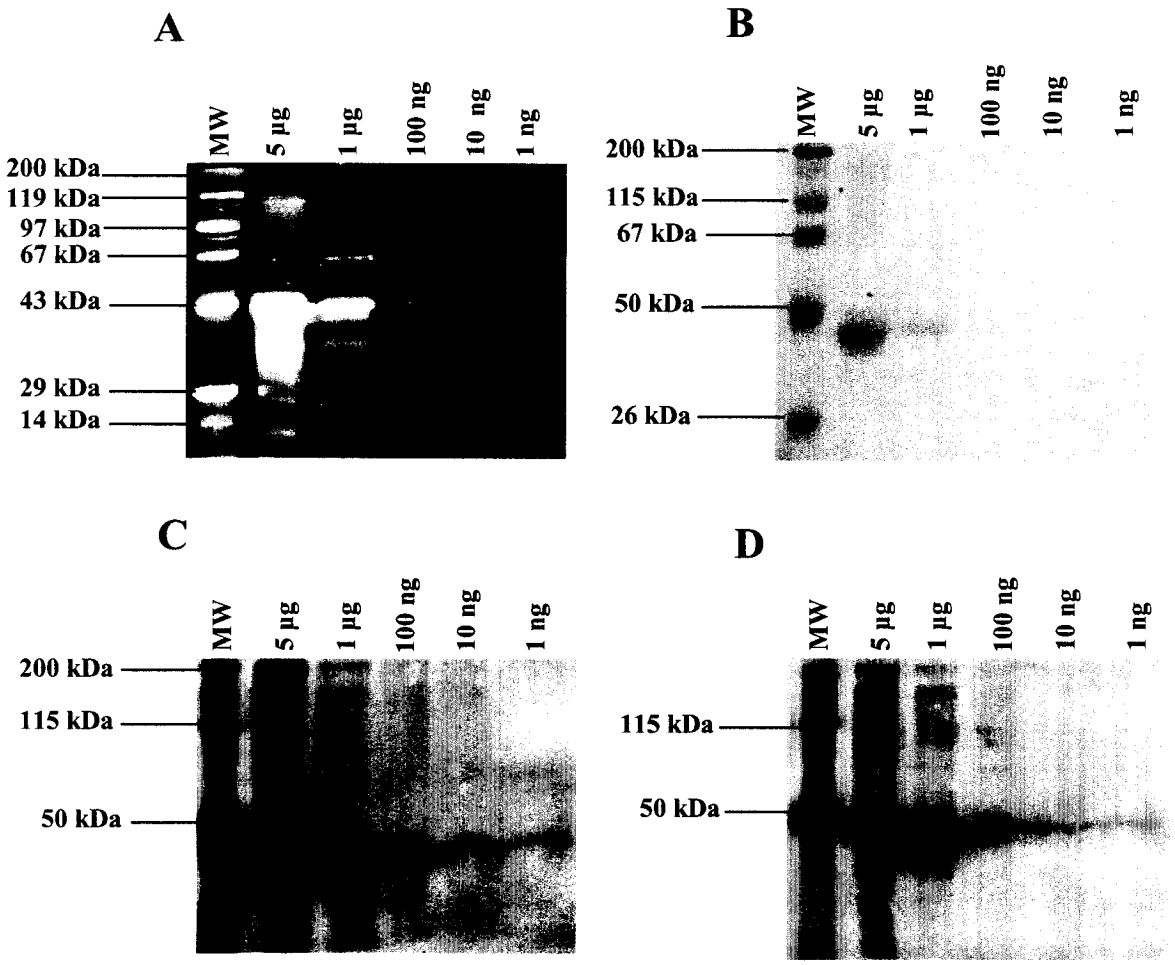

Figure 5.3.1 Western Blot analysis of ovalbumin using alkaline phosphatase labeled antibody conjugates. Ovalbumin was loaded in amounts as indicated on top of each blot, onto a 12.5 % SDS-PAGE along with a pre-stained molecular weight marker (Lane 1). **(A)** Gel stained with Sypro® Ruby Red Stain. The gel was transferred to a PVDF membrane, blocked with 1% casein blocking solution, incubated for one hour with primary rabbit anti-ovalbumin (3.4 mg/mL) at a dilution of 1:300 (except blot B), washed, incubated for 1 hour with secondary antibody conjugate (1.2 mg/mL) at 1:3000 dilution (except blot B), washed again, detected via the NBT/BCIP coloured reaction procedure for 0.5-2 min. **(B)** *In vacuo* cross-linked anti-ovalbumin-APase, 3 mg/mL at 1:300 dilution, **(C)** IgG-APase secondary antibody purchased from commercial source, 1.2 mg/mL and **(D)** *In vacuo* cross-linked IgG-APase, 1.2 mg/mL.

IgG-APase produced by *in vacuo* cross-linking shows a distinct band detecting ovalbumin at an amount of 1 ng (Figure 5.3.1D). An identical detection pattern of ovalbumin is also seen in Figure 5.3.1C, a blot probed with IgG-APase purchased from a commercial source, and 1 ng of ovalbumin is also detected. These preliminary results also indicated that APase labeling of IgGs by *in vacuo* cross-linking generated a reagent in which the enzyme and antibody retained full activity; a result that while expected from previous *in vacuo* cross-linking experiments, needs verification in the specific and sensitive application explored here. The washing of the blots with a detergent between steps and prior to detection with a detergent removes any non-specific binding of proteins to the blot. It can be concluded, therefore, any APase activity detected must be the result of the binding of an antibody that is highly specific for the primary antibody. Despite these promising preliminary results with APase-linked secondary antibodies, the high backgrounds on the membranes and the occasional insolubility problems encountered in lower grade APase products prompted a switch to horseradish peroxidase (HRP). As a smaller, more soluble reporter enzyme, HRP was considered well suited for this investigation.

5.3.3 *In vacuo* cross-linking of IgG to HRP

IgG and HRP were cross-linked in a 1:1 (w/w) ratio using the *in vacuo* method and the large molecular weight conjugates eluted from the gel filtration FPLC system were collected and prepared, by suitable dilution, for immunological testing. Figure 5.3.2B depicts a blot of a gel in which ovalbumin was loaded in decreasing amounts, and detected using goat anti-rabbit IgG-HRP produced by *in vacuo* cross-linking in conjunction with the ECL™ Western photochemical detection reagents provided by Amersham Biosciences to

expose an incubated film. The *in vacuo* cross-linked IgG-HRP product shows a distinct band at all higher loadings of ovalbumin including the lane corresponding to 1 ng of ovalbumin. Less distinct bands are also present at loading amounts of ovalbumin less than 1 ng but these bands are no more intense than those detected in those that appear to be non-specific or higher molecular weight products that are also detected in the ovalbumin preparation. The commercial IgG-HRP conjugate immuno-blot is shown in Figure 5.3.2A. In the case of the commercially available product, a band in the lane marked 1 ng is also visible but no further ovalbumin detected at lower levels of antigen loading. Comparison of equal concentrations of secondary antibody and identical blot incubation times, the IgG-HRP *in vacuo* conjugate appears to be slightly more sensitive than the commercially available enzyme-linked secondary antibody: bands at 1 ng, 5 ng, and 10 ng with the *in vacuo* product blot are more intense than the corresponding bands shown on the commercial IgG-HRP blot. These results also indicate that the activities of both HRP and IgG are fully retained after cross-linking by the *in vacuo* method demonstrating that this procedure does not alter the functionality of the antibody or the enzyme.

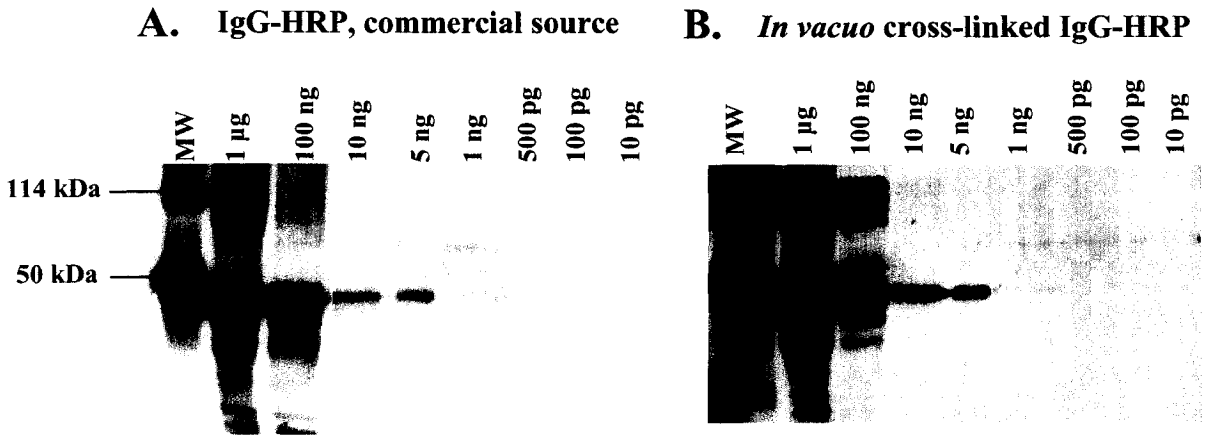

Figure 5.3.2 Western Blot analysis of ovalbumin using horseradish peroxidase labeled antibody conjugates. Ovalbumin was loaded in amounts as indicated on top of each blot, onto a 12.5 % SDS-PAGE along with a pre-stained molecular weight marker (Lane 1). The gel was transferred to a PVDF membrane, blocked with 1% casein blocking solution, incubated for one hour with primary rabbit anti-ovalbumin (3.4 mg/mL) at a dilution of 1:300, washed, incubated for 1 hour with secondary antibody conjugate (0.7mg/mL) at 1:20 000 dilution, washed again, detected via the ECL™ Western Blotting detection system as per described by Amersham Biosciences. **(A)** IgG-HRP secondary antibody purchased from commercial source, 0.7 mg/mL. **(B)** *In vacuo* cross-linked IgG-HRP, 0.7 mg/mL.

5.3.4 Cross-linking of multi-enzyme IgG conjugates for improved sensitivity

The apparent accomplishments in generating an IgG molecule tagged with a molecule of HRP demonstrating slightly improved immunoblot sensitivity was a springboard for the further development of HRP labeled antibodies with a potential for an even greater amplification in signal. Earlier results (reported in Chapter 4) show that enzymes, cross-linked to polypeptide chains such as poly-glutamic acid remain active. The retained activity opens the possibility that multiple units of HRP could be attached to chains of poly-glutamic acid and the ensuing multi-enzyme-linked scaffold, in a subsequent step, can be attached to a

single (or at least limited number) of IgG molecule(s). The product of such a process is expected to be a multi-enzyme immunoconjugate with a much amplified ability to detect antigen. Poly-glutamic acid (poly(glu)), chosen as a soluble scaffold to test this hypothesis, because of its good solubility and its carboxylic acid functionality presents a large number of potential attachment sites of HRP (through lysine residues on the protein). Co-lyophilization of HRP with poly(glu) was performed at a HRP:poly(glu) ratio of 100:1 (w/w) in order to optimize the amount of HRP cross-linking to each soluble scaffold chain. The large poly(glu)-HRP complexes elute on size exclusion chromatography as broad peaks that are easily separated from the unmodified material (Figure 5.3.3). The large molecular weight fractions collected from the SEC-HPLC column were found to contain a high amount of enzymatic activity in a peroxidase assay using OPD as a substrate (data not shown). The relatively mild conditions used in the *in vacuo* procedure have, once again, preserved the catalytic activity of the enzyme after cross-linking.

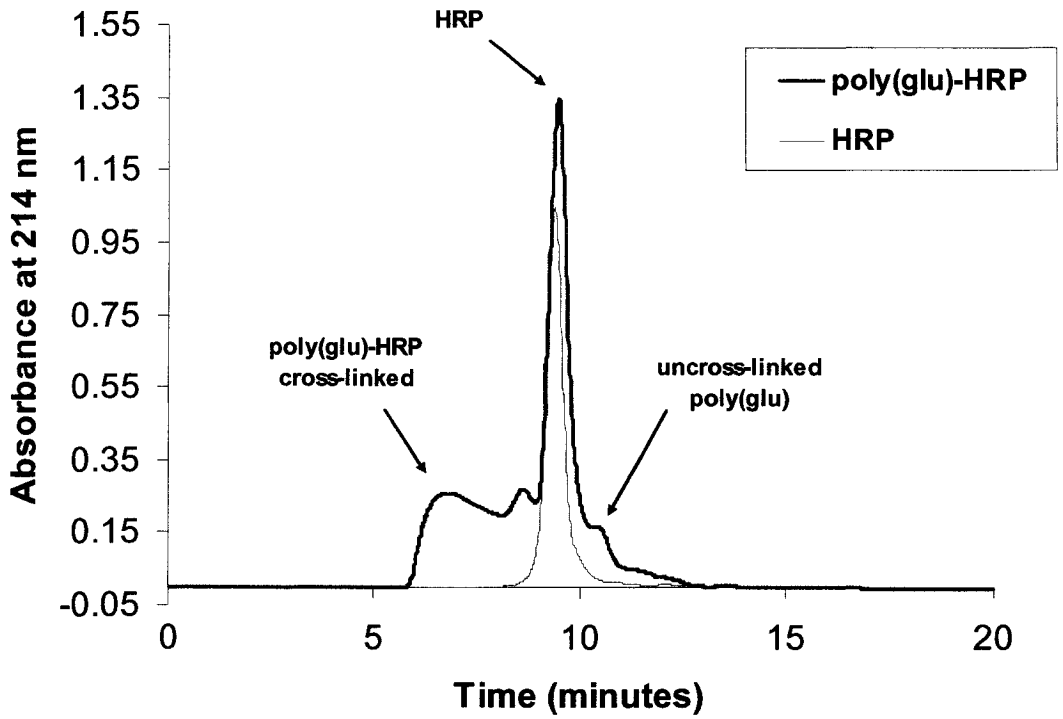

Figure 5.3.3 Size exclusion HPLC of HRP alone (blue line) and of poly(glu)-HRP cross-linked mixture (green line) by a TSK G3000SW$_{XL}$ column.

The next step in the development of the multi-enzyme immunoconjugate was to covalently attach the IgG to the poly(glu)-HRP complex. This attachment was accomplished by co-lyophilizing the IgG and the multi-enzyme-linked scaffold in a 1:10 (w/w) ratio, then incubating the sample under vacuum. The limiting number of IgG ensures that a small number of IgG molecules are attached to each multi-enzyme complex. The unmodified IgG was removed from the cross-linked mixture by size exclusion FLPC, and the very large IgG-poly(glu)-(HRP)$_n$ conjugates were collected and prepared (by appropriate dilution) for testing on immunoblots containing decreasing amounts of blotted ovalbumin. Figure 5.3.4 depicts the Western Blots of ovalbumin probed with IgG-poly(glu)-(HRP)$_n$ produced by *in*

vacuo cross-linking when incubated at equal concentrations (Figure 5.3.4A) used previously in Figure 5.3.2 (i.e. 1:20 000 dilution of 0.7 mg/mL) and three times more concentrated (Figure 5.3.4B) and ten times more concentrated (Figure 5.3.4C blot 1 and 2) than those concentrations. Ovalbumin is detected by a faint band in the lane corresponding to 500 pg in Figure 5.3.4A. This indicates that at an equal concentration to that used in the commercial product immunoblot shown in Figure 5.3.2A, 1:20 000 dilution of 0.7 mg/mL, the *in vacuo* IgG-poly(glu)-$(HRP)_n$ conjugate detects a smaller amount of ovalbumin (500 pg as opposed to 1 ng). Using a concentration three times higher, a 1:6 600 dilution, the IgG-poly(glu)-HRP reagent can detect ovalbumin down to 10 pg, as shown by a faint band in the corresponding lane in Figure 5.3.4C blot 2. A ten fold increase in the concentration, a dilution of 1:2 000, generates a very strong signal on all blotted amounts of ovalbumin, including the lane corresponding to 10 pg. Despite the expected higher backgrounds generated when the concentration of the IgG-poly(glu)-$(HRP)_n$ conjugate is increased, 10 pg of blotted ovalbumin is detected which corresponds to approximately 100 fold increase in sensitivity over the detection limit (1 ng) of the IgG-HRP product purchased from a commercial source.

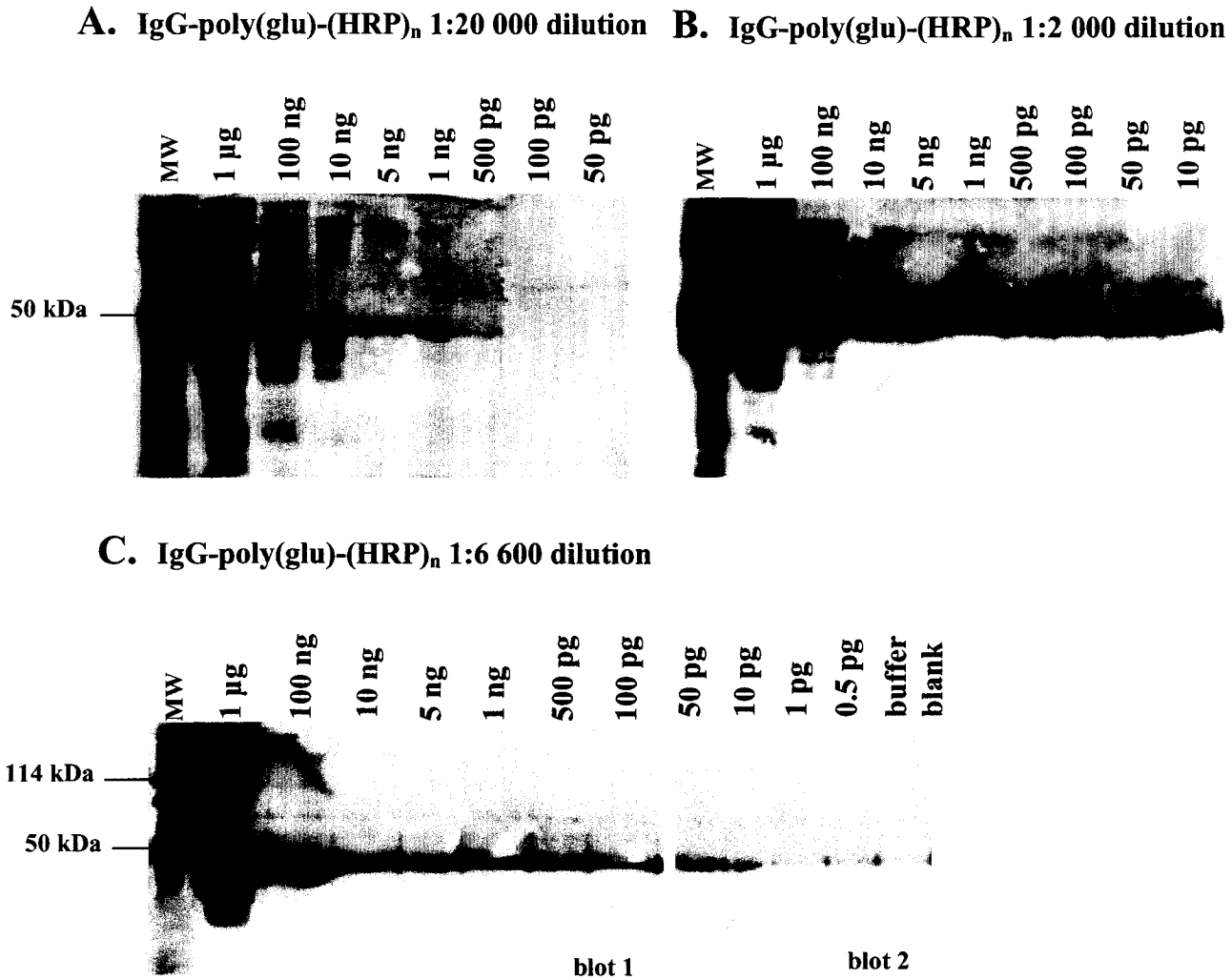

Figure 5.3.4 Western Blot analysis of ovalbumin using poly(glu)-$(HRP)_n$ labeled anti-rabbit IgG conjugates. Ovalbumin was loaded in the amount indicated on the top of each blot onto a 12.5 % SDS-PAGE along with a pre-stained molecular weight marker (Lane 1). The gel was transferred to a PVDF membrane, blocked with 1 % casein blocking solution, incubated for one hour with rabbit anti-ovalbumin (3.4 mg/mL) at 1:300 dilution, washed, incubated for 1 hour with secondary antibody anti-rabbit IgG-poly(glu)-$(HRP)_n$ conjugate, washed again detected with ECL™ Western Blot detection reagents from Amersham Biosciences. The IgG-poly(glu)-$(HRP)_n$ conjugate was quantified at 0.7 mg/mL and then diluted to 1:20 000 (A), 1:2 000 (B), and 1:6 6000 (C, blots 1 and 2).

5.3.5 *In vacuo* cross-linked antibody conjugates tested by ELISA

While the improved sensitivity in the detection of antigen by the enzyme-linked antibody produced by the *in vacuo* method is apparent on Western Blots, Western Blotting does not easily lend itself to accurate quantification. It was therefore necessary to confirm these results using a more quantitative method of immunodetection such as enzyme-linked immunosorbent assay (ELISA). In an ELISA, either an antigen or antibody is immobilized onto a surface, typically a microtitre plate well. That surface is incubated with the appropriately labeled antibody which can then be detected using a measurable colorimetric reaction read by a microtitre plate reader and a spectrophotometer. Because it is quantitative (unlike Western Blotting which is only semi-quantitative) ELISAs can help to assess the cross-linking efficiency of the *in vacuo* method and the quality of cross-linked antibody-enzyme product. In order to test the activity of the *in vacuo* cross-linked IgG-HRP products, rabbit anti-ovalbumin antiserum (5 µg/mL) was adsorbed onto polystyrene microtitre plates and the anti-rabbit IgG immunoconjugates were evaluated for their binding affinity to this primary antibody by means of a standardized colorimetric reaction of the oxidation of ODP (*o*-phenylenediamine dihydrochloride), a substrate for HRP (Bovaird et al., 1982).

Figure 5.3.5 shows the ELISA results of *in vacuo* cross-linked IgG-HRP and IgG-poly(glu)-$(HRP)_n$ at 0.7 mg/mL, incubated in decreasing dilutions, binding to the primary antibody (rabbit anti-ovalbumin) immobilized onto a polystyrene microtitre plate. After a 30 minute incubation with OPD (the substrate of HRP), the reaction was stopped with 3.0 M HCl, and the plate was read at 492 nm and the data collected. As the concentration of the immunoconjugate decreased, the absorbance plotted followed a sigmoidal curve, the data was fitted, and an equation was obtained representing the signal per HRP labeled antibody

bound. Titre is defined as the dilution of conjugate sufficient to give a change in absorbance of 1.0 at 492 nm after 30 minutes of substrate conversion at 25°C. In the assay containing the *in vacuo* cross-linked IgG-HRP product (blue line), a dilution of 1:18 300 was required to generate a signal of 1 absorbance unit (1 Au) for a 30 minute reaction time. The IgG-HRP product purchased from a commercial source (red line) required a higher concentration, a dilution of only 1:14 200, to achieve the same signal in the same reaction. These results are consistent with the results obtained by Western analysis, indicating the slight increase in sensitivity of the *in vacuo* cross-linked IgG-HRP conjugate relative to the commercial homologue. Both enzyme-linked secondary antibodies (commercial and *in vacuo* products) are expected to contain enzyme and antibody in a 1:1 ratio and the same concentration of both was applied in the experiment. The *in vacuo* methodology, therefore, appears to generate an immunoconjugate of higher quality, either by producing an enzyme with a greater retention of catalytic activity, or an antibody with greater binding affinity than in the commercially available conjugates produced by chemically activating with bifunctional reagents. It should be noted that the starting materials used in the *in vacuo* cross-linking procedure were obtained from the same supplier who provided the IgG-HRP conjugate for comparison.

The IgG-poly(glu)-$(HRP)_n$ conjugate was also tested under exactly the same conditions used above and compared with the singly enzyme-labeled IgG antibody conjugates. The results (green line in Figure 5.3.5) demonstrated that an even higher dilution (1:35 000) achieves a signal of 1 absorbance unit after a 30 minute reaction time. This indicated that it requires less IgG-poly(glu)-$(HRP)_n$ reagent, approximately 2.5-fold less, to generate the same signal as the singly labeled IgGs.

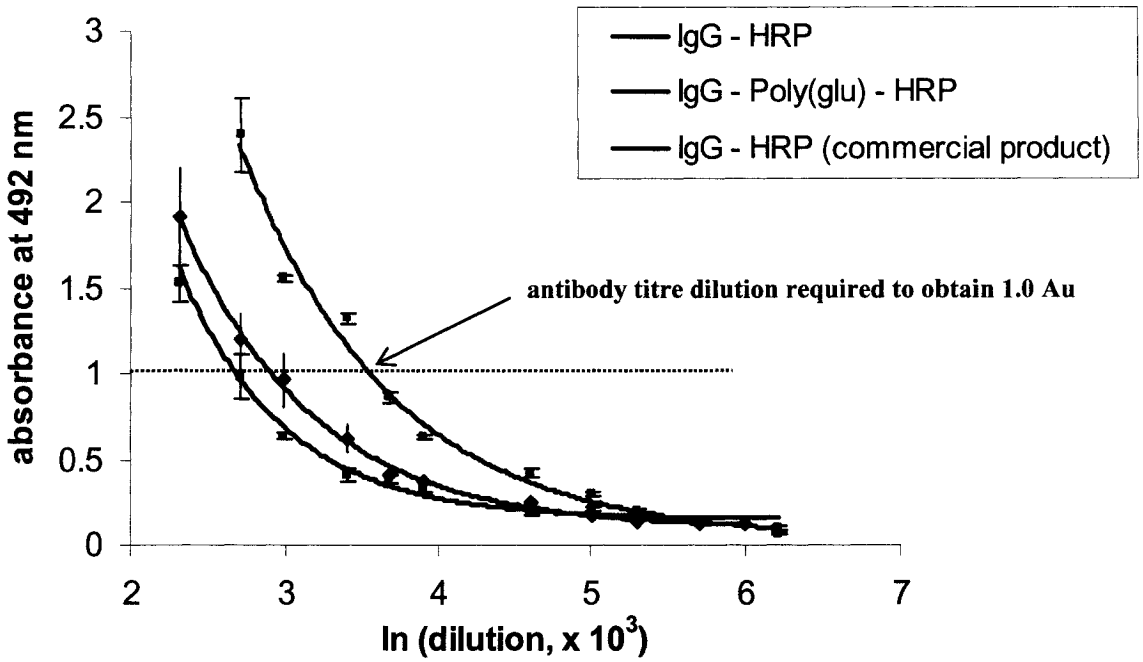

Figure 5.3.5 Titrating for optimal peroxidase activity of the IgG-HRP conjugates by increasing their dilution in a direct ELISA. IgG-HRP, IgG-poly(glu)-HRP by *in vacuo* cross-linking, and IgG-HRP from Sigma, all standardized to 0.7 mg/mL, were diluted to 1:400 000, 1:300 000, 1:200 000, 1:150 000, 1:100 000, 1:50 000, 1:40 000, 1:30 000, 1:20 000, 1:15 000, and 1:10 000, and incubated in a microtitre plate coated with 5 µg/mL of anti-chick egg ovalbumin for 2 hours at room temperature. Detection with OPD substrate for 30 min, after which the reaction was stopped by 50 µL of 3 M HCl, readings taken at A_{492nm}. Data were collected in triplicate readings by TECAN™ microtitre plate reader and sigmoidal curves were created by curve fit analysis by SigmPlot™.

5.3.6 Determination of antibody concentration

Assuming that the antibody is the limiting component in immunodetect assays, the concentration of antibody should be standardized to determine the signal generated per antibody bound and this allows direct comparisons between conjugated products. It is expected that the composition of the *in vacuo* cross-linked IgG-poly(glu)-$(HRP)_n$ conjugate differed from that of the IgG-HRP products. While IgG-ply(glu)-$(HRP)_n$ has undoubtedly

more enzyme molecules attached via the poly(glu) chain to each individual antibody molecule, less antibody per mg of total protein conjugate was applied. It is impossible to discern the precise amount of antibody per conjugate as methods to determine protein concentration cannot differentiate between the IgG and HRP in the sample. The following experiment, therefore, was designed to determine the amount of antibody present for a given amount of signal detected and thus standardize the amount of IgG in each conjugate. An ELISA was prepared testing the binding affinity of a fixed amount of labeled (enzyme-linked) IgG conjugate, a 1:20 000 dilution of 0.7 mg/mL, in the presence of unlabeled (no enzyme) IgG, added in decreasing amounts. The antibodies were allowed to compete with one another for binding to the immobilized primary antibody, and after equilibrium was achieved, the amount of bound labeled antibody was detected. The effective concentration of unlabeled IgG required to displace 50% of the bound labeled antibody, EC_{50} was then determined. The results of this "competitive ELISA" are shown in Figure 5.3.6.

As the amount of unlabeled IgG added increases, the signal representing bound labeled IgG-HRP decreases in a manner reminiscent of a hyperbolic decay curve the shape of which describes the binding affinity of the labeled IgG conjugate and its susceptibility to being displaced by the unlabelled IgG. As expected, the curves for the *in vacuo* produced IgG-HRP and the commercial IgG-HRP product show a similar decrease in signal as the amount of unlabeled IgG increases and hence a similar but not absolutely identical amount of antibody present in each mg of enzyme-linked IgG conjugate was applied (see discussion below). The IgG-poly(glu)-$(HRP)_n$ conjugate, although showing an enhanced signal, is considerably more susceptible to displacement by the unlabelled IgG as shown by a steeper depletion of signal as unlabeled IgG increases. This indicates that there is less antibody per

mg of total protein in this conjugate and hence more enzyme than in the singly conjugated products.

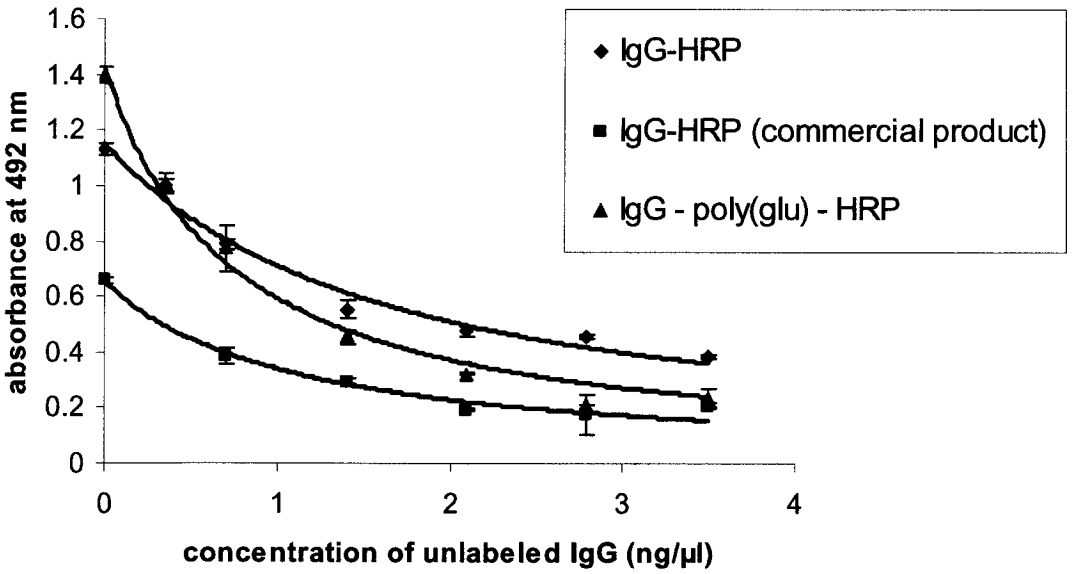

Figure 5.3.6 Competitive binding of HRP labeled IgG and unlabeled IgG (Sigma) by direct ELISA. IgG-HRP, IgG-poly(glu)-$(HRP)_n$ by *in vacuo* cross-linking, and IgG-HRP from Sigma, all at standard concentrations of 0.7 mg/mL, were diluted by 1:20 000 and 0.35 – 2.8 ng of unlabeled IgG was added in a total volume of 200 µL, incubated in an EIA well coated with 5 µg/mL of anti-chick egg ovalbumin for 2 hours at room temperature. Detection with OPD substrate for 30 minutes, after which reaction was stopped by 50 µL of 3 M HCl, and readings were taken at A_{492}. Data was collected in triplicate readings by TECAN™ spectrophotometer microtitre plate reader and hyperbolic decay curves were created by curve fit analysis by SigmPlot™.

If the absorbance values obtained in the competitive binding ELISA are considered to be "bound signal (B)" (by analogy to the radioactive competitive receptor-binding assays on which this experiment was modeled) and a ratio is formed between the signal in the presence

of competitor (unlabeled IgG) to the total signal in the absence of competitor (B_o), i.e. B/B_o, new hyperbolic curves are generated depicting the displacement of enzyme-labeled IgG conjugates upon the increase of unlabeled IgG added (Figure 5.3.7). These curves allow one to determine the amount of unlabeled IgG necessary to displace 50% of the bound signal (EC_{50}) for each conjugate thereby providing information on the relative amounts of antibody in the conjugate (EC_{50} values of each conjugate are listed in Table 5.3.1). Based on the interpolation into these curves, the *in vacuo* cross-linked IgG-HRP conjugate requires 1.65 ng/μL or 330 ng of unlabeled IgG to displace 50% of bound signal (blue line). The commercially purchased HRP labeled IgG, assayed at the exact same total protein concentration and dilution, required 1.05 ng/μL or 210 ng of unlabeled IgG to achieve the same depletion in signal. These results indicate that there is either more antibody per mg of total protein present in the *in vacuo* product compared to the commercial product or that the antibody has a higher affinity for the immobilized primary antibody. If the former proposition is correct and there are actually more antibody molecules present per mg of total protein conjugate applied in the assay, there would, as a necessary corollary, be less enzyme present. Given that the *in vacuo*-prepared conjugate actually produces more enzymatic activity than its commercial counterpart, this scenario seems unlikely. One must therefore conclude the latter explanation to be correct; the antibody present in the *in vacuo*-prepared conjugate has a higher affinity for the immobilized primary antibody than does the purchased IgG-HRP product. Considering that all starting materials are sourced from the same supplier and that the quality of the manufacturer's preparations can reasonably be presumed to be very similar from lot to lot, it is not unreasonable to assume that the IgG used in the cross-linking procedure has equal binding affinity to the IgG-HRP and the unlabeled IgG

purchased from the same supplier. If these assumptions are correct, the *in vacuo* method of cross-linking appears to have generated a product of higher binding affinity or rather to have preserved more of the antibody's original binding capacity after the cross-linking procedure.

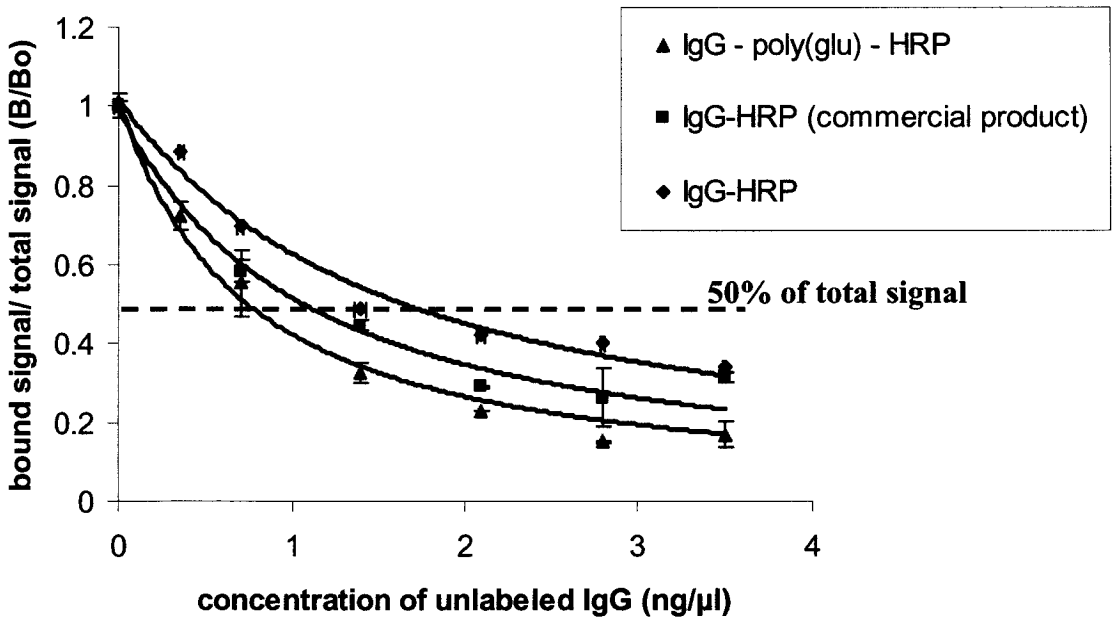

Figure 5.3.7 Competitive binding of HRP labeled IgG and unlabeled IgG (Sigma) by direct ELISA. IgG-HRP, IgG-poly(glu)-$(HRP)_n$ by *in vacuo* cross-linking, and IgG-HRP from Sigma, all at standard concentrations of 0.7 mg/mL, were diluted by 1:20 000 and 0.35 – 2.8 ng of unlabeled IgG was added in a total volume of 200 µL, incubated in an EIA well coated with 5 µg/mL of anti-chick egg ovalbumin for 2 hours at room temperature. Detection with OPD substrate for 30 minutes, after which the reaction stopped by 50 µL of 3 M HCl, readings taken at A_{492}. Data was collected in triplicate readings by TECAN® spectrophotometer microtitre plate reader. Total signal from each conjugate was determined and each absorbance reading collected from the addition of unlabeled IgG was divided by the total signal to get B/B_0. Hyperbolic decay curves were created by curve fit analysis by SigmaPlot®.

Table 5.3.1 EC_{50} values of *in vacuo* cross-linked IgG-HRP and IgG-poly(glu)-$(HRP)_n$ compared to IgG-HRP prepared by chemical cross-linking (commercial source).

IgG conjugate	EC_{50} (ng/µL)
IgG-HRP (commercial source)	1.05
IgG-HRP *in vacuo* cross-linked	1.65
IgG-poly(glu)-$(HRP)_n$	0.74

The curve resulting from the competitive binding assay from the displacement of the IgG-poly(glu)-$(HRP)_n$ conjugate (green line in Figure 5.3.7) by the unlabeled IgG was also analyzed in a similar manner. The IgG-poly(glu)-$(HRP)_n$ curve shows a steeper depletion in signal compared to the curve depicted by the singly labeled antibodies. Through interpolation into the IgG-poly(glu)-$(HRP)_n$ curve, it was determined that only 0.74 ng/µL or 148 ng of unlabeled IgG was required to displace 50% of the bound signal. This indicates that there is approximately 2.5 times less antibody per mg of total protein present in this conjugate compared to the IgG-HRP conjugate, which required 330 ng of unlabeled for the 50% signal displacement (148 ng/330 ng equals approximately 1/2.5). The smaller amount of antibody per total weight in the IgG-poly(glu)-$(HRP)_n$ *in vacuo* conjugate was expected, however, despite the limiting number of antibody molecules, the signal obtained per mg of the IgG-poly(glu)-$(HRP)_n$ conjugate in the absence of competitor is 3 fold higher. Hence, the binding event of one IgG molecule carries multiple units of HRP and enhances the detection signal beyond the capabilities of the singly enzyme-linked IgGs.

5.4 Conclusions

The *in vacuo* method of cross-linking protein has shown with good efficiency and efficacy the cross-linking of antibodies to reporter enzymes and generated antibody-based reagents with greater sensitivity than reagents currently available from commercial sources. The anti-rabbit IgG-HRP conjugate produced by the *in vacuo* procedure had a high sensitivity, detecting 1 ng, in the Western Blot analysis of ovalbumin, equal to the detection limit of IgG-HRP purchased commercially. In the ELISA studies, *in vacuo*-prepared IgG-HRP conjugates showed an increase in sensitivity relative to the commercial product, when equal concentrations were assayed, and also demonstrated an increase in binding affinity to a rabbit primary antibody. By simply heating a co-lyophilized mixture of HRP and IgG under vacuum, the resulting cross-linked IgG-HRP product is presumed to have retained its native protein structure and thus had a higher activity as demonstrated by its improved performance in immunoassays.

Multi-enzyme-linked antibodies have the potential to increase the detection signal many fold beyond the detection limits of singly-enzyme-linked antibodies. The *in vacuo* cross-linked IgG-poly(glu)-$(HRP)_n$ had a detection limit of 10 pg of ovalbumin, almost a 100 fold increase in sensitivity from the results obtained using singly-enzyme-linked IgG when equal amounts of antibody are applied. Although the total amount of bound HRP to the poly(glu) scaffold was not directly quantified, it is presumed that each molecule of poly(glu) carries a random distribution in the amount of HRP, and collectively, these conjugates generate a 100 fold increase in detection capability. Further development of multi-enzyme-linked polymer scaffolds will allow one to optimize the cross-linking efficiency to antibodies. Bulk mass transfer effects and steric hinderance on binding of IgG are factors

that affect the assay performance of the multi-enzyme-linked IgG and it will require further investigation to determine the ideal construction and size of the conjugate.

Current procedures in chemically cross-linking antibodies with enzymes, adopted by several manufacturers, include activating the proteins with bifunctional reagents followed by coupling through common functional groups, in most cases, primary amines. Even though these chemical cross-linking methods have successfully produced active immunoreagents, the presence of chemical modifying agents in the cross-linking reaction create possibilities of altering the function of the protein and generating the following limitations: (1) not all enzymes and antibodies will be efficiently coupled using the same sets of reagents; (2) loss of enzyme activity as a result of the introduction of a foreign linking group; (3) loss of antibody binding affinity; (4) cost demands for up-scaling large quantities and the use of large amounts of chemical reagents; and (5) poor yields and variant complexes.

The *in vacuo* method of cross-linking is an efficient and cost-effective method of coupling enzymes to antibodies for the following reasons: (a) the methodology is straightforward and results are highly reproducible; (b) no chemical activating reagents are present thereby increasing the likelihood that the activity of the enzyme and antibody will be retained; (c) good yields of single antibody-enzyme complexes; (d) few and selective linkages minimizing heterogeneous complexes; (e) flexible and controllable based on the ratios of enzyme:antibody added in the co-lyophilization mixture; and (f) and unmodified protein can be recovered and reused.

5.5 Acknowledgements

I would like to thank Sylvie Fournier (Centre for Biologics Research, Health Canada) for the technical assistance in the preliminary stages of this project. As well, my thanks go out to Dr. Mary King (Northern Center for Biotechnology and Clinical Research, Sudbury) for the intellectual input.

5.6 References

Avrameas, S. Detection of antibodies and antigens by means of enzymes. *Bull. Soc. Chim. Biol. (Paris)* **1968,** *50* (5), 1169-1178.

Avrameas, S.; Ternynck, T. The cross-linking of proteins with glutaraldehyde and its use for the preparation of immunoadsorbents. *Immunochemistry.* **1969,** *6* (1), 53-66.

Avrameas, S. Coupling of enzymes to proteins with glutaraldehyde. Use of the conjugates for the detection of antigens and antibodies. *Immunochemistry.* **1969,** *6* (1), 43-52.

Bovaird, J.H.; Ngo, T.T.; Lenhoff, H.M. Optimizing the *o*-phenylenediamine assay for horseradish peroxidase: effects of phosphate and pH, substrate and enzyme concentrations, and stopping reagents. *Clin. Chem.* **1982,** *28(12):*2423-2426.

Dhawan, S. Design and construction of novel molecular conjugates for signal amplification (II): use of multivalent polystyrene microparticles and lysine peptide chains to generate immunoglobulin-horseradish peroxidase conjugates. *Peptides* **2002,** *23* (12), 2099-2110.

Dhawan, S. Design and construction of novel molecular conjugates for signal amplification (I): conjugation of multiple horseradish peroxidase molecules to immunoglobulin via primary amines on lysine peptide chains. *Peptides* **2002,** *23* (12), 2091-2098.

Kala, M.; Bajaj, K.; Sinha, S. Magnetic bead enzyme-linked immunosorbent assay (ELISA) detects antigen-specific binding by phage-displayed scFv antibodies that are not detected with conventional ELISA. *Anal. Biochem.* **1997,** *254* (2), 263-266.

Kluger, R.; Alagic, A. Chemical cross-linking and protein - protein interactions - a review with illustrative protocols. *Bioorg. Chem.* **2004,** *32* (6), 451-472.

O'Sullivan, M. J.; Marks, V. Methods for the preparation of enzyme-antibody conjugates for use in enzyme immunoassay. *Methods Enzymol.* **1981,** *73* (Pt B), 147-166.

Smith, P. K.; Krohn, R. I.; Hermanson, G. T.; Mallia, A. K.; Gartner, F. H.; Provenzano, M. D.; Fujimoto, E. K.; Goeke, N. M.; Olson, B. J.; Klenk, D. C. Measurement of protein using bicinchoninic acid. *Anal. Biochem.* **1985,** *150* (1), 76-85.

Ternynck, T.; Weston, P.; Guilbert, B.; Avrameas, S. A new process for the preparation of insoluble proteins and of proteins coupled with peroxidase. *Ann. Inst. Pasteur (Paris)* **1972,** *123* (1), 146-147.

Ternynck, T.; Avrameas, S. Polyacrylamide-protein immunoadsorbents prepared with glutaraldehyde. *FEBS Lett.* **1972,** *23* (1), 24-28.

Ternynck, T.; Avrameas, S. A new method using p-benzoquinone for coupling antigens and antibodies to marker substances. *Ann. Immunol. (Paris)* **1976,** *127* (2), 197-208.

Ternynck, T.; Avrameas, S. Conjugation of p-benzoquinone treated enzymes with antibodies and Fab fragments. *Immunochemistry.* **1977,** *14* (11-12), 767-774.

Vermeer, A. W.; Norde, W. The thermal stability of immunoglobulin: unfolding and aggregation of a multi-domain protein. *Biophys. J.* **2000,** *78* (1), 394-404.

Wiechelman, K. J.; Braun, R. D.; Fitzpatrick, J. D. Investigation of the bicinchoninic acid protein assay: identification of the groups responsible for color formation. *Anal. Biochem.* **1988,** *175* (1), 231-237.

Wilson, M. B.; Nakane, P. K. *Immunofluorescence and related Staining Techniques;* Elsevier/North Holland BioMedical Press: Amsterdam, 1978.

Chapter 6: Dimer Formation in a Monomeric *De Novo* Design: Milk Bundle Proteins

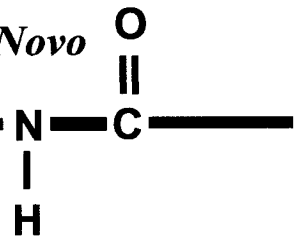

6.1 Introduction

Milk bundle proteins (MB) were designed by *de novo* methods to incorporate a large number of the nutritionally important amino acids, methionine, lysine, leucine, and threonine, for a dietary application in agriculture. The protein was originally engineered to fold into a stable four-helix bundle protein. The initial objective of Hefford and Beauregard (1995) was to select an amino acid sequence enriched in those specific amino acids that would adopt a stable tertiary structure and a helical bundle fold.

Secondary structure characterization of the first milk bundle construct, MB-1, indicated the protein was largely α-helical with a well packed hydrophobic core. However, physical evidence suggested that the protein was dimeric rather than monomeric in solution. In addition, as initially designed, MB-1 appeared to be relatively unstable in thermal and chemical denaturation studies (Hefford *et al*, 1999). Efforts were then focused on creating a series of variants (by site directed mutation) to encourage the conformer to adopt a stable monomeric fold.

If one assumes that the original design of the helical regions of MB-1 is sound (and the several reasons to do so are discussed in Parker and Hefford, 1998), one would predict that dimer formation results when one or another of the loops fails to form as designed. Figure 6.1.1 depicts possible dimers of MB-proteins, each resulting from the failure of a different loop to form the intended turn and fold helices against one another in the monomer. Each of these folds constitutes "domain swapping", a phenomenon recently defined by Eisenberg and co-workers (1995) and seen in a variety of other proteins under certain conditions. This "3D domain swapping" may be more probable in this particular 4-helix bundle design because it contains sets of identical helical domains linked covalently by

flexible hinges or loop regions (Saint-Jean et al., 1998). Opening of a "hinge" (loop) allows the helices to dissociate from each other and to re-associate with equivalent helices from a second monomer giving rise to a homodimer. This homodimer would contain two helix-helix interfaces, each identical to the interface that was designed to exist in the original monomer.

Four different domain-swapped dimers are possible. Two (the "1st helix swapped dimer" and the "4th helix swapped dimer") involve the swapping of one helix between the monomers in the dimer whereas the open-faced dimer involves the swapping of two helices. Two open face dimer conformers are possible as Helix 1 and Helix 3 have identical sequences except for one leucine residue that is replaced with a tyrosine. Helix 2 and 4 are also identical. The resulting set of two 4-helix bundles yields dimers both with equivalent cores. However, the open face dimer II (as shown in Figure 6.1), is expected to be less favourable because steric hinderance resulting from the proximity of the two tyrosine residues in two Helix 3 partners is predicted to interfere with the proper packing of the bundle core. The open face dimer I is, therefore, theoretically the more plausible structure. The 3D domain swapping of the 1st helix (N-terminal domain), and the 4th helix (C-terminal domain) are also possible homodimer conformers and each would result in the designed packing of the bundle core.

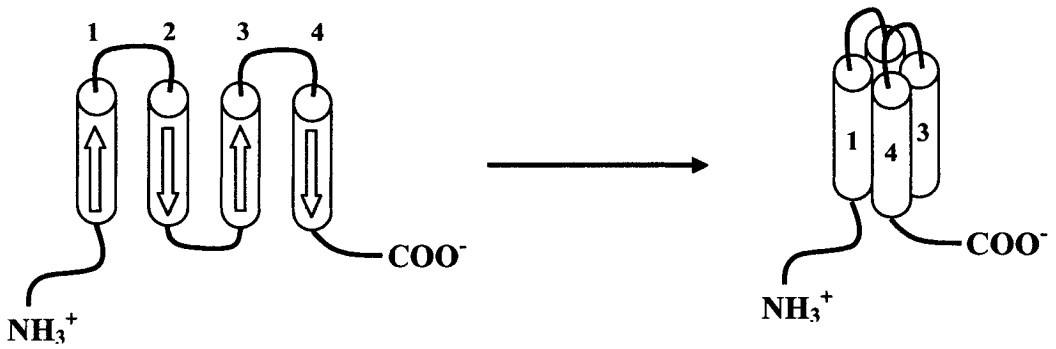

4-helix bundle design **4-helix bundle folded**

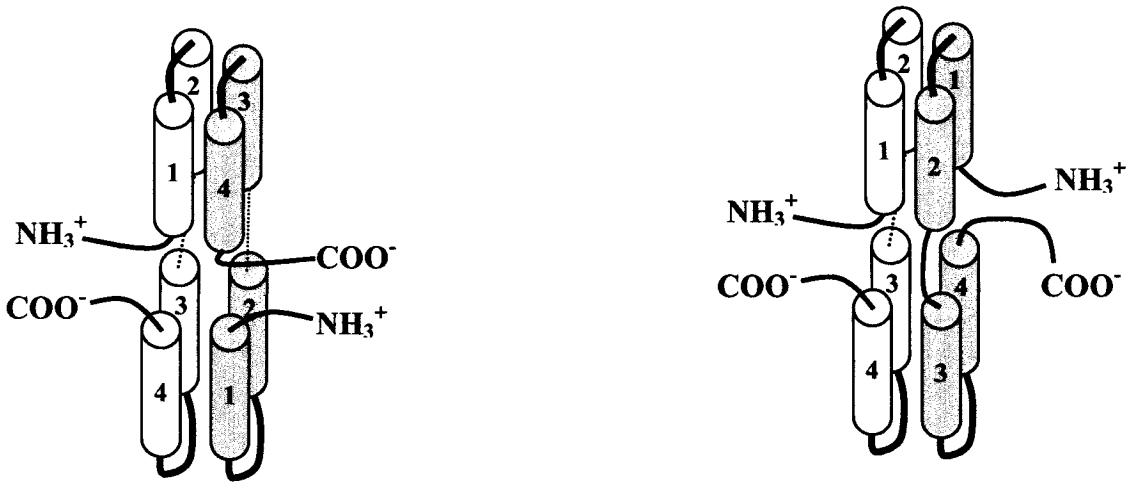

open face dimer I **open face dimer II**

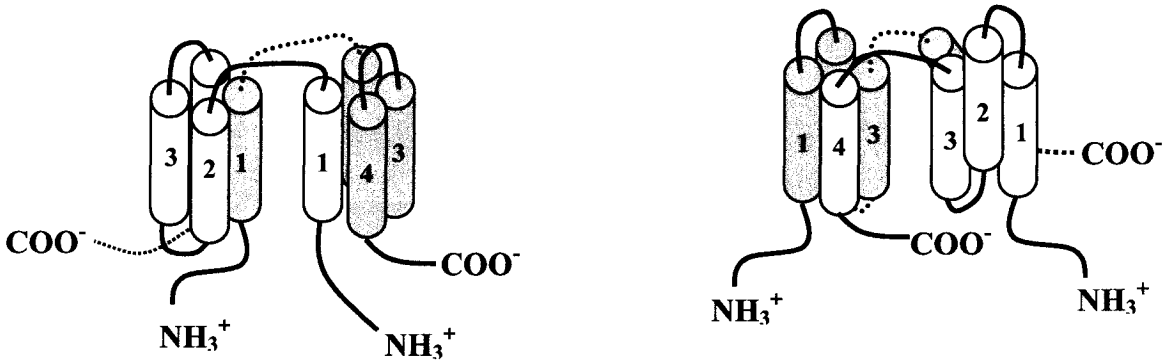

1st helix swapped dimer **4th helix swapped dimer**

Figure 6.1.1 MB-1 four-helix bundle design and its possible homodimeric conformers.

While the dimeric nature of MB-proteins does nothing to detract from their practical utility as a source of essential amino acids for high-producing dairy cattle or other agricultural applications, the original design intent was a monomeric protein and the reasons for deviation from the design remains of theoretical interest. This section of the thesis work began as a secondary project to attempt to resolve the reasons for dimer formation in MB-variants by making changes in the residues of the loops between helices. As the characterization of new variants progressed, it became evident that the *in vacuo* cross-linking procedure had at least the potential to help resolve this issue. This chapter, therefore, describes the results of both the initial characterization of MB-variants with altered loop residues and the application of the *in vacuo* method to attempt to ascertain the form of the dimer formed by MB-1 and its variants.

6.2 Materials and Methods

6.2.1 Mutant construction (performed by Drs. Dean Scholl and Alain Doucet)

The gene for MB-16 and MB-13/16 were made by site directed mutagenesis of the MB-1 and MB-13 genes, respectively, using the primer 5'-ATGCAGAAGGGTGGAGGAGGTGGAGAGGATATG-3' in the Kunkel method (Kunkel et al., 1991). Genes for both MB-16 and MB-13/16 were cloned as fusions to the gene for maltose binding protein (MBP) using the pMal-c2 vector (New England Biolabs, Beverly, MA, USA) and the resultant plasmid used to transform DH5αF' *E. coli* cells (Gibco® Invitrogen, Burlington, ON, CAN). Gene sequences were verified by dideoxy-sequencing using ^{35}S-ATP.

6.2.2 Protein purification of MB-1 and MB-16

MB-1, MB-16, and MB-13/16 were expressed and purified from *E. coli* as per the protocol described by Beauregard et al., 1995, with only minor variations in the gradient of the ion exchange chromatography to enhance the separation of the different variants from MBP. Milk bundle proteins were expressed as a MBP fusion protein by using a construct (Beauregard et al., 1995) in the pMALc2 plasmid (New England Biolabs, Beverly, MA, USA) which is induced by the addition of 100mM IPTG (isopropyl-beta-D-thiogalactopyranoside) to each 1 L of media. The bacteria (grown in 2YT broth (Invitrogen, Burlington, ON, CAN)) was pelleted at 8600 rpm for 30 min at 4°C and the cell pellet was reconstituted into amylose column buffer (0.01 M Tris-HCl, 0.2 M NaCl, 1 mM EDTA (ehtylenediamine tetraacetic acid), and 1mM NaN_3 at pH 7.4) with 10 µL of PMSF (phenylmethyl sulfonyl fluroride). The cells were sonicated and the soluble fraction separated by centrifugation at 5600 rpm for 30 min at 4°C.

The soluble fraction was removed and subjected to affinity purification chromatography using Amylose resin (New England Biolabs). The fusion protein is preferentially retained onto the column resin because of the maltose binding domain while all other cellular proteins pass through. The fusion protein was pumped onto the column at 1 mL/min using an FPLC system (Amersham Biosciences, Baie d'Urfée, PQ, CAN) and the eluted proteins were detected by a UV detector (Bio-Rad Laboratories, Mississauga, ON, CAN) set at 280 nm. The fusion protein was eluted from the column by a solution of 100 mM maltose in amylose column buffer and collected. The fusion protein was cleaved through a Factor Xa site, by dialysis into 20 mM Tris-HCl, 200 mM NaCl, 2 mM $CaCl_2$ at pH 8.0 with the addition of 140 µL of 1 mg/mL Factor Xa. After a 2 hour incubation at

room temperature, the cleaved fusion protein was dialyzed into 10 mM Tris-HCl, 1 mM EDTA at pH 8.25 for 2 changes of 2 L over 12 hours at 4°C.

After cleavage of the fusion protein, the milk bundle protein was separated from the maltose binding protein by weak anion exchange chromatography using DEAE sepharose fast flow resin (Amersham Biosciences). The cleaved fusion protein was loaded onto a 30 cm column equilibrated with 10 mM Tris-HCl and 1 mM EDTA at pH 8.25 and pumped through by an FPLC system at 1 mL/min. The proteins were separated by retention in the column and eluted by a gradient of 0 to 200 mM NaCl. The steepness of the gradient was optimized for each variant to maximize its separation from MBP. The fractions containing milk bundle protein were collected and concentrated using Amicon® Ultra 5 kDa MWCO centrifugal filtering devices (Millipore, Nepean, ON, CAN) to a volume of approximately 2 mL. The protein sample was stored at 4°C or lyophilized from a solution of 0.1 M NH_4HCO_3 at pH 8.0 for long-term storage at -20°C.

All protein preparations were examined by silver staining (BioRad Laboratories, Mississauga, ON,CAN) of SDS-PAGE 16.5% Tricine gels (Schagger and von Jagow, 1987) and judged to be at least 95% pure.

6.2.3 Size exclusion chromatography of MB-proteins

MB-proteins were prepared for SEC by dialysis or reconstitution into the mobile phase: 0.1 M Na_2PO_4 and 0.2 M NaCl at pH 7.5. A 20-50 µg injection of the protein was made into a TSK G2000SWxl, 30 cm x 7.5 mm i.d. (Sigma-Aldrich, Oakville, ON, CAN) column operated by a Water 600E Multisolvent delivery system HPLC with Waters 717plus autosampler and followed by a Waters 486 UV detector set at 214 nm (Waters, Mississauga,

ON, CAN). The proteins and protein standards (Amersham Biosciences, Mississauga, ON, CAN) were eluted in mobile phase at a flow rate of 0.5 mL/min and the resulting chromatograms were generated by Waters HPLC operating software.

6.2.4 Mass spectroscopic analysis of intact MB proteins

MB-protein samples, submitted for MS analysis, were buffer exchanged using a C_{18} ZipTip® (Millipore) in a final organic solvent/water mixture of 95% ACN/5% dH_2O/0.1% TFA , centrifuged at 6000 rpm for 2 min, and then 2 µL was loaded into a gold coated nanospray needle (New Objectives Picotip, Woburn, MA, USA). The positive ion ESI-MS nanospray mass spectrum was generated by a Micromass Q-TOF instrument (Waters Inc.). The key variable MS voltages included: capillary (+950 V), cone (+47 V), and RF lens 1.05; the source temperature was 80°C, and the data for each scan were collected for 5 seconds over the range of 400 to 2500 Da, using a NaTFA solution for external calibration. The MS data was deconvoluted using MaxEnt1™ software (Masslynx™, Micromass, Mississauga, ON, CAN) to provide the singly charged average masses.

6.2.5 Circular dichroism studies of MB-proteins

Protein concentrations used for calculations in the circular dichroism (CD) and SEC studies were determined using a Bicinchoninic Acid (BCA) Protein Assay Kit purchased from Sigma-Aldrich (B9643, Oakville, ON, CAN) developed by Smith et al., 1985 and Wiechelman et al., 1988; a 1 mg/mL bovine serum albumin solution served as the protein standard. CD spectra were recorded on a Jasco 800 spectropolarimeter (Jasco Inc., Easton, MD, USA) interfaced with an IBM compatible computer. Samples were placed in a water-

jacketed 0.1 mm circular cell and the temperature was controlled using a Neslab RT111 water circulating bath (Fisher Scientific, Ottawa, ON, CAN). The data represent the average of 5 scans with a step size of 1 nm and a response time of either 8 seconds (in the case of the full scans or the denaturation with choatropic agents) or 1 second (in the case of the thermal denaturation data).

Stock solutions of MB-1 or MB-16 in buffer (100 mM potassium phosphate, pH 7.2) were mixed with the appropriate amounts of stock solutions of either 8 M urea or 6 M guanidinium hydrochloride in the same phosphate buffer to achieve the appropriate concentrations of protein and denaturant for the chemical denaturation studies. Each solution was allowed to equilibrate overnight at 4°C to ensure complete denaturation. A total volume of 100 µL of each protein solution was placed into the cell and read by CD.

6.2.6 Data manipulation and calculations

Mean residue molar ellipticity values from the CD spectra at each temperature were used to calculate secondary structure according to the algorithm of Johnson (1999). Both α-helix and total helix (the sum of all contribution identified by the algorithm as α- or 3_{10}-helix) were calculated. The fraction of protein unfolded at each temperature or molarity of denaturant was calculated using Equation 6.2.1 (Hu et al., 1992).

$$f_U = \frac{(y_f - y)}{(y_f - y_U)}$$

Equation 6.1 The fraction of protein unfolded (f_U) is calculated by the CD ellipticity value of the sample at 222 nm (y) and the extrapolated values from the denatured (y_u) and native (y_f) ellipticity base-line values (Hu et al., 1992).

The difference in Gibbs free energy (ΔG) values were calculated using Equation 6.2.2. Non-linear regression analysis was performed using SigmaPlot® (Systat Software Inc., Point Richomond, CA, USA) and the curves were fitted to an exponential function, 4 parameter equation.

$$\Delta G = -RT \ln K \quad \text{.....(1)}$$

$$K = \frac{2C(f_U)^2}{f_f} \quad \text{.....(2)}$$

Equation 6.2 Gibbs free energy is calculated by (1) assuming an equilibrium exists between the folded dimer and unfolded monomer according to (Hu et al., 1992) (2) where C is the total molar protein concentration and f_f and f_U are the fraction of folded and unfolded proteins (Neet and Timm, 1994).

6.2.7 In vacuo *cross-linking of MB-proteins*

MB-16 (5 mg) was dialyzed against water for 3 changes of 1 L over 4 hours to rid the sample of all buffers and salts. The pH of the protein solution was then adjusted to 7.5 using 1.0 N NaOH, placed in a glass tube, frozen, and lyophilized. After lyophilization, the sample tube was narrowed, sealed under vacuum (50 mtorr), and incubated at 85°C for 96 hours. After incubation, the sample tube was cracked and the protein was reconstituted into 0.1 M Tris-HCl and 0.15 M NaCl at pH 7.2 to produce a solution of 5 mg/mL.

The cross-linked MB protein products were visualized on a 16.5 % Tricine SDS gel electrophoresis and subsequently stained with Sypro® Ruby Red (Molecular Probes, Eugene, OR, USA). Approximately 10 μg of the total protein cross-linked mixture was loaded onto the gel, and the gel was electrophoresed for 90 min at 150 volts. The gel was

fixed in 7% acetic acid and 10% methanol solution for 20 min before being stained in Sypro® Ruby Red UV stain overnight. Bands were visualized by UV light at 312 nm.

6.2.8 Purification of MB-16 dimer

To purify the covalent MB-16 dimer from the non-covalent MB-16 dimer, a preparatory electrophoretic unit (Bio-Rad Laboratories), encompassing a tubular 3 cm 16.5% Tricine SDS-PAGE apparatus, was employed. A 16.5% Tricine gel was poured and submersed between top and bottom solution reservoirs containing cathode buffer (0.1 M Tris and 0.1% SDS, pH 9.0) and anode buffer (0.1 M Tris-HCl, pH 8.9), respectively. The MB-16 *in vacuo* cross-linked mixture (~3 mg) was reconstituted in 2 mL of SDS gel loading buffer and the sample was loaded onto the gel, then subjected to electrophoresis for 8 hours at 12 Watts. The eluant (in 4 mL fractions) was collected from the gel into a TBS (50mM Tris-HCl, 300 mM NaCl, at pH 7.4) elution buffer. To determine the elution profile of monomeric and dimeric MB-16 from the gel, a 10 µL aliquot from each collected fraction was electrophoresed on a 16.5% tricine SDS-PAGE using the standard Mini-PROTEAN II gel electrophoresis apparatus and the gel was electrophoretically transferred to a polyvinylfluoro membrane (Millipore) for subsequent Western Blot analysis.

Blotted membranes were blocked with 1% casein blocking solution (Amersham Biosciences), washed with three changes of 20 mM Tris-HCl at pH 7.6, 100 mM NaCl, and 1% Tween-20 (TBS-Tween), and incubated for 1 hour at room temperature with a solution (3.9 mg/mL) of rabbit anti-MB (previously prepared by inoculating rabbits with isolated MB-1 protein, Hefford et al., unpublished results), which had been diluted 1:100 in TBS. After incubation with the primary antibody, the blot was washed with 3 changes of TBS with

0.1% Tween 20 and then the secondary antibody (goat anti-rabbit IgG linked to horseradish peroxidase, prepared as described in Chapter 5) was applied at a dilution of 1:20 000 in TBS and allowed to incubate for 1 hour at room temperature. After incubation of the secondary antibody, the membrane was washed, according to the procedure described above, and the bound horseradish peroxidase was detected using the standard reagents and protocols described by the ECL™ Western Blot Detection System (Amersham Biosciences).

The fraction containing the covalent MB-16 *in vacuo* cross-linked dimer was pooled and dialyzed extensively against distilled water and finally 20 mM ammonium bicarbonate.

6.2.9 Enzymatic digestion of MB-16 dimer and peptide mapping by HPLC

The MB-16 *in vacuo* cross-linked dimer and native proteins (2 mg/mL) were digested with trypsin (40 µg) (Promega, Madison, WI, USA) at a 25:1 (w/w) trypsin:protein ratio in 500 µL of 0.1 M NH_4HCO_3 at pH 8.0 for 24 hours at 37°C. After digestion, the samples were heated at 90°C for 5 min then evaporated to a final volume of 20 µL.

Peptide separation by RP-HPLC required the reconstitution of each tryptic digestion sample in 5% ACN and 0.1% TFA then a 50 µL injection (by Waters 770E autosampler) into a 0.46 x 30 cm C_{18} RP-HPLC column (Grace Vydac, Massachusetts, USA) that was attached to a Waters 600E HPLC system interfaced by Millennium HPLC software (Waters). At a flow rate of 1 mL/min, peptides were eluted in a solvent system A (5% ACN, 0.1% TFA) and B (95% ACN, 0.1% TFA) following a linear gradient from 0% to 50% B in 60 min. Peptides were detected by a Waters 486 UV detector set at 214 nm.

6.2.10 Mass spectrometric analysis of MB-16 tryptic peptides

After the separation and collection of tryptic fragments by HPLC, each eluted peak was prepared for mass spectrometry. The eluted fragments were concentrated (by evaporation) to a volume of ~ 10 µL. These samples were then reconstituted into 0.2 % formic acid (v/v) to an estimated final concentration of 50 pmol/µL per sample.

Samples were analyzed by LC-ESI-MS with use of a Q-TOF Global mass spectrometer (Waters/Micromass™ Inc. Manchester, UK) coupled to a Waters CapLC XE system (Waters). Tryptic peptides (1.0 µL) were loaded and desalted at a flow rate of 20 µL/min on a 300 µm id/5mm length C_{18} Pepmap trapping column (LC Packings, San Francisco, CA, USA). The peptide mixture was eluted with an acetonitrile solvent gradient from 0 to 40% B in 60 min then 40% to 95% B in 10 min (where solvent A was 98% dH_2O, 0.2% formic acid, 2% ACN and solvent B was 10% dH_2O, 90% ACN, 0.2% formic acid) at a flow rate of 10 µL/min. The flow was split to 200 nL/min prior to the analytical column. The analytical column was an Atlantis™ Waters C18 75 µm x 150 mm NanoEase™ column (Waters). Mass data acquisitions were piloted by MassLynx™ software (Waters, Micromass Inc.) using automated switching between MS and MS/MS acquisition modes. The survey scan (1 s) was obtained over the mass range m/z 300-1200 in the positive ion mode with a cone voltage of 40 V. When the signal reached a user-defined threshold of 10 counts/sec, and the isotope pattern demonstrated that the ion was multiply charged, the peptide precursor ions could be selected for MS/MS scan (2s) over the mass range m/z 50-2000. Fragmentation was performed using argon as the collision gas and with a collision energy profile (20-40 eV) depending on the change state and the mass. External calibration was

achieved using a multipoint calibration from the MS/MS of doubly charged glu-fibrinopeptide B (Sigma-Aldrich) at various concentrations in 0.2% formic acid.

6.3 Results and Discussion

To evaluate the "misfolding" of MB-1 to form dimers rather than the intended monomer, attempts were made to adjust the loop length and flexibility of loop II. Subsequent to publication of the original MB-1 design (Beauregard et al., 1995), Nagi and Regan (1997) investigated the effects of loop length and flexibility on the oligomerization state of another helical bundle protein, ROP. Their results indicate that loops of less than 5 residues may be too short to allow the turn to fold one helix back on another. MB-1 has one loop, Loop II, between Helix 2 and Helix 3 that, in the original design, is only 4 residues in length. In addition, this loop contains 2 lysine residues, both of which are expected to be positively charged under physiological conditions (see Figure 6.3.1). One can easily envision a scenario in which the failure of this sequence to form the expected interhelical turn would result in one or the other of the open-faced dimers shown in Figure 6.1.1. Indeed, MacBeath et al., (1998) have recently shown that insertion of a loop-forming sequence into the long helix of just such a dimeric 4-helix bundle protein (choismate mutase) converts that dimeric enzyme into a monomeric, 4-helix bundle protein with near native activity.

The MB-16 variant was created by replacing the 4 residues (lys, thr, lys, and gln) in this loop with 5 glycine residues (refer to Figure 6.3.1). It was thought that additional length and flexibility of this new Loop II could relocate the positioning of the helices, allow the folding of Helix 2 back on Helix 3 of the same monomeric unit and create a more tightly packed core. To determine the contribution of the shorter, less flexible Loop II of the

original design, the ability of MB-1 and MB-16 to assume the designed monomeric fold was compared and their stabilities examined by heat denaturation, and by chaotropic agent denaturation using urea and guanidinium hydrochloride denaturation.

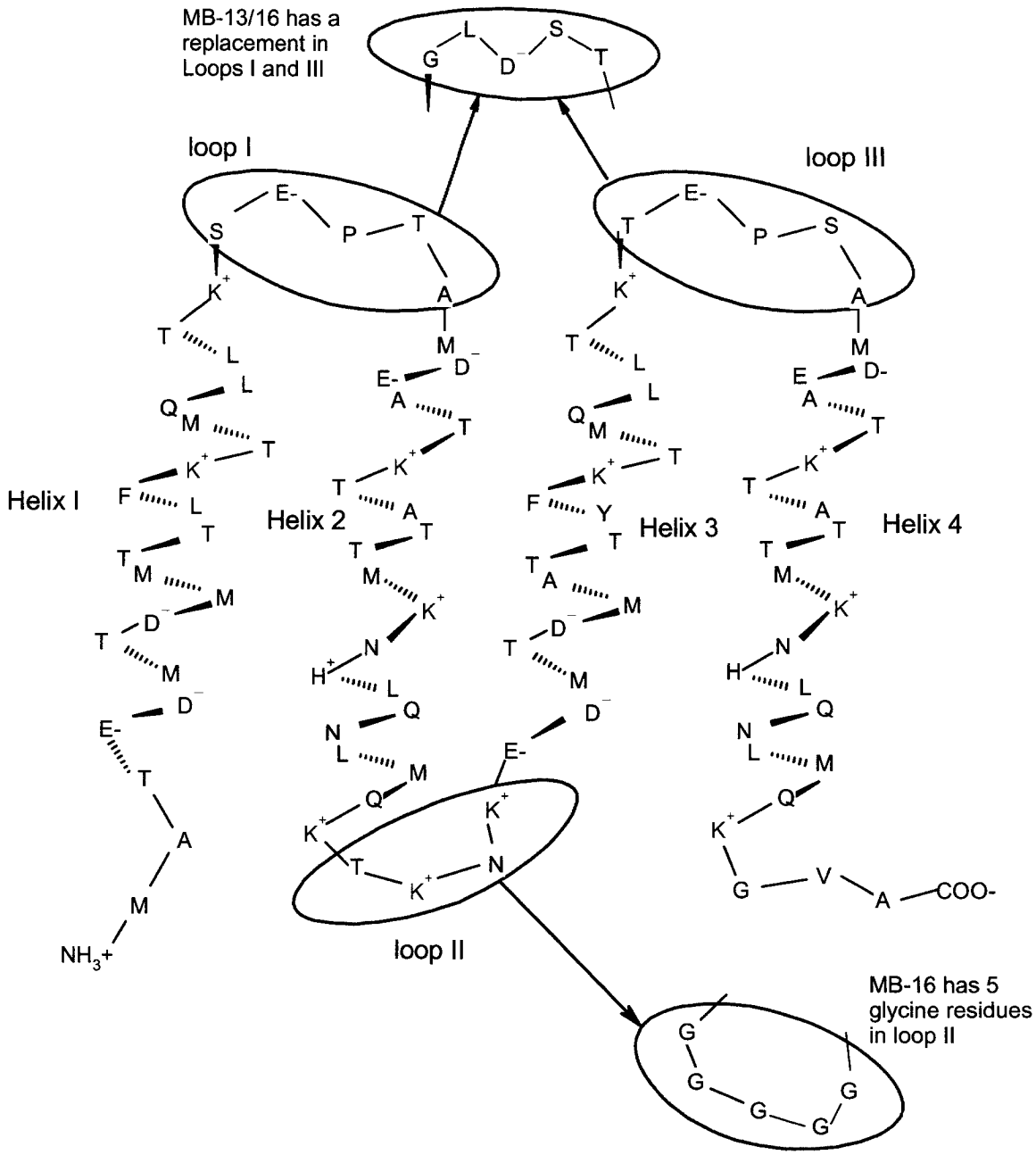

Figure 6.3.1 Sequence and designed folding of MB-1 (modified from Hefford *et al*, 1999). Positively charged lysine residues are labeled in blue and negatively charged aspartic and glutamic acid residues are labeled in red. MB-16 has the exact same sequence and folding of MB-1 except for the replacement of 5 glycine residues in loop II. MB-13/16 had a replacement sequence in Loops I and III.

6.3.1 Analysis of the loop II variant MB-proteins

The designed amino acid sequences of MB-1 and its variants were analyzed using secondary structure prediction algorithms. Predictions using GOR IV (Garnier, Gibrat, and Robson, 1996) indicated that the replacement of TKNK loop in the original MB-1 sequence with 5 glycine residues significantly enhances the tendency for loop formation in this section of the protein. The successful replacement of the TKNK loop II in MB-1 with the GGGGG loop specified for MB-16 was confirmed by gene sequencing (data not shown). Induction of *E. coli* clones containing the MB-16 gene resulted in stable expression of a new, largely helical protein (results not shown). The identities of expressed MB-1 and MB-16 mutant proteins were also confirmed by mass spectrometry. The mass spectrums of MB-16 and MB-1 are shown in Figure 6.3.2 in panels A and B. Introduction of this all-glycine loop in MB-16 resulted in a protein with 101 residues but a slightly reduced molar mass (11149.2 Da) as compared to that of MB-1 (11335.4 Da) both ±1 Da. The fact that both purified proteins generate single peaks of the expected molecular mass indicates that in each case, the full-length protein has been isolated with high purity.

MB-13/16 variant was generated with the intent to combine the all-glycine loop II of MB-16 with the loop substitution of ser-glu-pro-thr-ala with gly-leu-asp-ser-thr into loops I and III. The latter loop substitutions were designed to introduce helix capping residues and had been shown (in the MB-13 variant, Parker and Hefford, 1998) to increase both the degree of helicity of protein and its conformational stability but do not result in the formation of monomeric helical bundle proteins. None-the-less, these helix capping moieties should encourage the tight turn needed in loops I and III allowing the Helix 1 to fold back onto Helix 2 and Helix 3 to fold against Helix 4 and prevent "flipping out" at these loops causing

the kind of interaction with a second monomer seen in 1st helix swapped dimer and 4th helix swapped dimer depicted in Figure 6.1.1 above. MB-13/16 expression and purification likewise resulted in a sample of high purity which was analyzed by mass spectrometry. Figure 6.3.1 panel C shows the mass spectrum of MB-13/16 revealing only one peak of 11126 ± 1 Da, representing the expected mass of MB-13/16.

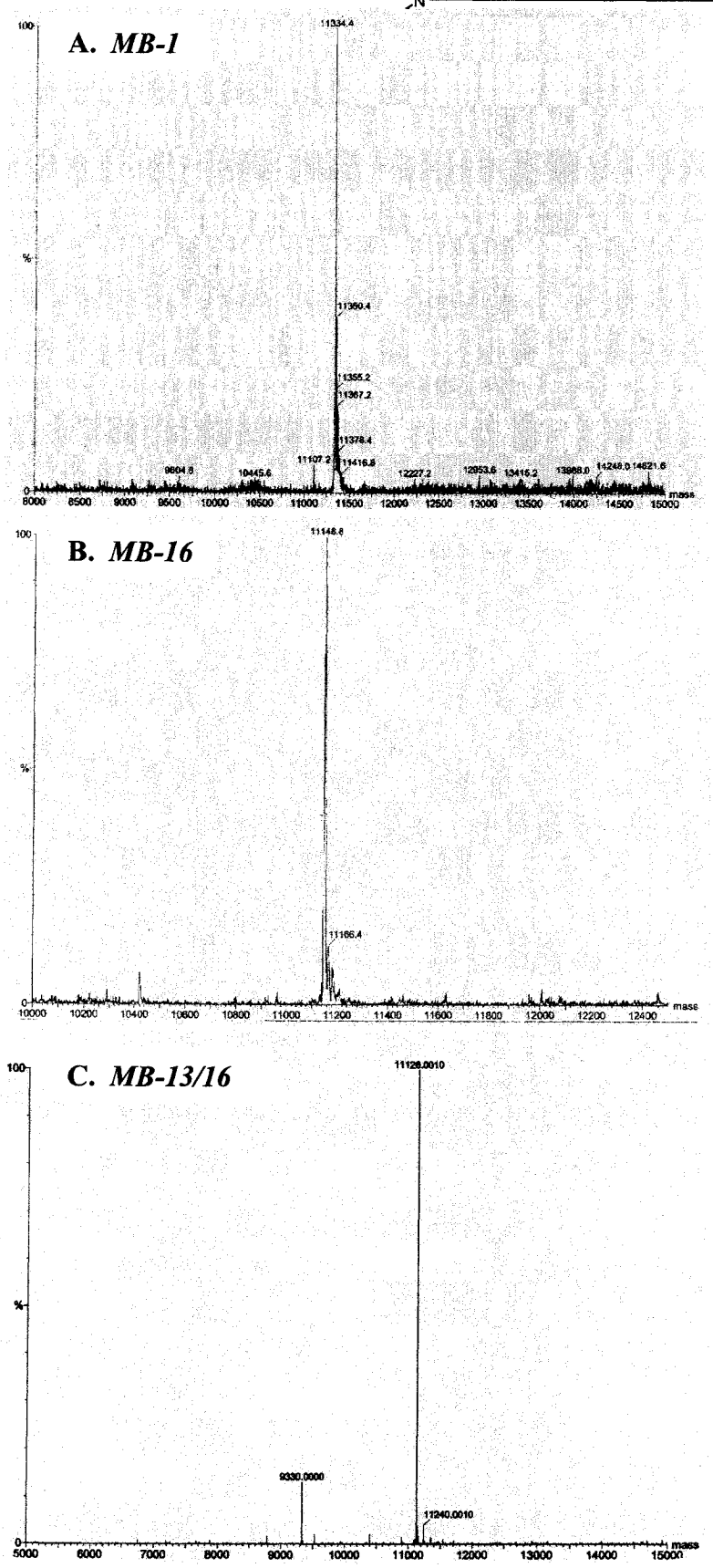

Figure 6.3.2 Deconvoluted ESI-TOF mass spectrum of MB-1 (A), MB-16 (B), and MB-13/16 (C).

6.3.2 Size exclusion chromatography of the MB mutants

The substitution of GGGGG in loop II of MB-16 and MB13/16 was expected to have two effects: First, the increased length and flexibility should facilitate the formation of the turn and allow better packing of Helix 2 against Helix 3 (Figure 6.3.3). Second, the removal of two lysine residues removes the potential for electrostatic repulsion that might prevent turn formation in MB-1. Both of these effects are expected to enhance the turn formation in loop II of MB-16 variants by removing constraints that would prevent it. The loop, however, does not contain any residues that would force the turn; it is still the hydrophobic collapse of one helix against the other that is expected to drive the folding process.

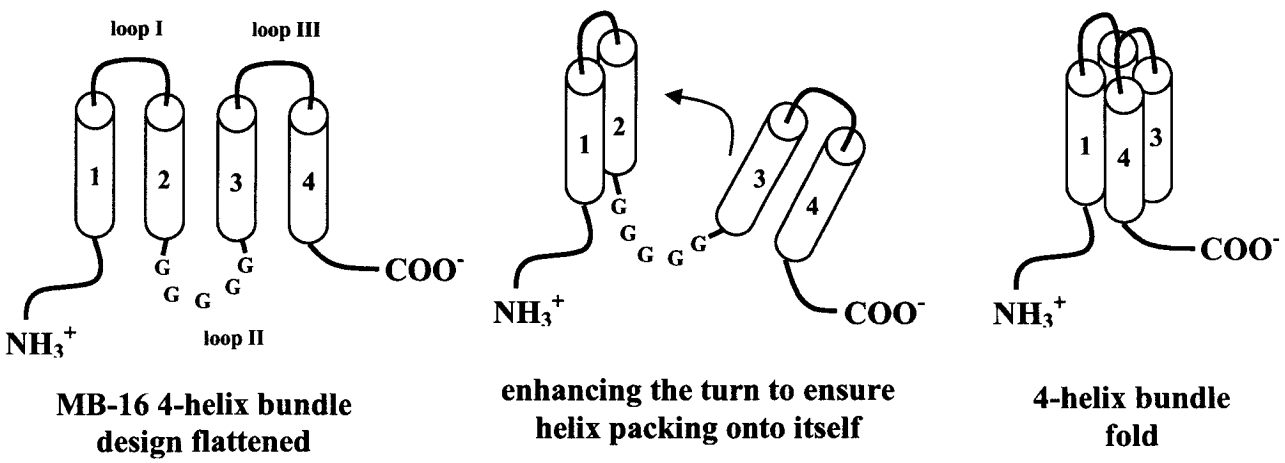

Figure 6.3.3 Proposed folding intent of the 5 glycine loop replacement in MB-16.

The size exclusion chromatographic data of MB-16 (Figure 6.3.4) indicates that MB-16 is, for the most part, dimeric like MB-1. The majority of the protein elutes from a TSK G2000SW$_{xl}$ SEC-HPLC column in a volume consistent with a dimeric species ($M_r \sim 22\,000$), but a small amount of protein elutes in a volume expected for the monomer ($M_r \sim 11\,000$). A third intermediate peak eluting at an estimated $M_r \sim 16\,000$ is also observed. This intermediate peak was originally thought to represent a dimer of a degraded form of MB-16. However, since the mass spectrometric analysis of MB-16 results in a single peak and shows little to no breakdown of the protein, an alternate explanation is required. Peaks consistent with species of intermediate mass are often seen on size exclusion chromatography when monomeric and dimeric species are in rapid equilibrium (Frenz et al., 1990). In these cases, however, one rarely sees peaks consistent with the size of either the monomeric or dimeric moiety as these are rapidly exchanging as the protein passes through the column. This unexpected chromatographic peak, therefore, is unlikely to result directly from the conversion of monomer to dimer but may result from an alternately folded form of MB-16 which, whether or not it results indirectly from this conversion process, has a different mobility in the SEC column. Given that both MB-1 and MB-16 exist as predominantly dimeric conformations in solution, the identity of this peak was not pursued further and, after a more thorough characterization of this variant to test the design tenets, efforts were again focused on finding variants with more monomeric character.

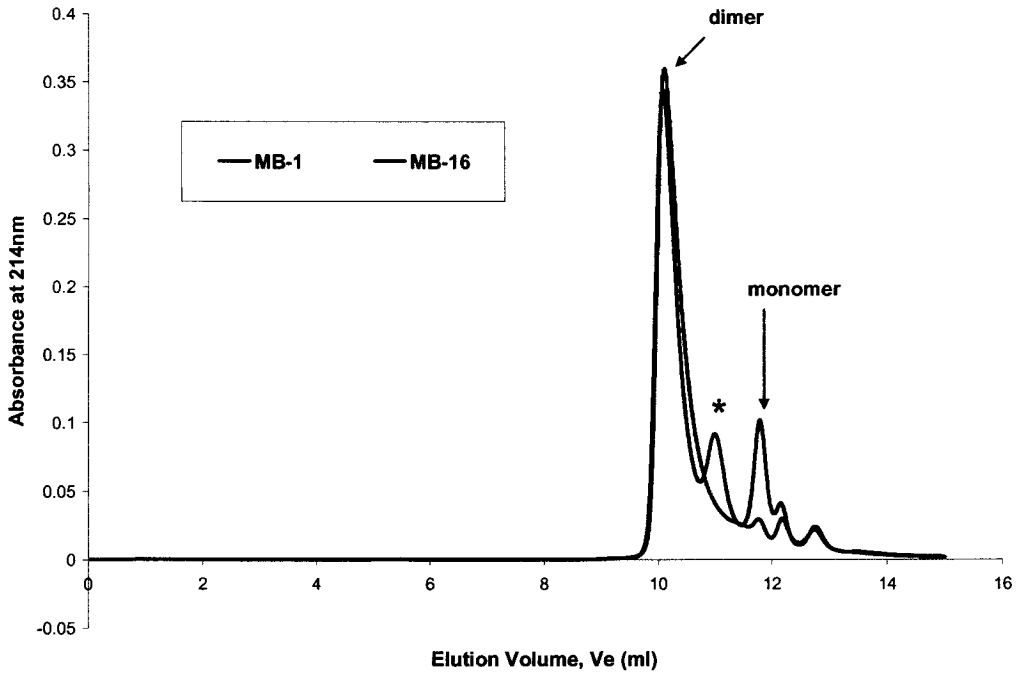

Figure 6.3.4 Size exclusion chromatography of MB-1 (blue line) and MB-16 (red line). Proteins were prepared in the mobile phase 0.1 M Na_2HPO_4 and 0.15 M NaCl at pH 7.5 and approximately 20 µg of total protein was injected into a TSK G2000Sxl SEC column and eluted at 0.5mL/min. The arrows indicate the elution of monomeric and dimeric conformers. The asterisk "*" indicates the MB-16 species with estimated M_r ~ 16 000.

6.3.3 Relative stability of MB proteins by thermal denaturation

Despite the failure in design of MB-16 to result in a stable monomeric conformation as the predominant fold, the presence of some monomeric protein in solution equilibrium with the dimer was encouraging. Further characterization of this mutant was carried out to assess whether the design affected the structural (conformational) stability of the protein to heat and choatropic agent-induced denaturation.

CD analysis of both MB-1 and MB-16 structures under "physiological" conditions (data not shown) was performed. The mean residue ellipticity data taken between 178 and

260 nm were analyzed using the algorithm of Curtis Johnson (Johnson, 1999) and gave an estimate of approximately 45% helical content in both the MB-16 variant and the original MB-1 protein. Therefore, the introduction of the 5 glycine loop sequence did not improve the helicity of the overall MB structure under these conditions. The protein samples were then heated, and mean ellipticity at 222 nm was measured at 5°C intervals from 25 to 95°C. These data were used to calculate the fraction of protein unfolded at each temperature using Equation 6.2.1. Figure 6.3.5 shows the thermal denaturation curves of MB-1 and MB-16, where fraction unfolded is plotted against temperature. MB-16 is slightly more resistant to thermal denaturation, with a T_m approximately 5°C higher than that of MB-1. This translates into an increased stability ($\Delta(\Delta G)$) at 25°C of approximately 2 kcal/mol. The higher melting temperature is indicative of an increase in tertiary interactions in MB-16 relative to MB-1 and suggests a more tightly packed structure. Likewise, the slight increase in co-operativity of the unfolding process, as indicated by the increase in steepness of the denaturation curve, supports this notion.

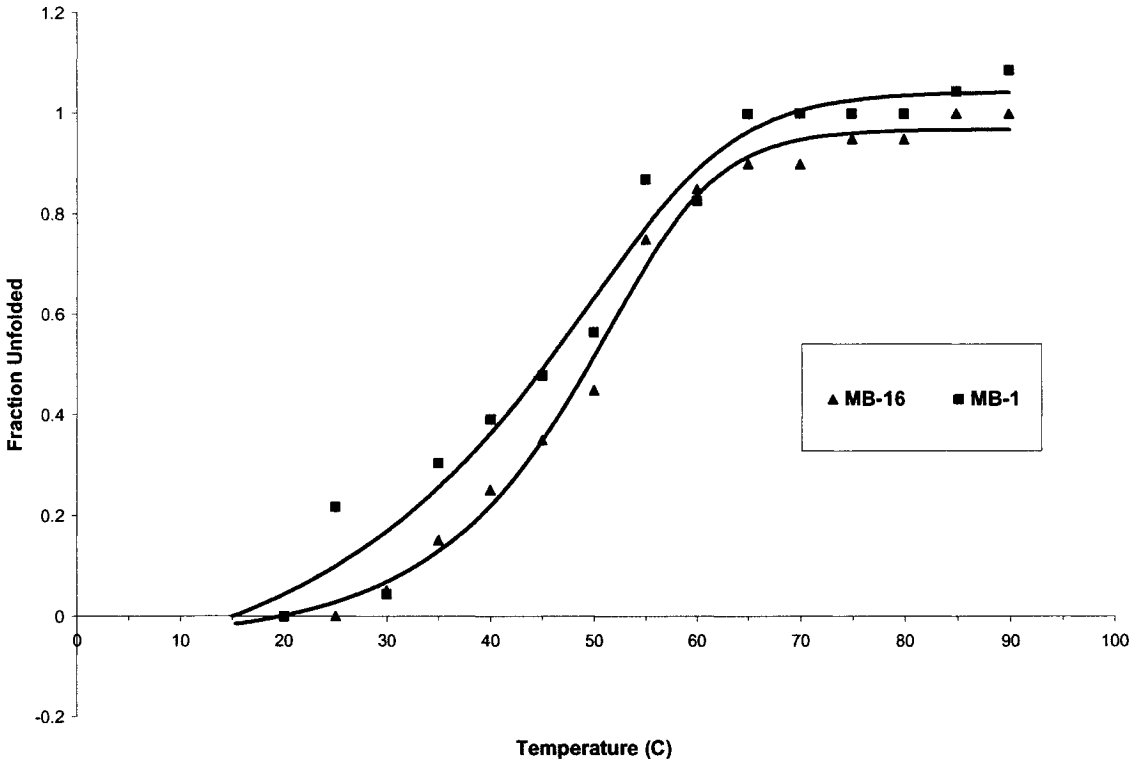

Figure 6.3.5 Thermal denaturation of MB-16 (red line) and MB-1 (blue line). CD spectra were taken from 20 – 90°C and the mean residue ellipticity values at 222 nm (monitors the % of helix) were taken to calculate the fraction unfolded at each temperature increment. The melting temperature, T_m, is the temperature at which 50% of the protein is unfolded.

6.3.4 Relative stability of MB proteins towards chaotropic agents

A similar stability study was performed by monitoring the structure of both MB-1 and MB-16 when the amount of chemical denaturant was increased. Guanidinium hydrochloride and urea were titrated into the sample in increasing amounts, and CD spectra were compiled, particularly monitoring the loss of helical structure at 222 nm. Fraction unfolded against concentration of guanidinium and fraction unfolded against concentration of urea is shown in Figure 6.3.6 A and B. As shown by the overlaying curves on these plots, MB-16 does not show an appreciable increase in resistance towards denaturation by either

guanidinium hydrochloride or urea. In addition, calculations indicate that MB-1 stability, as estimated by the exposure to the ionic chaotropic agent guanidinium hydrochloride, is approximately the same as that estimated when urea is used as the denaturant. If the relative proximity of the two lys residues in Loop II and MB-1 were to result in a negative (repulsive force) interaction in the folded protein, one would expect that the relative stability of MB-1 would be higher in guanidinium hydrochloride (where ionic interactions are masked) than in urea (Kohn and Allen, 1995). These data therefore suggests that the limited stability observed in MB-1 is not the result of the unfavourable juxtaposition of two like charges in Loop II and the charges located in this loop may not be a detriment to the overall stability in the protein.

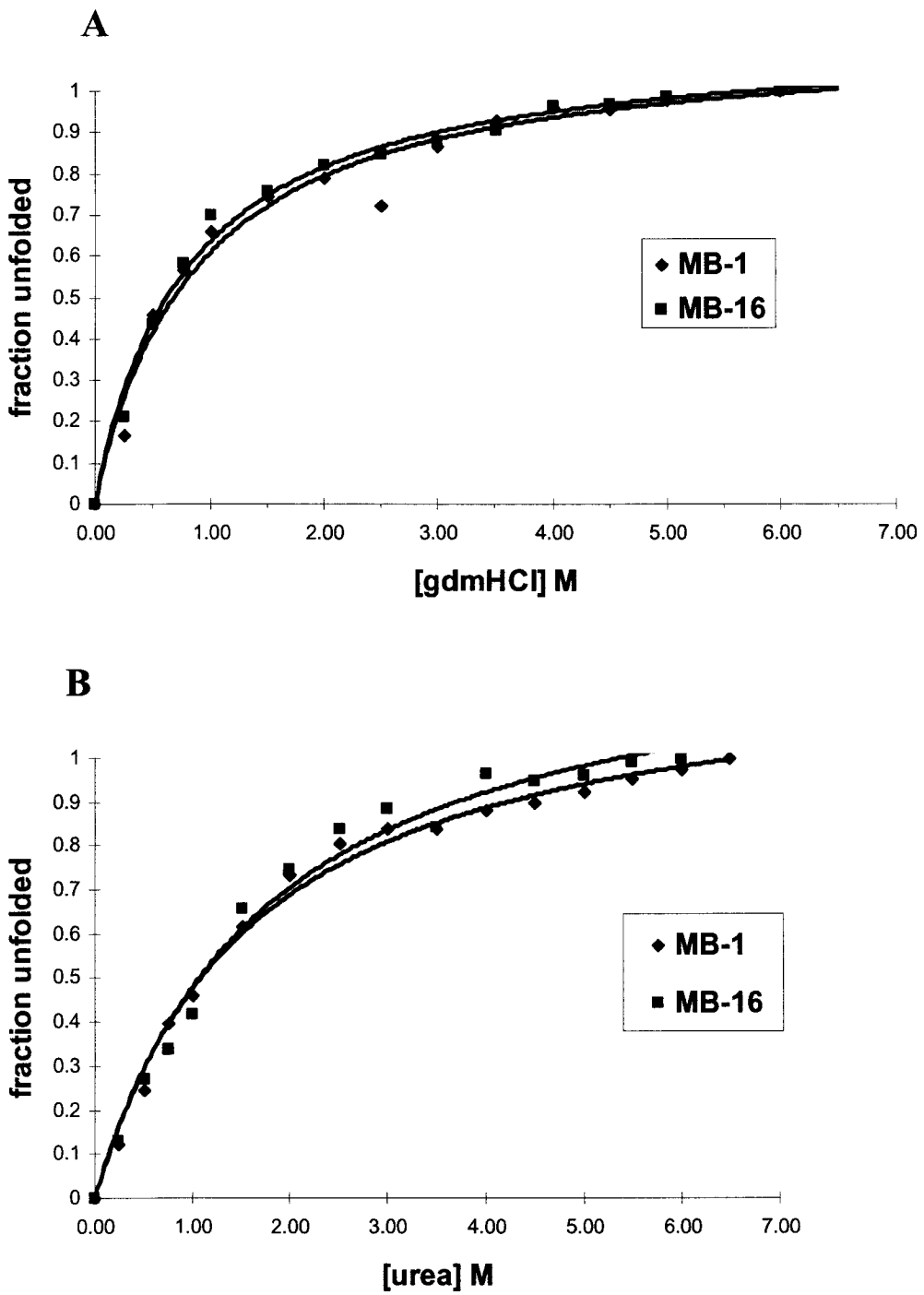

Figure 6.3.6 Chemical denaturation of MB-1 (blue line) and MB-16 (red line) in guanidinium hydrochloride (A) and urea (B). Mean residue molar ellipticity was monitored by CD at 222 nm as the concentration of denaturant was increased.

6.3.5 Size exclusion chromatography of the MB-13/16 mutant

The existence of even some monomeric protein in the MB-16 preparation is encouraging and indicates that, in some of the dimer formed by MB-1 is a result of the lack of turn formation at loop II (i.e., that one of the two open faced dimers depicted in figure 6.1.1 is forming). There is no evidence however, to absolutely rule out the possibility that the 1st and 4th helix swapped dimer may not exist, to some extent at least, in the equilibrium mixture of dimers formed by MB-1. While it is true that variants such as MB-11 and MB-13 should preclude the formation of these particular conformers, they do not preclude formation of the open-faced dimers. Similarly, while the open-faced dimers are less likely to be formed by the MB-16 variant, MB-16 has no helix capping in loops I and III can form both the 1st helix swapped dimer and 4th helix swapped dimer. These single helix-swapped dimers may be less favourable than open-faced dimer formation but responsible for at least some of the dimers observed in MB-16 preparations. In order to assess these possibilities, the MB-13/16 variant was also tested for its ability to form monomeric helical bundles. MB-13/16 contains the helix capping residues in loops I and III that, in the MB-13 variant, increased helicity and stability but not monomer formation as well as the flexible, all-glycine loop II of the MB-16 variant.

Figure 6.3.7 shows the SEC chromatogram of MB-13/16 run under the same conditions as MB-1 and MB-16. The MB-13/16 protein elutes into two major peaks (labeled as 1 and 4) corresponding to $M_r \sim 22\,000$ and $M_r \sim 11\,000$. These correspond to the expected sizes of the dimer and monomer, respectively. There is also a much smaller, intermediary peak, labeled as "2", eluting at approximately $M_r \sim 17\,000$, a peak that was also observed in the SEC elution profile of MB-16. Although the conformation of the protein

eluting in this intermediary peak 2 remains unclear, it is apparent that the ratio MB-13/16 monomer to dimer in solution is very close to 1:1.

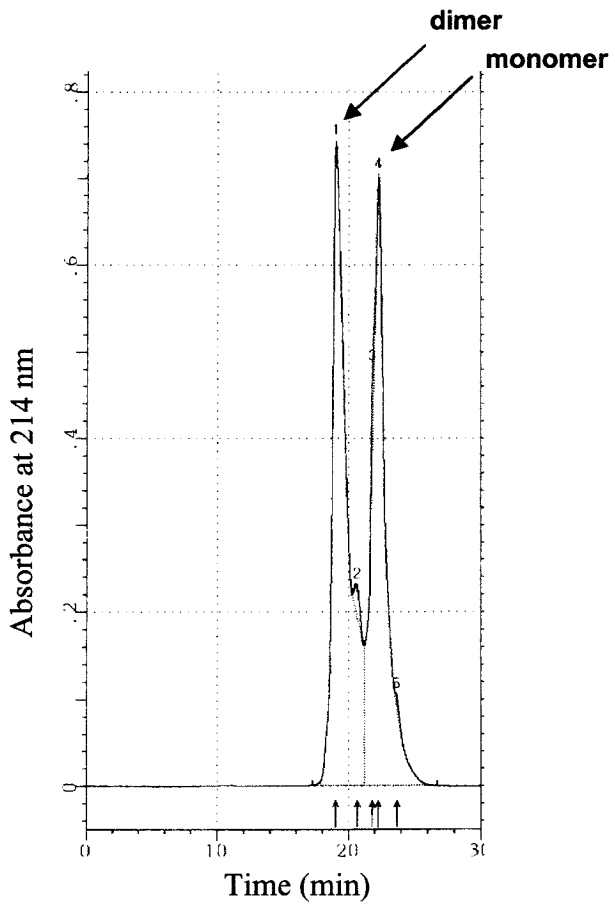

Figure 6.3.7 Size exclusion chromatography of MB-13/16 eluted from a TSK G 2000SW_{xl} column in mobile phase 0.1 M Na_2HPO_4 and 0.15 M NaCl at pH 7.5. Approximately 30 µg of total protein was injected into HPLC and eluted at 0.5 mL/min. Elution volume is determined by the elution time x flow rate. The arrows indicate the integrated peaks 1 to 4.

The replacement of ser-glu-pro-thr-ala with gly-leu-asp-ser-thr into loop I and III along with the 5-glycine loop II sequence has pushed the MB design into a conformer with more monomeric character. From these data alone, however, it is unclear why this occurs. It may be that, when formation of the open-faced dimer(s) is less likely, the 1st helix swapped dimer and/or 4th helix swapped dimer would form in the absence of the helix capping residues in loop I and III that are present in this variant. Alternately the prevention of helix fraying and the ensuing increase in stability resulting from the introduction of the loop I and III changes may merely increase the relative stability of the monomer with respect to the open-faced dimer(s) when, with the more flexible loop II, the monomeric bundle does form. The *in vacuo* cross-linking method suggests a means of perhaps covalently "freezing" the MB-16 dimer present in solution and the possibility of acquiring data that may help to resolve this issue.

6.3.6 *In vacuo* cross-linking of MB proteins

The MB-13/16 variant shows an increase in monomeric structure compared to MB-16, however, it does not fully fold into a stable monomeric bundle. The effect of substituting for a stronger helix capping motif in loops I and II while maintaining the 5 glycine residue turn in loop II did not seem to fully promote the independent folding of each monomeric unit. Earlier studies with MB-1 included the characterization of the interactions at the dimeric interface (Hefford *et al*, 1999). The results of hydrophobic affinity probing with ANSA dye (Hefford et al., 1999) led to the conclusion that there is no exposed hydrophobic interface on MB-1 in solution. These data, in conjunction with size exclusion chromatography in the presence of increasing concentrations of salt (Hefford et al.,

unpublished results), indicate that MB-1 monomers do not interact to form a dimer merely via a hydrophobic interface but rather an electrostatic association between opposed charges. As apparent in Figure 6.3.1, the primary structure of MB-1 affords several possibilities of salt bridge formation between helices, through interacting lysine and aspartic or glutamic acid residues, as one helix packs against another. The presence of these potential salt bridges suggested that the *in vacuo* cross-linking procedure may provide information as to which interfaces are strongly interacting and thus help elucidate the interactions that appear to confer such propensity for the dimeric conformer. If salt bridge interactions occur at the monomer-monomer interface and contribute to the formation of the dimer, cross-linking through these interactions, using the *in vacuo* cross-linking method, will result in a covalent dimer which could then be characterized to elucidate the linkages and, presumably, the residues that contribute to dimer stabilization. This evaluation would therefore yield information resulting in renovation of the design itself.

Figure 6.3.8 shows a denaturing SDS-polyacrylamide gel of MB-16 before (Figure 6.3.8 lane 3) and after *in vacuo* cross-linking (Figure 6.3.8 lane 2). As shown by the Sypro® Red staining on the gel, a band corresponding to the expected mass of dimeric MB-16 (M_r~24 000) appears after the *in vacuo* cross-linking treatment on the MB protein sample. Because MB-16, without any treatment, forms a stable non-covalent dimer in solution (as shown by the size exclusion chromatography elution profile, Figure 6.3.3, above) separation of the *in vacuo* cross-linked dimer from this natural non-covalent dimer by molecular sieving techniques such as dialysis, gel filtration, or size exclusion chromatography was expected to be difficult. Therefore, a preparatory electrophoretic cell under denaturing SDS conditions was employed. The denaturing conditions induced by the presence of SDS assure that all

non-covalent interactions are disrupted and the proteins are separated by the size of their covalent structures. The covalent dimer and monomer present in the MB-16 cross-linked mixture were thus separated by their difference in mobility through the gel. Fractions of the eluant containing the covalent dimer were determined by taking a small aliquot of each fraction of eluant collected and reloading it onto SDS-PAGE and observing the elution pattern of covalent dimer and monomer (data not shown). These were pooled and extensively dialyzed against ammonium bicarbonate at pH 8.0 to remove all electrophoretic buffers and SDS. The purified MB-16 dimer is shown in Figure 6.3.8 lane 4.

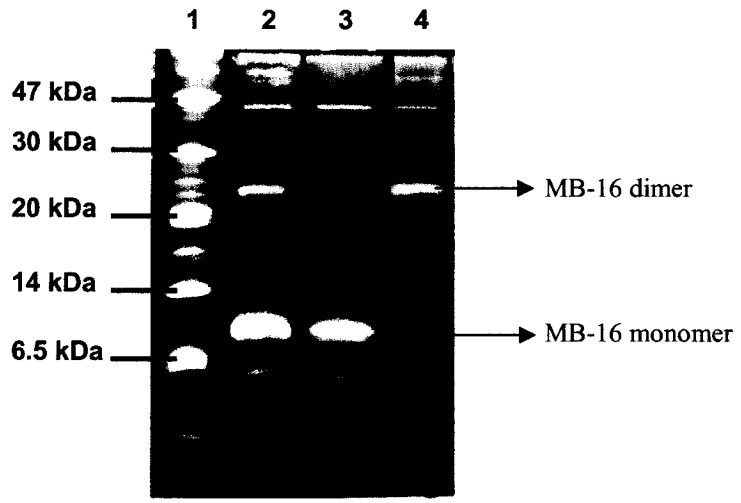

Figure 6.3.8 16.5% Tricine SDS-PAGE of MB-16 before and after *in vacuo* cross-linking. Total protein load per lane is approximately 10 µg. Lane 1: low range molecular weight marker; Lane 2: *in vacuo* cross-linked MB-16 mixture; Lane 3: MB-16 monomer; Lane 4: purified MB-16 covalent dimer. The gel was stained with Sypro® Ruby Red Stain.

6.3.7 Peptide mapping of the *in vacuo* cross-linked MB-16 dimer

After achieving a sample of covalent MB-16 dimer with sufficient purity, the covalent dimer sample and a noncross-linked sample of MB-16 were enzymatically digested

with trypsin and the resulting peptides mapped using reverse phase HPLC and mass spectrometry, a strategy previously used for the peptide mapping of dimeric RNase A in Chapter 3. The elution profiles (from a C_{18} reverse phase HPLC column) of tryptic peptides of both the untreated MB-16 sample and the covalent dimer are shown in Figure 6.3.9 A and B, respectively. The tryptic digestion of untreated MB-16 is expected to yield 11 peptides from cleavages at 10 lysine residues but only 7 of these peptides have unique sequences. (The sequence of MB-16 consists of two sets of repeating motifs: Helix 1 and 3 and Helix 2 and 4, with the exception of a leucine residue replaced by a tyrosine in Helix 3.) As shown by the tryptic digestion chromatogram of untreated MB-16, six major peaks were detected and are labeled with numbers 1 to 6. The seventh expected peptide is the C-terminal tripeptide, resulting from a cleavage at Lys_{98}, which is not easily detected and may elute early in the void volume.

The repetitive nature of MB-16 and the fact that several peaks in the elution profile contains peptide from two different parts of the primary structure of the protein makes the differences in the eluted peaks in the two chromatograms of Figure 6.3.9 difficult to observe. The most apparent difference in these two chromatograms is the appearance of a new peak in the MB-16 cross-linked dimer digest that elutes at approximately 52 minutes and is labeled "X" in chromatogram of Figure 6.3.9B. In addition, in the covalent dimer digestion, peaks 3 and 5 appear to have a decrease in height relative to the remaining peaks in the profile and relative to the noncross-linked MB-16 profile. This small loss of intensity, however, is consistent with the loss of one of four possible "copies" of each peptide to a new, cross-linked peptide. Other than these small differences, the two peptide maps look identical in terms of peak elution and baseline noise.

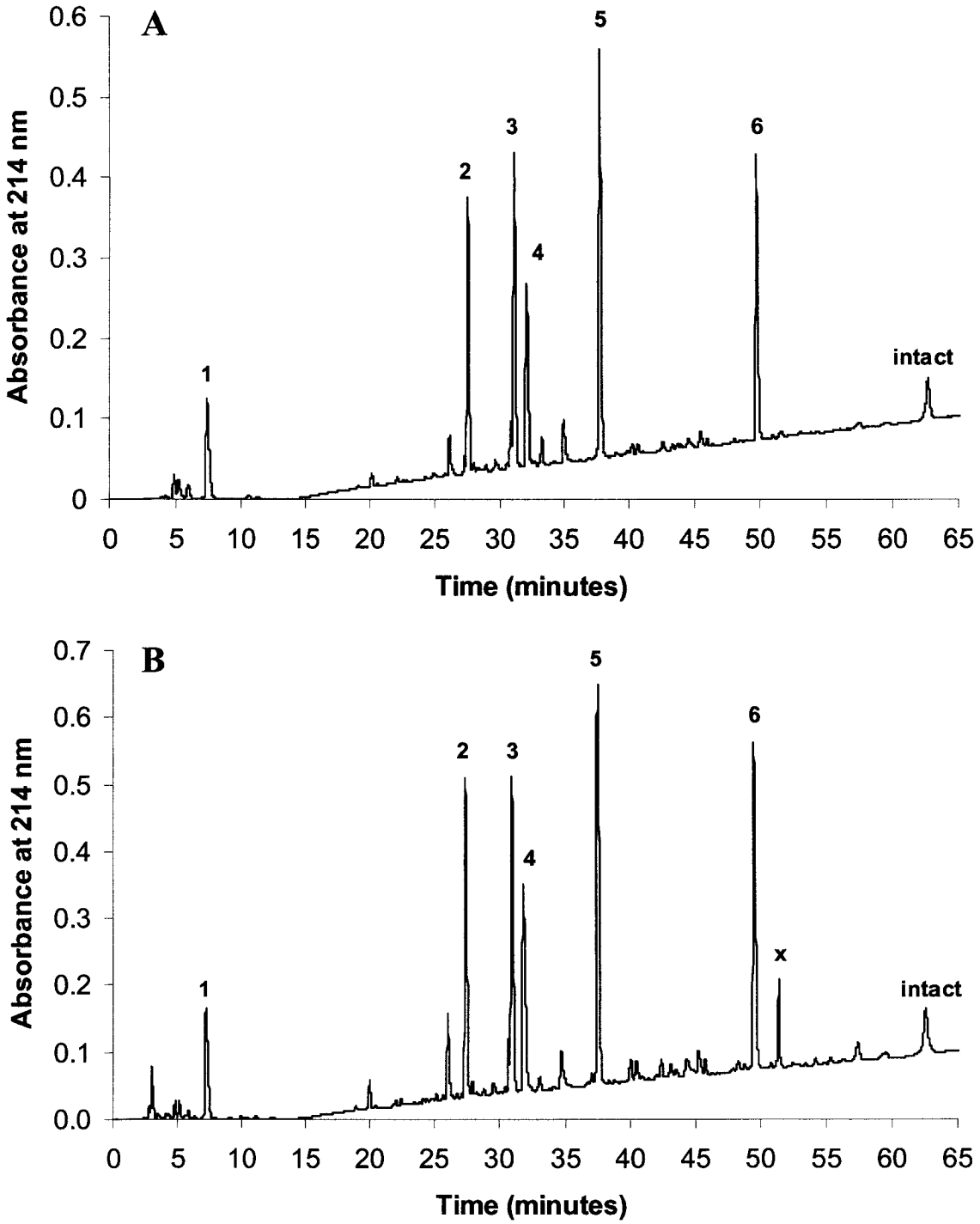

Figure 6.3.9 Reverse Phase HPLC elution profile of tryptic digests of noncross-linked MB-16 (A) and *in vacuo* cross-linked MB-16 (B) separated by a C_{18} column and a linear solvent gradient from 100% A (5% ACN, 0.1% TFA) to 50% B (where B = 95% ACN, 0.1% TFA) in 60 minutes. 25 µg of total digested MB-16 protein was injected and detected by a UV detector at 214 nm.

6.3.8 Mass spectrometric analysis of the tryptic peptides of the cross-linked MB-16 dimer

Given the slight differences in the RP-HPLC digestion profiles of the noncross-linked and covalent dimer MB-16 samples and simplicity of the peptide maps, individual peaks were not collected for analysis. Instead, the fully digested peptide mixture of each sample (untreated and covalently cross-linked MB-16) was injected into a mass spectrometer equipped with a pre-analytical C_{18} reverse phase column. This allowed the identification of each tryptic fragment, including the new peptide X, which is presumed to be a cross-linked peptide. The resulting mass spectra of the noncross-linked MB-16 sample allowed for the identification of all the expected tryptic fragments from the amino acid sequence of MB-16 (data not shown). The mass spectra generated from the injection of the *in vacuo* cross-linked MB-16 sample also lead to the identification of these same tryptic peptides and that of a new mass peak. This latter peak eluted late from the analytical C_{18} column which preceded the mass spectrometer, an observation that is consistent with the results of the eluted peaks from the RP-HPLC. Mass analysis of this peak, shown in Figure 6.3.10A, indicates a doubly charged entity with an m/z of 1073 and a triply charged ion peak of m/z equal to 1431 (circled in red) in the cross-linked MB-16 dimer sample. The m/z peak of 1073 appears in all late eluting MS scans from the analytical column and may be the result of a keratin or trypsin impurity but does not match to any expected MB-16 digestion product. The triply charged peak at 1431, however, does correspond to a peptide in the mass range anticipated for a larger cross-linked peptide. Deconvolution of the spectra was performed in the range spanning from 3500 to 45000 mass units (m.u.) (Figure 6.3.10B), where there are no tryptic fragments expected to appear. A peak of 4292 m.u. is detected; this mass equals to the sum of the masses of the fragment corresponding to residues 49-72 (2572 m.u.) plus the fragment

corresponding to residues 49-65 (1737 m.u.) minus 18 mass units (representing the loss of a water molecule). The cross-link in the covalent dimer was therefore postulated to join tryptic peptide 49-72 to 49-65.

To confirm this postulation, MS/MS was performed on this 4292 m.u. peak. From the resulting data, an amino acid sequence consistent with residues 51-65 and residues 69-71 (with 85% confidence) was identified. These MS/MS data, in conjunction with the mass of the parent ion (4292 m.u.) suggest the proposed cross-linked chains: residues 49-72 on one monomer linked to residues 49-65 on a second monomer. The fragment spanning residues 49-72 contains a lysine residue at position 65 that is uncut by trypsin, presumably because it is cross-linked to the second tryptic fragment of residues 49-65 from a second monomer containing the acid function. This proposed cross-linking site is shown in Figure 6.3.11.

In the initial 4-helix bundle design of MB-16, residues 49-72 are contained in Helix 3. The proposed amide cross-linked joins residues 49-72 (through Lys_{65}) to residues 49-65 of the second monomeric chain through an acidic side chain, either aspartic or glutamic acid. As shown in Figure 6.3.11, there are 3 possible acid functions in this second peptide, Glu_{49}, Asp_{50}, and Asp_{53}. The mass spectrometric data does not conclusively determine the actual acid residue involved in the cross-link as the MS/MS sequencing results displayed residues 49-65 which is also the major component of the lysine containing fragment and the mass peak corresponding to the inter-residue fragmentation of the actual amide linked residues was not detected. Full determination of the residue containing the acid function in the cross-linking site may be possible but would require further mass spectrometry with samples containing a purified cross-linked peptide. Even so, considerable optimization of fragmentation methods would be needed to enable the identification of the exact two

residues linked together. The data obtained, however, is enough to satisfy the main objective in cross-linking MB-16: the identification of the helices that are strongly interacting to form the dimer. The evidence indicates that Helix 3 from one molecule is packing against Helix 3 from a second molecule.

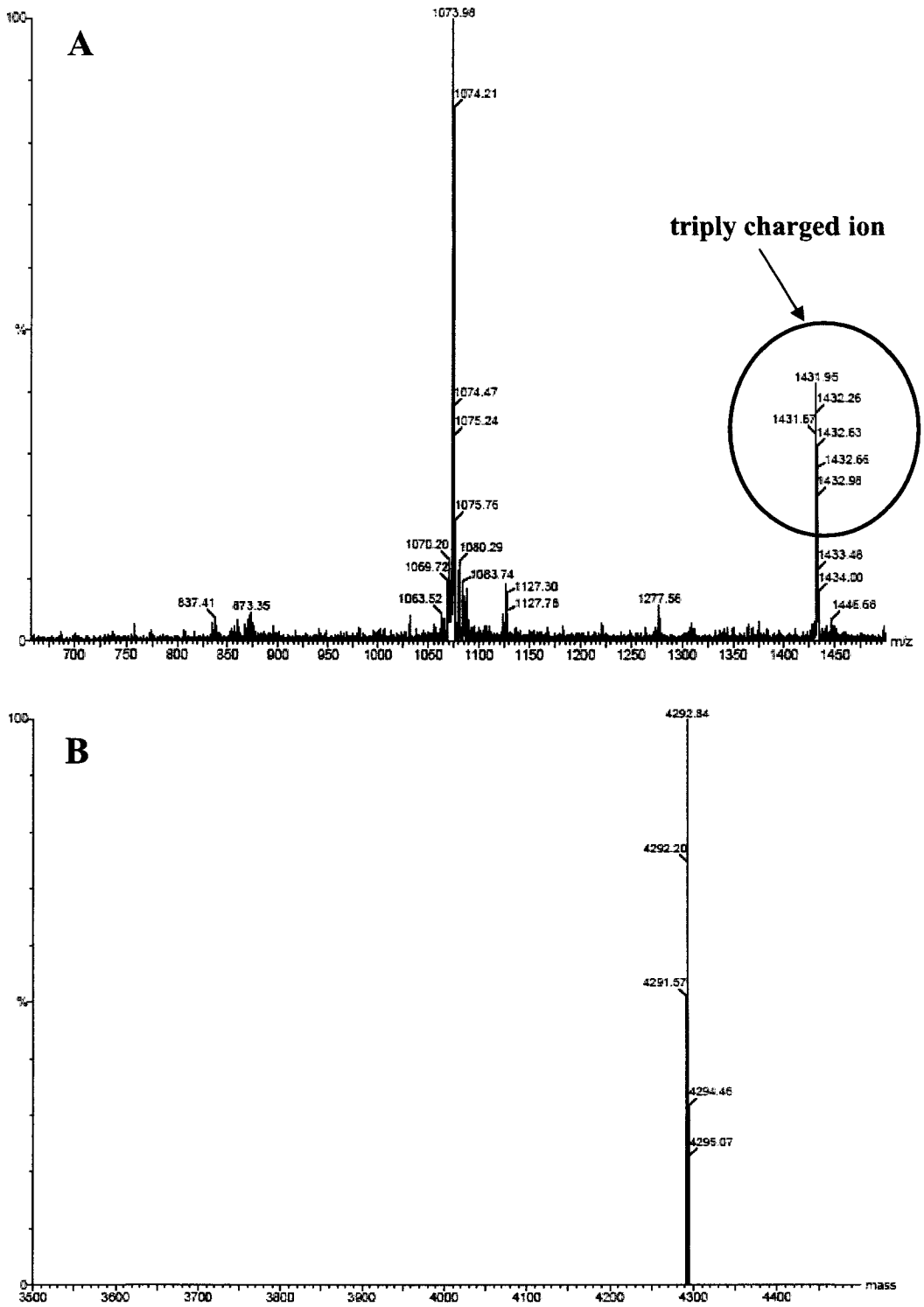

Figure 6.3.10 Electrospray ionization TOF mass spectrum of MB-16 cross-linked peptide (A) and deconvoluted spectrum (B). The cross-linked peptide has an apparent mass of 4292 ± 1 m.u.

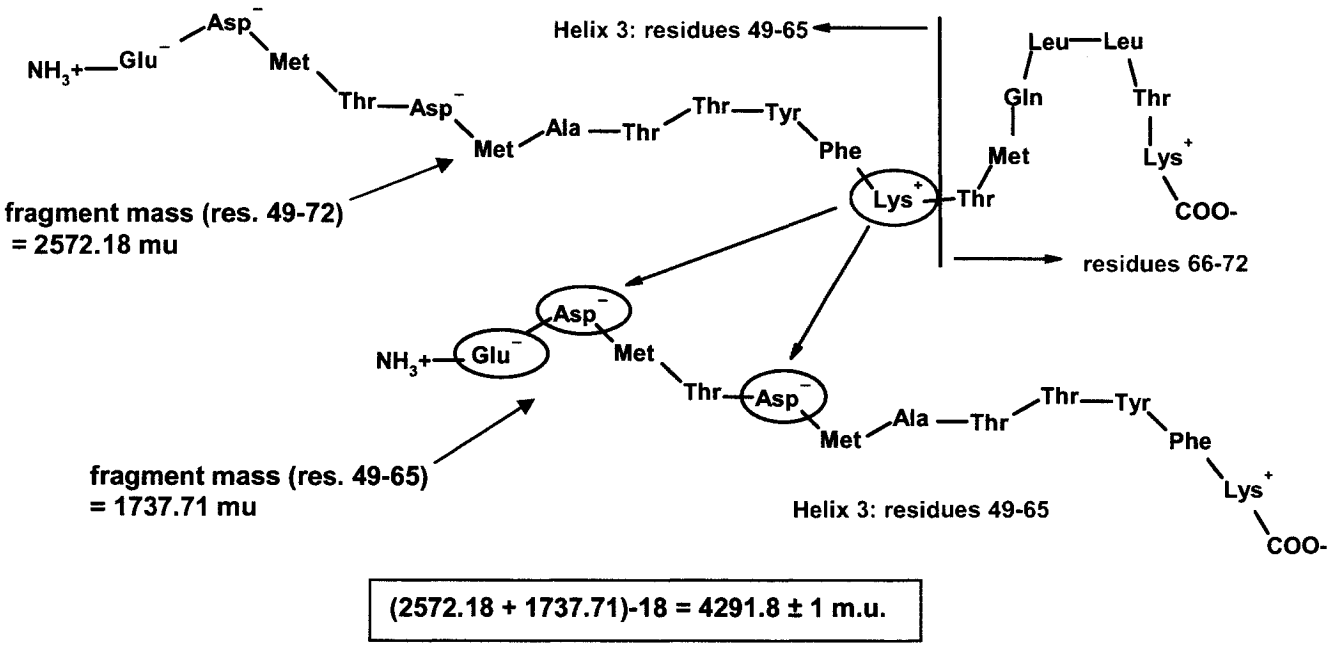

Figure 6.3.11 Schematic of the cross-linking site in the *in vacuo* cross-linked MB-16 dimer; two MB-16 tryptic fragments covalently attached by an amide bond at Lys_{65} to an acid residue on a second fragment. The resulting mass from a condensation reaction between a protonated amino group from lys and a deprotonated carboxylic acid group from an acid residue is 4291.8 ± 1 m.u.

6.3.9 Proposed "misfolding" of MB-16 to give the dimeric conformer

The interaction of Helix 3 of one MB-16 monomer with Helix 3 from a second monomer to form a non-covalent dimer suggests an opened face dimeric conformation. As indicated in Figure 6.1.1 in the introductory section of this chapter, an opened face dimer may occur if the Loop II does not enforce a proper turn and Helix 3 and 4 can swing away allowing the formation of two 4-helix bundles composed of two interacting monomers (also shown in Figure 6.3.12). Because Helix 1 and 3, and, Helix 2 and 4 are equivalent, two opened face dimeric conformers are possible, and, in view of theoretical considerations, the

open face dimer I was predicted to be more likely (see introduction, above). The cross-linking data, however, is consistent only with the formation of the open face dimer II (this representation is shown in Figure 6.3.12). These results suggest that not only is there no steric constraint to the juxtaposition of the two tyrosine residues from the two monomeric units, but that the stacking of the *pi* electron systems may in fact promote the formation of this dimer. Closer analysis of the schematic in Figure 6.3.12 and the positions of the amino acids within the ensuing open-faced helix structure leads to the speculation that the strongest intermolecular salt-bridge would occur between Lys_{65} and Asp_{53}, perhaps further supported by the stacking interaction of neighboring tyrosine residues bringing the salt-bridging residues closer in proximity. The exact positioning of the helices in the dimeric bundle fold is purely speculative but is consistent with both theoretical considerations and the data obtained here and previously as to the nature of the interface. Further analysis of the *in vacuo* cross-linked MB-16 dimer may in fact reveal the presence of other minor cross-links in the structure which were not apparent during these preliminary experiments.

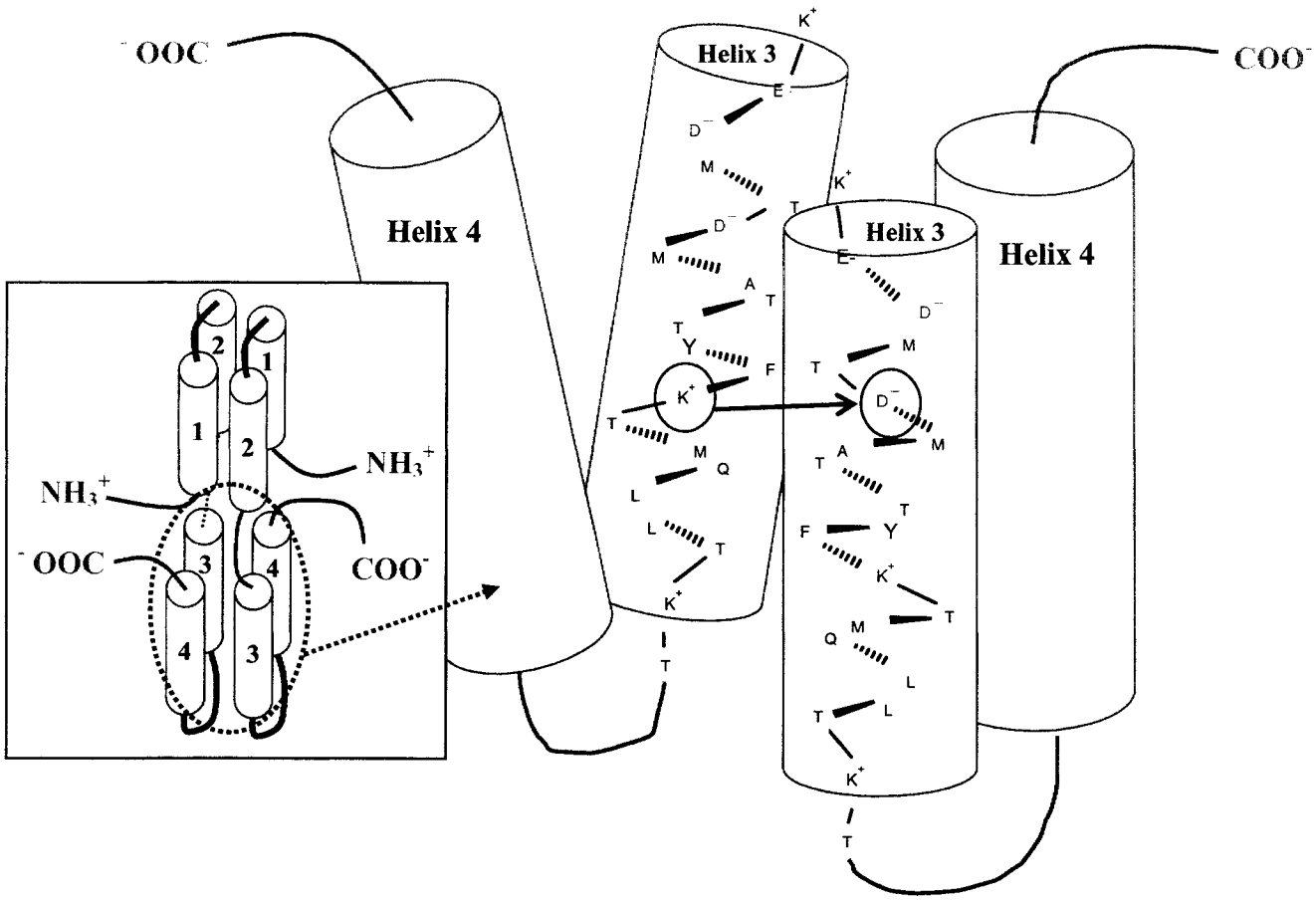

Figure 6.3.12 Proposed folding of MB-16; open face dimer II conformer with the proposed cross-linking site circled in red.

6.4 Conclusions

The ability of some proteins to self-associate to form non-covalent dimers, trimers, and higher oligomers in solution has been an area of study highly pursued in an effort to provide further understanding of the relationships between the primary structure of proteins and their tertiary and quaternary folds. (Bennett et al., 1995; D'Alessio, 1999). In the case of the designed milk bundle proteins, the misfolding of the original monomeric 4-helix bundle design reflects the challenges of engineering a primary structure to adopt that stable tertiary

structure once recombinantly expressed and purified in solution using an algorithm-based prediction of a helical fold. The work presented here, along with previously published work in this laboratory and that of colleagues (Parker and Hefford, 1998; Doucet et al., 2002) adds, at least incrementally, to the common understanding of structure and fold.

The comparison of MB-1 and MB-16 in terms of conformational and chemical stability reveals that the repulsion between the two positively charged lysine residues in the TKNK loop sequence of MB-1 does not result in a destabilization of the folded structure. Replacing the TKNK loop with 5 glycine residues does result in some improvements in terms of obtaining a small amount of monomeric structure and whose overall structure is slightly more resistant to thermal denaturation, but is not sufficient to direct the folding of MB-16 into a stable monomeric 4-helix bundle fold. Glycine residues were inserted into loop II in MB-16 because they are excellent 'helix-breakers', a property that may well explain the secondary structure predictions of GGGGG as a very strong 'loop' sequence. Glycine's lack of a side chain also allows the formation of a sharp turn in the direction of the peptide chain without steric hindrance. This flexibility serves both to stop helix propagation (Serrano et al., 1992) and to allow the formation of the capping hydrogen bonds found in paperclip motifs such as the α_L and the Schellman motifs (Aurora et al., 1994).

The 5 glycine residue sequence in MB-16 should allow the formation of the C-capping motif. In our laboratory's previous work with capping motifs (Parker and Hefford, 1998), a C-capping motif was introduced into loops I and III. Unlike MB-16, the resultant protein in that case, MB-11, was both more helical than MB-1 and more resistant to urea denaturation. In addition to the C-capping motif, the loops I and III sequences in MB-11 also had the potential to form a motif at the N-termini of the alpha helix folllowing the

loop sequence known as the 'N-capping box' (Harper and Rose, 1993). The formation of an N-capping box at the beginning of Helix 3 is not possible in MB-1 as it lacks the appropriate Ncap and N3 residues to make the requisite reciprocal hydrogen bonds. The introduction of the 5-glycine residue loop in MB-16 does not rectify this situation. N-capping boxes can substantially increase the stability of both proteins (Serrano, et al., 1992; Aurora et al., 1994). In their design of 3-helix-bundle proteins, Bryson and co-workers (1998) introduced an N-capping box (N-X-X-E) into each loop sequence. This was sufficient to convert the self-associating, oligomeric α_3A protein to the monomeric α_3B. Given the observation that MB-16 can form some monomer (particularily in dilute solutions), it may well be that the GGGGG loop sequence can allow but does not force the turn which would juxtapose Helix 2 and Helix 3 for the formation of a monomeric milk-bundle protein.

The MB-16 covalent dimer produced by the *in vacuo* procedure resulted in the formation of an intermolecular amide linkage between Helix 3 from one monomer and Helix 3 from a second monomer. The dimer was then proposed to have a structure consistent with an open face dimer II conformation composed of two 4 helix bundles in which two Helix 3 domains, one from each monomer, are packed against each other. If this covalent dimer is reflective of the non-covalent dimer present in solutions, it provides several additional pieces of information about the original design of the MB helical bundle proteins and suggests modifications of the design. Firstly, it confirms earlier results (Gagnon et al., 2000) that, contrary to the original design premise, the bundle packing does allow for a bulkier residue in the core of the bundle. Indeed, the side chains of two tyrosine residues appear to be accomodated in the core created by packing of four helices and may actually stabilize the dimer. "Negative design" might well be undertaken to replace the three alanine residues that

were, in the original design, thought to "make room for" the tyrosine side chain in the core with residues with bulkier side chains. This added "crowding" of the tyrosine side chain may make it difficult to fit two tyrosine residues into a core and thus prevent the formation of a dimer. Secondly, the covalent dimer is an open face dimer. This result explains why earlier variants like MB-11 and MB-13, while both more stable and more helical than the original design, were not monomeric proteins. Both MB-11 and MB-13 had the original loop II design and thus could "flip out" to form open face dimers. It is curious, however, that MB-13/16 (a variant that contains the loop I and III mutations of MB-13 and the loop III mutation of MB-16) is more monomeric than MB-16. That result suggests that loops I and III play some role in dimerization; perhaps more than one type of dimer is possible. In this regard, it would be interesting to use the *in vacuo* procedure to probe the dimer(s) formed by MB13/16. Alternately, characterization of another variant produced further modification/improvement of loop II of MB-16 to introduce N-capping would also be interesting. If such a modification could force the turn at loop II, only the 1st helix swapped dimer and the 4th helix swapped dimer would be possible. The *in vacuo* cross-linking method could determine which if any was more likely.

Whether the covalent dimer of MB-16 formed on lyohilization in the *in* vacuo cross-linking procedure is accurately depicting the actual non-covalent interface this protein displays in solution is certainly a question that requires further investigation. The evaluation of the ability of *in vacuo* cross-linking to covalently capture, through amide bond formation, strongly interacting salt-bridged residues that are present when the protein structures are solvated would require directly testing the location and strength of salt-bridges in dimeric interfaces of known solution structures by some other means (for example, probing dimeric

interfaces for hydrogen/deuterium exchange with the use of H/D MS (Busenlehner and Armstrong, 2005) and comparing that to H/D exchange after the formed amide linkages induced by the *in vacuo* cross-linking procedure. This experiment, of course, is beyond the scope of this thesis and is best left to future graduate students.

6.5 Acknowledgements

The construction of the MB-1 and its MB-16 and MB-13/16 variants was done by Dr. Dean Scholl, Dr. Matt Parker and Dr. Marc Beauregard in Dr. Hefford's laboratory at Agriculture and Agri-food Canada in Ottawa and, subsequently, by Dr. Alain Doucet in Dr. Marc Beauregard's laboratory at the Université du Québec à Trois-Rivières.

This work was funded by grants from Dairy Farmers of Canada and from the Natural Science and Engineering Council of Canada. I would like to thank Sophie D'Aoust for technical assistance on several experiments and help in the preparation of some figures in the chapter.

6.6 References

Aurora, R.; Srinivasan, R.; Rose, G. D. Rules for alpha-helix termination by glycine. *Science* **1994,** *264* (5162), 1126-1130.

Beauregard, M.; Dupont, C.; Teather, R. M.; Hefford, M. A. Design, expression, and initial characterization of MB1, a de novo protein enriched in essential amino acids. *Biotechnology (N. Y.)* **1995,** *13* (9), 974-981.

Bennett, M. J.; Schlunegger, M. P.; Eisenberg, D. 3D domain swapping: a mechanism for oligomer assembly. *Protein Sci.* **1995,** *4* (12), 2455-2468.

Bryson, J.W.; Desjarlais, J.R.; Handel, T.M.; DeGrado, W.F. From coiled coils to small globular proteins: design of a native-like 3-helix bundle. *Protein. Sci.* **1998**, *7(6)*, 1404-1414.

Busenlehner, L.S. and Armstrong, R.N. Insights into enzyme structure and dynamics elucidated by amide H/D exchange mass spectrometry. *Arch. Biochem. Biophys.* **2005**, *433(1),* 34-46.

D'Alessio, G. The evolutionary transition from monomeric to oligomeric proteins: tools, the environment, hypotheses. *Prog. Biophys. Mol. Biol.* **1999,** *72* (3), 271-298.

Doucet A,; Williams M,; Gagnon MC,; Sasseville M,; Beauregard M. Engineering nutritious proteins: improvement of stability in the designer protein MB-1 via introduction of disulfide bridges. *J Agric Food Chem.* **2002**, 50 (1):92-8.

Gagnon MC,; Williams M,; Doucet A,; Beauregard M.; Replacement of tyr62 by trp in the designer protein milk bundle-1 results in significant improvement of conformational stability. *FEBS Lett.* **2000,** 484(2):144-8.

Garnier, J.; Gibrat, J. F.; Robson, B. GOR method for predicting protein secondary structure from amino acid sequence. *Methods Enzymol.* **1996,** *266:540-53.*, 540-553.

Frenz, J.; Hancock, W.S.; Henzel, W.T., and Horváth, C. "Reversed Phase Chromatography in Analytical Biotechnology of Proteins", *HPLC of Biological Macromolecules: Methods and Applications.* K. M. Goodings and F. E. Regnier, (Editors), Marcel Dekker, N.Y., **1990**, pp. 145-177.

Harper, E. T.; Rose, G. D. Helix stop signals in proteins and peptides: the capping box. *Biochemistry* **1993,** *32* (30), 7605-7609.

Hefford, M. A.; Dupont, C.; MacCallum, J.; Parker, M. H.; Beauregard, M. Characterization of MB-1. A dimeric helical protein with a compact core. *Eur. J. Biochem.* **1999,** *262* (2), 467-474.

Hu, C. Q.; Sturtevant, J. M.; Thomson, J. A.; Erickson, R. E.; Pace, C. N. Thermodynamics of ribonuclease T1 denaturation. *Biochemistry* **1992,** *31* (20), 4876-4882.

Johnson, W. C. Analyzing protein circular dichroism spectra for accurate secondary structures. *Proteins* **1999,** *35* (3), 307-312.

Kohn, R. A.; Allen, M. S. Prediction of protein degradation of forages from solubility fractions. *J. Dairy Sci.* **1995,** *78* (8), 1774-1788.

Kunkel, T. A.; Bebenek, K.; McClary, J. Efficient site-directed mutagenesis using uracil-containing DNA. *Methods Enzymol.* **1991,** *204:125-39.*, 125-139.

MacBeath, G.; Kast, P.; Hilvert, D. Probing enzyme quaternary structure by combinatorial mutagenesis and selection. *Protein Sci.* **1998,** *7* (8), 1757-1767.

MacCallum, J. D.; Hefford, M. A.; Omar, S.; Beauregard, M. Prediction of folding stability and degradability of the de novo designed protein MB-1 in cow rumen. *Appl. Biochem. Biotechnol.* **1997,** *66* (1), 83-93.

Nagi, A. D.; Regan, L. An inverse correlation between loop length and stability in a four-helix-bundle protein. *Fold. Des.* **1997,** *2* (1), 67-75.

Neet, K.E.; and Timm, D.E. Conformational stability of dimeric proteins: quantitative studies by equilibrium denaturation. *Protein Sci.* **1994,** *3* (12), 2167-2174.

Pace, C. N. Conformational stability of globular proteins. *Trends Biochem. Sci.* **1990,** *15* (1), 14-17.

Parker, M. H.; Hefford, M. A. A consensus residue analysis of loop and helix-capping residues in four-alpha-helical-bundle proteins. *Protein Eng* **1997,** *10* (5), 487-496.

Parker, M. H.; Hefford, M. A. Introduction of potential helix-capping residues into an engineered helical protein. *Biotechnol. Appl. Biochem.* **1998,** *28* (Pt 1), 69-76.

Saint-Jean, A. P.; Phillips, K. R.; Creighton, D. J.; Stone, M. J. Active monomeric and dimeric forms of *Pseudomonas putida* glyoxalase I: evidence for 3D domain swapping. *Biochemistry* **1998,** *37* (29), 10345-10353.

Serrano, L.; Sancho, J.; Hirshberg, M.; Fersht, A. R. Alpha-helix stability in proteins. I. Empirical correlations concerning substitution of side-chains at the N and C-caps and the replacement of alanine by glycine or serine at solvent-exposed surfaces. *J. Mol. Biol.* **1992,** *20;227* (2), 544-559.

Serrano, L.; Neira, J. L.; Sancho, J.; Fersht, A. R. Effect of alanine versus glycine in alpha-helices on protein stability. *Nature* **1992,** *356* (6368), 453-455.

Smith, P. K.; Krohn, R. I.; Hermanson, G. T.; Mallia, A. K.; Gartner, F. H.; Provenzano, M. D.; Fujimoto, E. K.; Goeke, N. M.; Olson, B. J.; Klenk, D. C. Measurement of protein using bicinchoninic acid. *Anal. Biochem.* **1985,** *150* (1), 76-85.

Wiechelman, K. J.; Braun, R. D.; Fitzpatrick, J. D. Investigation of the bicinchoninic acid protein assay: identification of the groups responsible for color formation. *Anal. Biochem.* **1988,** *175* (1), 231-237.

Chapter 7: Conclusions and Future Work

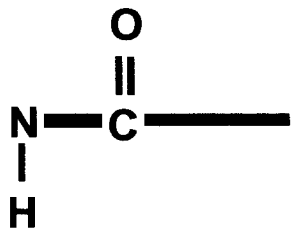

This thesis describes the discovery that interacting ammonium and carboxylate groups of proteins in the lyophilized state, such as those functional groups involved in an intermolecular salt bridge, can undergo a condensation reaction *in vacuo* resulting in the formation of an amide linkage. In practical terms, the discovery provides new non-aqueous methodology for the cross-linking of proteins without the use of chemical reagents. The research focused on characterization of the reaction mechanism, efficiency, and potential applications of this discovery. The *in vacuo* reaction has been shown to be general in its applicability as all proteins tested showed intermolecular cross-linking, whether in homogeneous or heterogeneous preparations or interacting with functionalized solid supports. Some theoretical insights into protein-protein interactions, potential therapeutic proteins, protein analytical products have resulted from this research. Furthermore, this *in vacuo* chemistry has opened new avenues of research into theoretical and practical applications arising from *in vacuo* cross-linking. The *in vacuo* cross-linking process is currently being developed in the research groups of Drs. Kaplan and Hefford as a platform technology for the study of protein stability, protein-protein interactions and the development of novel protein products. This chapter discusses the insights gained from using the *in vacuo* cross-linking process to cross-link proteins and its potential for further development.

7.1 Theoretical Findings

One of the most interesting theoretical aspects arising from the results obtained is based on the observation that reactions that are unfavourable in aqueous solution proceed readily when the proteins are in the lyophilized state under certain conditions (elevated

temperatures and reduced pressures). Specifically, protonated amine groups, which are poor nucleophiles and expected to be unreactive in a solvated environment, can react with a deprotonated carboxylic acid, a functional group that would, in aqueous conditions, be considered a poor electrophile. This observation gives evidence that a proton transfer occurs amongst ionizable functional groups in the lyophilized state under *in vacuo* conditions: an initial step of a proton transfer from the protonated amine to the carboxylate ion produces both a good nucleophile (a primary amine) and an electrophile (a protonated carboxylic acid). If such a proton transfer and subsequent reaction produces a volatile leaving group, and this gaseous product is drawn out of the reaction by the vacuum, a covalent amide bond is formed. This mechanism was proposed based on the experimental evidence obtained from the *in vacuo* cross-linking of RNase A. Evidence was obtained for the involvement of interacting protonated amine and deprotonated carboxyl groups in the condensation reaction forming the RNase A covalent dimer by an intermolecular amide linkage (Simons et al., 2002). Such a condensation reaction is thermodynamically unfavourable under aqueous conditions; however, the effect of the vacuum removing a product of the reaction, *viz.* water, drives the reaction and promotes the formation of an amide bond – in accordance with Le Châtelier's principle. The *in vacuo* cross-linking technique challenges the traditional view of protonated amino groups as unreactive and reveals new insight into the nucleophilic capabilities of such groups in the dried state. Additionally, this reaction is carried out at neutral to mildly alkaline pH values, conditions where proteins, in most cases, retain their native conformations and thereby preserving biological activity.

The results obtained in the study characterizing the RNase A dimer (primarily one amide bond resulting from one condensation reaction) indicated that protein cross-linking via the *in*

vacuo method, unlike aqueous methods of cross-linking protein mediated by bifunctional activating reagents, does not result in uncontrolled random cross-linking. In solution, the conformational mobility of proteins is, for the most part, unrestricted and the intermolecular interactions between side chains are highly dynamic resulting in variations in the chemical reactivities of the functional groups contained on those side chains (Creighton, 1993). Upon the introduction of bifunctional reagents, any available and reactive functional group on the protein will become derivitized and thus leaving the protein chemically modified even if the cross-linking reaction remains incomplete. Lyophilization removes the aqueous environment, locks the protein into low energy conformations, and restricts the movements of side chains and, as a result, functional groups become fixed into defined ionization states. This effect of "freezing-out" the ionization states of reactive functional groups is called the pH memory effect and allows one to gain much more control over reactions carried out *in vacuo*. Intermolecular interactions between molecules in the dried state also become stronger; in particular, salt-bridge interactions are stronger due to the absence of the solvation shell around the protein. The *in vacuo* method of cross-linking exploits these advantages that occur in lyophilized protein preparations and selectively promotes the formation of an amide bond only between strongly interacting ammonium and carboxylate groups found in an intermolecular salt bridge. This technique, therefore, allows for the permanent marking of strong electrostatic interactions between molecules and thus enabling for the characterization of the site of interaction.

7.2 Practical Applications

The practical advantages of the *in vacuo* method can be summed up by the following points: (1) the procedure is general in its applicability and all proteins or compounds will cross-link to some extent providing the correct functionality is available; (2) a wide range of protein quantities, *viz.* gram to picogram quantities, can be used, thus making it applicable to both microscale and larger scale reactions; (3) cross-linking reactions can be performed at elevated temperature or for longer durations to increase yields but without concomitant loss of native structure; (4) the extent of cross-linking can be controlled by either adjusting the ratios of the starting materials or by the addition of excipients in the lyophilized mixture; (5) all uncross-linked material remains unmodified and thus can be recovered and reused; and lastly (6) no chemical reagents are used, therefore purified protein therapeutics produced by this method cannot be contaminated by the presence of traces of reagents that might give rise to immunogenic or toxic reactions in patients – a fact that may expedite their assessment by regulatory authorities.

7.2.1 Investigation of protein-protein interactions

The use of protein cross-linking to investigate multi-protein structures is a rapidly developing area of interest. The *in vacuo* method of cross-linking proteins can selectively form an amide bond between residues that are strongly interacting in a salt bridge, forming a physical linkage through which to investigate electrostatic interactions between proteins and biological macromolecules. The ability to produce controlled linking sites between protein molecules or protein domains can allow one to deduce information about even transient domain-domain or protein-protein interfaces in order to solve structures more rapidly or to gain insight into relationships between structure and function. This utility is demonstrated in

the *in vacuo* cross-linking of the *de novo* designed milk bundle proteins (Chapter 6): cross-linking between specific salt-bridged residues, suggested that Helix 3 from one molecule was interacting with Helix 3 from a second molecule resulting in the formation of a stable dimeric conformation rather than Helix 3 packing against Helix 1, 2 and 4 in the monomeric form of the protein intended in the design. Although only two direct examples with proteins were investigated in this study (RNase A dimers and MB protein), the generality of the cross-linking reaction observed with other proteins and non-protein supports (*vide infra*) indicates that all proteins that form stable non-covalent complexes or domain-domain interactions involving strong electrostatics (once freeze dried) will form cross-links through these salt bridging residues thus allowing one to capture these interactions and physically examine them in terms of their number and location.

7.2.2 Protein Immobilization

Given the success and relative efficiency of cross-linking proteins to themselves, to other proteins, and to poly-glutamic acid polypeptide polymers, the *in vacuo* cross-linking method was tested for its applicability to non-protein surfaces that contain the required functionality. Alkaline phosphatase was covalently attached to functionalized glass filter disks and glass particles and its activity was retained, even after six consecutive activity assays where the immobilized enzyme was washed and re-assayed. While alkaline phosphatase derivitized glass surfaces do not have any apparent commercial applications, these immobilization experiments have initiated several projects with trypsin (an enzyme of considerable commercial interest) that are currently ongoing in the Kaplan research group. For example, native trypsin, glycated trypsin, and reductively methylated trypsin were *in*

vacuo cross-linked to functionalized glass beads. All immobilized trypsin products retain catalytic activity and increased thermal stability compared to the free enzyme (Kaplan unpublished results, 2004). Not only has this method shown to be an effective procedure for attaching proteins to surfaces, to date all cross-linked materials appear to retain their native conformations, resulting in high quality immobilized products. All uncross-linked protein remains completely unmodified and can therefore be simply washed off, recovered and reused.

7.3 Novel Cross-linked Products

The *in vacuo* cross-linking method has shown to be an efficient procedure for cross-linking enzymes and forming active protein complexes (Chapter 5). Conjugating enzymes to antibodies has several medicinal and diagnostic based applications, and to date, such cross-linking has only been successfully achieved by chemical activation of the proteins in solution using bifunctional reagents (Avrameas, 1969; Kala et al., 1997; Dhawan, 2002). The *in vacuo* cross-linking of horseradish peroxidase to anti-rabbit IgG has been shown to produce a high quality immunoconjugate with a slightly improved sensitivity when compared to a comparable immunoconjugate produced by solution cross-linking chemistry (Wilson and Nakane, 1978). The *in vacuo* cross-linking of multiple units of HRP and IgG to polypeptide supports has produced an antibody conjugate with a 100 fold increase in sensitivity for the detection of low levels of antigen on Western Blots and ELISAs. While solution methods using some chemical modifying reagents have yielded active enzyme-antibody complexes with good efficiency, there is no general procedure employing a universal reagent, and no two sets of proteins/antibodies will be conjugated with exactly the same efficiency using the

same aqueous strategy. Furthermore, exposing the antibodies/enzymes to highly reactive reagents may induce conformational changes and thus altering binding affinities and biological activity - a significant disadvantage that the *in vacuo* method of cross-linking overcomes. Once again all uncross-linked material remains unmodified and can be recovered and reused.

Oligomerized enzymes often show modulated biological activity (Bennett et al., 1995). Dimers of RNase A (both natural, non-covalent dimers and chemically cross-linked RNase A dimers produced using the bifunctional reagent submerimidate as the cross-linking reagent have been widely pursued as a protein therapeutic based on their anti-tumor and cytotoxicity effects in certain cancer cell lines (Gotte and Libonati, 1998; Di Donato et al., 1994). Certain ribonucleases have been engineered as toxins, acting either alone or as part of chimeras or fusion proteins, for targeted cancer treatment (Wu et al., 1995). The RNase A dimer produced by *in vacuo* cross-linking has also shown an increase in enzymatic activity against dsRNA and an ability to resist inhibition by the known cellular inhibitor - traits that are consistently observed to transform RNase A into a cytotoxic agent. This dimer, therefore, or the heterodimer produced by the cross-linking of RNase A and Onconase™ molecules (to afford facile and selective cellular entry) may eventually find application as a potent cytotoxic and therapeutic agent after further investigation and more complete characterization of their interactions, structures, and biological activities.

7.4 Future Work

This thesis described the development of a novel method for cross-linking proteins and the characterization of some of the cross-linked products that can be formed using this method. It can easily be elaborated upon and expanded to several new applications with either medicinal or industrial uses. This method of cross-linking protein can now be viewed as a platform technology, opening up opportunities for commercialization of the method itself and the products resulting from the use of the method.

Some experiments described in this thesis are preliminary and require further detailed exploration. For instance, the RNase A dimer produced by *in vacuo* cross-linking has shown potential to become further developed into a cancer therapeutic, but, further work is required to fully assess the cytotoxicity of this dimer. To this end, preliminary cell proliferation assays using HL-60 (cancerous) cell lines compare the dimer's activity to that of Onconase™ and a RNase A – Onconase™ heterodimer also produced by the *in vacuo* method. These experiments, however, are only very preliminary and need to be repeated and expanded. In addition, the mechanism by which RNase A and Onconase enter the cell and are routed through it to act upon RNA has only been recently elucidated (Matousek et al., 2003). These mechanisms will require further understanding and experimentation before *in vacuo* cross-linked ribonucleases could be effectively assessed, work that would require further collaboration with people who have expertise with cell culture and cytotoxicity studies.

Antibody-enzyme complexes continue to be valuable in diagnostics and research. The *in vacuo* cross-linked antibody complexes have been shown to increase detection of low levels of antigen in a one antigen/antibody system. Further development of this application is required, extending the cross-linking to a variety of different antibodies (primary and

secondary) and different reporter moieties like biotin, radio labels and fluorescein, for example. The labeling of antibodies using the *in vacuo* technology would represent a cost efficient means of producing custom immunoreagents with improved sensitivity - no matter how small or large the quantity of starting materials.

The most apparent application of the *in vacuo* cross-linking technology is protein immobilization onto solid supports, whether applied to an industrial process or as a bench-top, research-based tool. The immobilization of enzymes onto glass surfaces was only a preliminary experiment but provides proof of the concept. In theory, any solid support that can be derivitized with either amino or carboxyl functionality can be employed for the cross-linking of protein. Surfaces such as ceramic, agarose, or polystyrene, should be investigated. As well, it would be beneficial to test the efficiency and efficacy of the immobilization of some commercially valuable enzymes such as *Taq* Polymerase, DNase I and II, and proteolytic enzymes. This strategy is currently being pursued in the Kaplan research group.

With further experimentation, the *in vacuo* method of cross-linking protein may prove to be a useful method for identifying strong salt bridge interactions between proteins that are members of multi-protein complexes with physiological importance. As many proteins exert their biological effect through interactions with other protein or parts of proteins, the development of methods to analyze these interactions at a molecular level continues to be important. Moreover, the common methods in proteomics research (i.e. 2D electrophoresis and tryptic peptide mapping by MALDI mass spectrometry) have limited ability to identify the protein-protein interactions that underpin the observed differences in comparative proteomics. New methods to study "interactomics" are currently under development and the *in vacuo* method of cross-linking, if it proves to have the ability to

covalently "freeze" in lyophilized samples under vacuum the salt bridge interactions that occur between proteins in solutions, may be useful in this regard.

In closing, one of the most satisfying aspects of this thesis research is that the *in vacuo* method of cross-linking protein gave rise to many new avenues of investigation; this thesis simply introduces the opportunities the method presents. It was impossible, within a reasonable timeframe, to investigate in sufficient depth those systems that were studied let alone investigate the many exciting possible applications the method suggests. No matter in what direction the future focus lies, however, this facile technique to cross-link proteins represents a novel discovery about the reactivity of proteins in the dried state, under vacuum. It can produce protein conjugates that would be difficult or impossible to accomplish by current solution methods and it does so without the involvement of any chemical activating reagents.

7.5 References

Avrameas, S. Coupling of enzymes to proteins with glutaraldehyde. Use of the conjugates for the detection of antigens and antibodies. *Immunochemistry.* **1969,** *6* (1), 43-52.

Bennett, M. J.; Schlunegger, M. P.; Eisenberg, D. 3D domain swapping: a mechanism for oligomer assembly. *Protein Sci.* **1995,** *4* (12), 2455-2468.

Creighton, T.E. Chemical properties of peptides; In *Proteins, Structures and Molecular Properties,* 2nd edition, W.H. Freeman and Company. **1993**. pp. 6-10.

Dhawan, S. Design and construction of novel molecular conjugates for signal amplification (II): use of multivalent polystyrene microparticles and lysine peptide chains to generate immunoglobulin-horseradish peroxidase conjugates. *Peptides* **2002,** *23* (12), 2099-2110.

Di, Donato, A.; Cafaro, V.; D'Alessio, G. Ribonuclease A can be transformed into a dimeric ribonuclease with antitumor activity. *J. Biol. Chem.* **1994,** *269* (26), 17394-17396.

Gotte, G.; Libonati, M. Two different forms of aggregated dimers of ribonuclease A. *Biochim. Biophys. Acta* **1998,** *1386* (1), 106-112.

Kala, M.; Bajaj, K.; Sinha, S. Magnetic bead enzyme-linked immunosorbent assay (ELISA) detects antigen-specific binding by phage-displayed scFv antibodies that are not detected with conventional ELISA. *Anal. Biochem.* **1997,** *254* (2), 263-266.

Matousek, J.; Soucek, J.; Slavik, T.; Tomanek, M.; Lee, J. E.; Raines, R. T. Comprehensive comparison of the cytotoxic activities of onconase and bovine seminal ribonuclease. *Comp Biochem. Physiol C. Toxicol. Pharmacol.* **2003,** *136* (4), 343-356.

Monti, D. M.; D'Alessio, G. Cytosolic RNase inhibitor only affects RNases with intrinsic cytotoxicity. *J. Biol. Chem.* **2004,** *279* (38), 39195-39198.

Schlunegger, M. P.; Bennett, M. J.; Eisenberg, D. Oligomer formation by 3D domain swapping: a model for protein assembly and misassembly. *Adv. Protein Chem.* **1997,** *50:61-122.*, 61-122.

Simons, B. L.; King, M. C.; Cyr, T.; Hefford, M. A.; Kaplan, H. Covalent cross-linking of proteins without chemical reagents. *Protein Sci.* **2002,** *11* (6), 1558-1564.

Wilson, M. B.; Nakane, P. K. *Immunofluorescence and related Staining Techniques;* Elseiver/North Holland BioMedical Press: Amsterdam, **1978,** pp. 158-162.

Wu, Y.; Saxena, S. K.; Ardelt, W.; Gadina, M.; Mikulski, S. M.; De, L. C.; D'Alessio, G.; Youle, R. J. A study of the intracellular routing of cytotoxic ribonucleases. *J. Biol. Chem.* **1995,** *270* (29), 17476-17481.

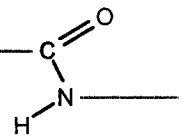

Publications (Refereed)

(I) **Brigitte L. Simons**, Mary-Alice Hefford, and Harvey Kaplan (2005). HRP labeling of antibodies by *in vacuo* cross-linking. Manuscript in preparation.

(II) Russell Taylor, Sylvie Fournier, **Brigitte L. Simons**, Mary Alice Hefford, and Harvey Kaplan (2004). Immobilization of alkaline phosphatase onto solid supports. *Journal of Biotechnology*, Accepted.

(III) **Brigitte L. Simons**, Mary C. King, Terry Cyr, Mary Alice Hefford, Harvey Kaplan (2002). Covalent cross-linking of proteins without chemical reagents. *Protein Science* 11(6): 1558-1564.

(IV) **Brigitte L. Simons**, Dean Scholl, Terry Cyr, and Mary Alice Hefford. (2001) Effects of Increased Loop Flexibility on the Structure and Stability of a De Novo Designed Helical Protein. *Protein and Peptide Letters*, 2001; Vol. 8, No. 2; 89-96.

Canada and U.S.A. Patent Applications

(i) Mary Alice Hefford, Havey Kaplan, and **Brigitte Simons**. Zero-length cross-linking of proteins. Filed, August 2001.

(ii) Mary Alice Hefford, Havey Kaplan, and **Brigitte Simons**. Covalent cross-linking of antibody-enzyme complexes for Western blots. Filed, November 2002.

(iii) Mary Alice Hefford, Havey Kaplan, and **Brigitte Simons (PROTEOVAK INC)**. *In vacuo* cross-linking of proteins. PCT # 46723.

Collaborative International Study and Publication (refereed)

(I) **Brigitte Simons** and Michel Girard. Proficiency Testing (PTS 037): Molecular size distribution of Haemophilus Type B conjugate vaccine. Under the auspices of the Official Medicine Control Laboratories, European Directorate for the Quality of Medicines, 2001.

Conference Poster Presentations (Refereed)

(I) **Brigitte L. Simons**, Sylvie Fournier, Mary Alice Hefford, and Harvey Kaplan. Novel Covalently Cross-linked Enzyme-Antibody Complexes for ELISA and Western Blots. *Protein Society 18th Annual Symposium.* August 14-18, 2004, San Diego, CA. Abstract no. 152. (PhD work)

(II) **Brigitte L. Simons**, Sylvie Fournier, Mary Alice Hefford, and Harvey Kaplan. Improved Western Blot Reagents: Covalent Cross-linking of Enzyme-Antibody Complexes. *Heath Canada Science Forum 2004.* October 18-19, Ottawa, Canada. Abstract no. 315. (PhD work)

(III) Harvey Kaplan, Mary Alice Hefford, Mary C. King, Nicholas A. Stewart, and **Brigitte L. Simons**. Covalent Cross-linking of Proteins Without Chemical Reagents. *5th European Symposium of the Protein Society*, Florence, Italy. Mar. 29 – Apr. 2, 2003. Abs 249.

(IV) **Brigitte L. Simons**, Sylvie Fournier, Mary Alice Hefford, and Harvey Kaplan. Covalent cross-linking of ribonuclease A without chemical reagents. *Protein Society 16th Annual Symposium.* August 17-21, 2002, San Diego, CA. Abstract no. 519. (PhD work)

(V) **Brigitte L. Simons**, Mary Alice Hefford, and Harvey Kaplan. A novel, non-aqueous method of cross-linking protein. *Ottawa Life Sciences Council BioNorth Conference 2002, Ottawa, Ontario.*

(VI) **Brigitte Simons**, Mary Alice Hefford, Harvey Kaplan. A novel, non-aqueous, method of cross-linking protein. BioNorth-Ottawa Life Sciences Conference 2001. Ottawa, Ontario; I107.

CLAIMS TO ORIGINAL RESEARCH

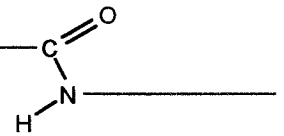

1. The development of a novel method to covalently cross-link proteins *in vacuo* without the use of solvents or chemical reagents.

2. To characterize the formation of amide cross-links between interacting protonated amino groups and deprotonated carboxyl groups between protein molecules in the lyophilized state, optimally at an LpH range between 7 and 10.

3. The *in vacuo* cross-linking of Ribonuclease A (RNase A) produces a covalent dimer with a single amide cross-link at positions Lys 66 and Glu 9 between interacting monomeric units. This novel covalent RNase A dimer displays a unique structure.

4. The demonstration of the enhanced enzymatic activity of the *in vacuo* RNase A dimer, both in the presence and absence of the cytosolic ribonuclease inhibitor.

5. Preliminary experimental set-up to test the cytotoxicity of RNase A monomer and *in vacuo* dimer compared to Onconase™, a cytotoxic ribonuclease, to exhibit their potentials as anti-cancer protein therapeutics.

6. Proteins immobilization onto functionalized solid supports by the *in vacuo* cross-linking method; immobilized alkaline phosphatase retains its catalytic activity after 6 consecutive washings and reuses.

7. Antibody-Enzyme conjugates were produced by the *in vacuo* method of cross-linking protein to produce effective immunoreagents for Western Blot and ELISAs. IgG cross-linked *in vacuo* to HRP demonstrated an improved sensitivity over the commercial enzyme-linked antibodies produced by chemical cross-linking methods.

8. The development of a novel multi-enzyme based immunoconjugate whereby an excess of HRP is linked to poly-D-glutamic acid prior to its attachment to IgG by the *in vacuo* cross-linking procedure. The IgG-poly(glu)-$(HRP)_n$ conjugate is shown to increase the signal of antigen detection by 100-fold beyond the detection limits of a single enzyme-linked antibody.

9. The *de novo* designed milk bundle proteins, MB-1, MB-16, and MB-13/16, have been characterized for their apparent molecular size, thermal stability, and chemical stability.

10. The *in vacuo* cross-linking of MB-16 produced a covalent dimer with an amide cross-link between Helix 3 from one molecule and Helix 3 from a second molecule. The characterization and location of the amide cross-link revealed a strong ionic interaction that was stabilizing the non-covalent dimeric structure of MB-16. MB proteins are thought to adopt a open face 4-helix bundle, non-covalent dimer.